



# PLASMA DIAGNOSTICS

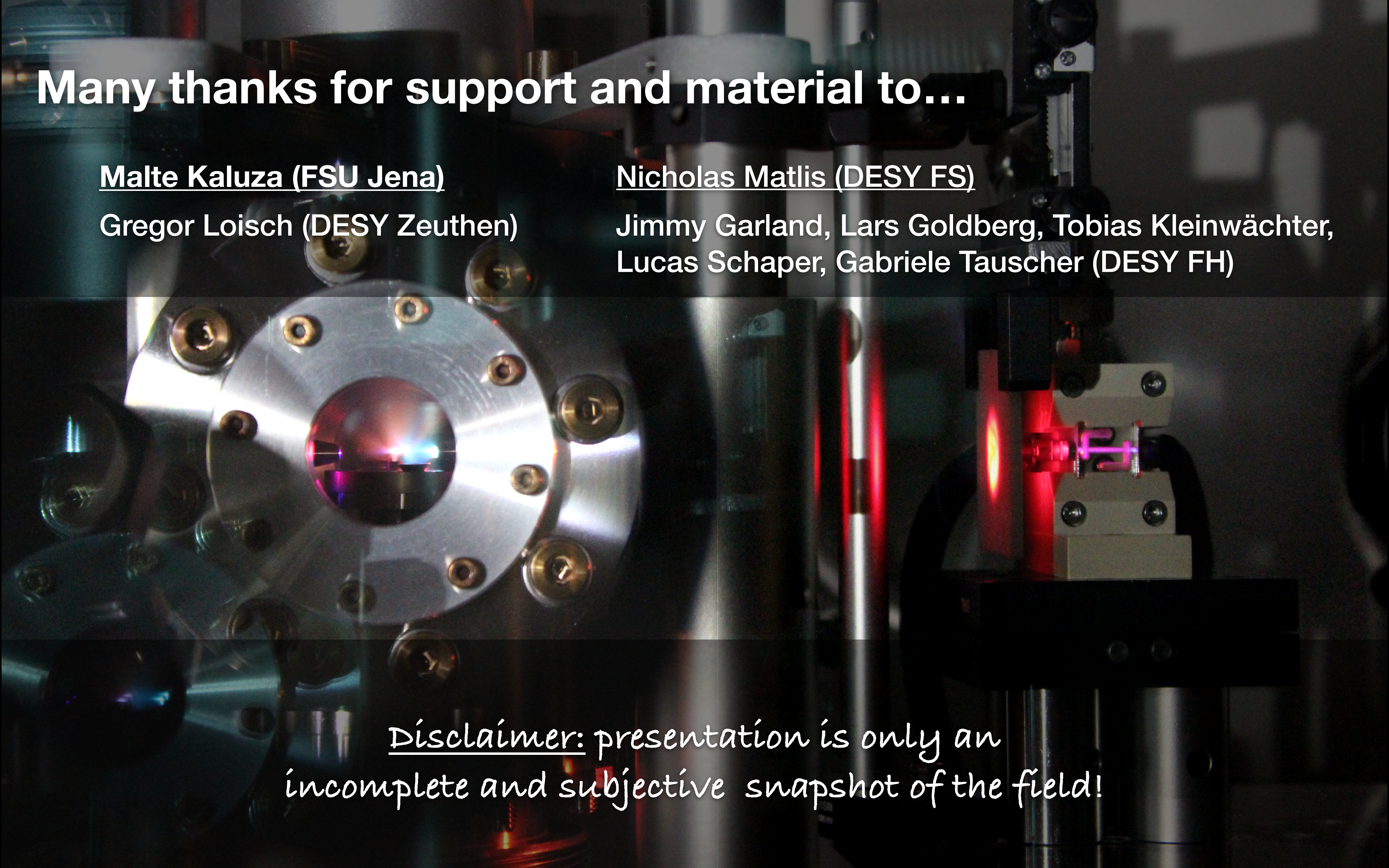
Jens Osterhoff

**FLASHFORWARD** | Research Group for Plasma Wakefield Accelerators  
Deutsches Elektronen-Synchrotron DESY, Particle Physics Division, Hamburg, Germany

Accelerator Research and Development, Matter and Technologies  
Helmholtz Association of German Research Centres, Berlin, Germany



**HELMHOLTZ**  
RESEARCH FOR GRAND CHALLENGES



**Many thanks for support and material to...**

Malte Kaluza (FSU Jena)

Gregor Loisch (DESY Zeuthen)

Nicholas Matlis (DESY FS)

Jimmy Garland, Lars Goldberg, Tobias Kleinwächter,  
Lucas Schaper, Gabriele Tauscher (DESY FH)

Disclaimer: presentation is only an  
incomplete and subjective snapshot of the field!

# Lecture Series on Plasma Sources and Diagnostics

## > Plasma Sources I

- Thursday, March 14, 9:00 - 10:00
- **Conceptual aspects**

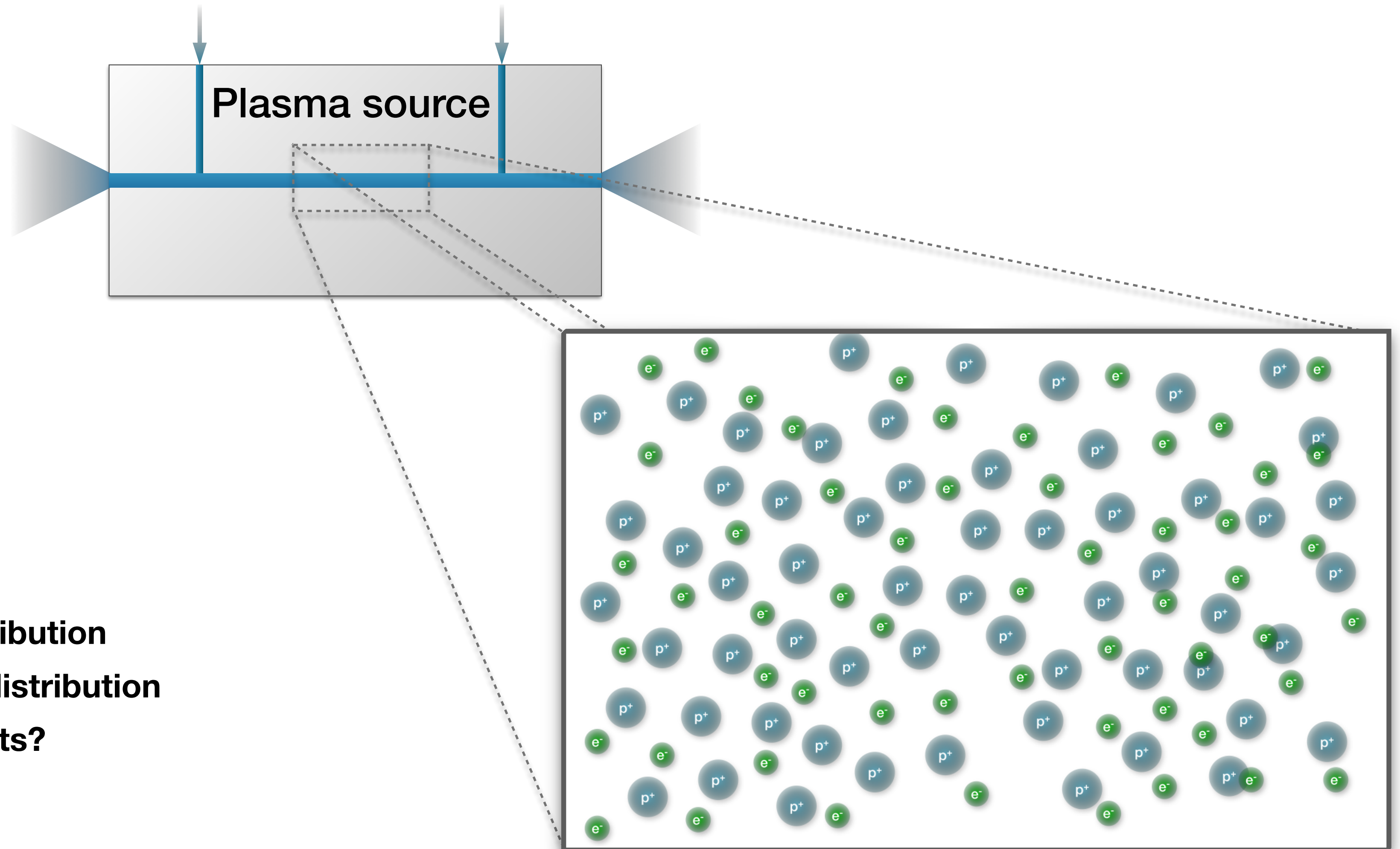
## > Plasma Sources II

- Friday, March 15, 9:00 - 10:00
- **Technical aspects**

## > Plasma Diagnostics

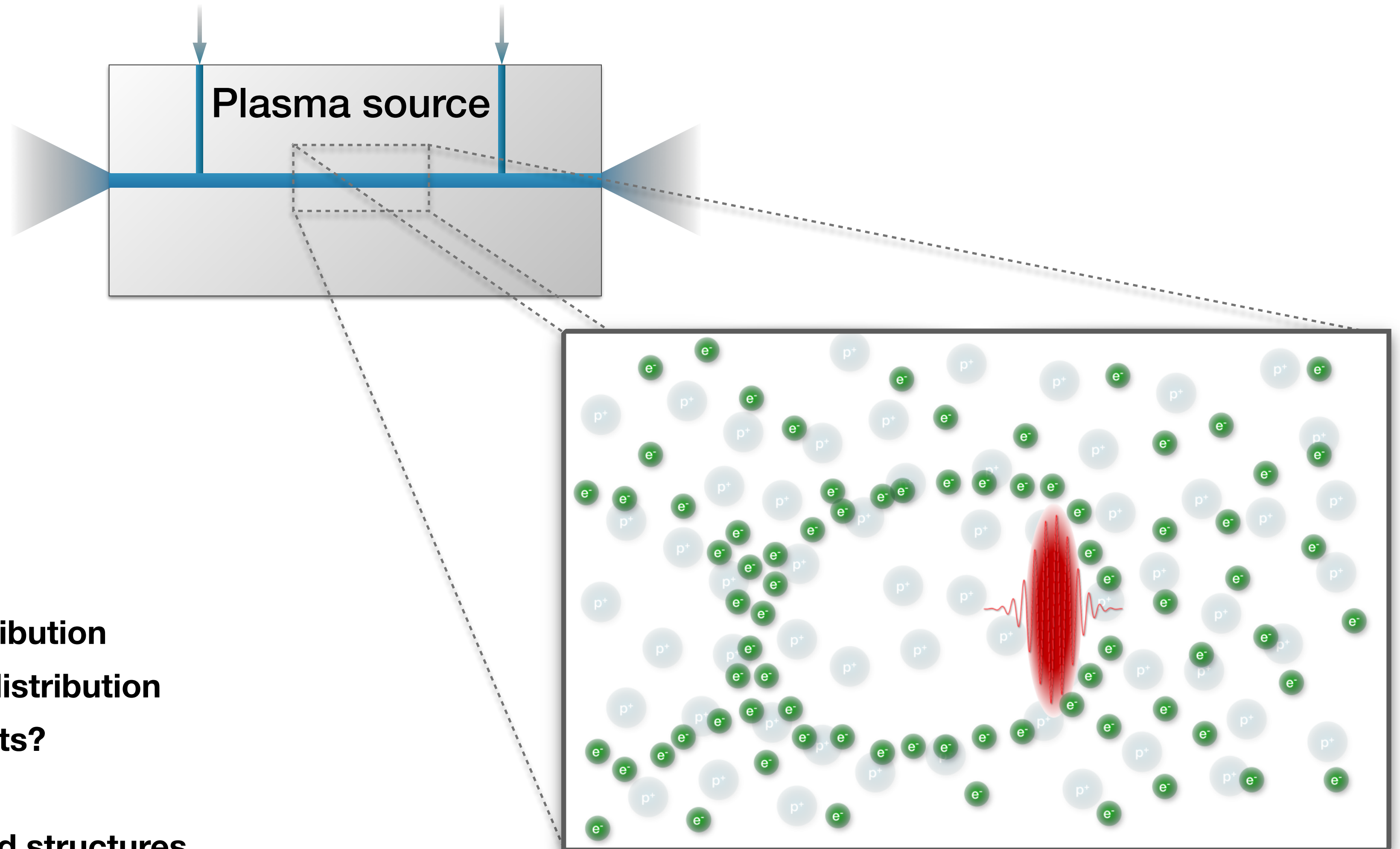
- Tuesday, March 19, 10:00 - 11:00
- **Diagnostics: how to measure what is going on in plasmas**

# Outline - Plasma Diagnostics - What to measure?



- > Gas density distribution
- > Plasma density distribution
- > Other constituents?
- > Temperature

# Outline - Plasma Diagnostics - What to measure?



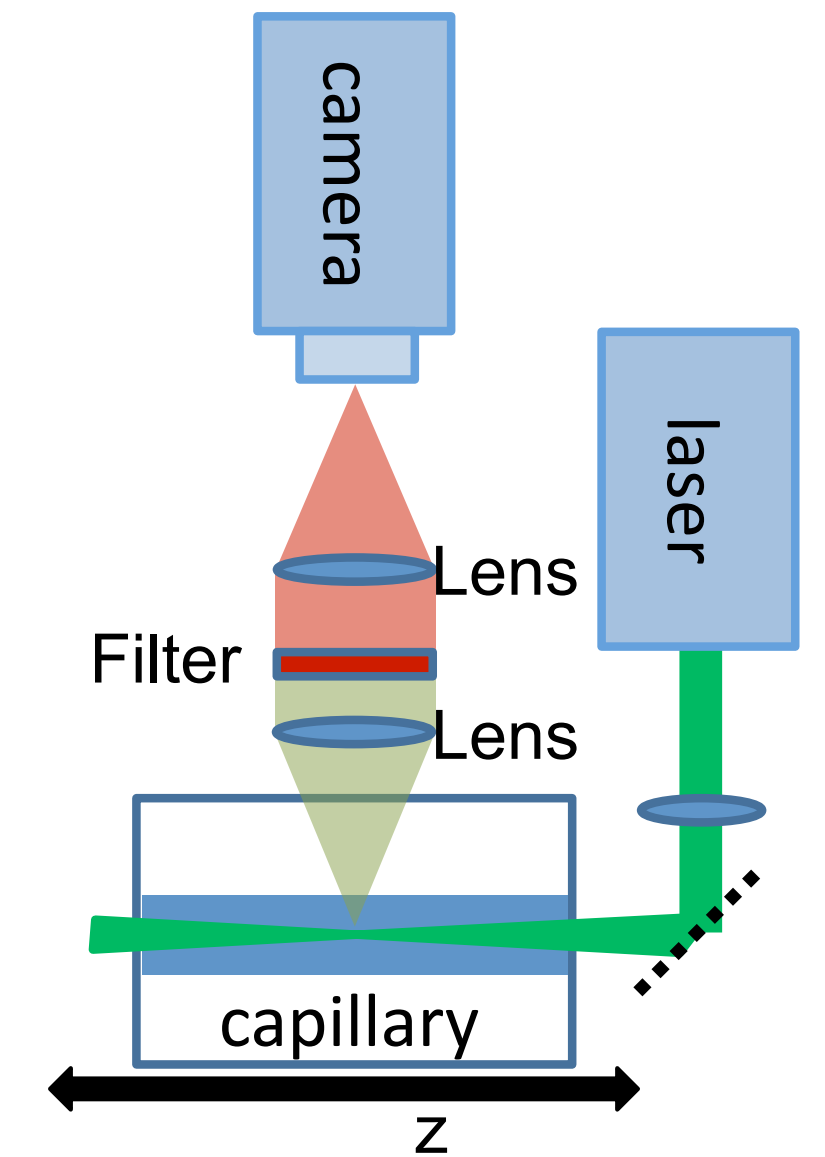
- > Gas density distribution
- > Plasma density distribution
- > Other constituents?
- > Temperature
- > Internal fields and structures

## **Initial gas density distribution**

- Raman scattering
- Laser interferometry
  - plasma density measurements

# Laser scattering

- > Scattering of (laser) light on bound electrons (gas, plasma) can be used as density diagnostic



# Laser scattering

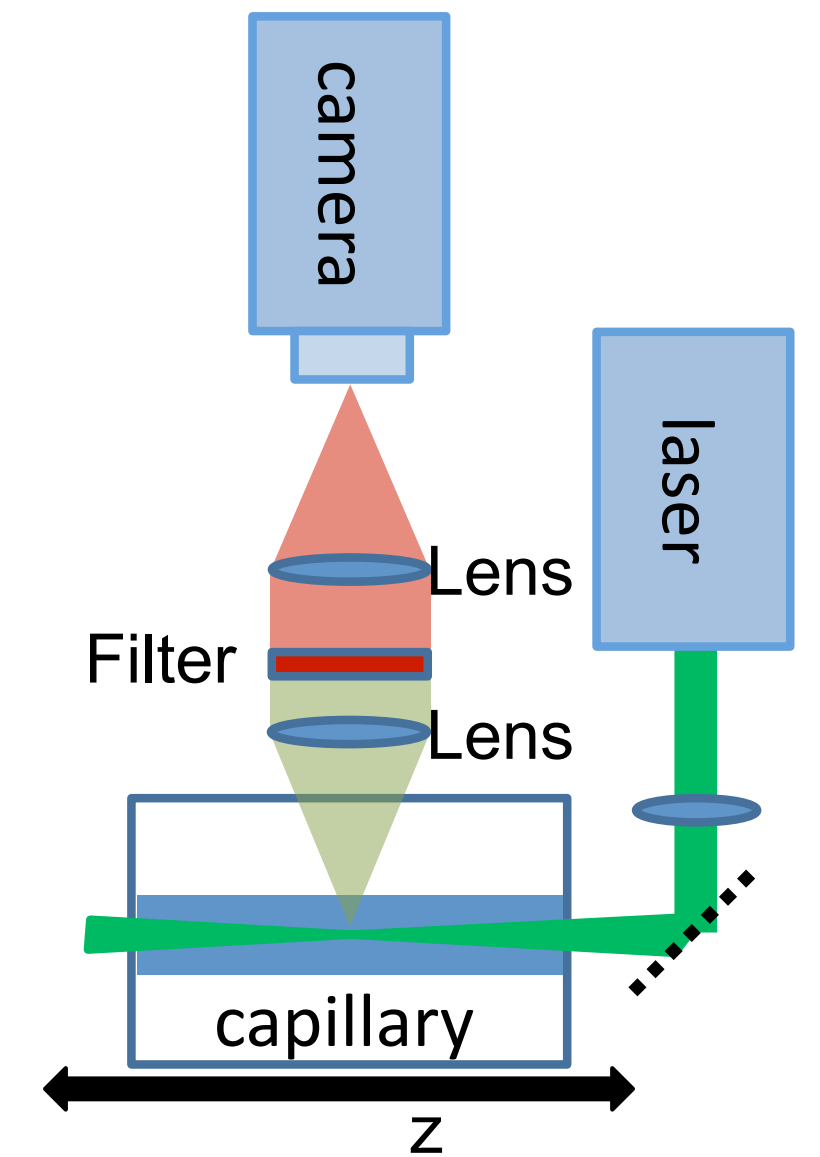
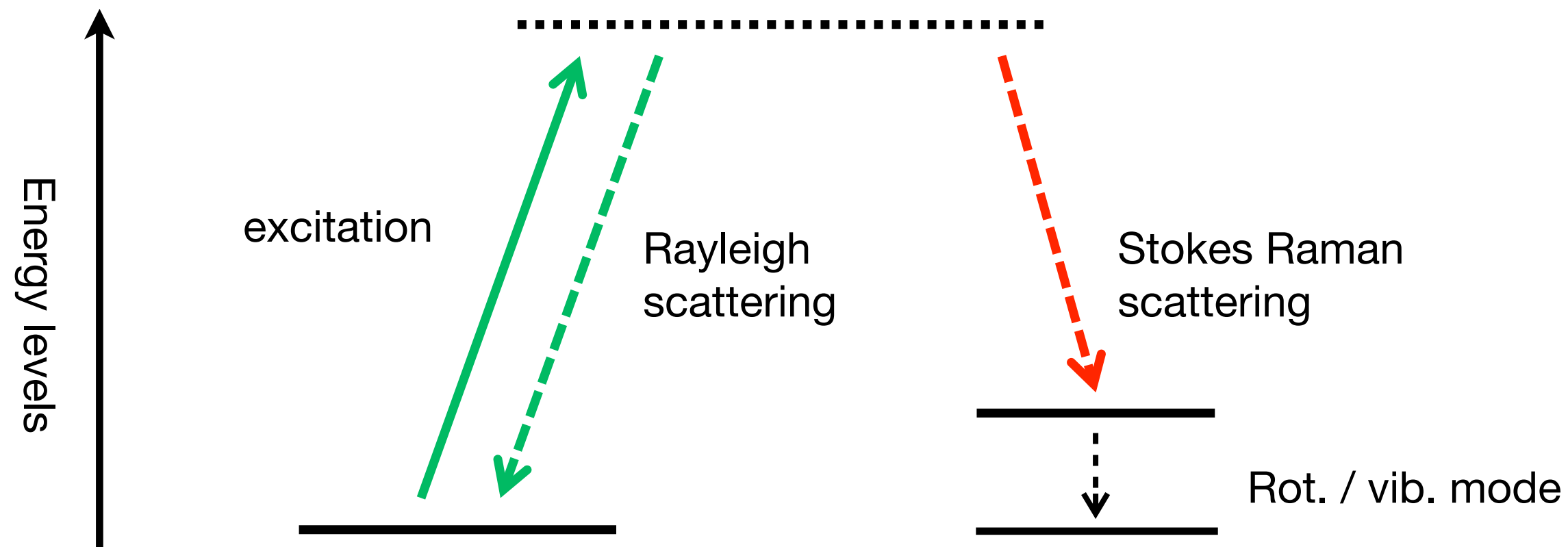
- > Scattering of (laser) light on bound electrons (gas, plasma) can be used as density diagnostic

## Elastic scattering (Rayleigh)

leaves species in same quantum state  
scattered photons of same energy

## Inelastic scattering (Raman)

changes the quantum state of the species  
energy difference excitation to emission



# Laser scattering

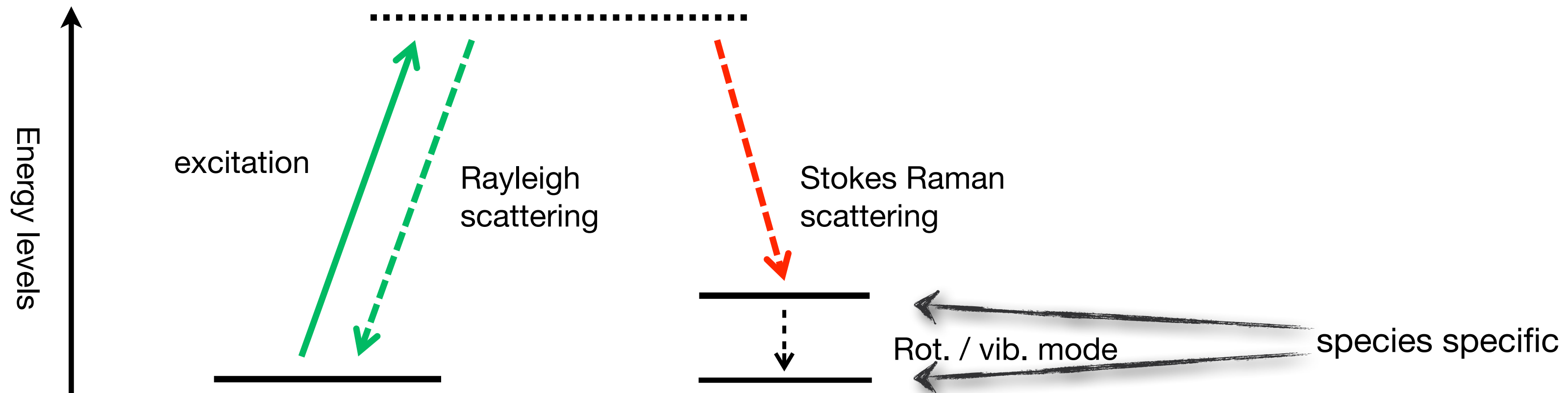
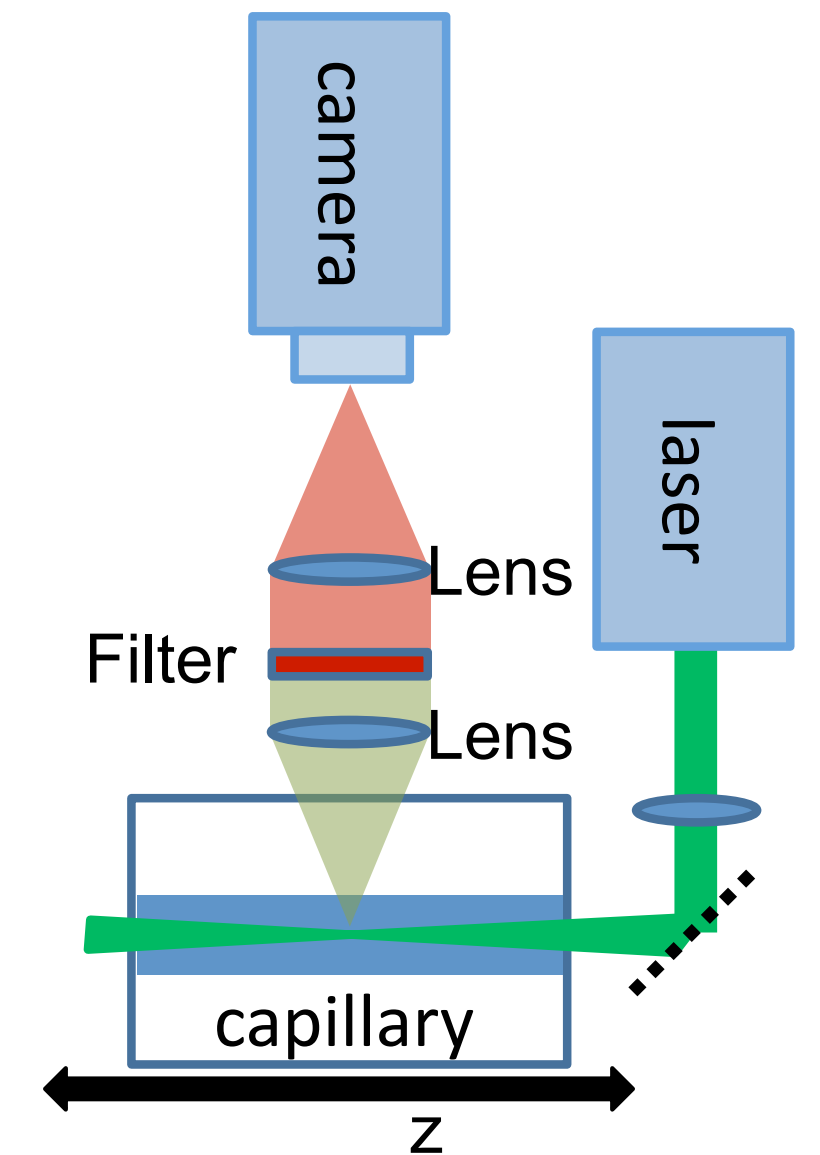
- > Scattering of (laser) light on bound electrons (gas, plasma) can be used as density diagnostic

## Elastic scattering (Rayleigh)

leaves species in same quantum state  
scattered photons of same energy

## Inelastic scattering (Raman)

changes the quantum state of the species  
energy difference excitation to emission



- > Rayleigh scattering allows in principle for measuring densities, but scattering off plasma difficult to distinguish from scattering off walls (+ much more intense!)
- > Raman scattering photons at species specific wavelength → differentiation between scattering sources

# Raman scattering

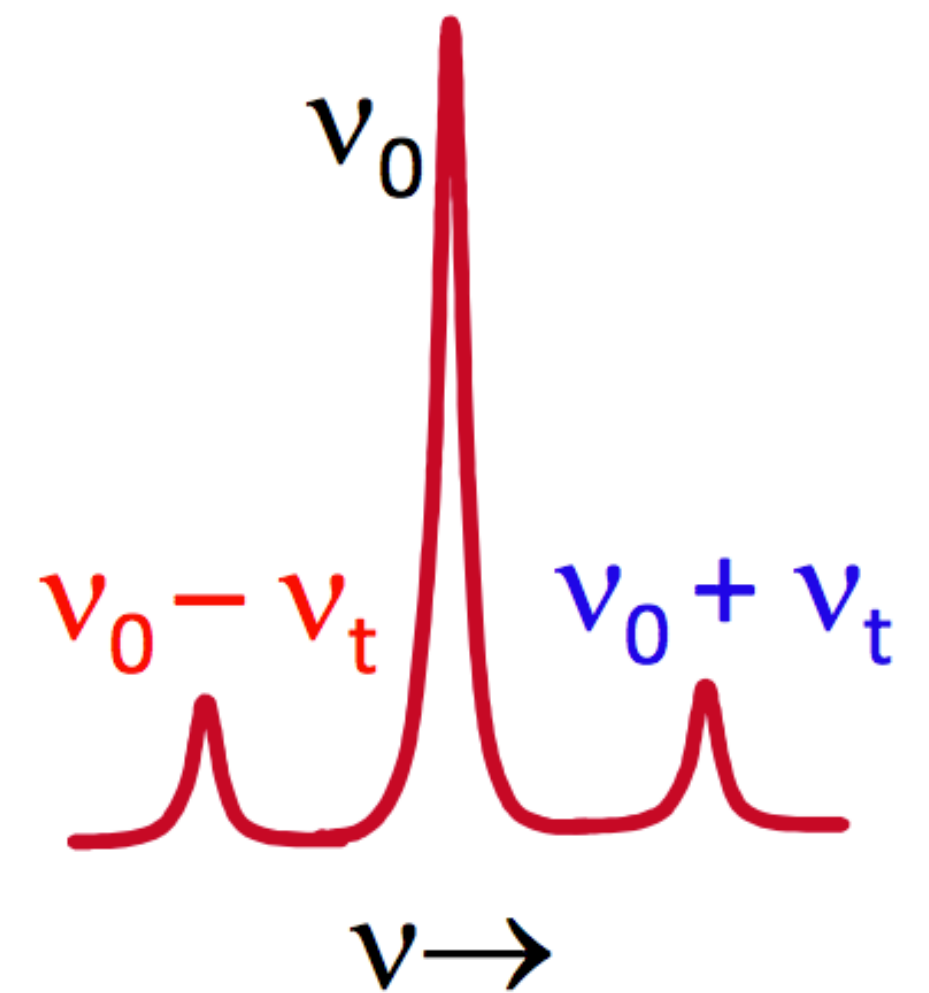
- > Inelastic process in which energy can be transferred to or from the scatterer
- > When energy is transferred to the scatterer: **Stokes lines**  $\nu_s = \nu_0 - \nu_t$
- > When energy is transferred from the scatterer: **Anti-Stokes lines**  $\nu_{as} = \nu_0 + \nu_t$
- > Raman scattering cross section larger than Rayleigh scattering cross section

$$I_{Raman} = I_0 \frac{\partial \sigma}{\partial \Omega} n \Omega_{eff}$$

$\Omega_{eff}$ : Optics and detector efficiency

T. Weineisen *et al.*, Phys. Rev. ST Accel. Beams **14**, 050705 (2011)

- > Rotational and vibrational Raman scattering modes exist
- > Upper state can be virtual or real electronic transition (resonance Raman spectroscopy)

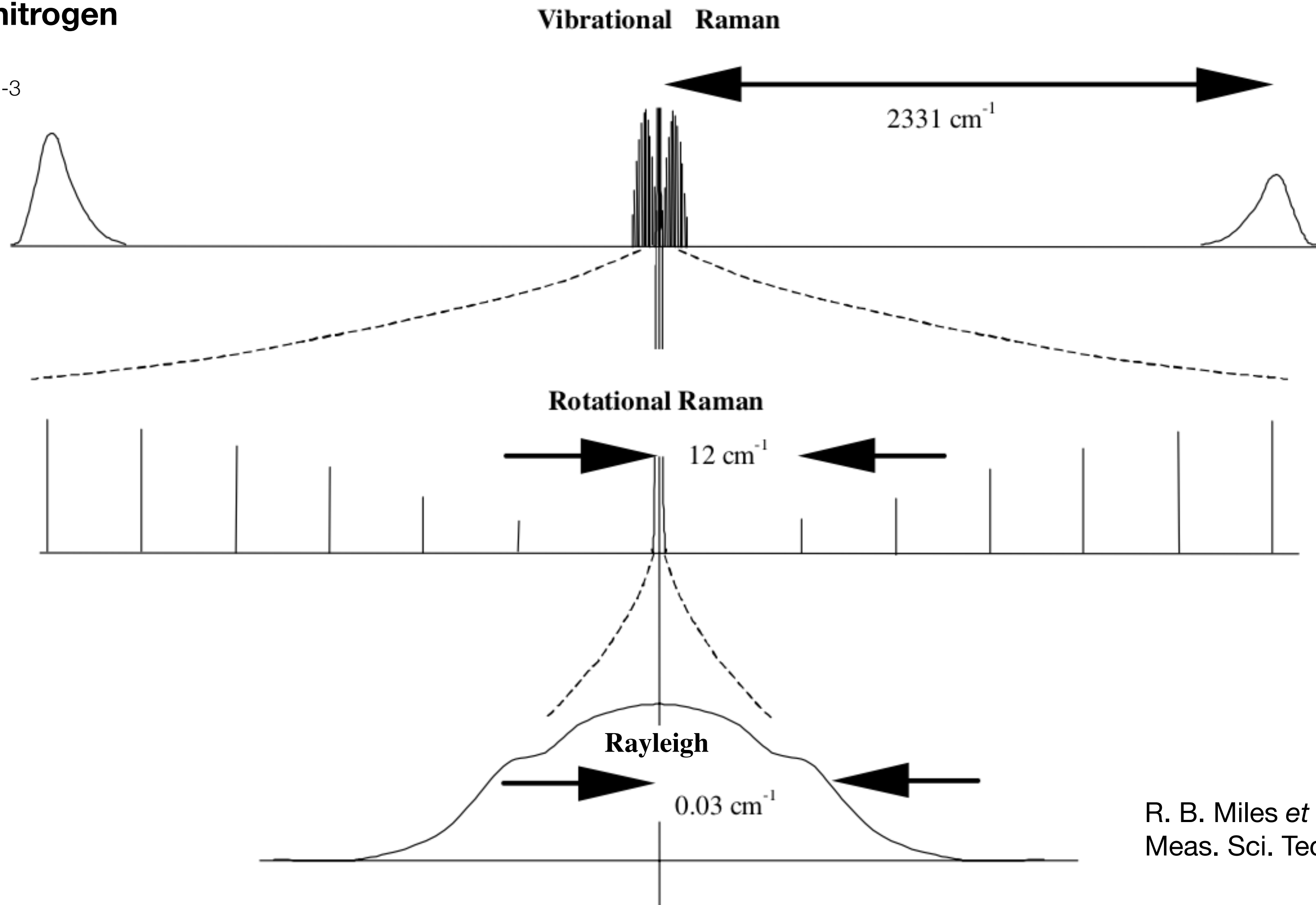


# Raman scattering

## Molecular nitrogen

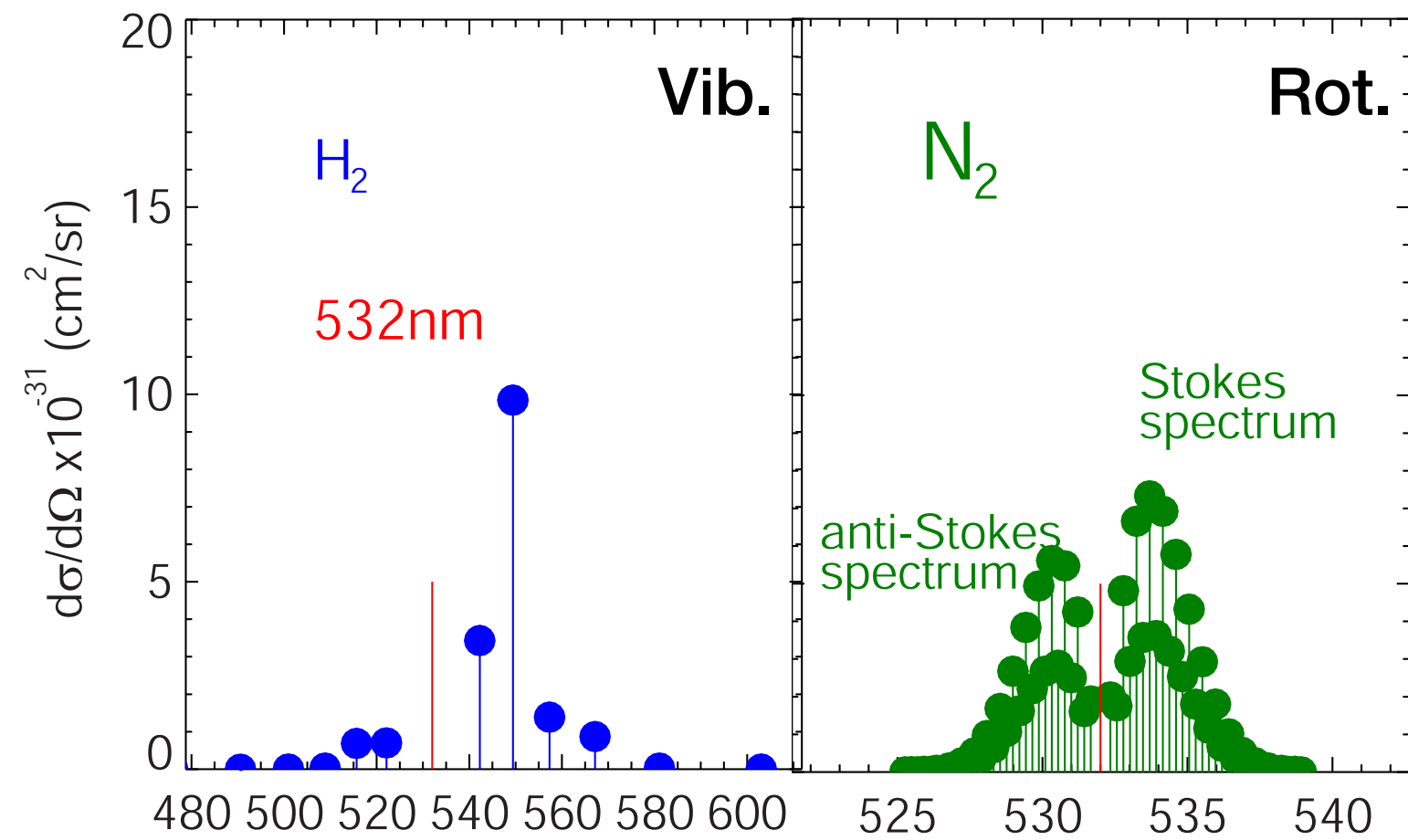
$T = 300\text{K}$

$n = 10^{25}\text{ m}^{-3}$



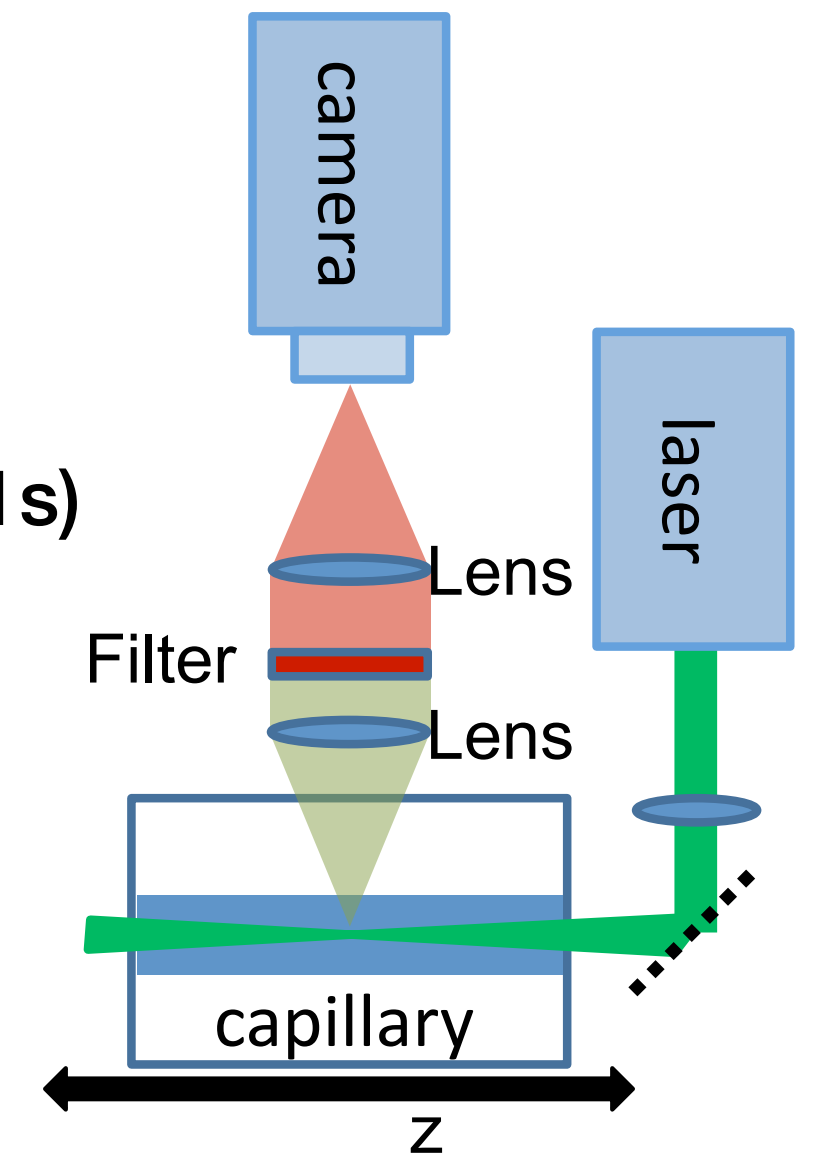
R. B. Miles *et al.*,  
Meas. Sci. Technol. **12**, R33-R51 (2001)

# Raman scattering

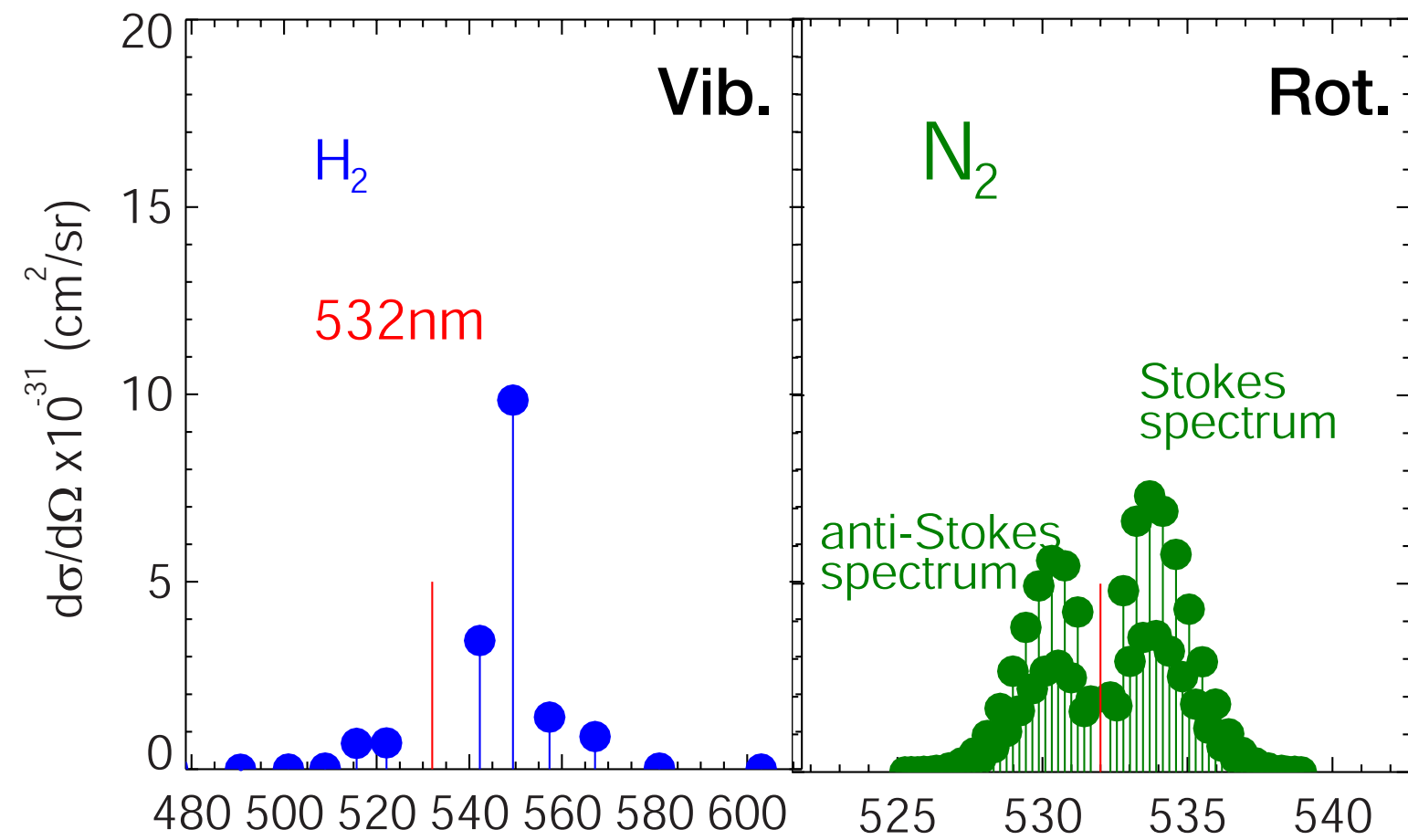


- > Weak signals require long interaction times ( $\sim 1\text{ s}$ )
- > Raman scattering allows for species discrimination
- > Raman scattering only works for molecules, no atoms

R. Scannell *et al.*,  
Rev. Sci. Instrum. **81**, 045107 (2010)

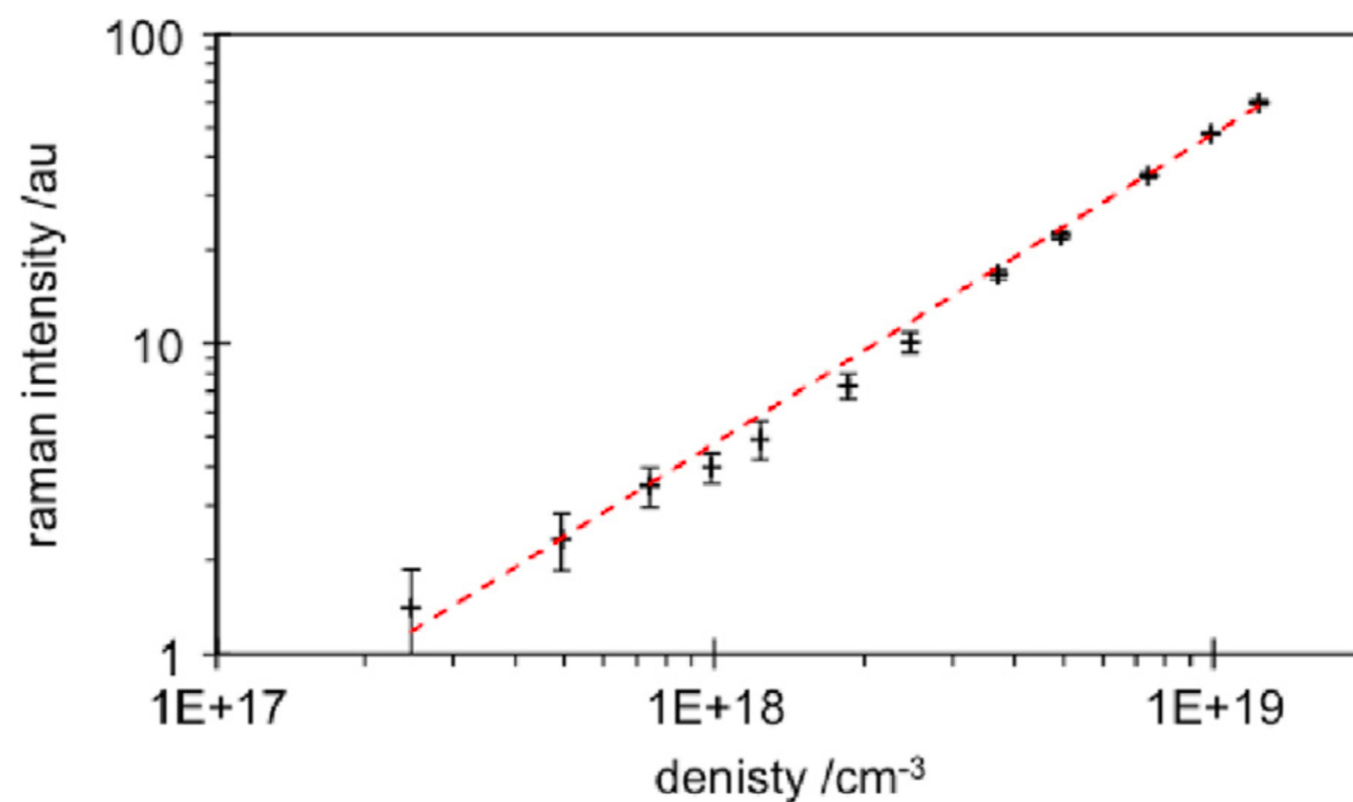
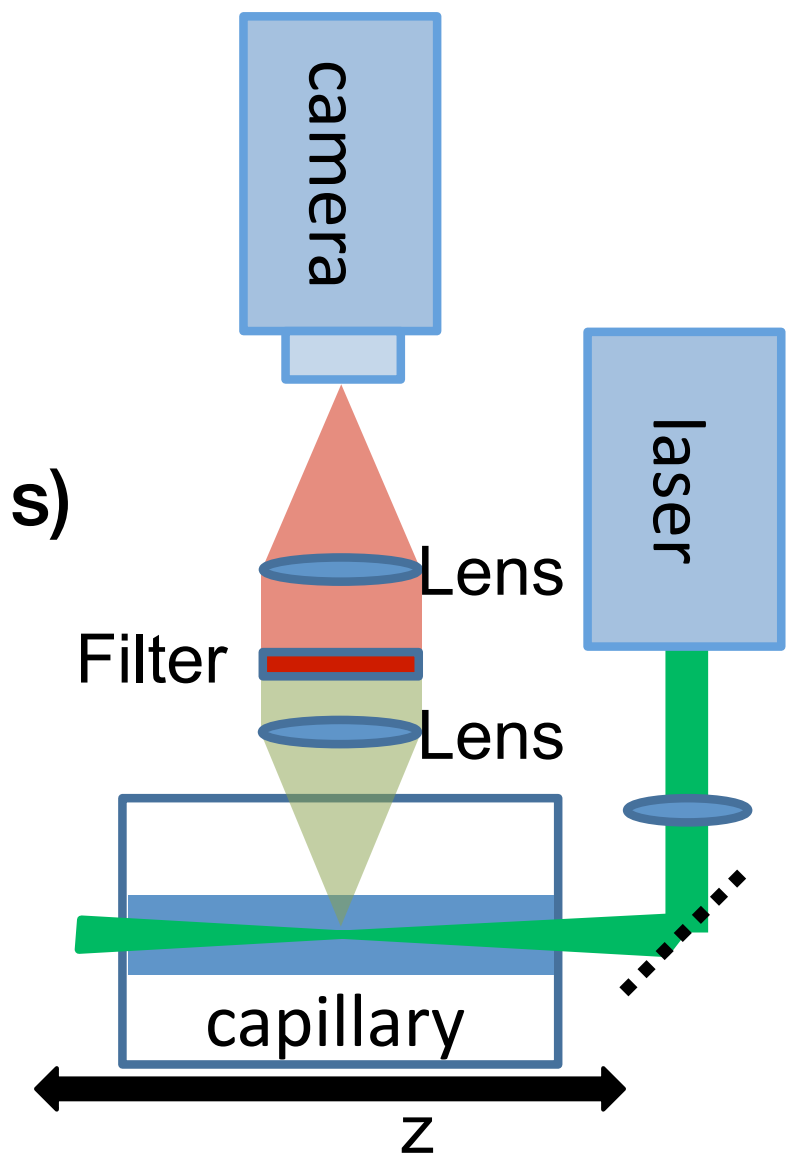


# Raman scattering



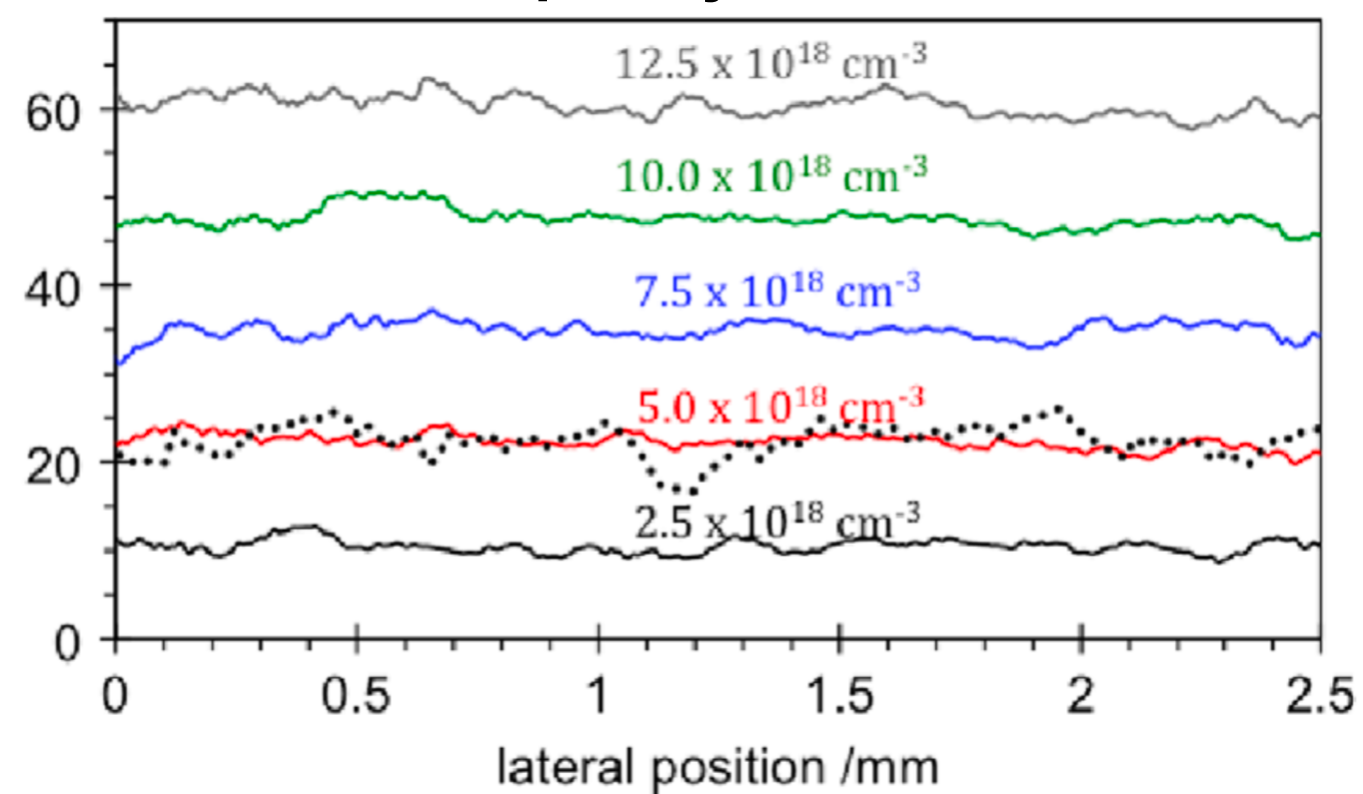
- > Weak signals require long interaction times (~ 1s)
- > Raman scattering allows for species discrimination
- > Raman scattering only works for molecules, no atoms

R. Scannell *et al.*,  
Rev. Sci. Instrum. **81**, 045107 (2010)

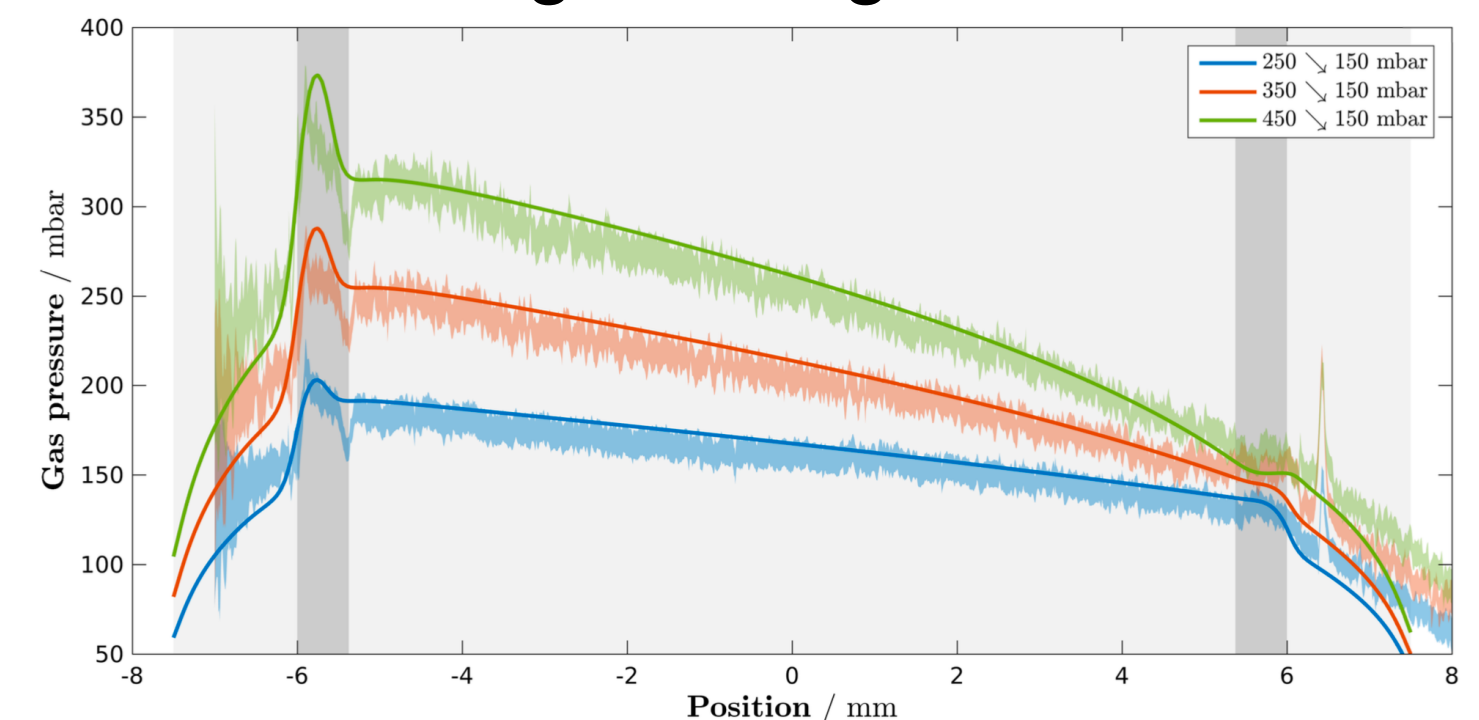


L. Schaper *et al.*, NIM A **740**, 208 (2014)

## Capillary center



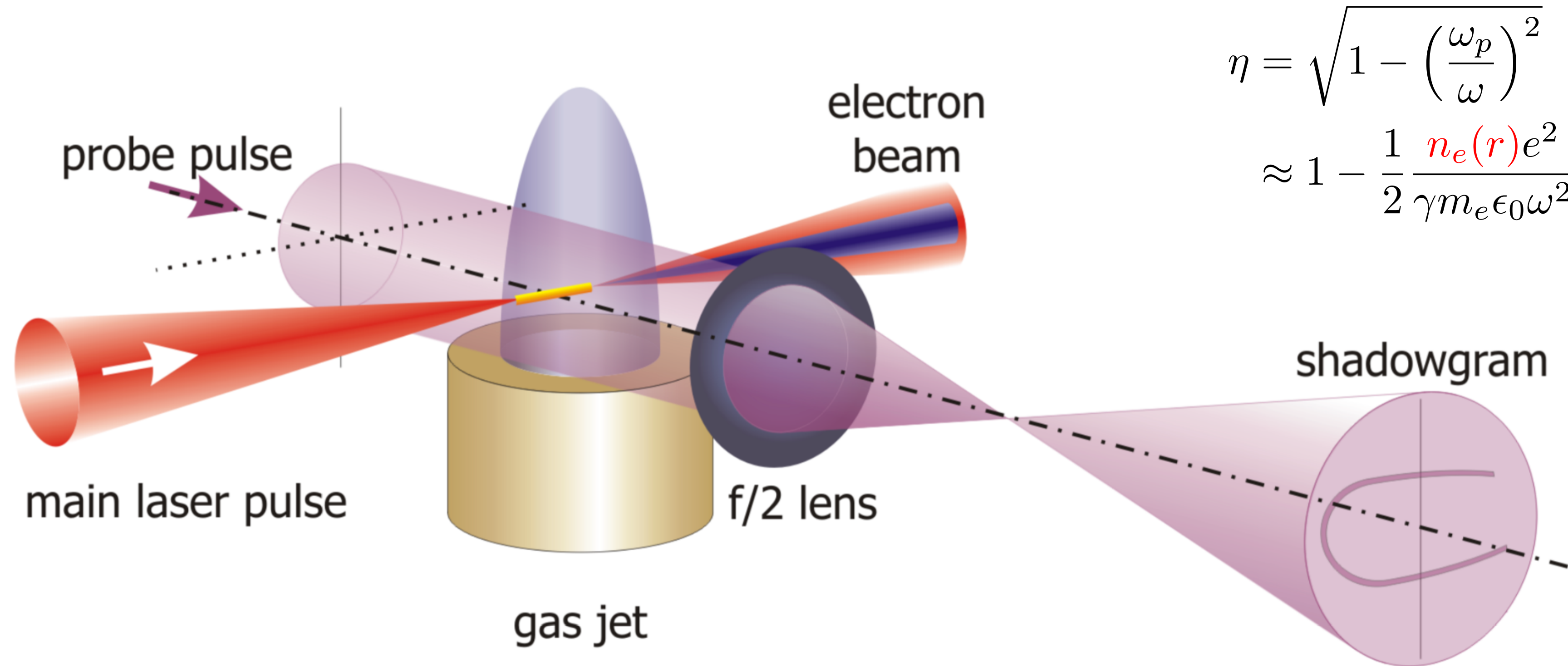
## Longitudinal gradients



# **Plasma density distribution and constituents**

- Schlieren/dark-field imaging
- Laser interferometry
- Two-color phase delay spectral interferometry
- Plasma spectroscopy

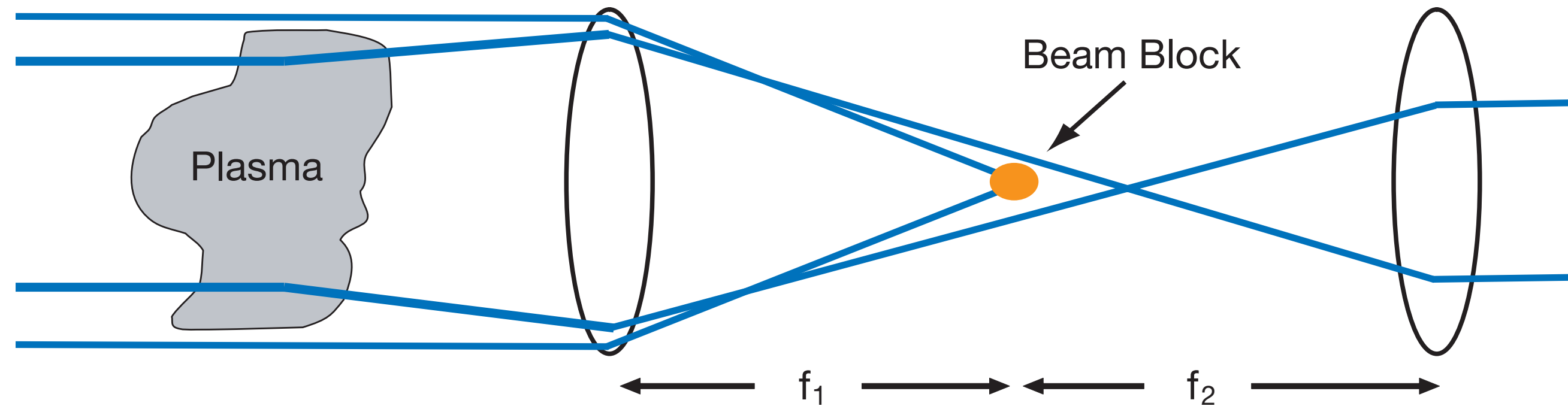
# Schlieren/dark-field imaging or shadowgraphy



$$\eta = \sqrt{1 - \left(\frac{\omega_p}{\omega}\right)^2}$$
$$\approx 1 - \frac{1}{2} \frac{n_e(r) e^2}{\gamma m_e \epsilon_0 \omega^2}$$

- > Index of refraction gradients cause distortion of probe phase front  
→ intensity structures in beam

# Schlieren/dark-field imaging or shadowgraphy



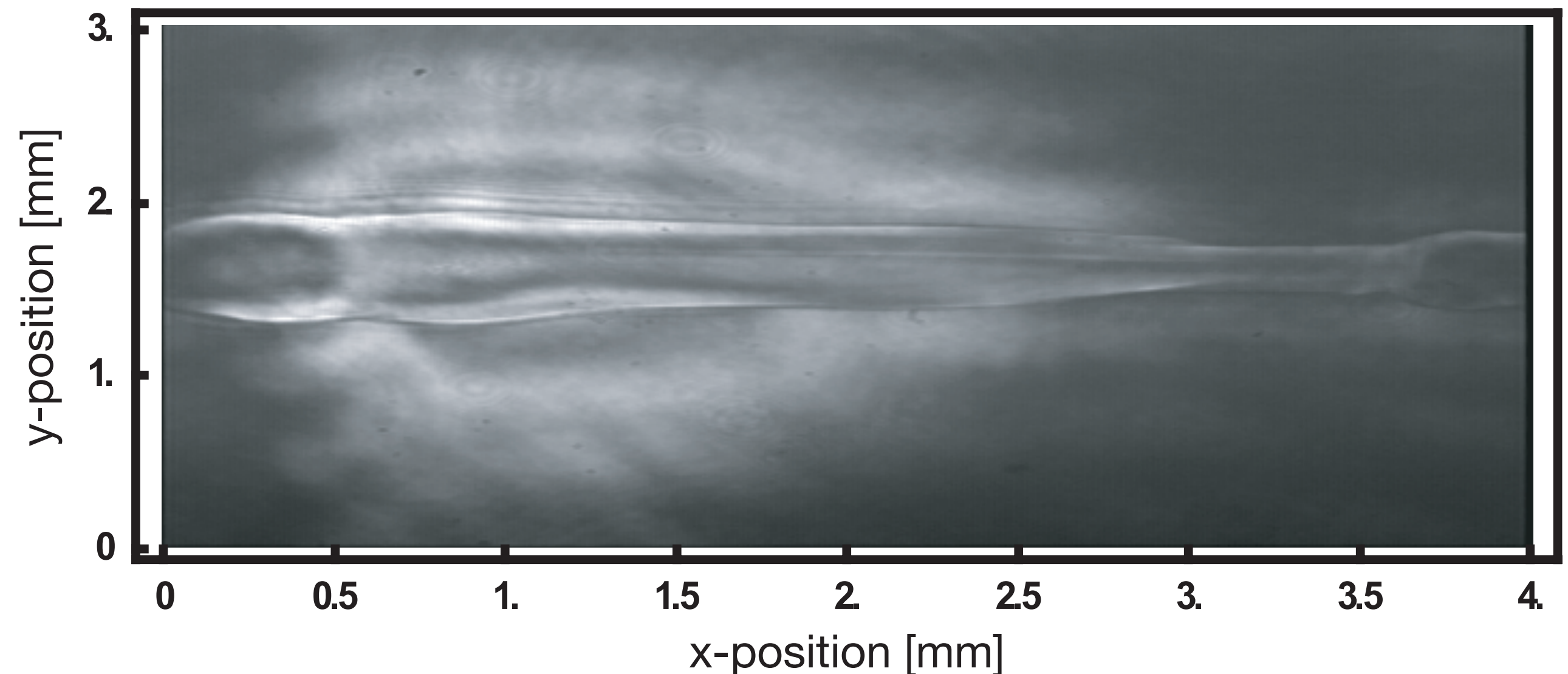
$$\eta = \sqrt{1 - \left(\frac{\omega_p}{\omega}\right)^2}$$

$$\approx 1 - \frac{1}{2} \frac{n_e(r) e^2}{\gamma m_e \epsilon_0 \omega^2}$$

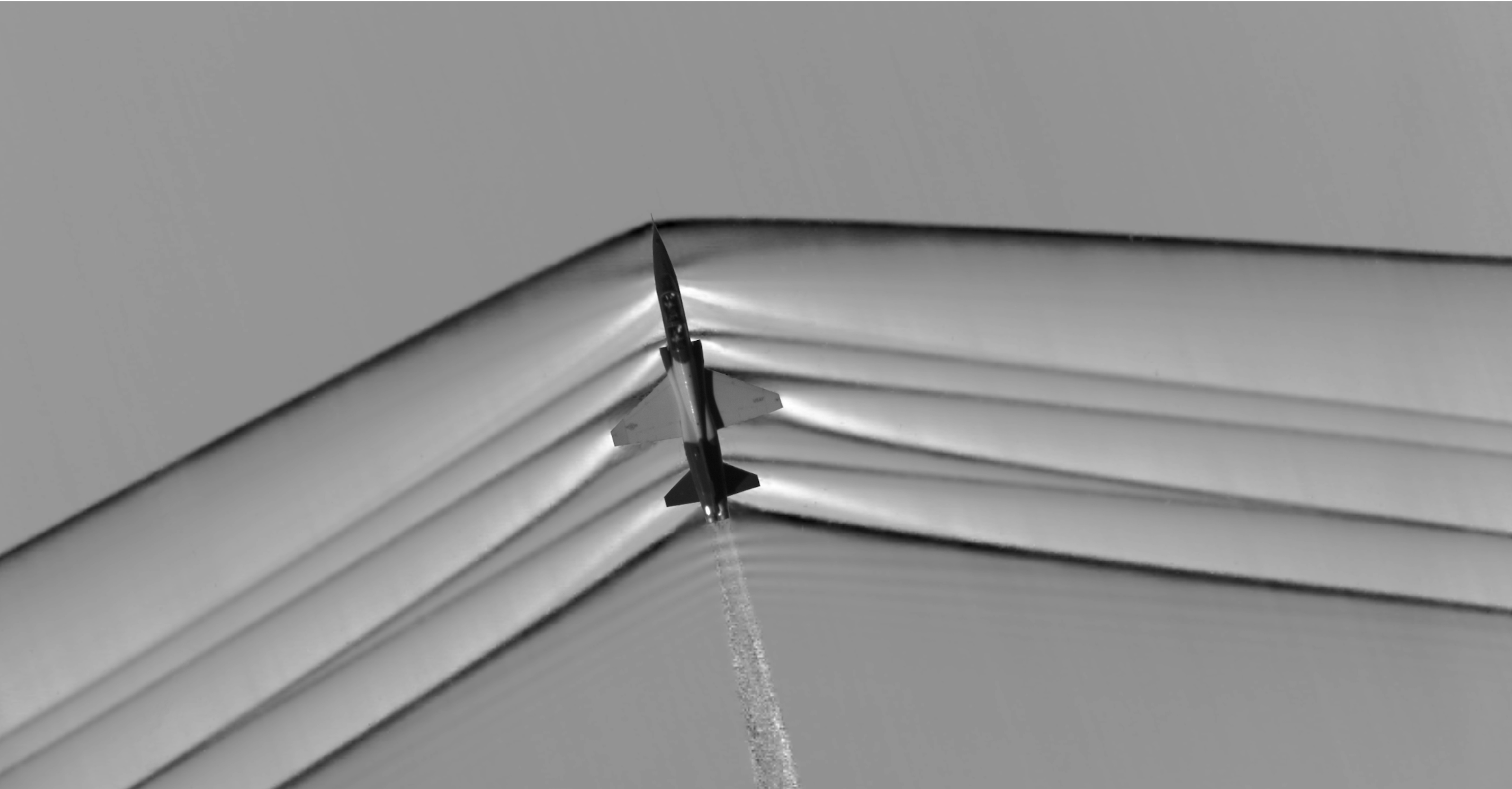
- > Angular deviation of ray

$$\epsilon_y = \frac{1}{n} \int \frac{\partial n}{\partial y} dz$$

- > Sensitive to density gradients
- > Absolute density measurements not straightforward

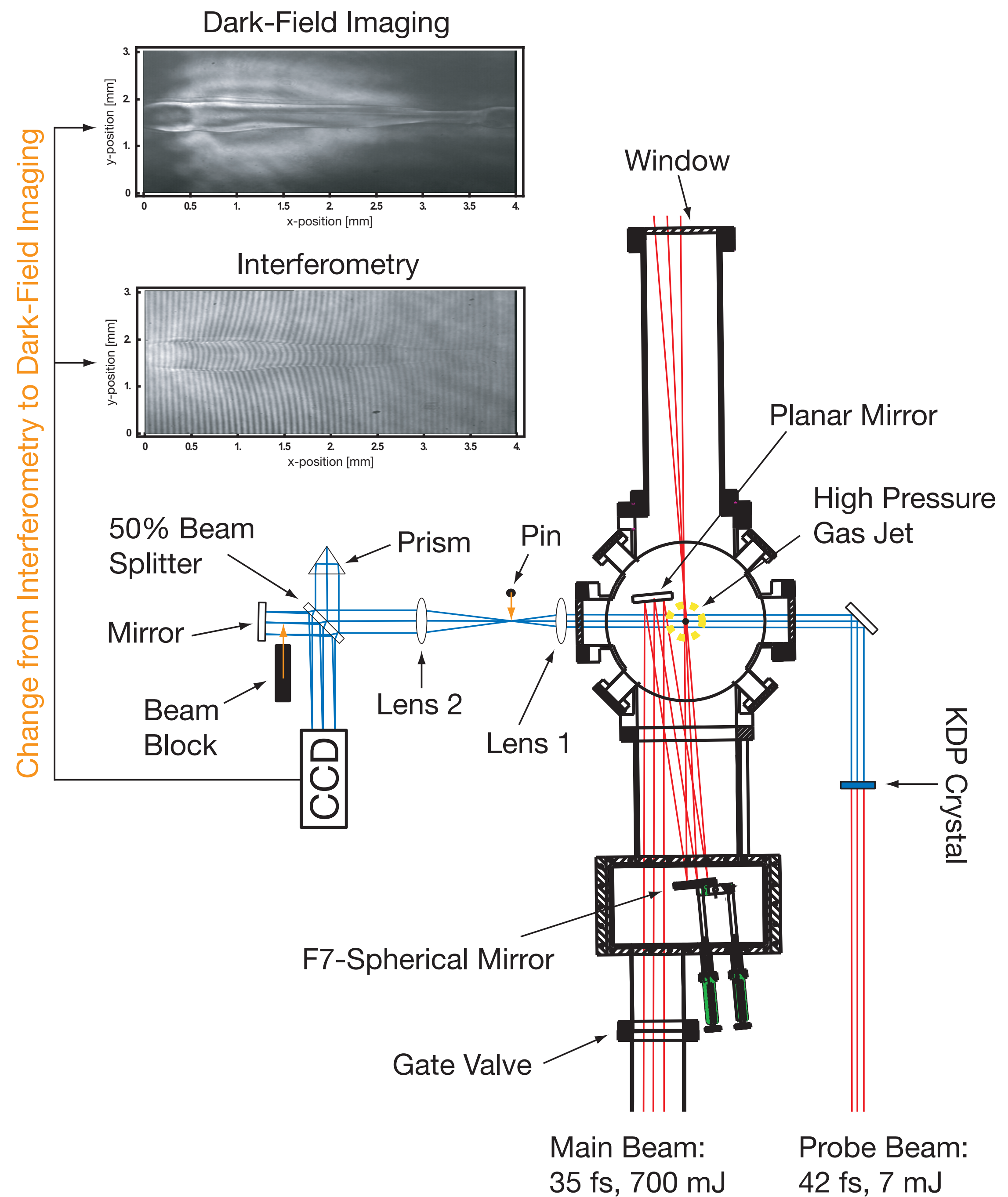


# Schlieren/dark-field imaging or shadowgraphy



# Laser interferometry

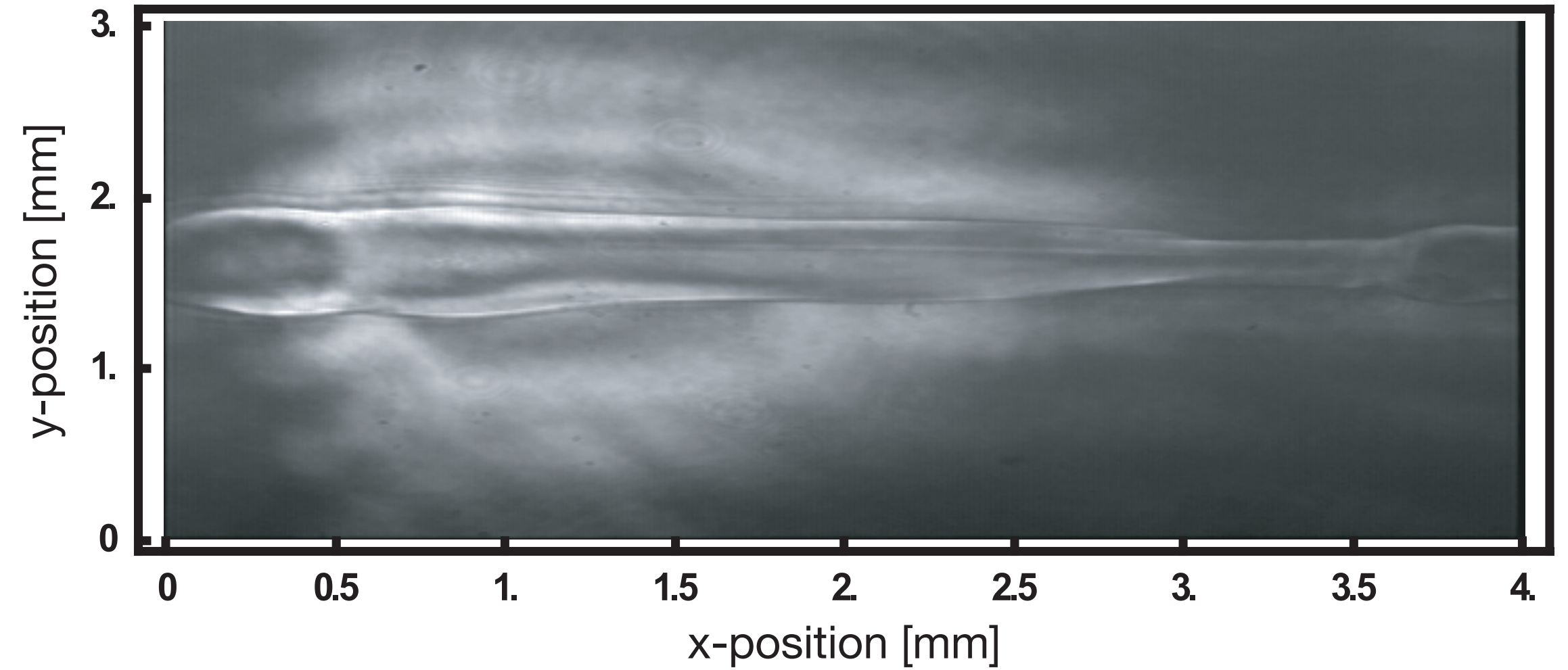
- > Laser interferometry allows for absolute density measurements
- > *Here:* setup compatible with dark-field imaging



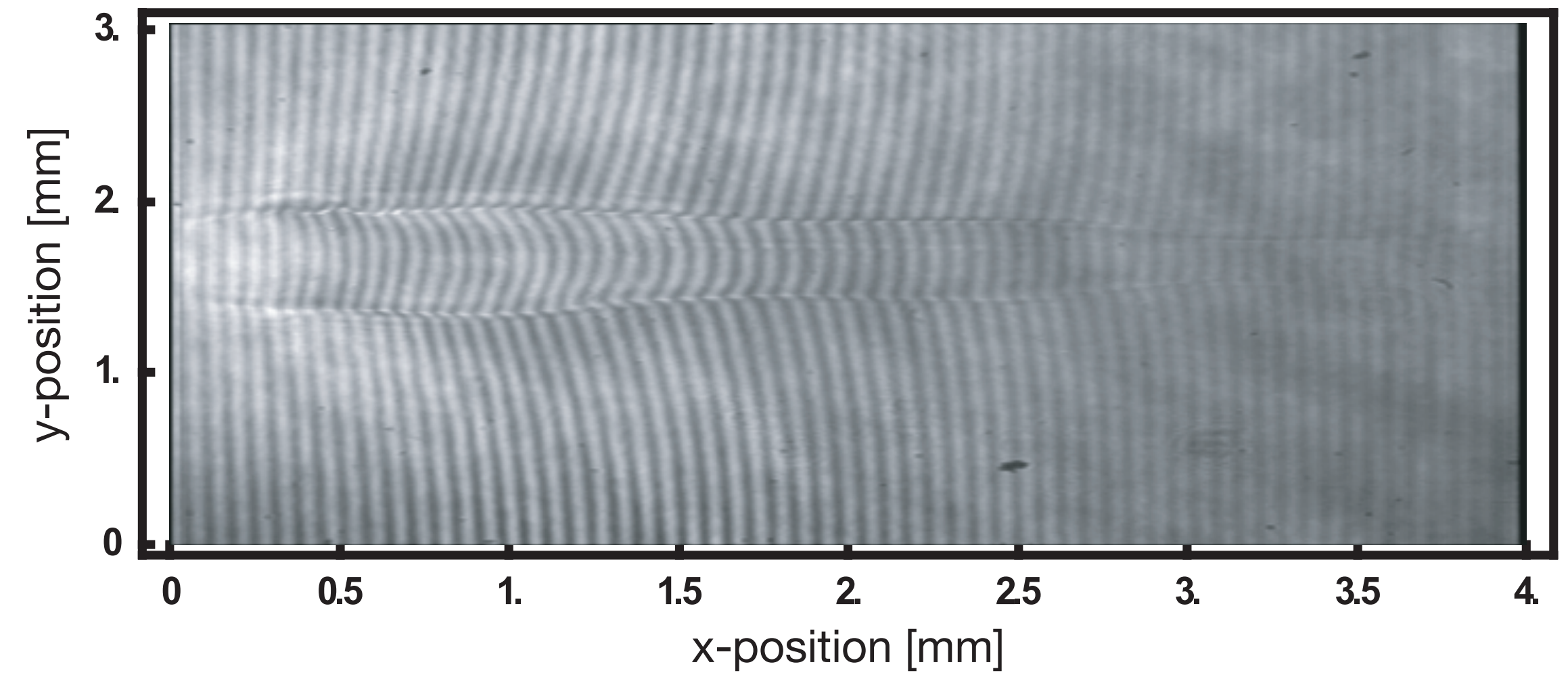
# Laser interferometry

- Laser interferometry allows for absolute density measurements

## Dark-Field Imaging

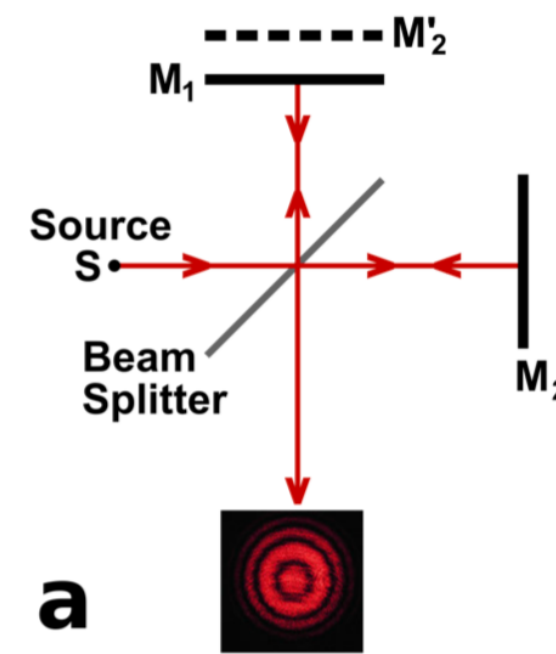
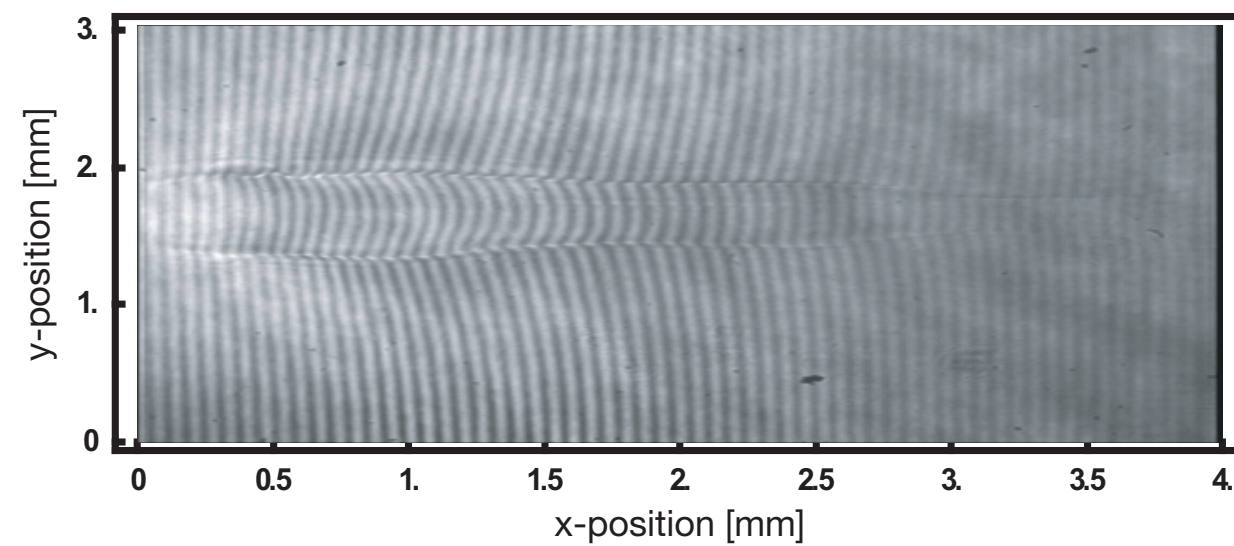


## Interferometry

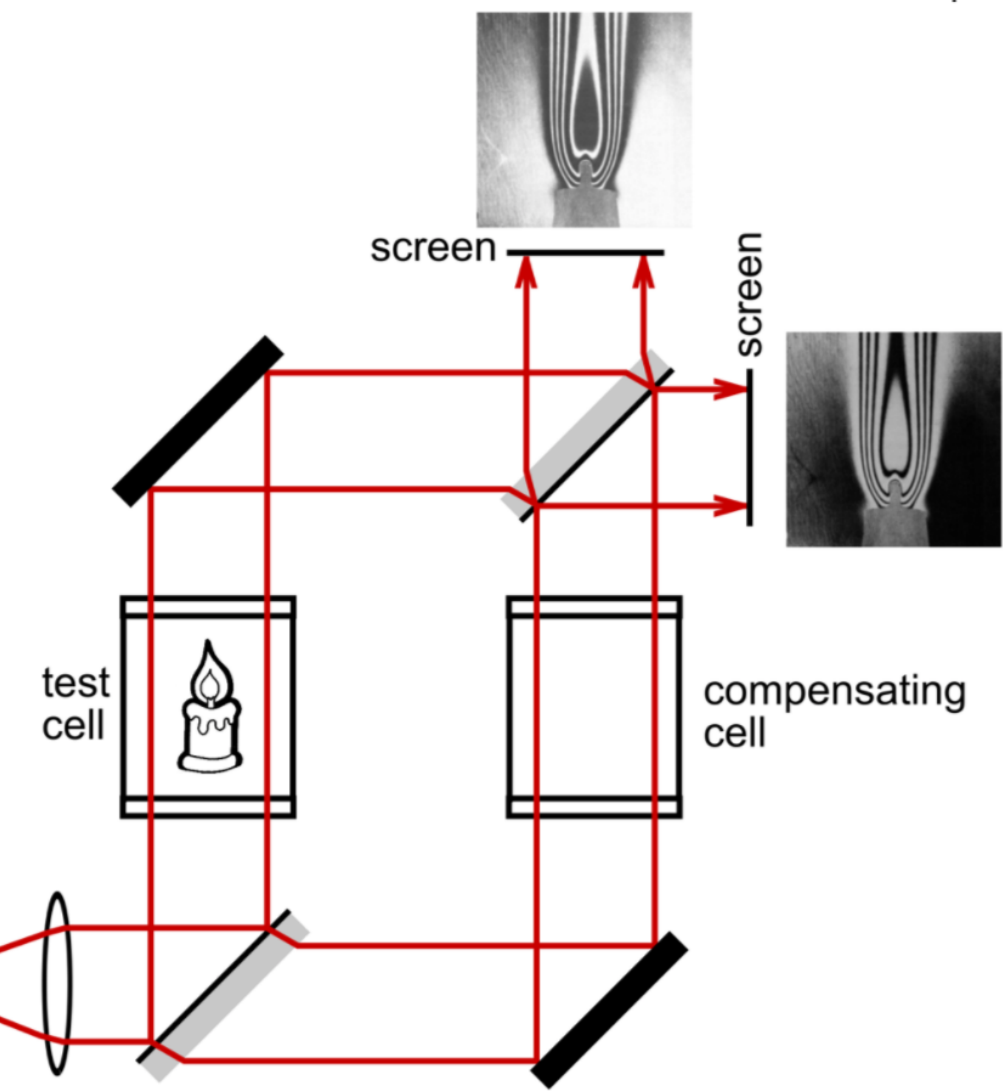
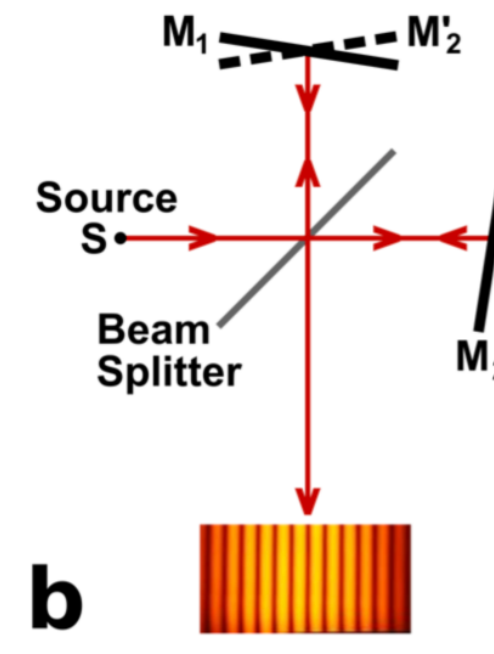


# Laser interferometry

- > Laser interferometry allows for absolute density measurements



*Michelson interferometer*

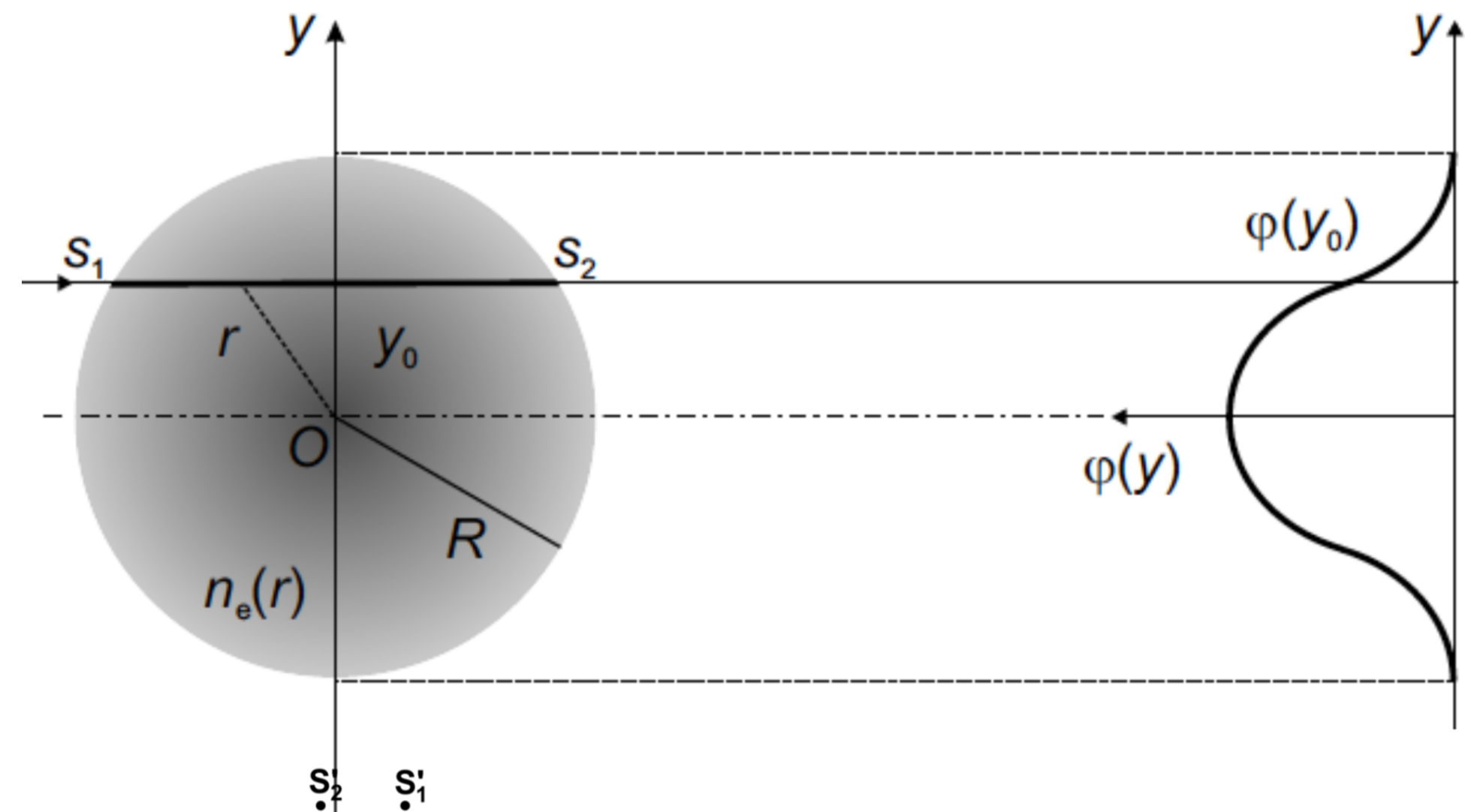


*Mach-Zehnder interferometer*

- > Integrated optical path length or phase  $\phi$  depends on integrated index of refraction

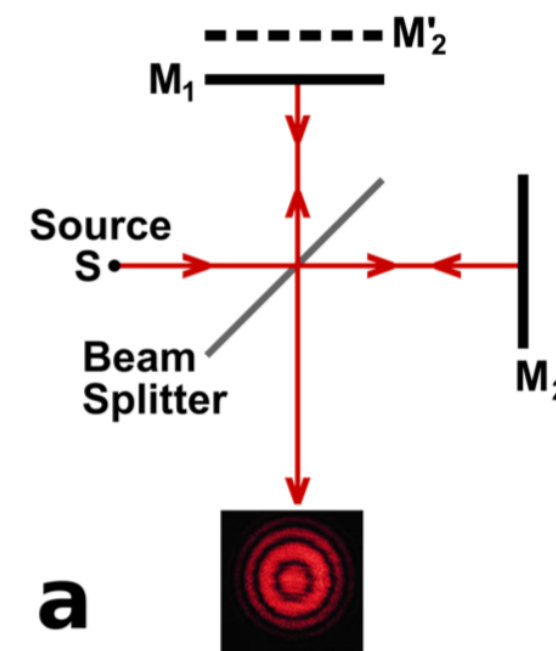
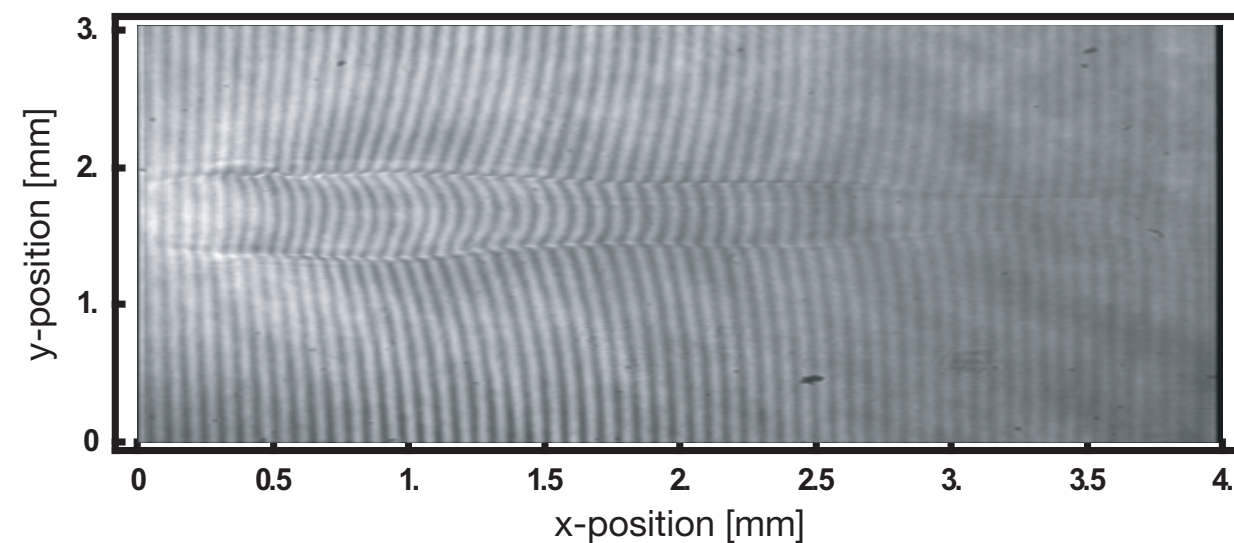
$$\eta = \sqrt{1 - (\omega_p/\omega_L)^2} = \sqrt{1 - n_e/n_c}$$

- > Visualize phase difference to unaffected reference by interference

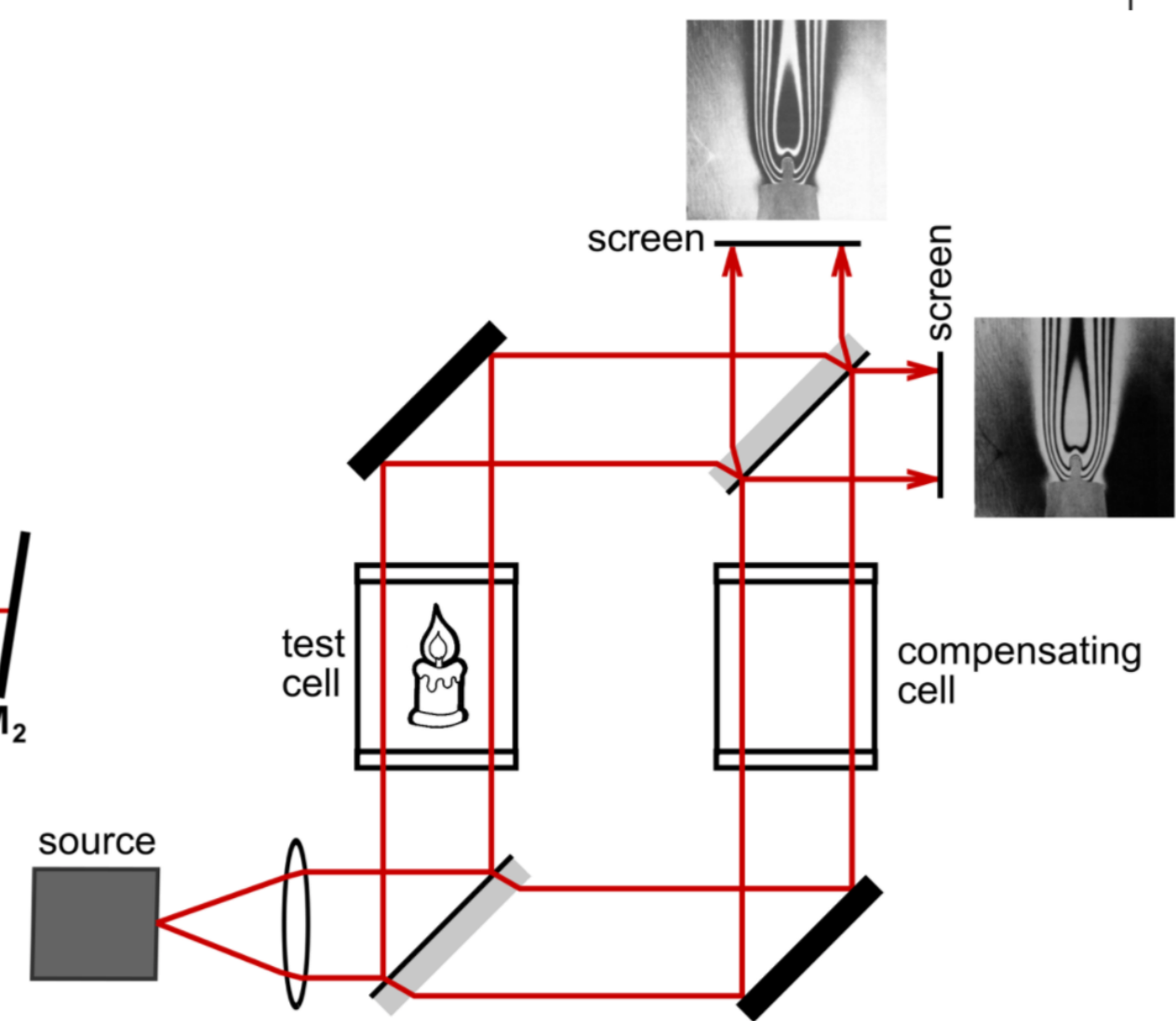
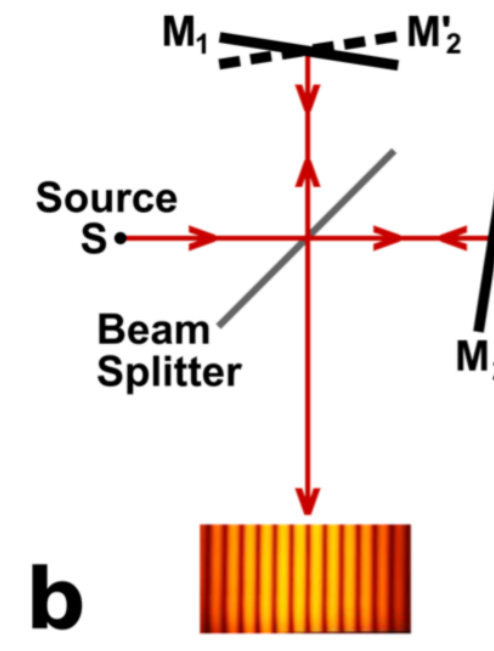


# Laser interferometry

- > Path lengths need to be within laser coherence length (typical  $\sim$  few  $\mu\text{m}$ ), otherwise no fringes

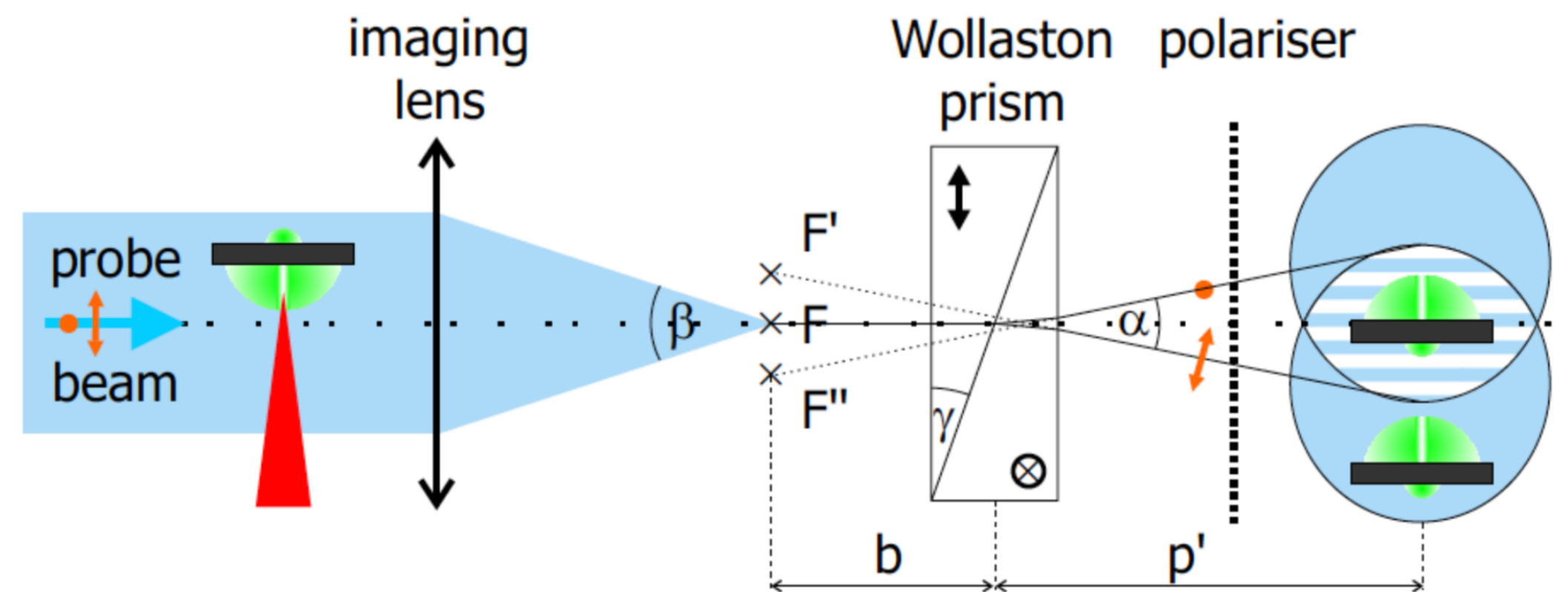


*Michelson interferometer*



*Mach-Zehnder interferometer*

- > Simple-to-align alternative: Wollaston prism (polarizing beam splitter, combination of two birefringent prisms)
- > Probe is polarized under  $45^\circ$  wrt optical axes
- > Two replica, separated by  $\alpha$ , polarized  $\perp$
- > Polarizer under  $45^\circ$ , so interference possible
- > Probe and reference sides overlapp

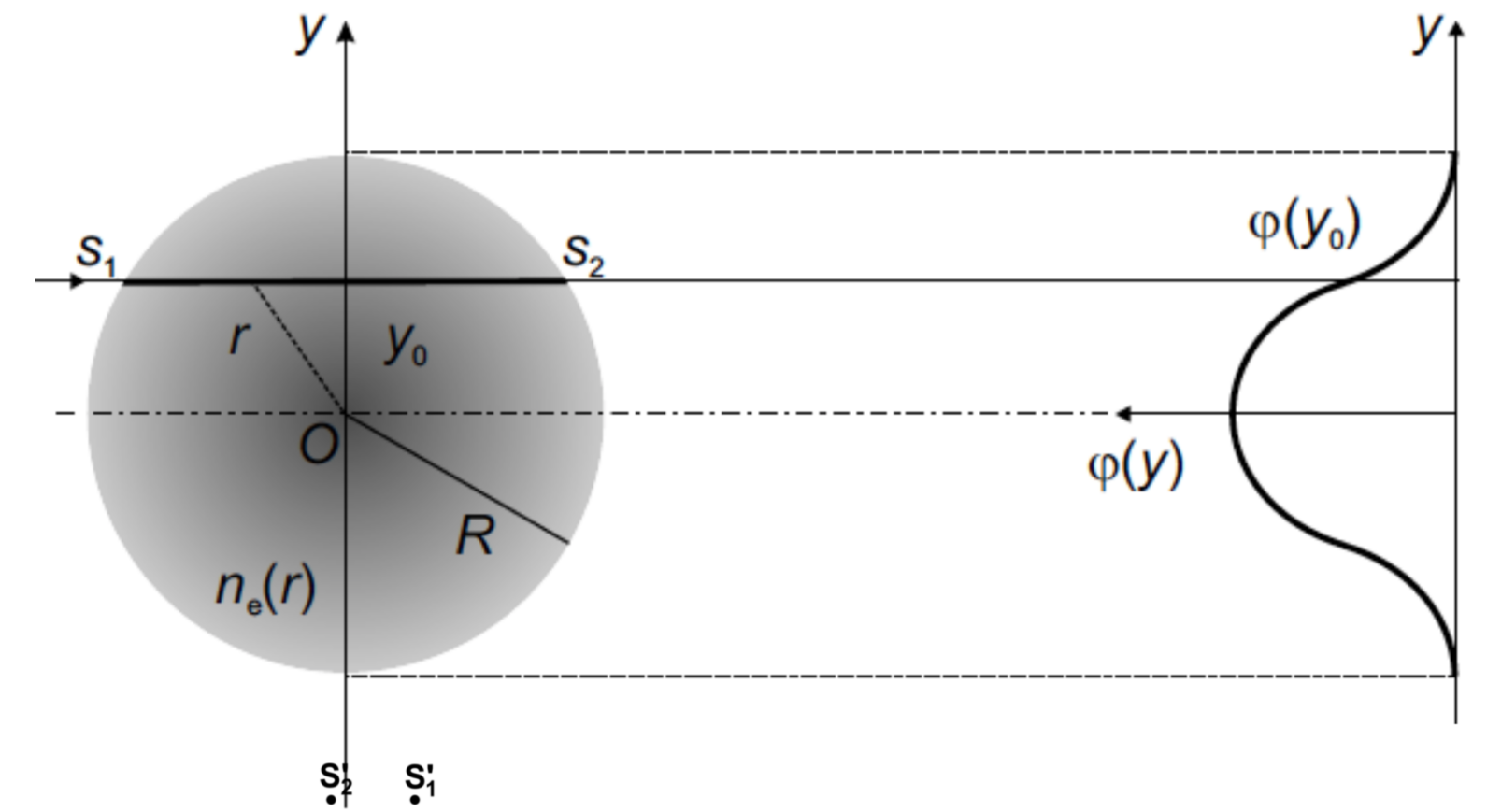


# Laser interferometry

- > Phase shift difference between probe and reference ray

$$\Delta\varphi(y_0) = \Phi(y_0) = \frac{2\pi}{\lambda_L} \int_{x_1}^{x_2} [1 - \eta(x)] dx$$

$$\approx \frac{\pi}{n_{cr}\lambda_L} \int_{x_1}^{x_2} n_e(x) dx = \frac{2\pi}{n_{cr}\lambda_L} \int_{y_0}^R \frac{n_e(r)r}{\sqrt{r^2 - y_0^2}} dr$$

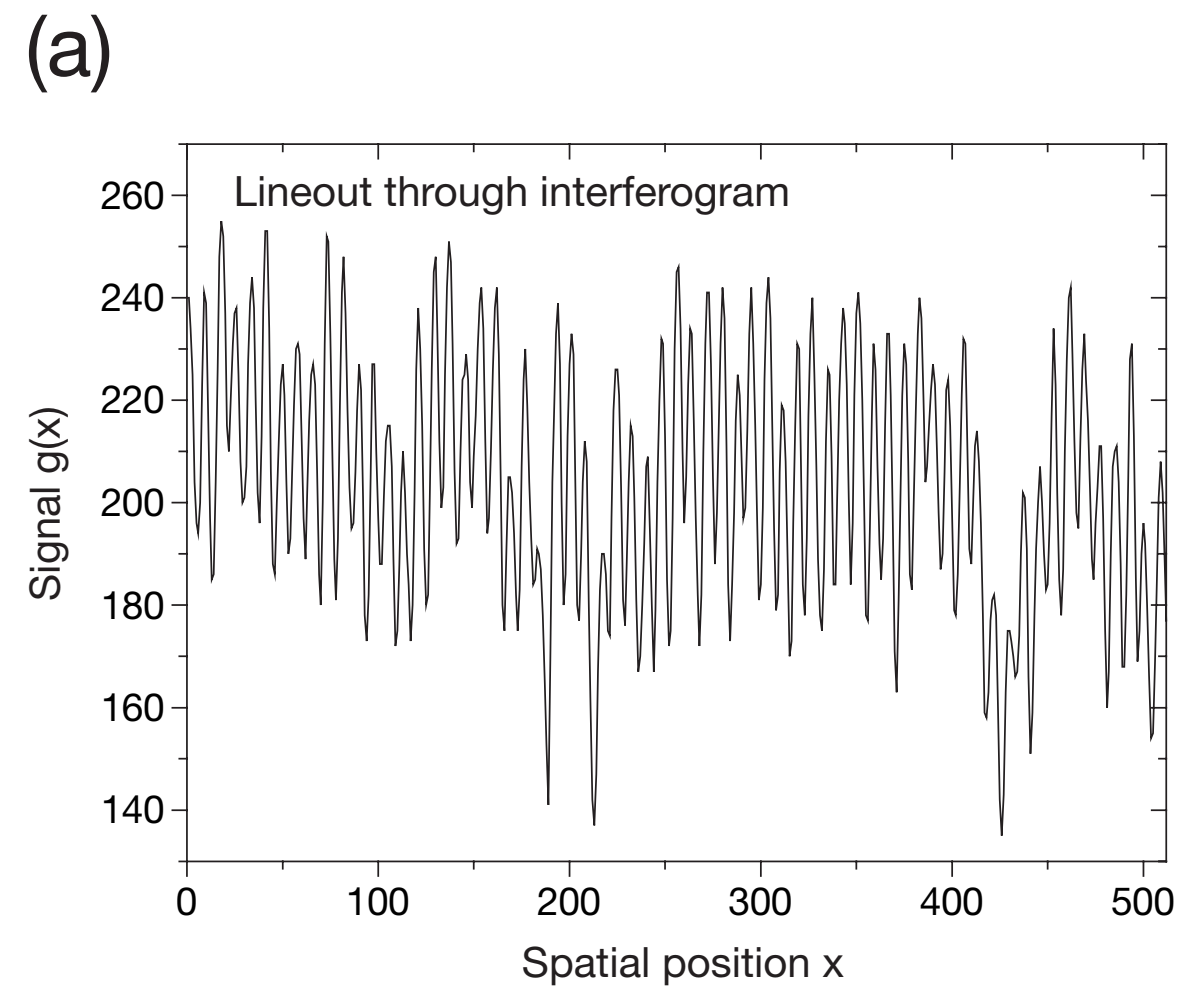


- > If cylindrical symmetry can be assumed → density reconstruction by Abel inversion (otherwise tomography)

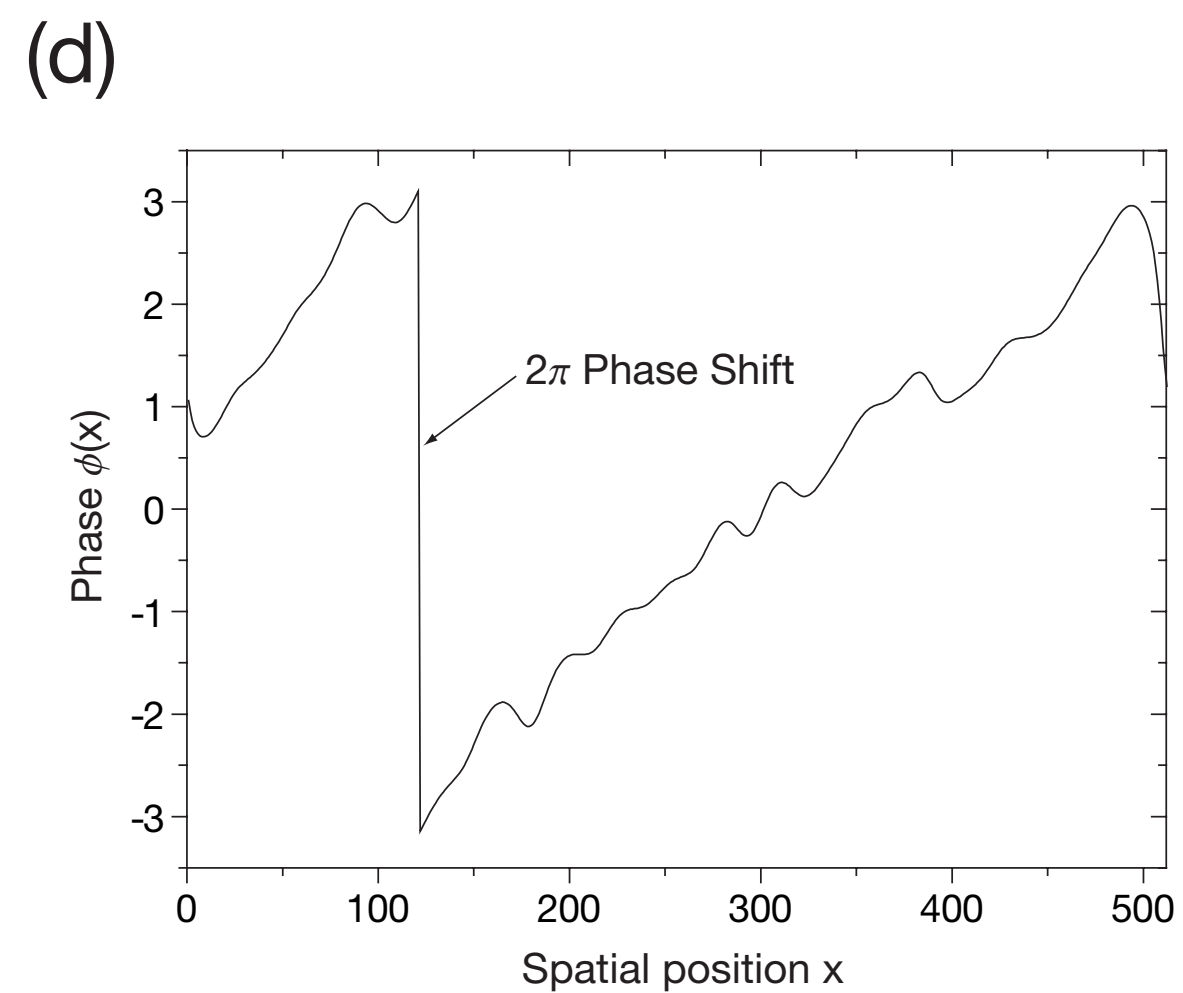
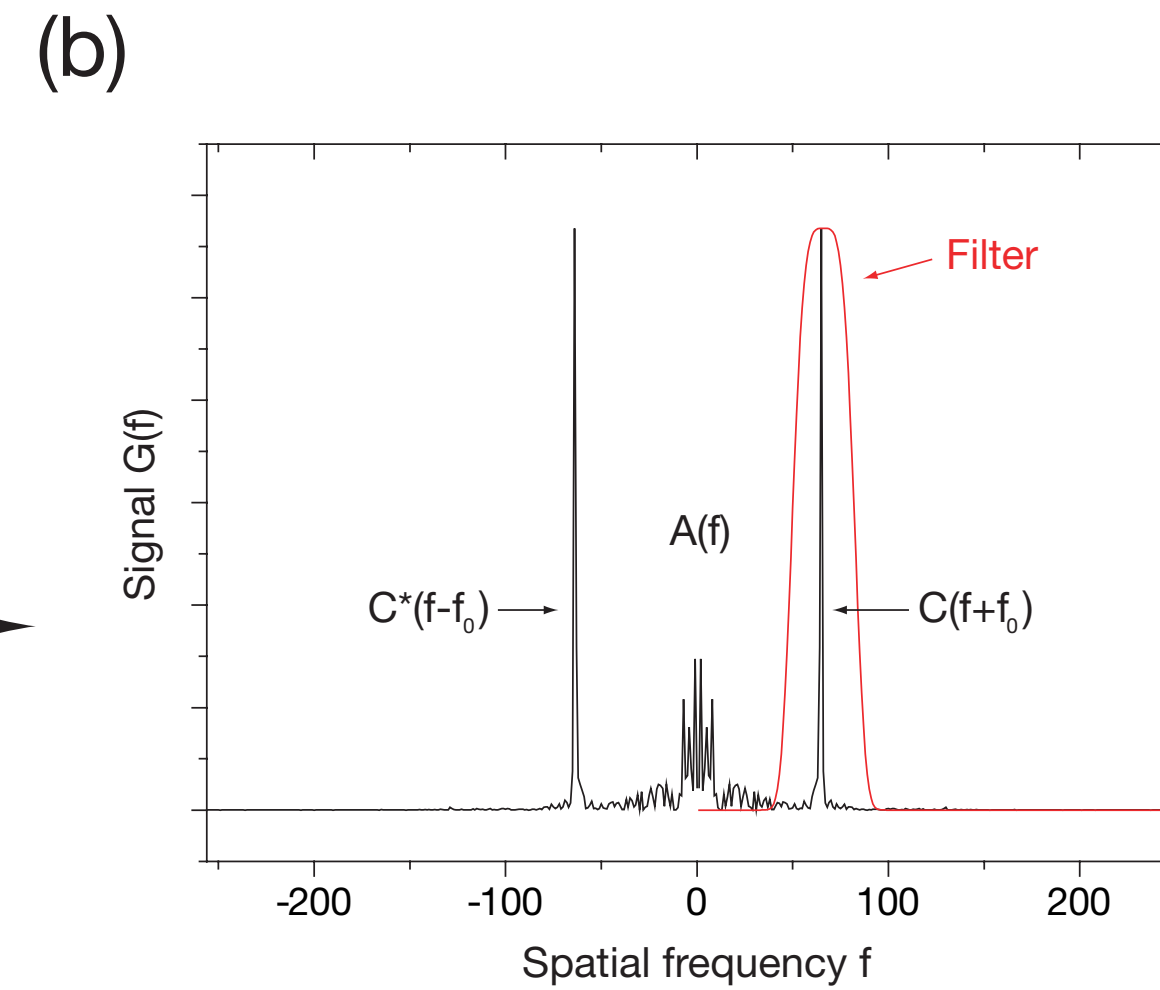
$$n_e(r) = -\frac{n_{cr}\lambda_L}{\pi^2} \int_r^R \frac{d\Phi(y)}{dy} \cdot \frac{dy}{\sqrt{y^2 - r^2}}$$

- > *Important:* Phase shift needs to be measurable, i.e.  $\lambda_L$  needs to see significant phase shift, not too far away from critical density  $n_{cr}$  or long plasma
- > *In practice:* densities below  $10^{18} \text{ cm}^{-3}$  difficult to diagnose in transverse geometry with  $1 \mu\text{m}$  lasers

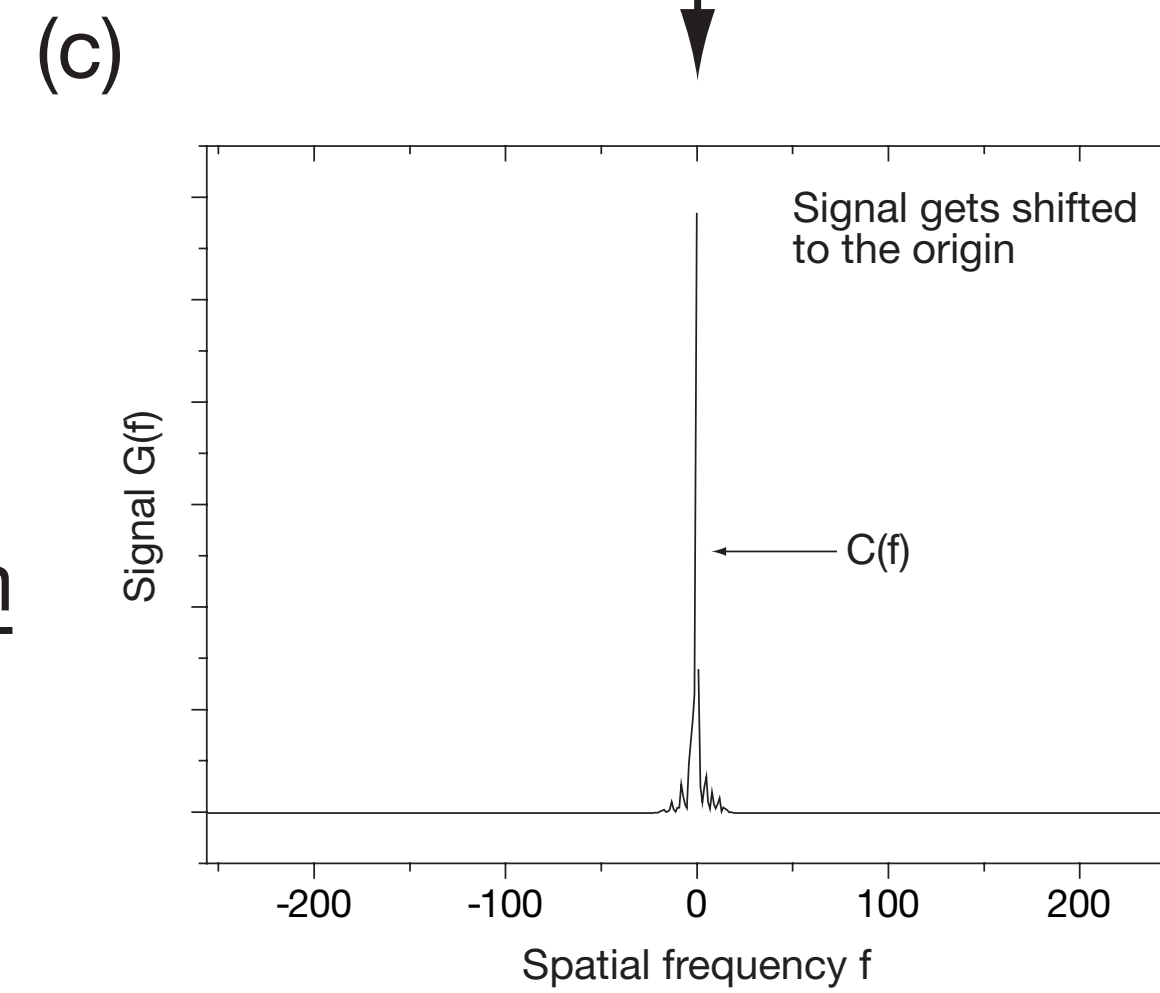
# Laser interferometry



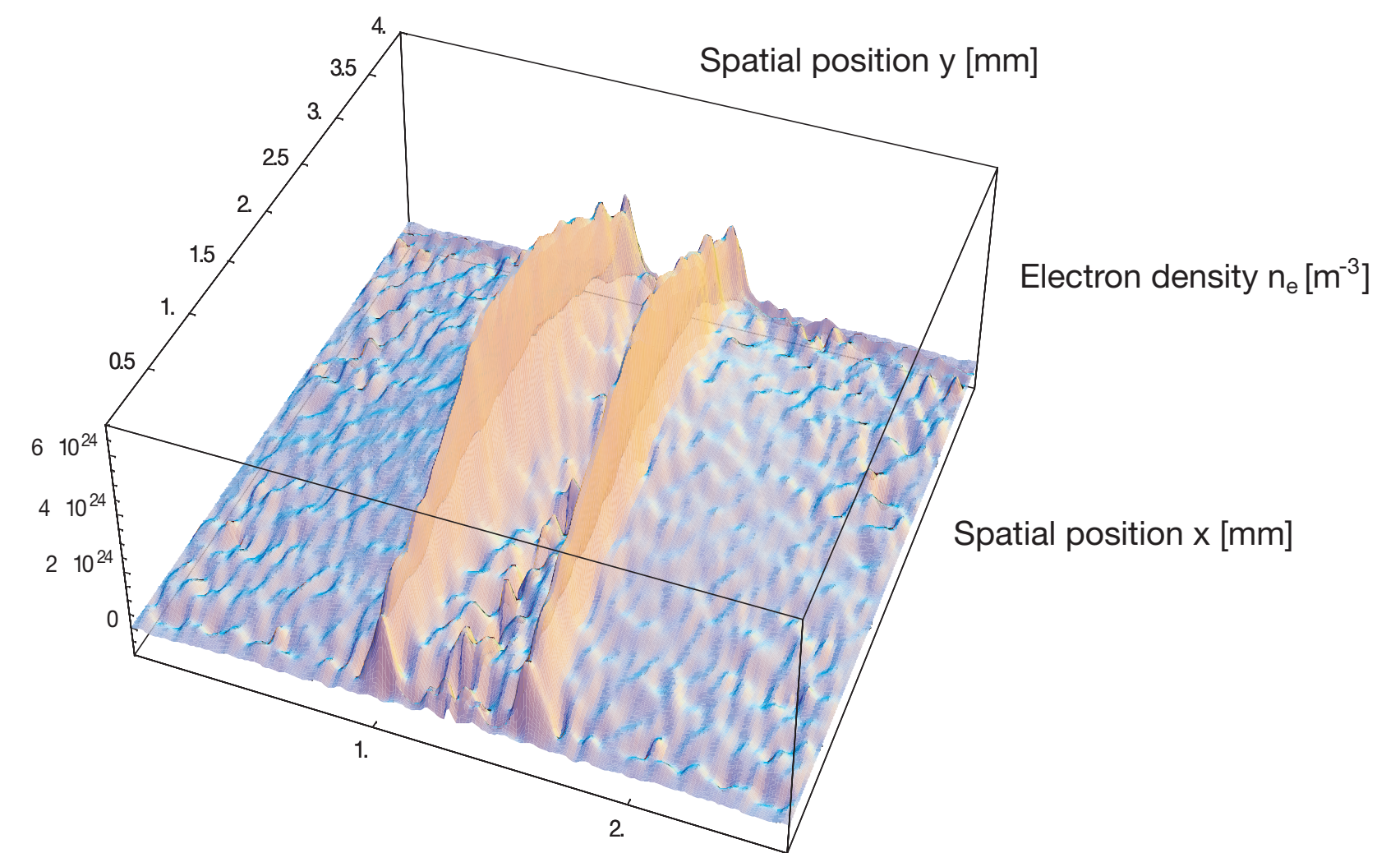
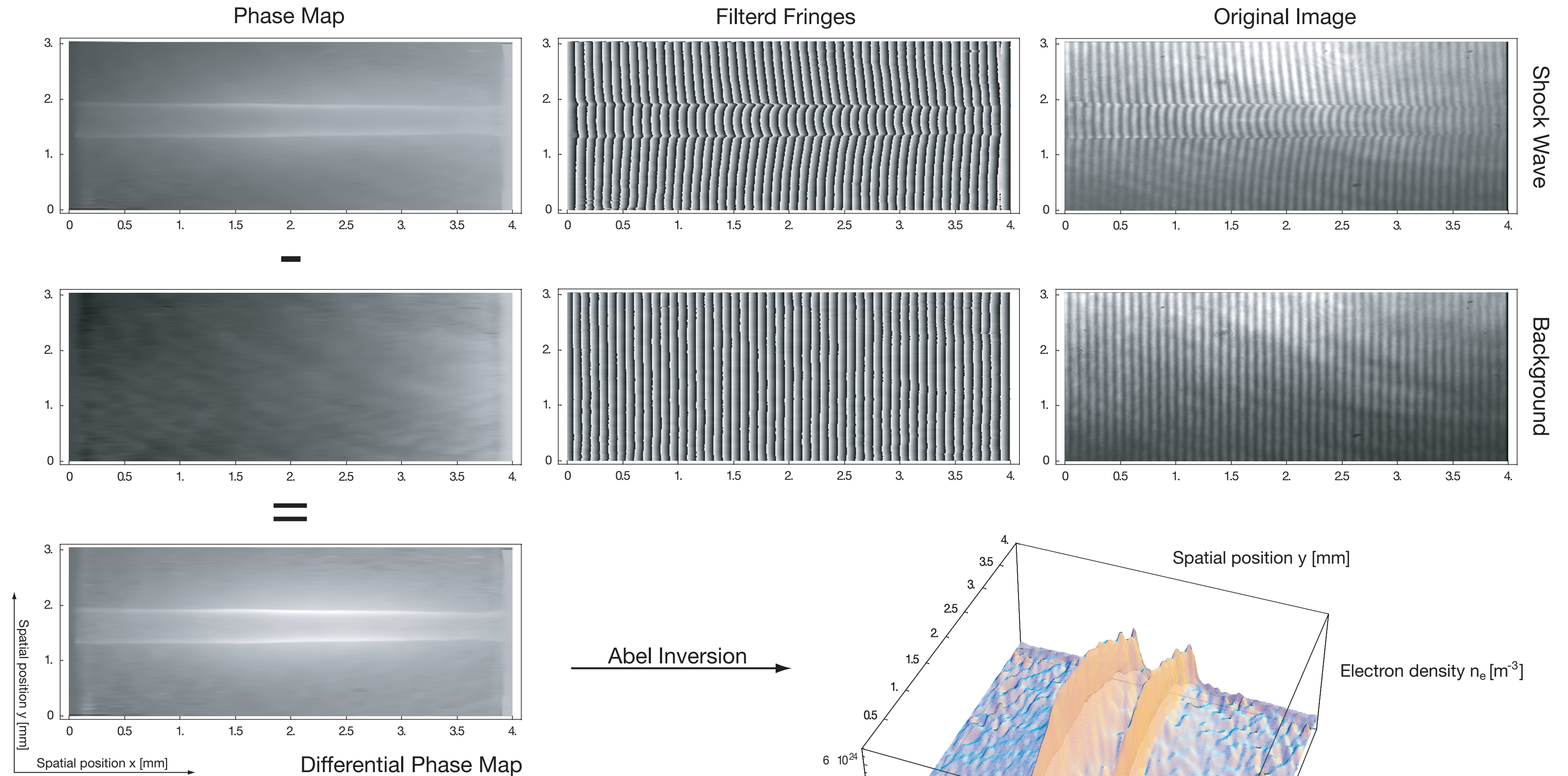
Fourier Transform



Inverse Fourier Transform

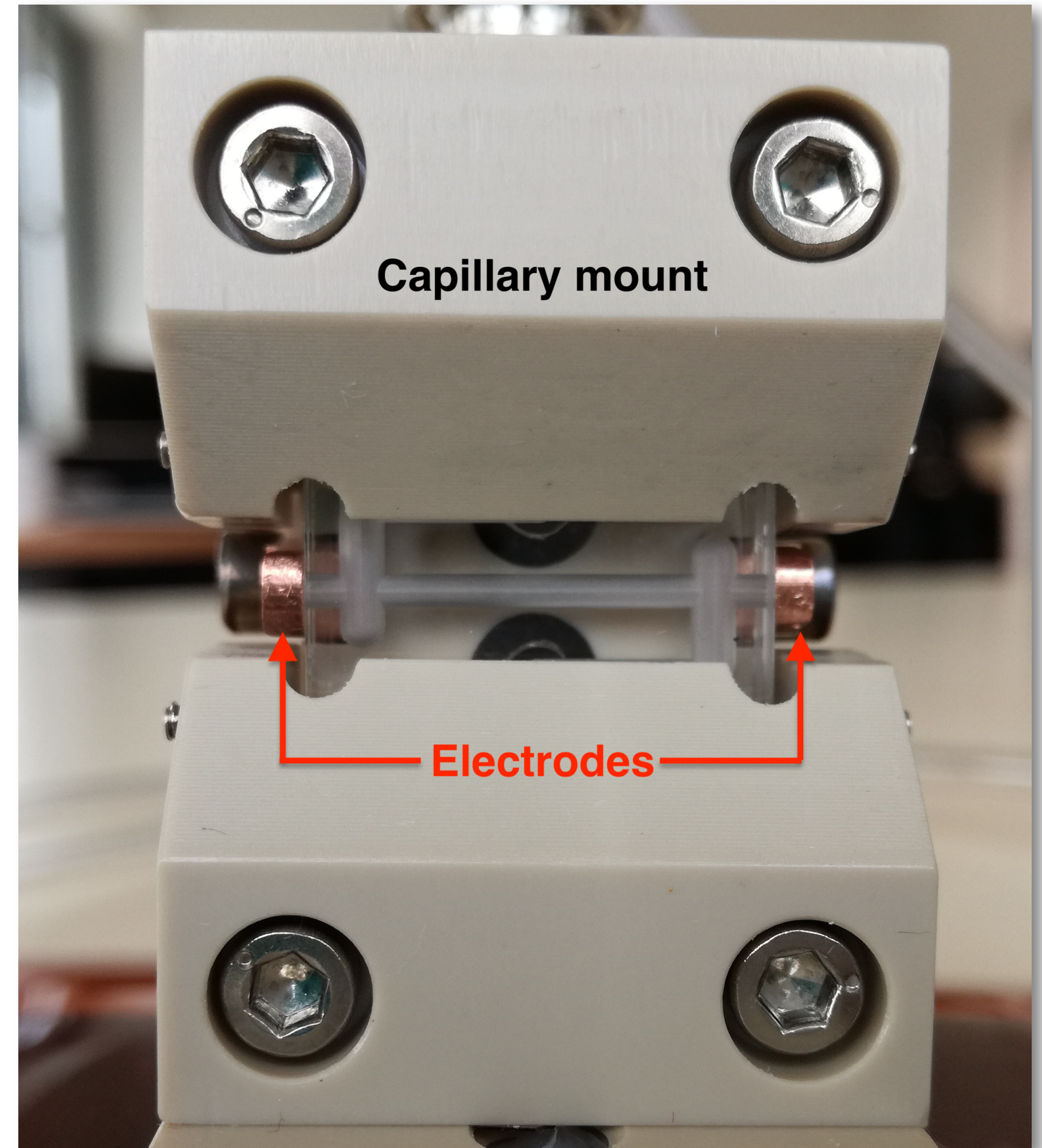
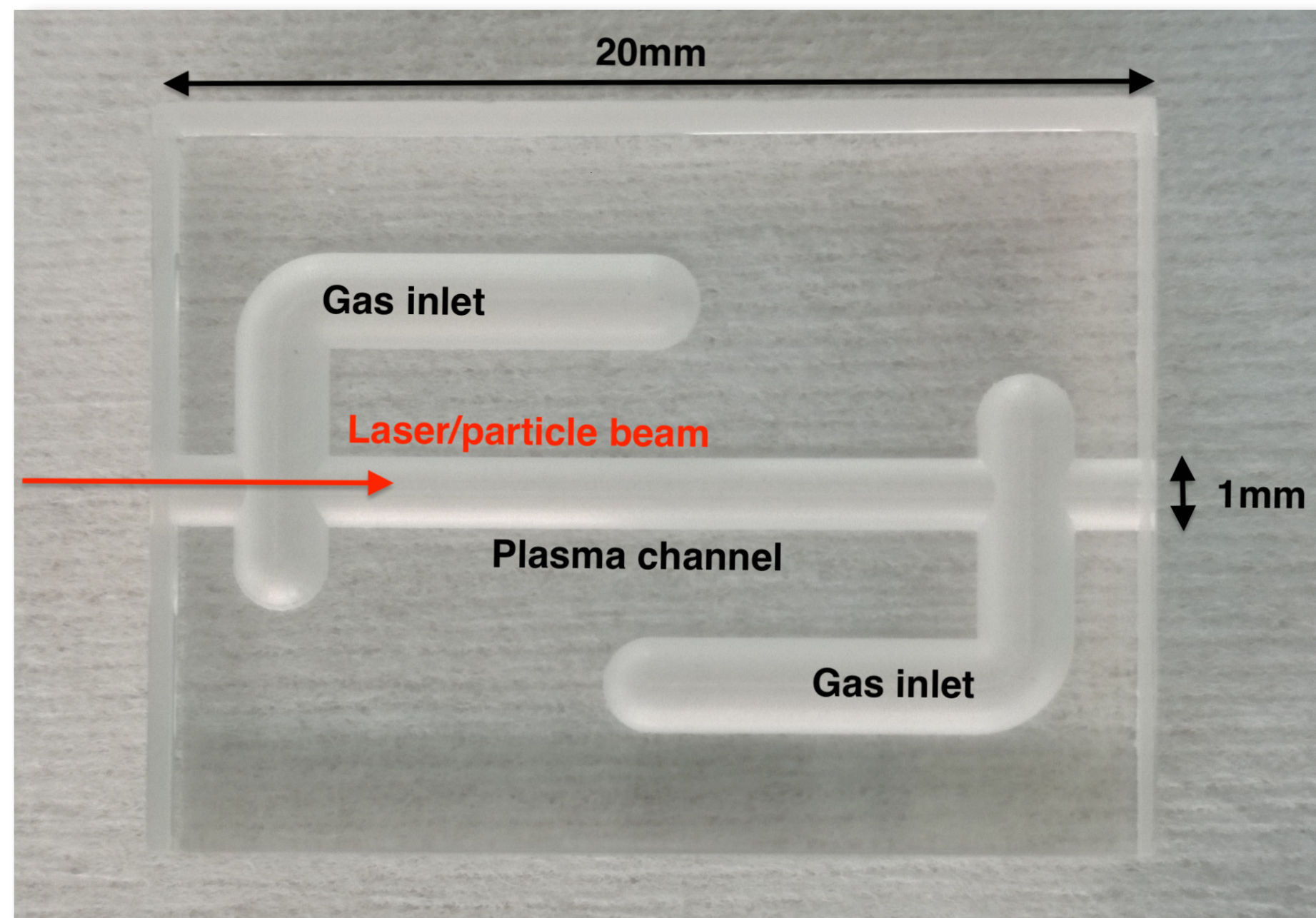


# Laser interferometry



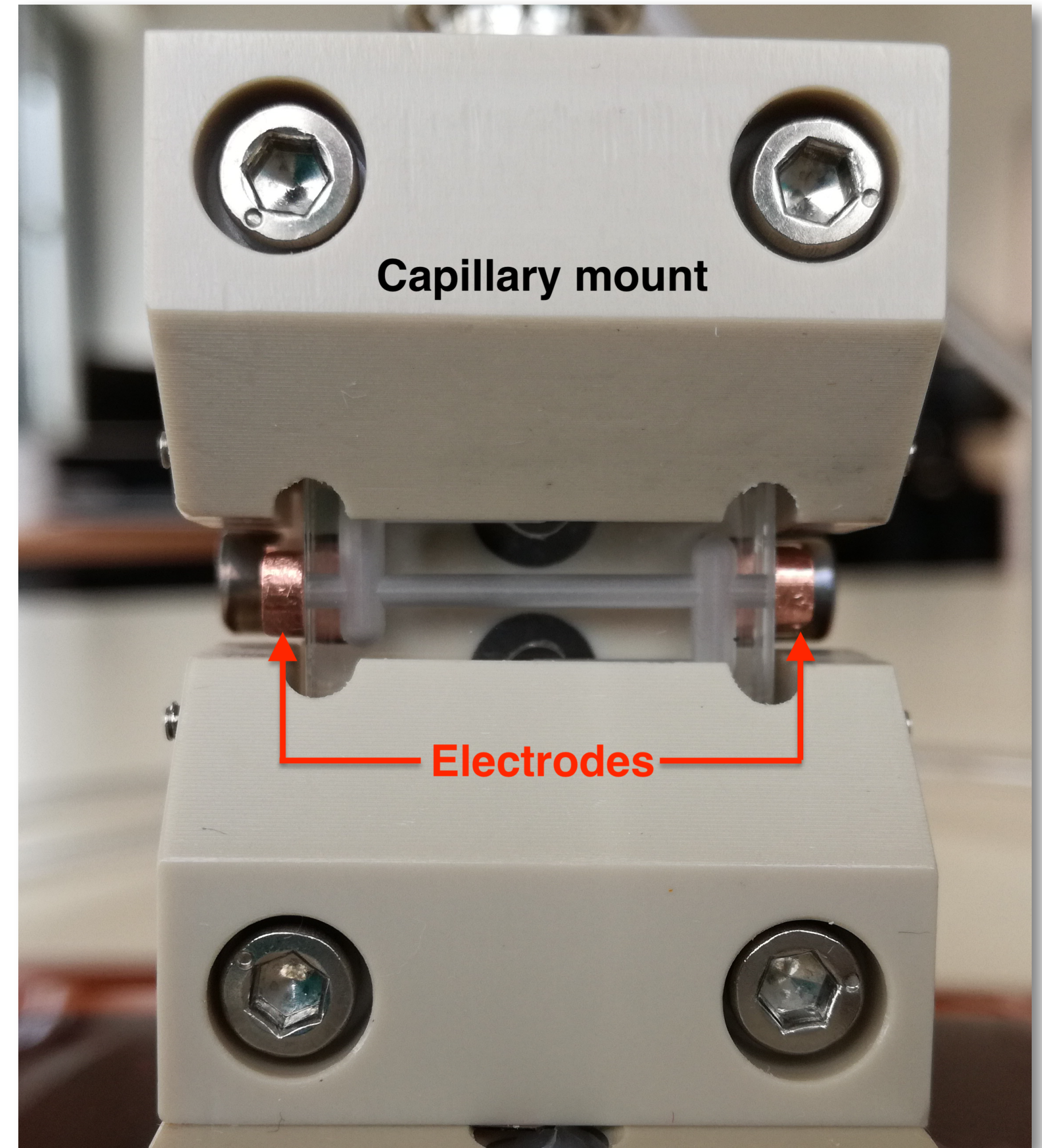
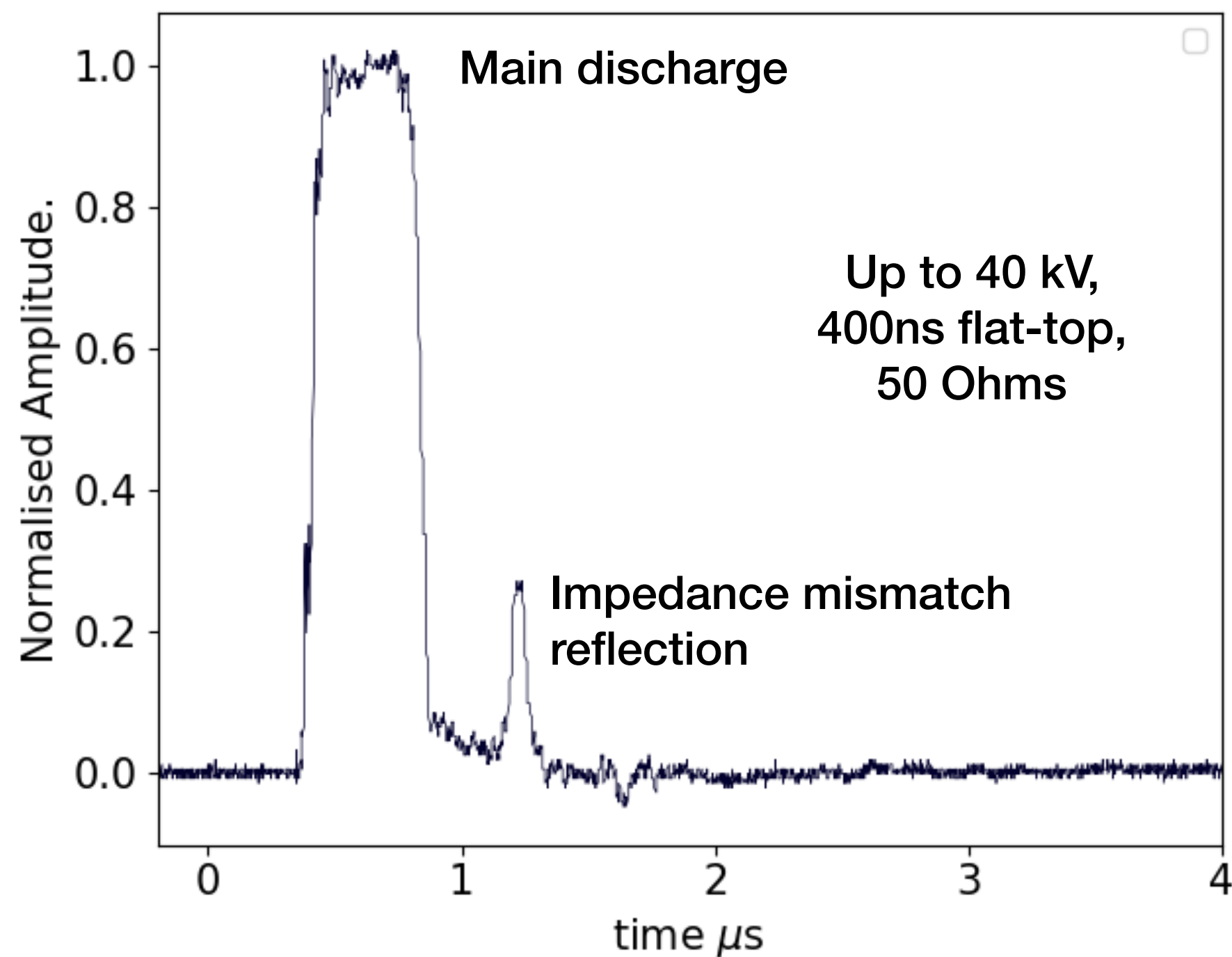
# Two-color phase delay spectral interferometry

- System to be investigated: discharge capillary
  - Cylindrical, sapphire milled channel
  - Length: 20 mm; Diameter: 1.0 mm
  - Electrically discharge-ignited plasma



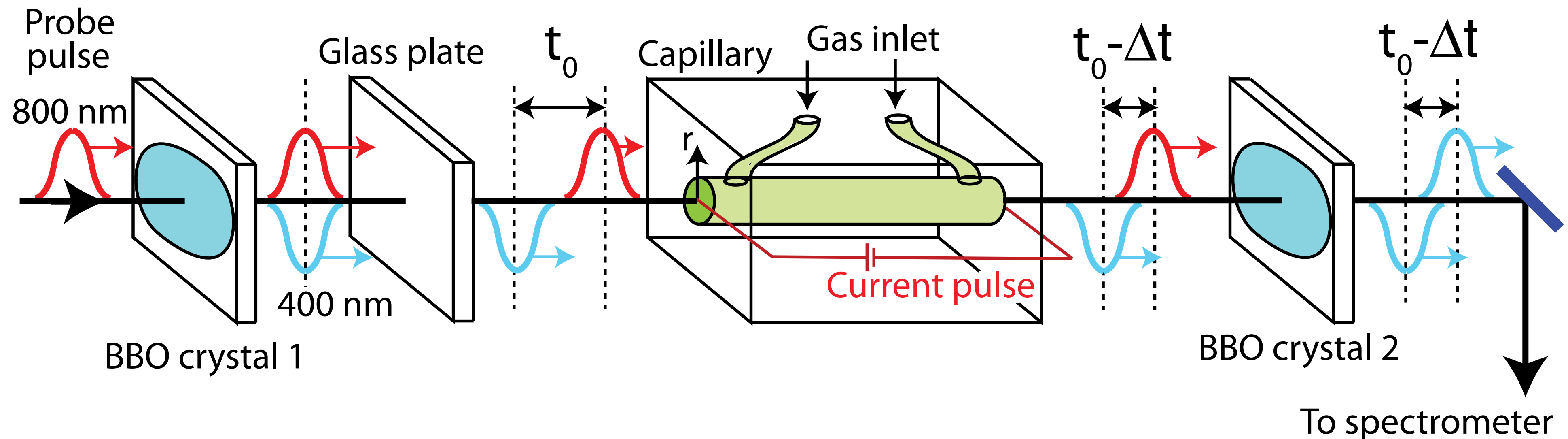
# Two-color phase delay spectral interferometry

- > System to be investigated: discharge capillary
  - Cylindrical, sapphire milled channel
  - Length: 20 mm; Diameter: 1.0 mm
  - Electrically discharge-ignited plasma



# Two-color phase delay spectral interferometry

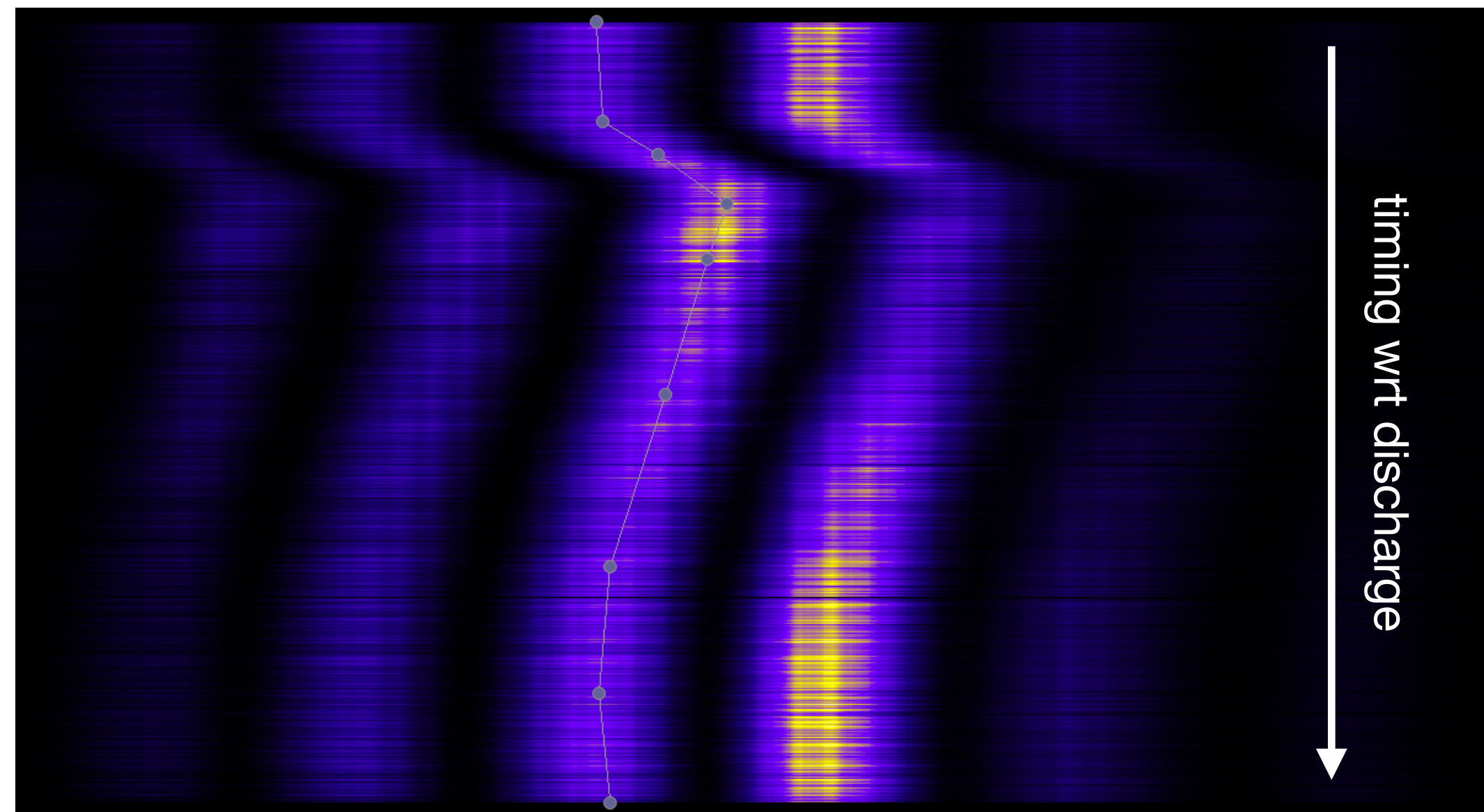
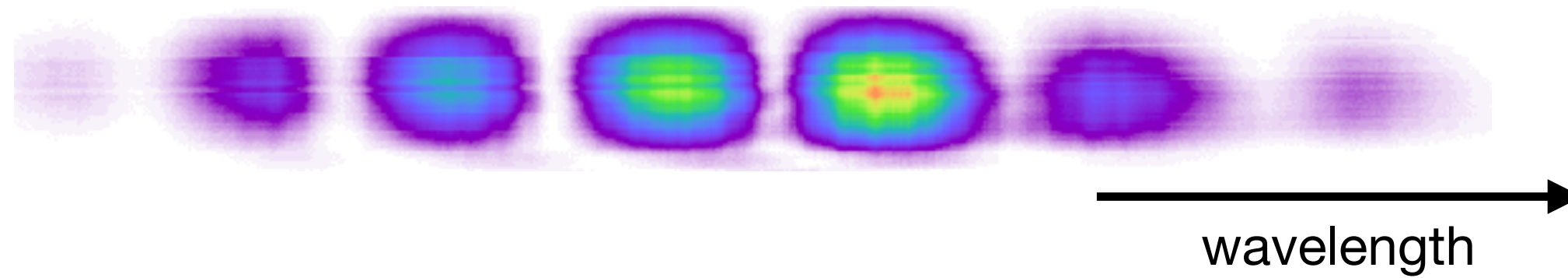
- > Single laser pulse frequency doubled → two co-propagating harmonics at 800 and 400 nm (red and blue)
- > Two pulses have different group and phase velocities in plasma → the pulses acquire a  $\Delta t$  and phase shift
- > On exiting the plasma, remaining 800 nm pulse is also doubled (all blue)
- > Spectral interference pattern reveals information about temporal delay, phase shift, and the plasma density



J. Van Tilborg *et al*, Optics Letters 43, 12 (2018)

# Two-color phase delay spectral interferometry

## > Interference pattern

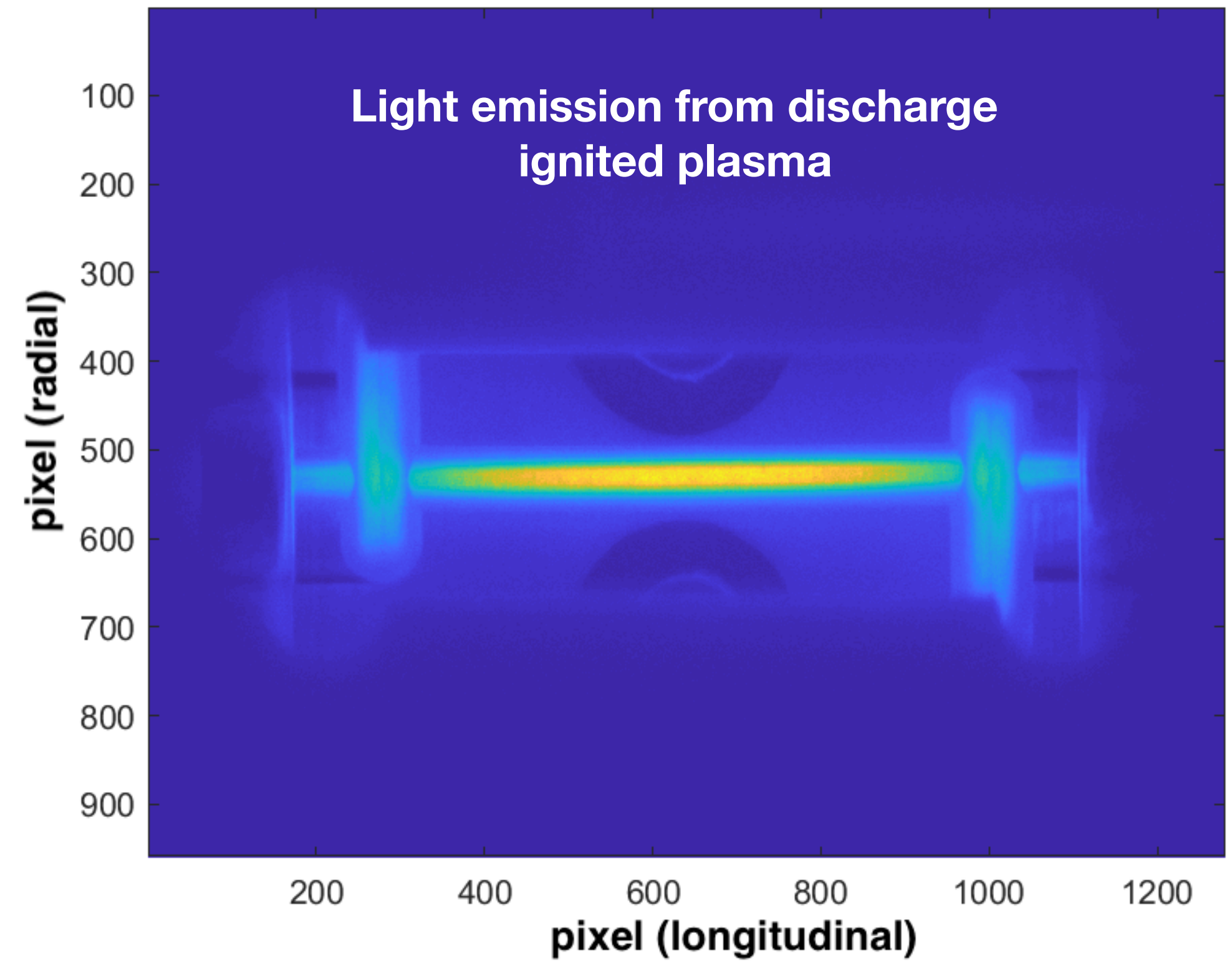
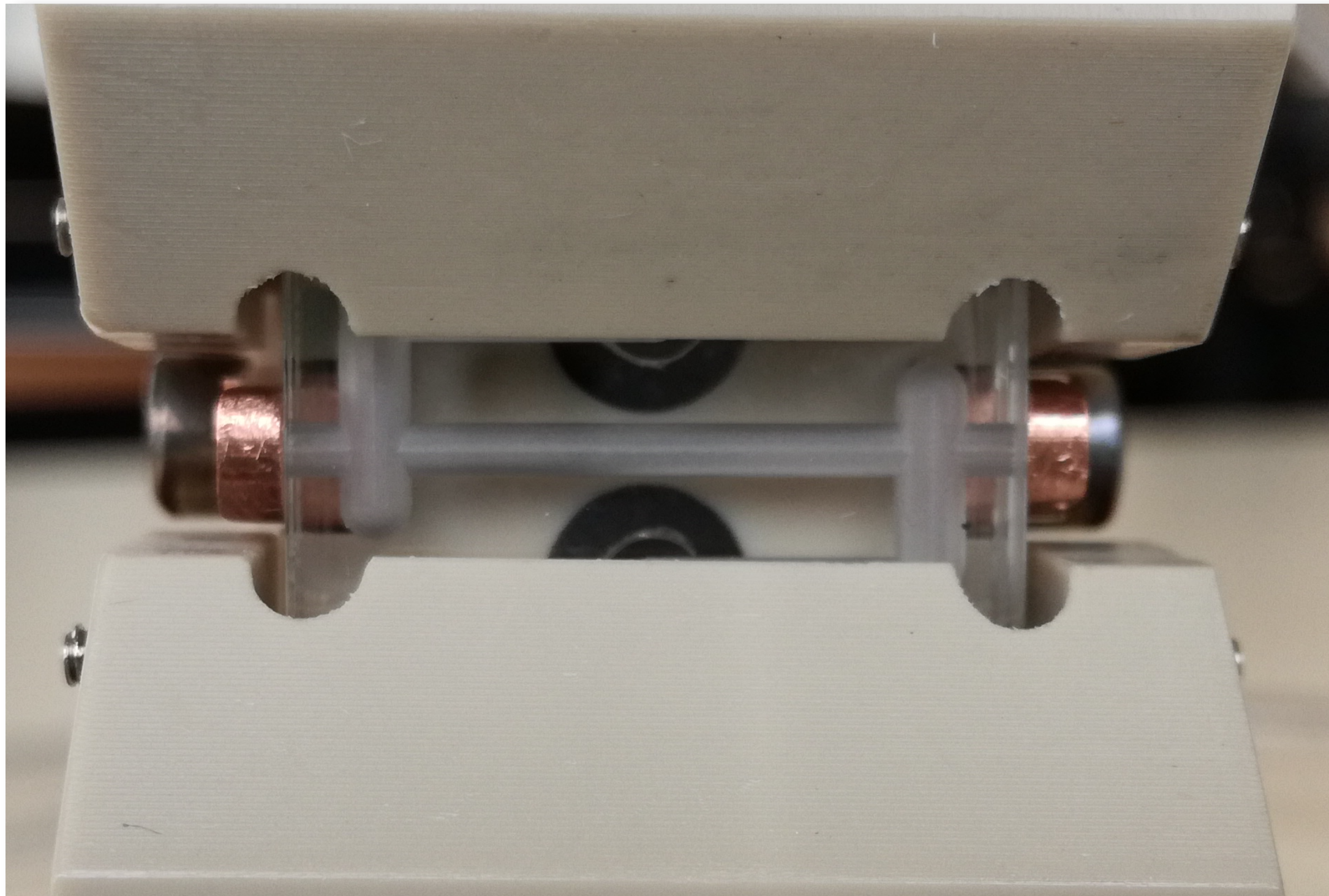


- > Fringe frequency → pulse separation
- > Fringe position → phase delay

- > Spatial resolution:  
longitudinally integrated
- > Temporal resolution:  
sub-ns (depending on capillary traversal time)

# Plasma spectroscopy

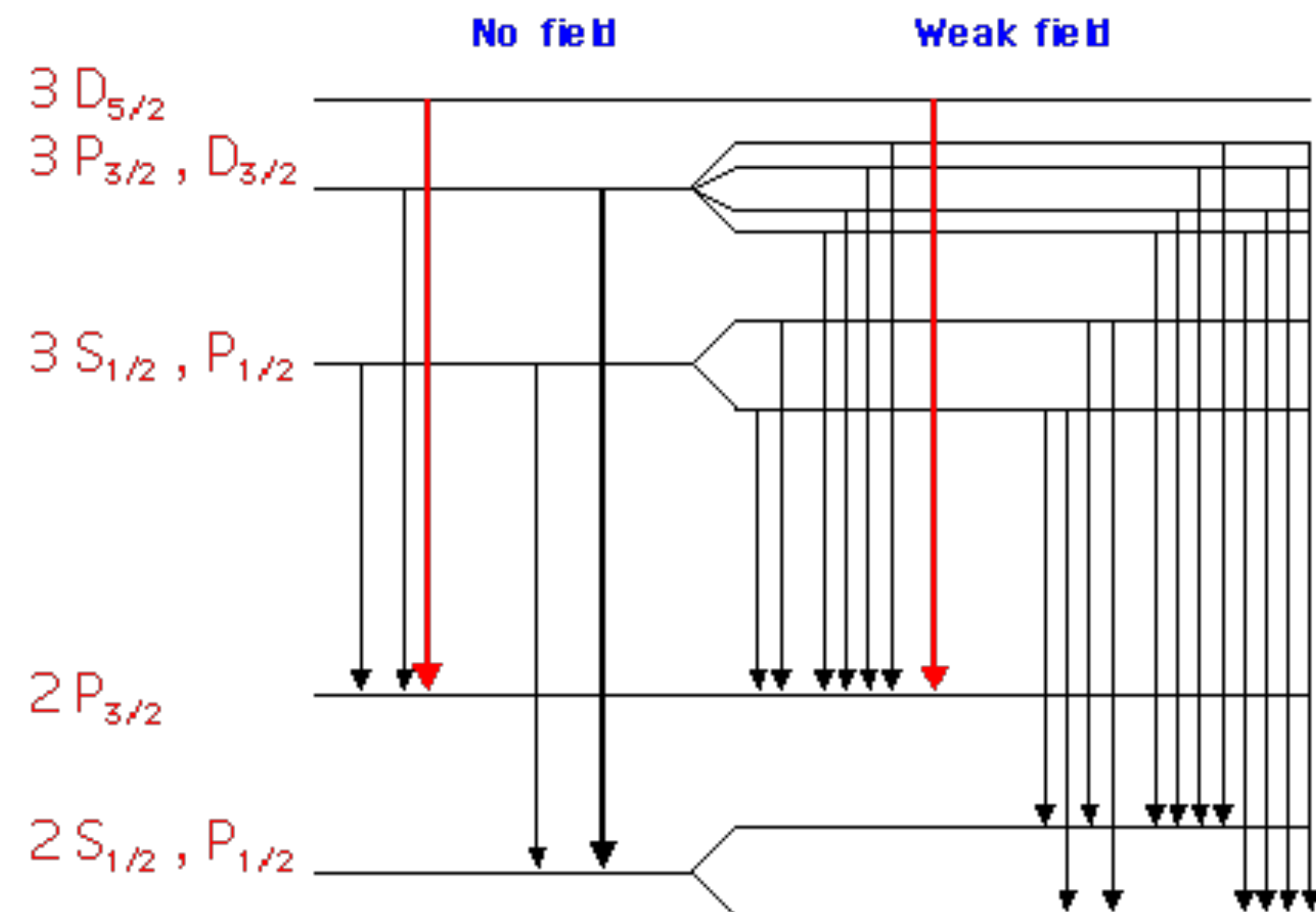
- Plasma emission may be used to acquire information about plasma



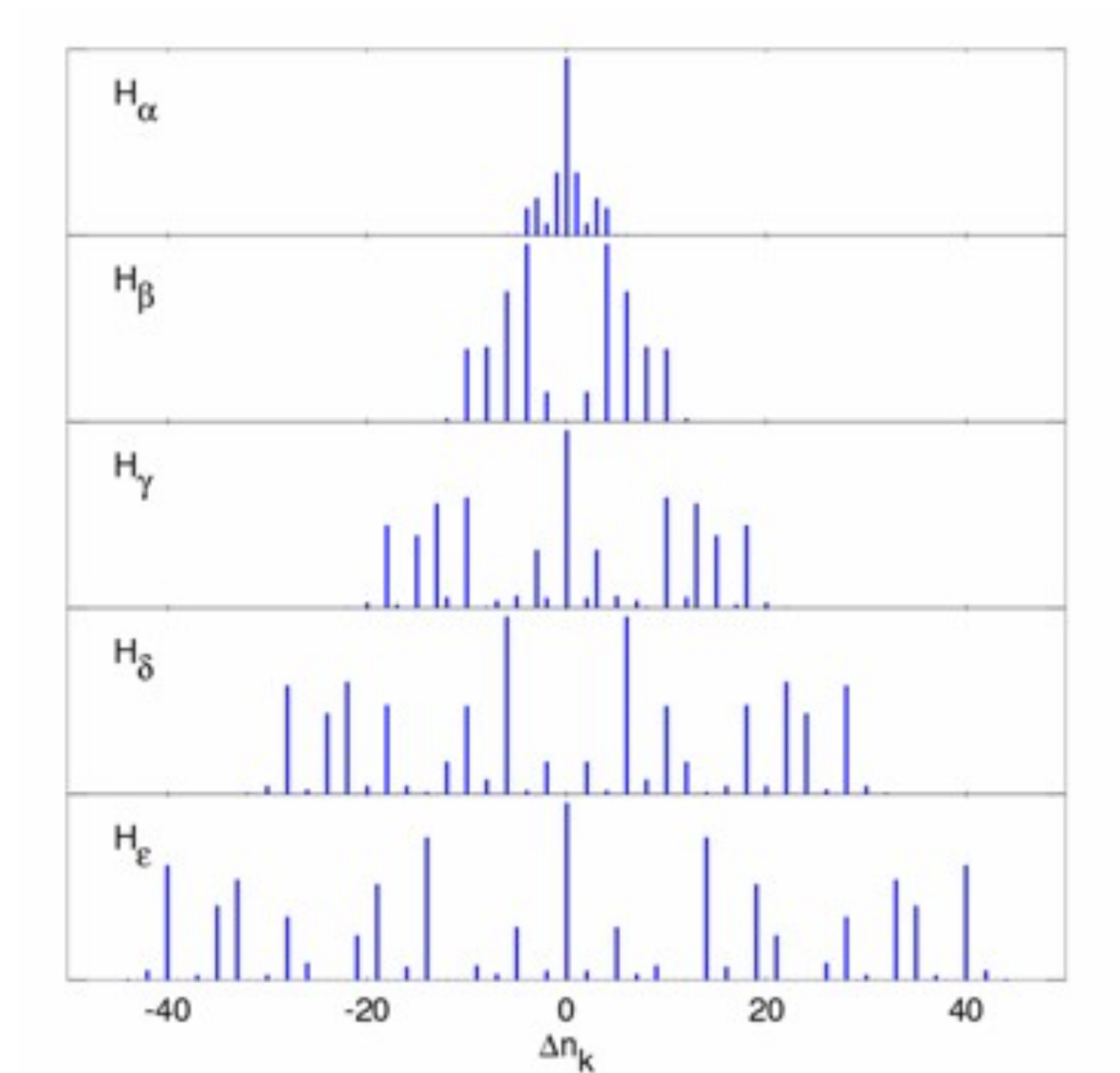
# Plasma spectroscopy

- > Stark broadening of electric relaxation lines depends on local electric field strength in plasma (Debye shielding)
  - contains information about local plasma electron density

**Stark effect for Hydrogen H<sub>α</sub>**



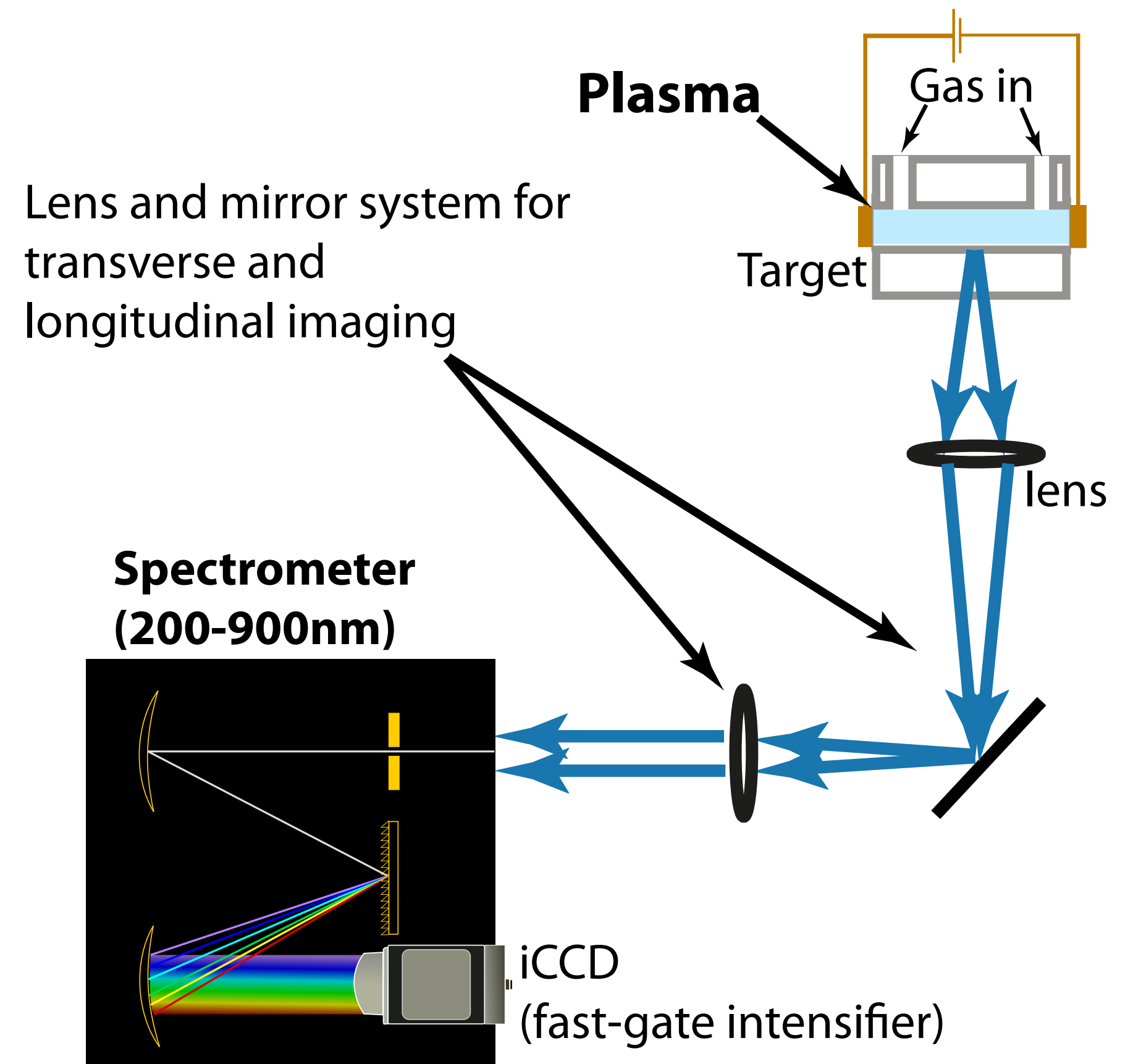
**Line splitting of Balmer Series of Hydrogen**



- > Number of degenerate states:  $g = 2 \sum_{l=0}^{n-1} (2l + 1)$

# Plasma spectroscopy

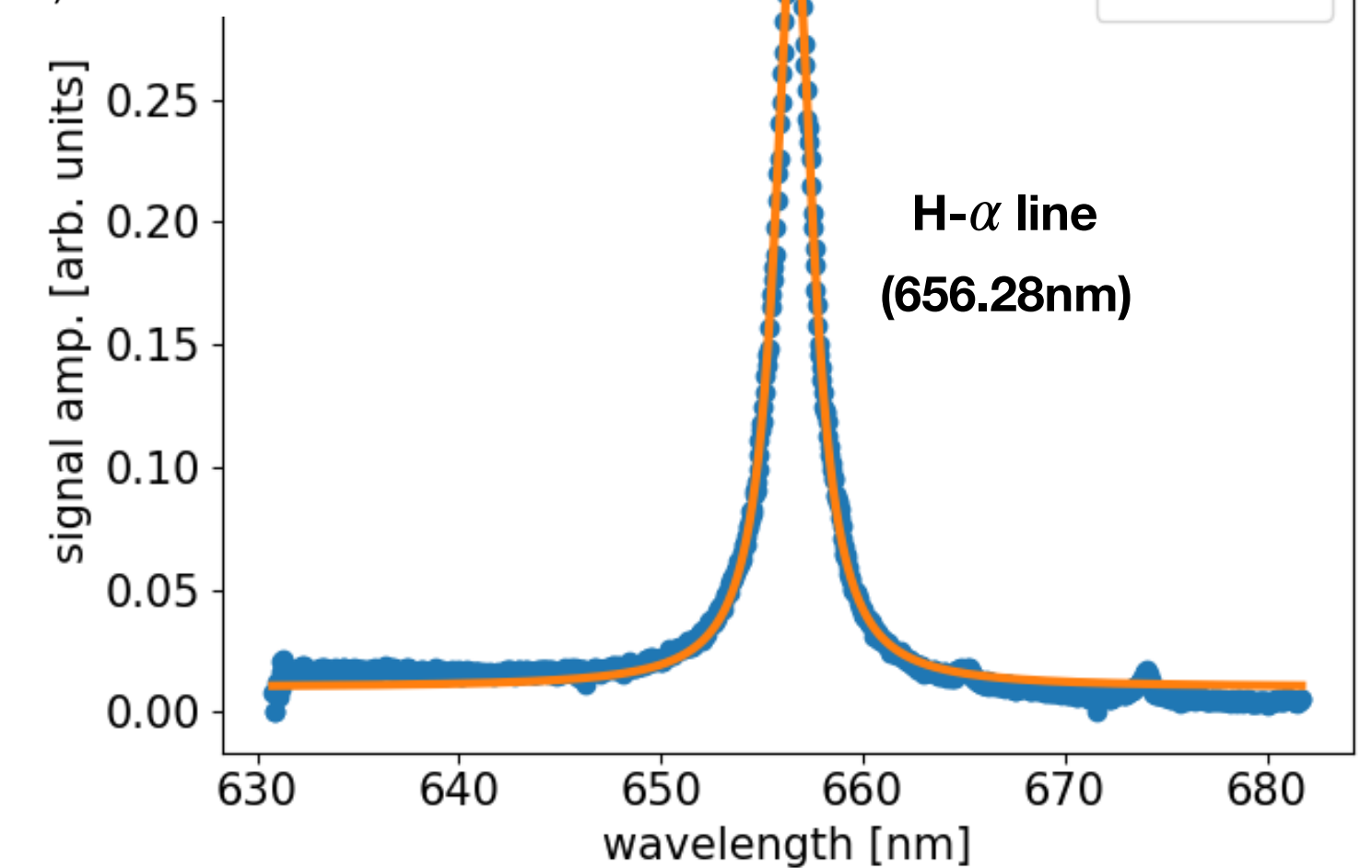
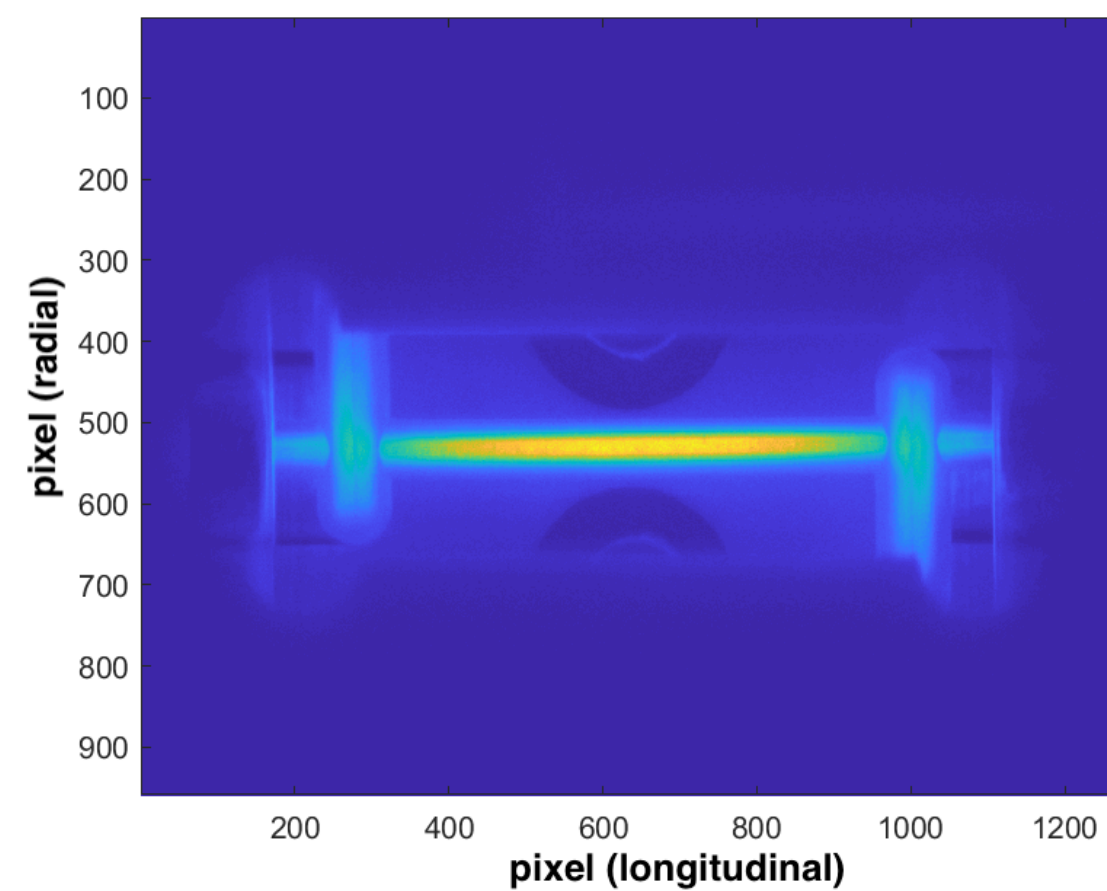
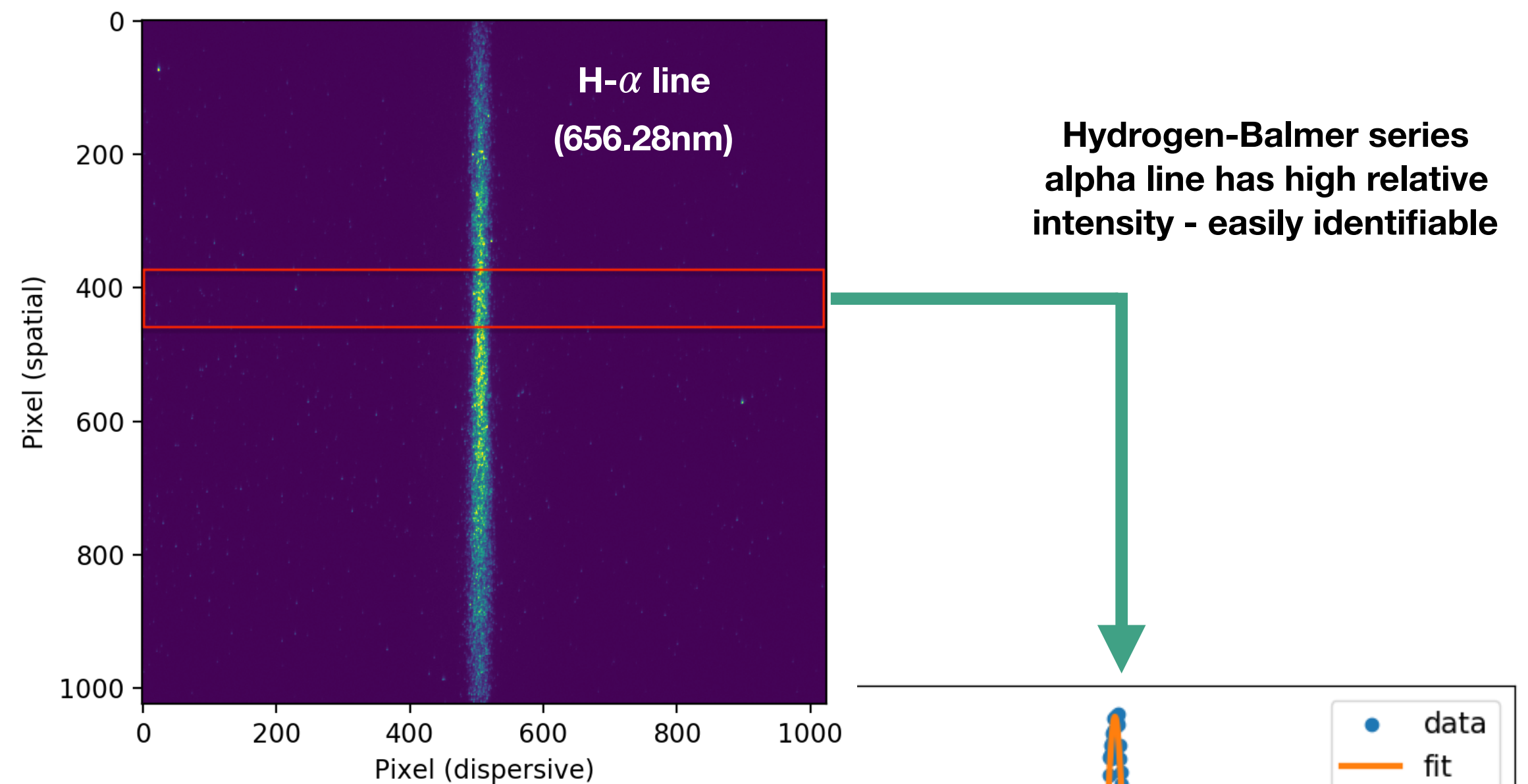
- > Stark broadening of electric relaxation lines depends on local electric field strength in plasma (Debye shielding)  
→ contains information about local plasma electron density
- > Observe spectroscopic light emission from atoms in plasma
- > Fast-gate intensifier (2 - 50 ns) before CCD camera
- > Width of spectral lines reveals information about plasma density



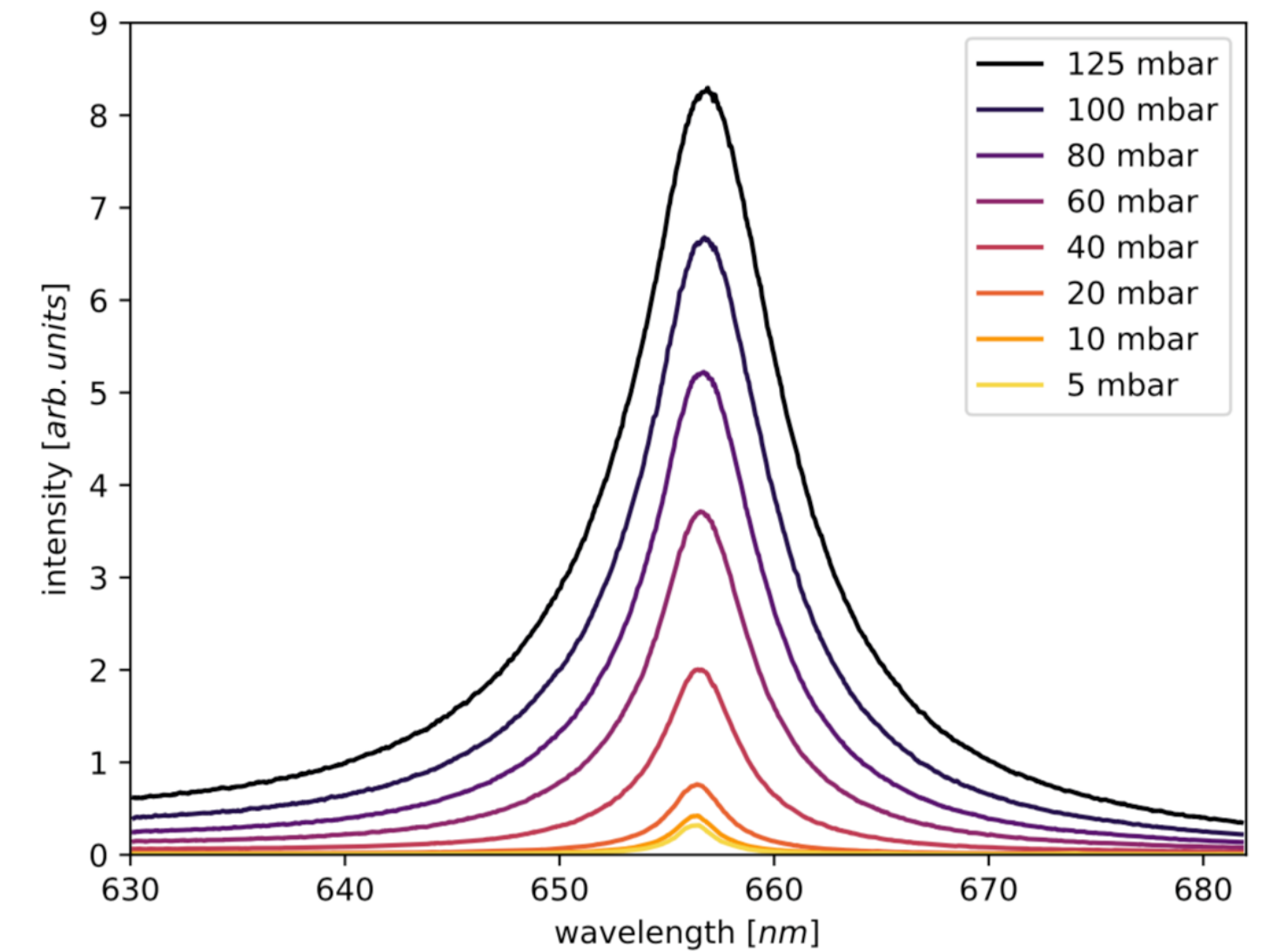
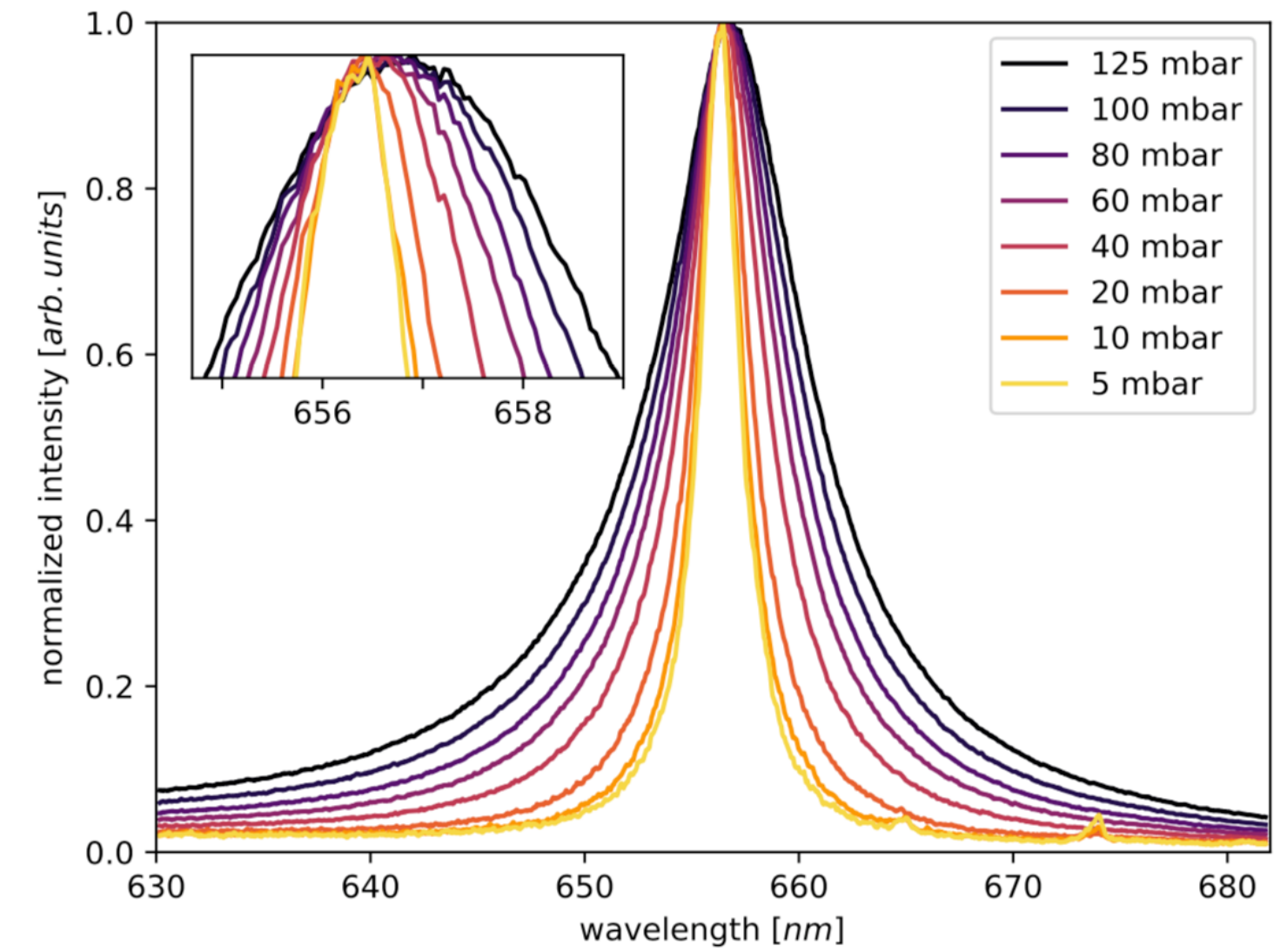
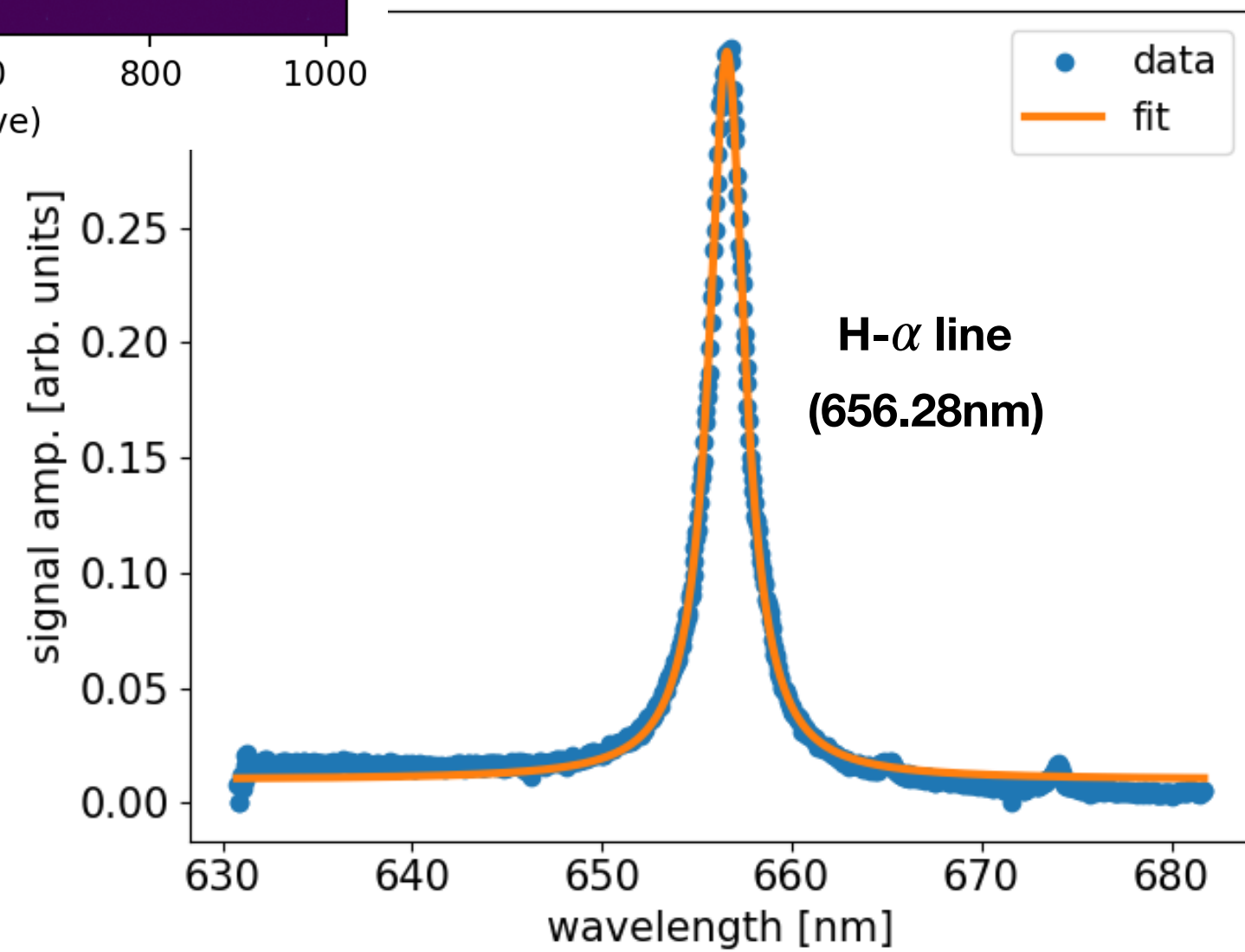
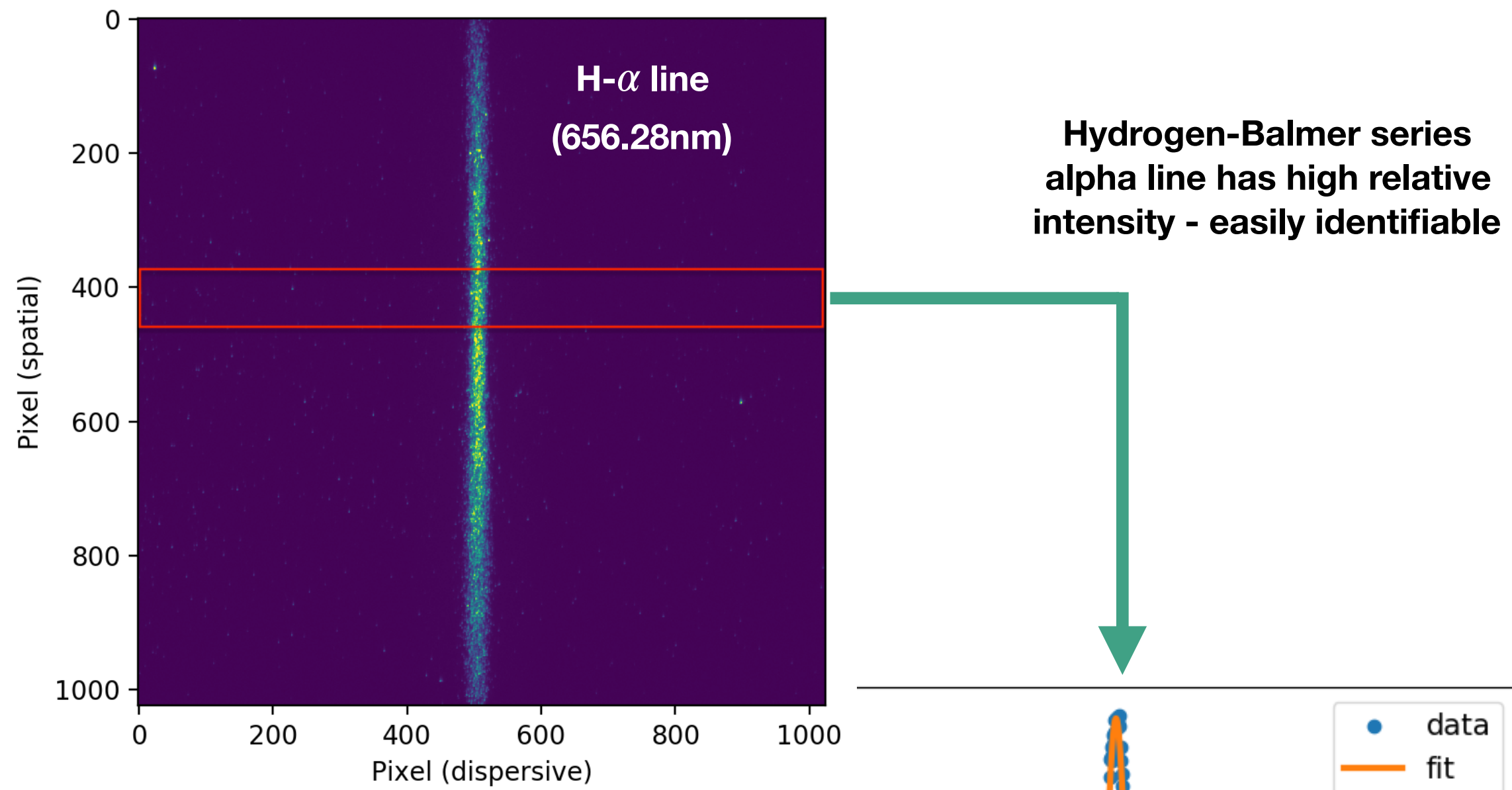
Methodology references: M.A. Gigosos *et al*, *Spectrochimica Acta B* **58** (2003)  
P. Kepple and H.R. Griem, *Phys. Rev.* **173** (1968)

# Plasma spectroscopy

- > Spatial resolution:  
longitudinally xor radially  
resolved density slices, ~ 10  $\mu\text{m}$  resolution
- > Temporal resolution:  
shortest gating time over which  
S/N is sufficient (typically 2 - 50 ns)



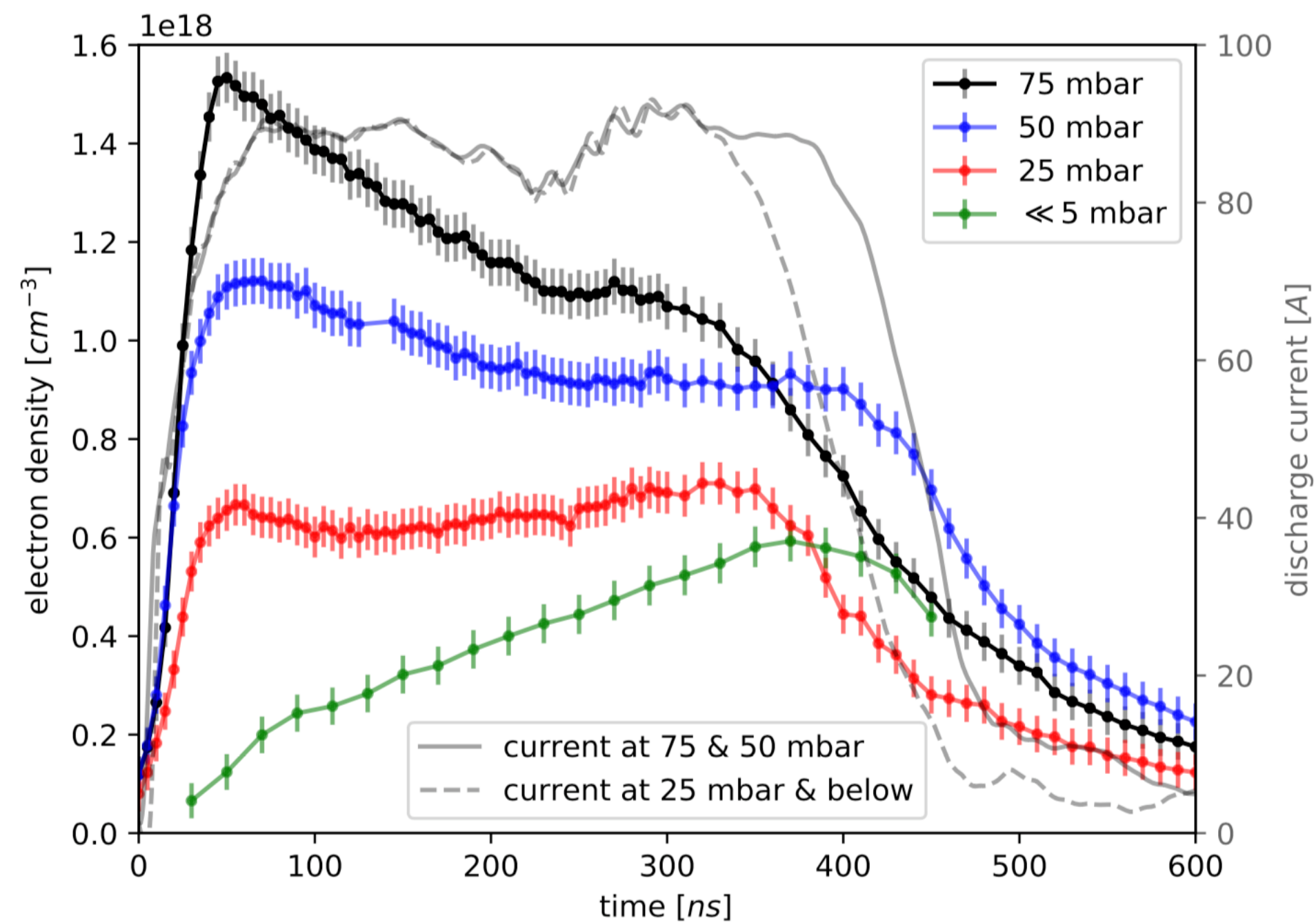
# Plasma spectroscopy



# Plasma spectroscopy

- Different capillary with 300  $\mu\text{m}$  inner diameter capillary

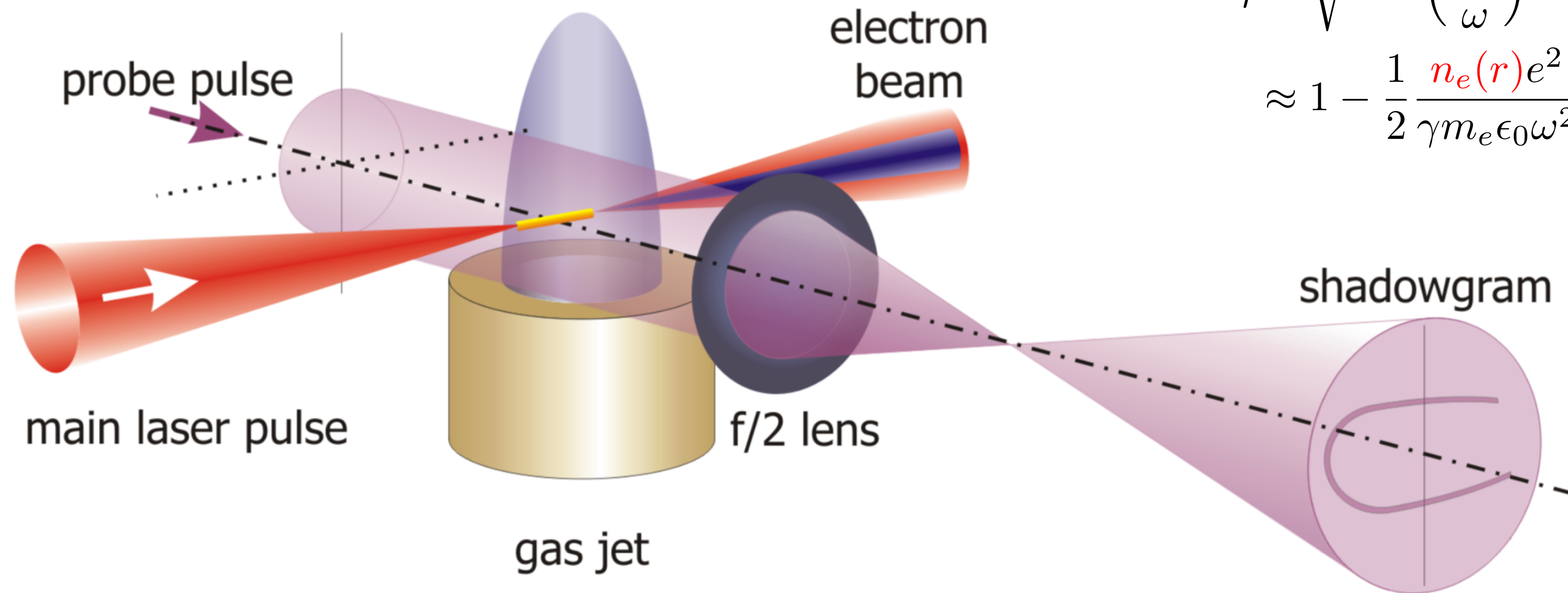
“100%” Hydrogen temporal evolution



# **Internal E- & B-fields, and wake structures**

- Polarimetry
- Particle beam probes
- Frequency Domain Holography

# Reminder: Shadowgraphy

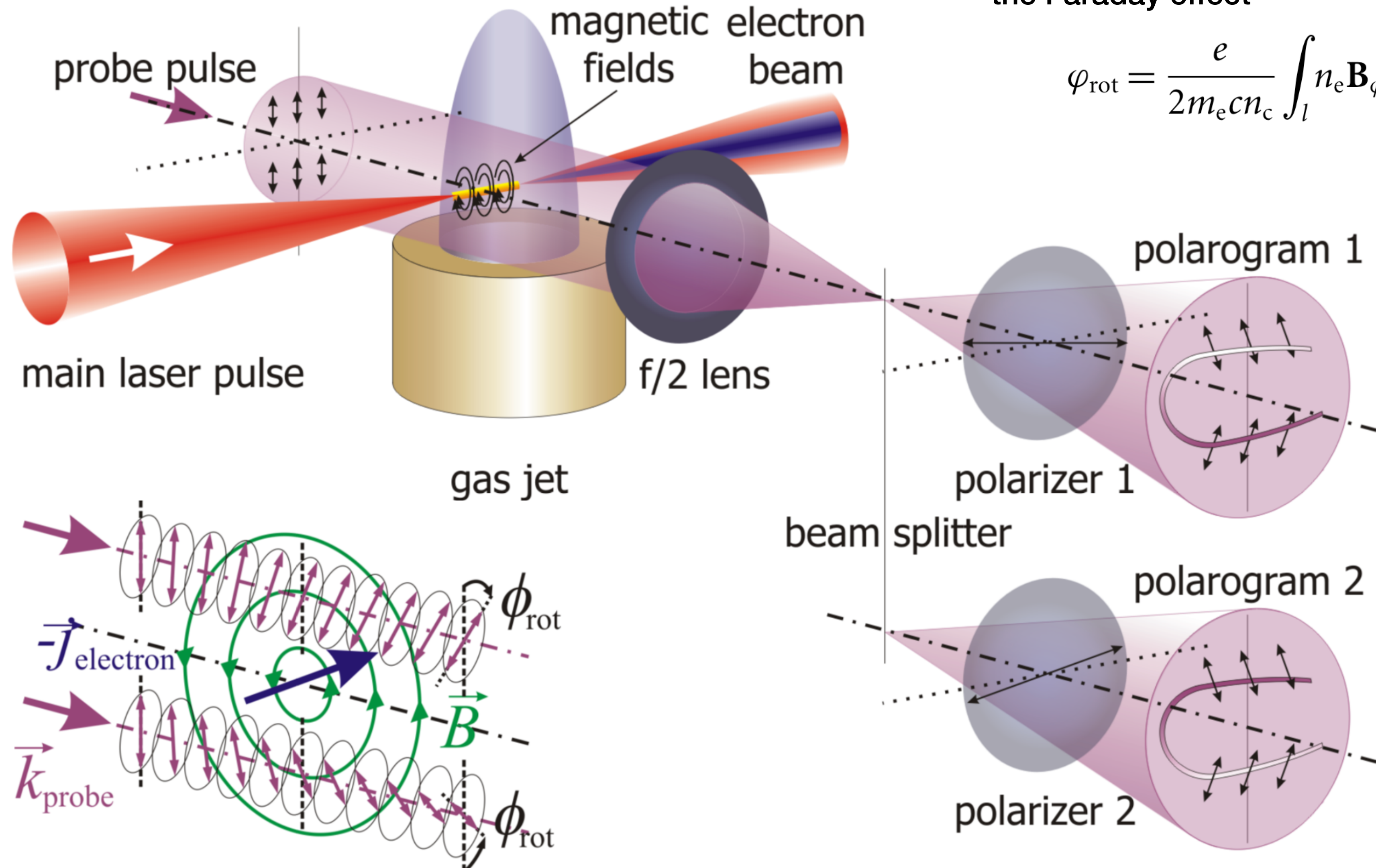


$$\eta = \sqrt{1 - \left(\frac{\omega_p}{\omega}\right)^2}$$
$$\approx 1 - \frac{1}{2} \frac{n_e(r) e^2}{\gamma m_e \epsilon_0 \omega^2}$$

- > Index of refraction gradients cause distortion of probe phase front  
→ intensity structures in beam

# Polarimetry

> Plasma can be an active medium for the Faraday effect



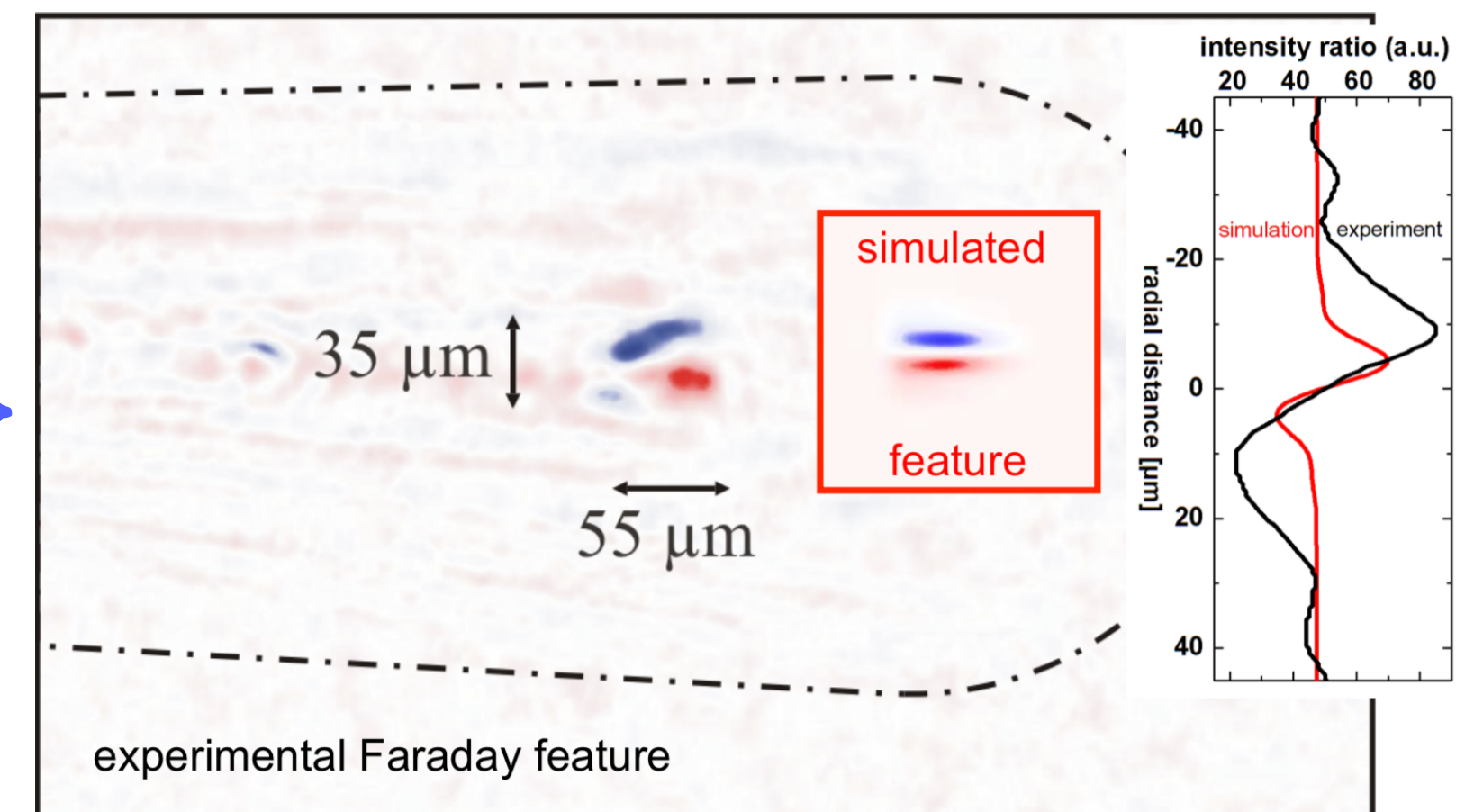
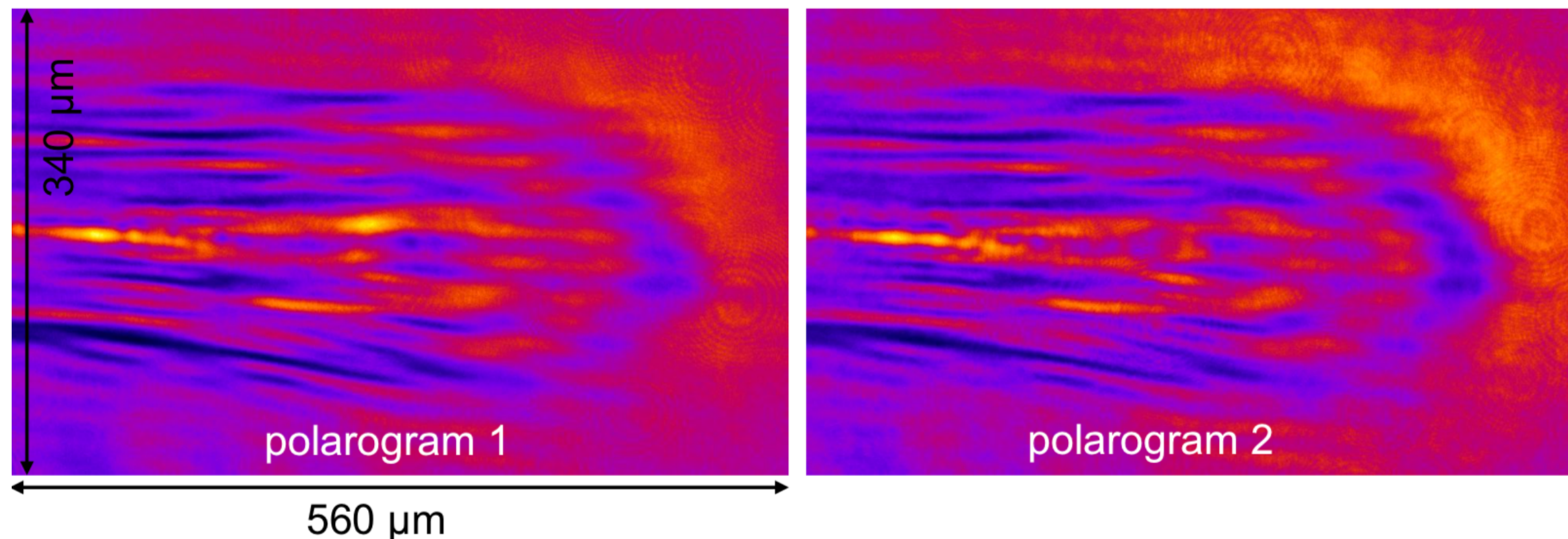
$$\varphi_{\text{rot}} = \frac{e}{2m_e c n_c} \int_l n_e \mathbf{B}_\varphi \cdot d\mathbf{s}$$

# Polarimetry

- Plasma can be an active medium for the Faraday effect

$$\varphi_{\text{rot}} = \frac{e}{2m_e c n_c} \int_l n_e \mathbf{B}_\varphi \cdot d\mathbf{s}$$

Two polarograms from two (almost) crossed polarizers:



Experimental evidence for B-fields from MeV electrons and bubble!  
MCK *et al.*, Physical Review Letters **105**, 115002 (2010)

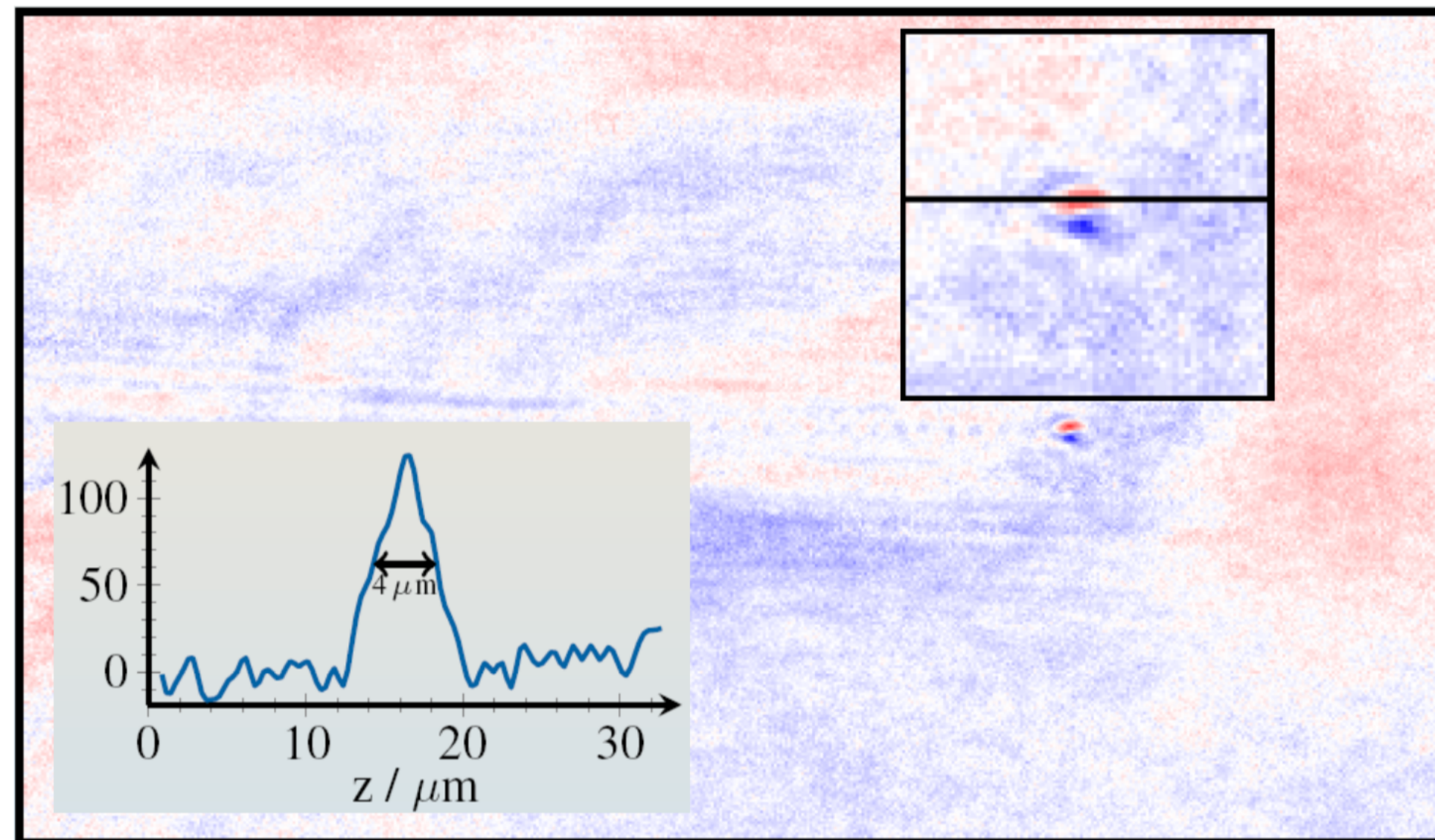
$$I_{\text{pol1}} = I_0 [1 - \beta_1 \sin^2(90^\circ - \theta_{\text{pol1}} - \phi_{\text{rot}})] \quad I_{\text{pol2}} = I_0 [1 - \beta_2 \sin^2(90^\circ + \theta_{\text{pol2}} - \phi_{\text{rot}})]$$

Deduce rotation angle  $\phi_{\text{rot}}$  from pixel-by-pixel division of polarogram intensities:

$$I_{\text{pol1}}(x, y) / I_{\text{pol2}}(x, y)$$

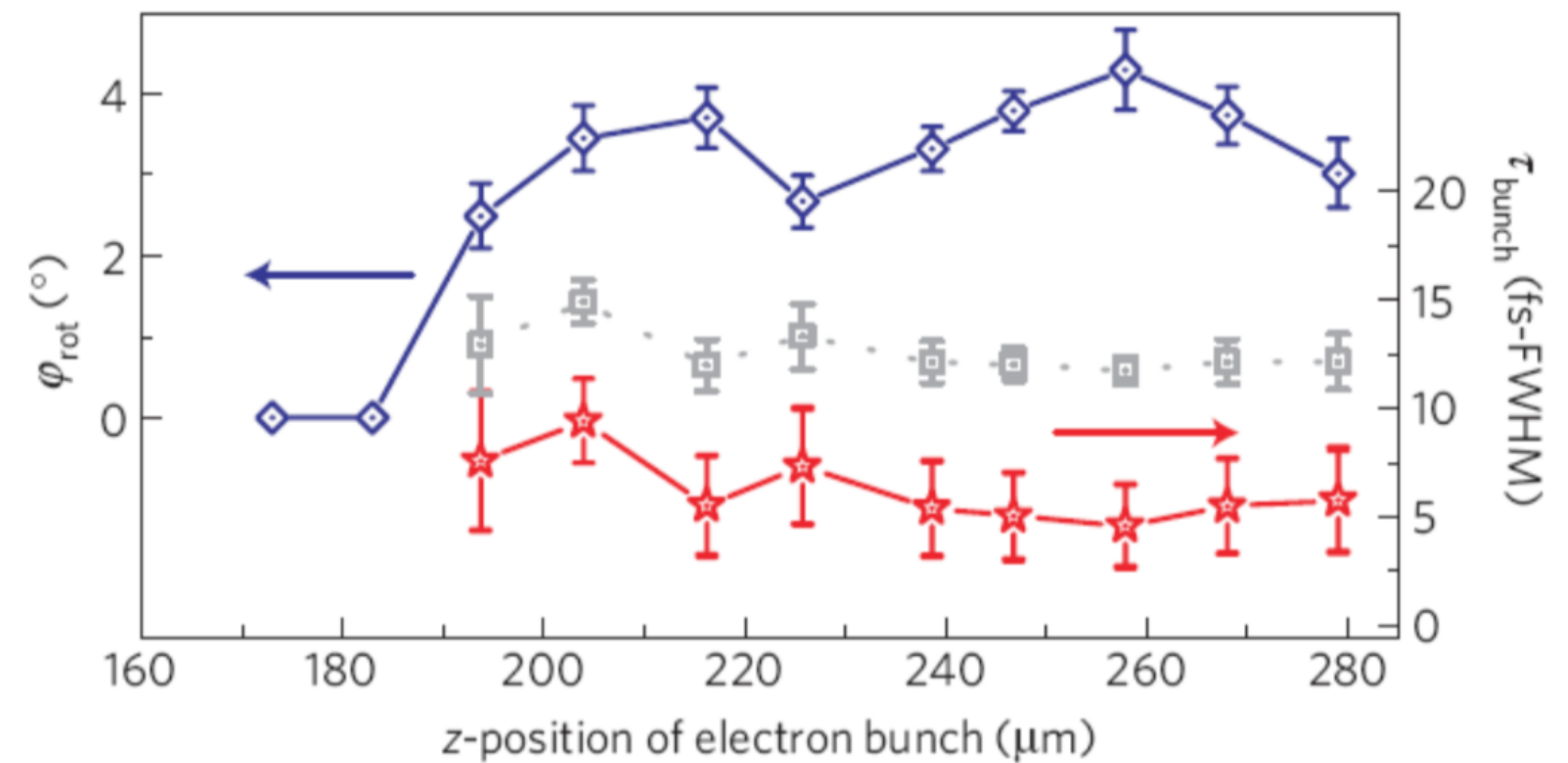
# Polarimetry

- > Bunch length measurements with few cycle laser pulses



Electron bunch length:  $\Delta z = 4 \mu\text{m}$   
 $\tau_{\text{FWHM}} = (6 \pm 2) \text{ fs}$ ,  $\tau_{\text{RMS}} = (2.5 \pm 0.9) \text{ fs}$

- > Online observation of electron bunch formation in an LWFA

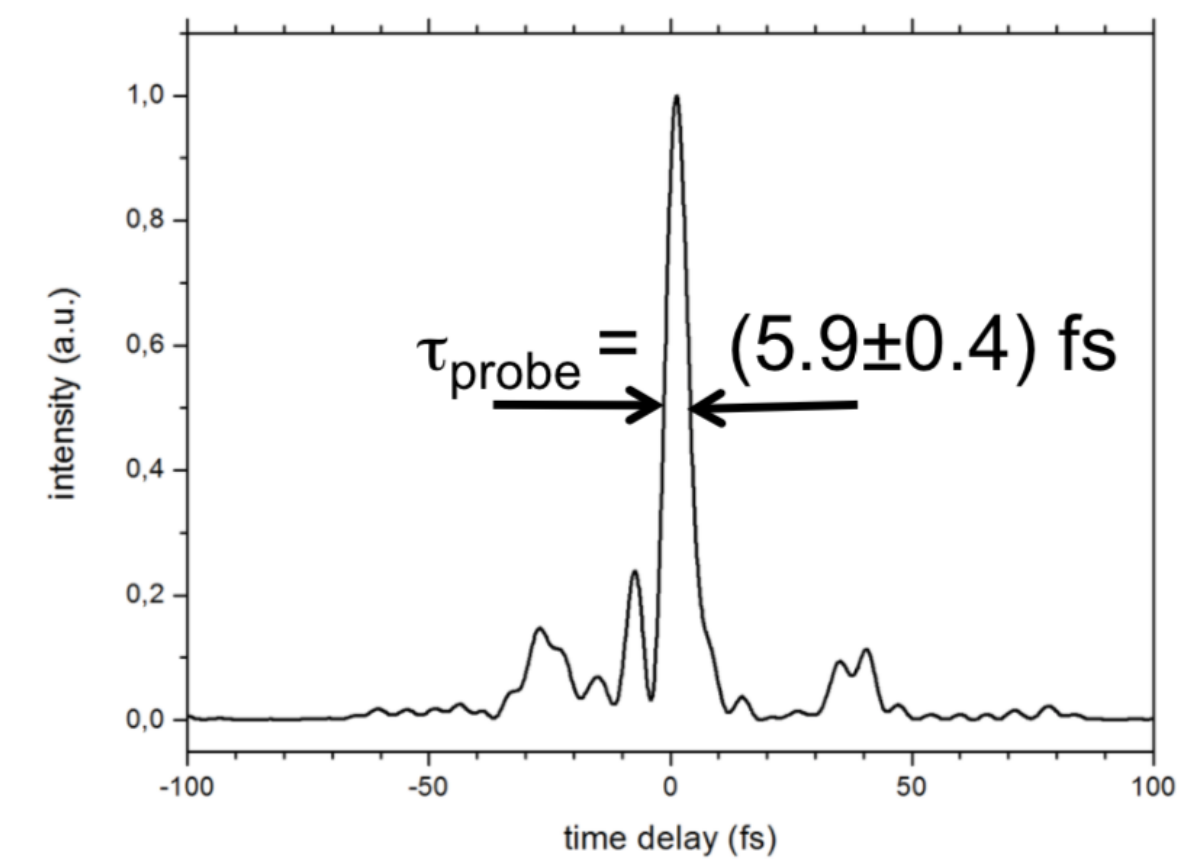
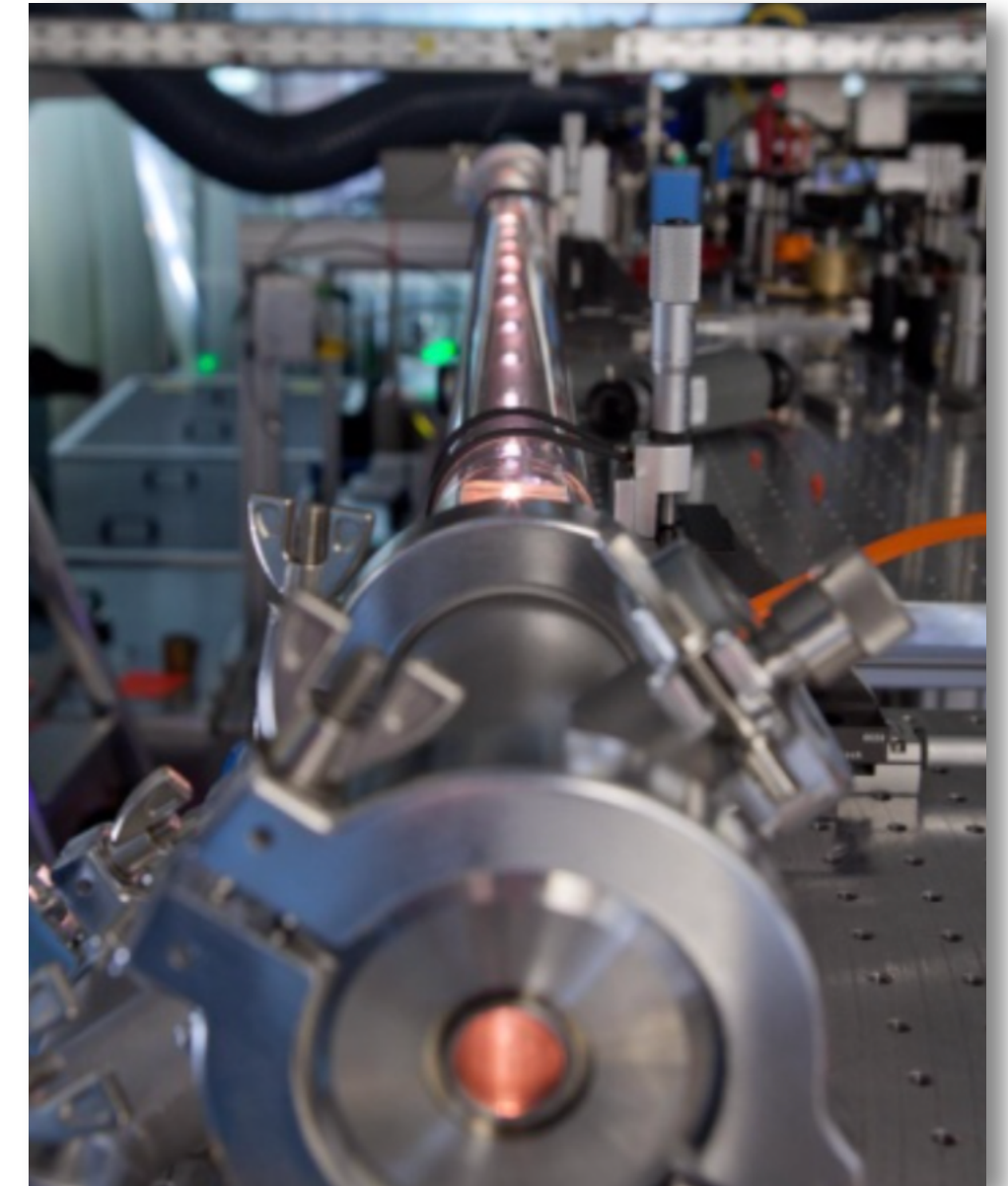


A. Buck *et al.*, Nature Physics 7, 543 (2011)

# Back to Shadowgraphy with few-cycle beams

- > Few-cycle probe pulse generation with hollow-core-fiber chirped mirror compressor
- > 5.9 fs beam generated from 35 fs FWHM Ti:sa pulse

M. Schwab *et al.*,  
Appl. Phys. Lett. 103, 191118 (2013)

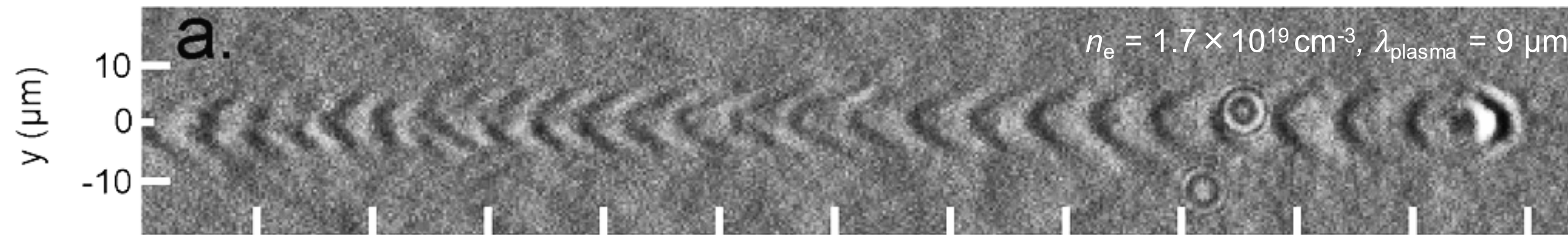


# Back to Shadowgraphy with few-cycle beams

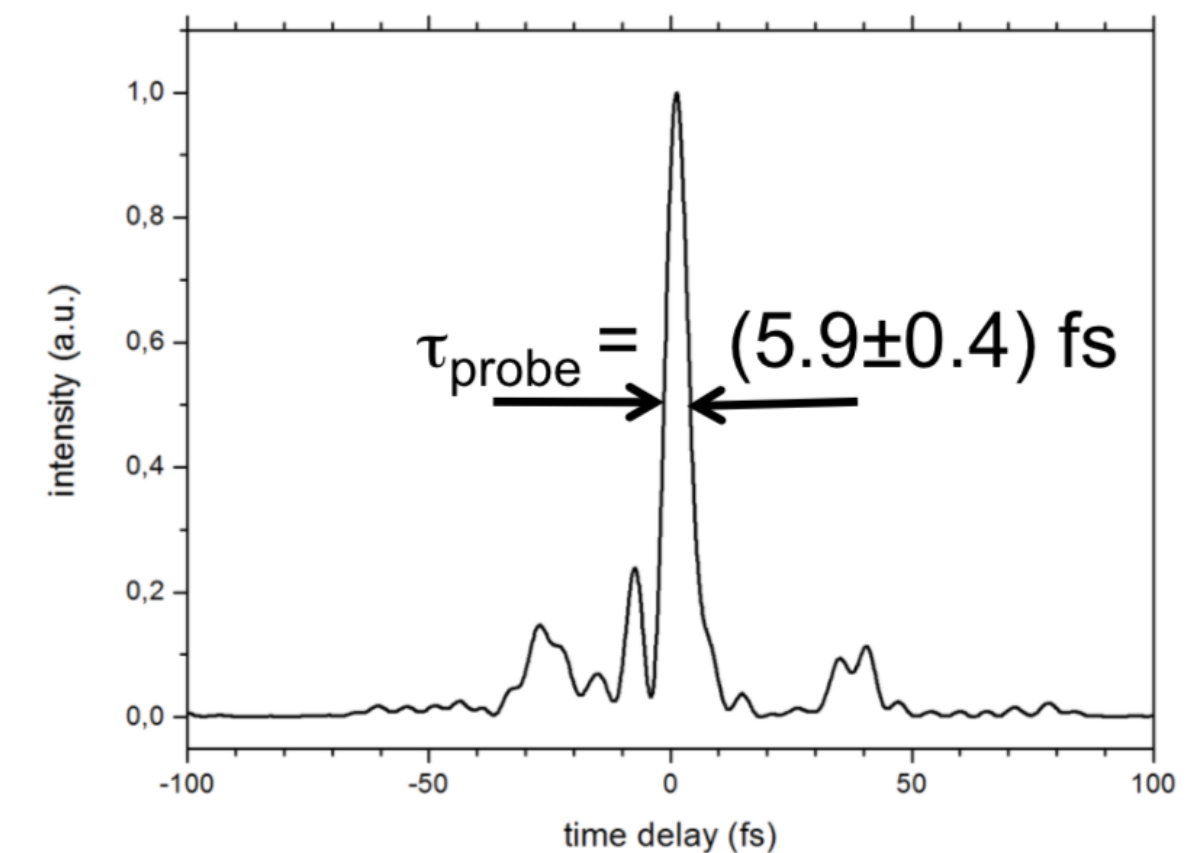
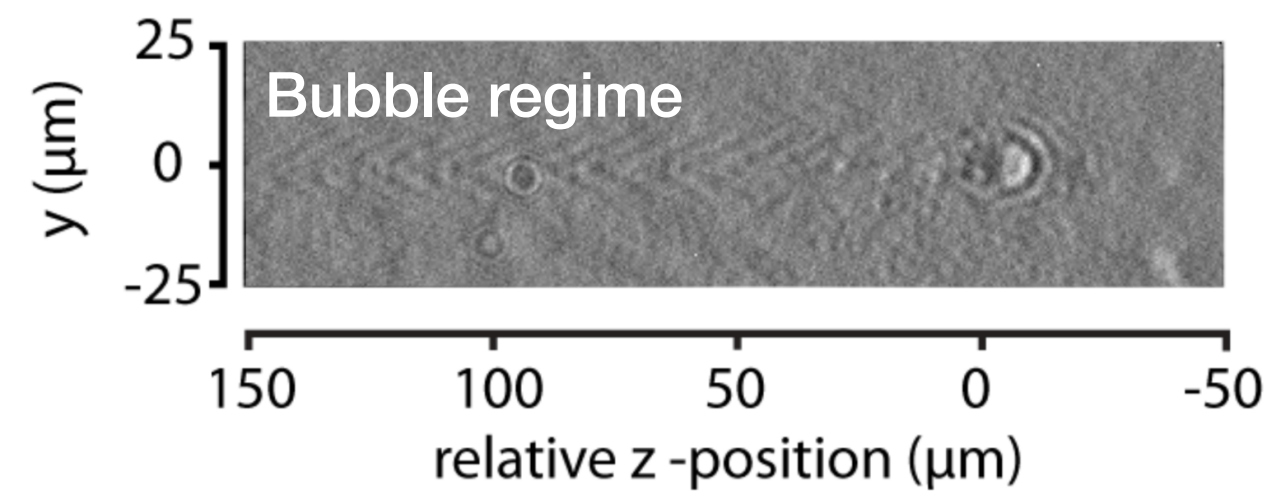
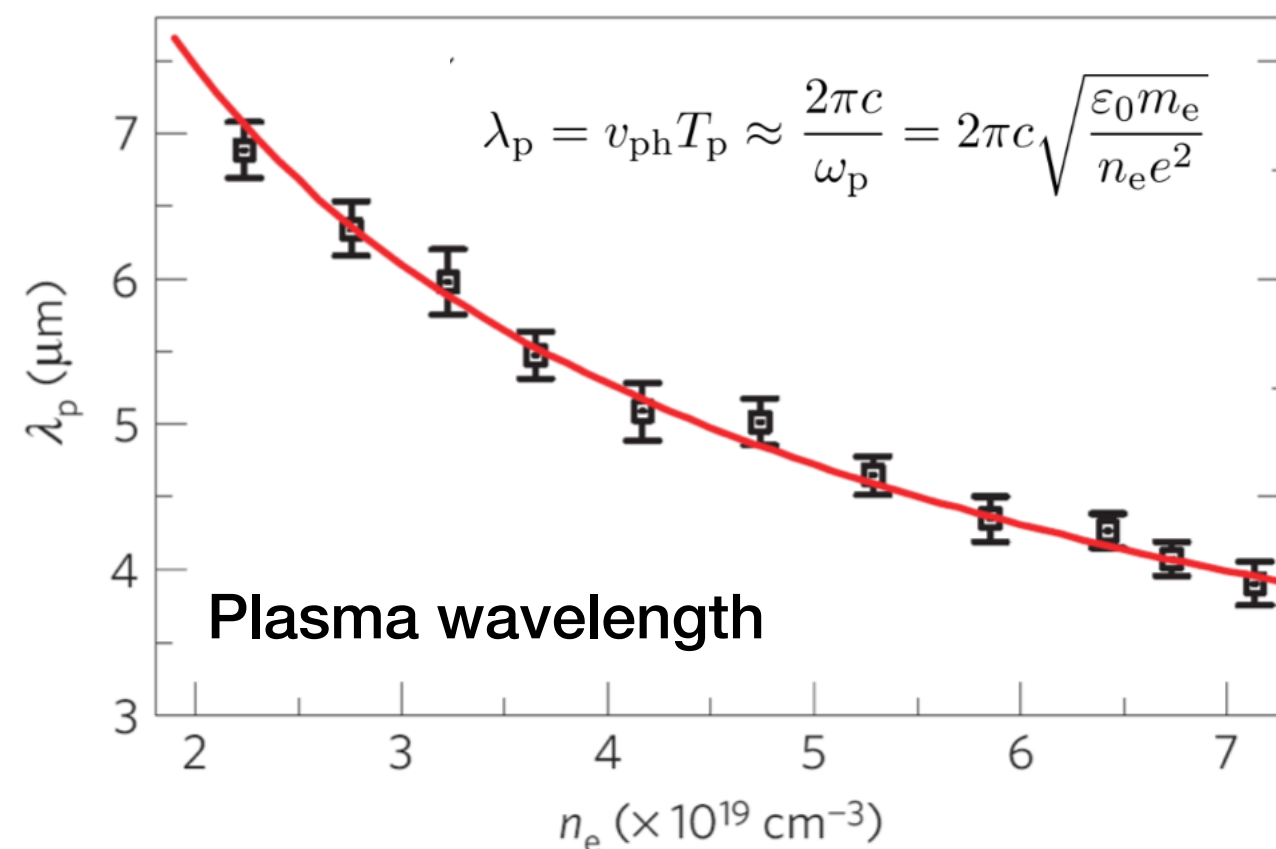
- > Few-cycle probe pulse generation with hollow-core-fiber chirped mirror compressor
- > 5.9 fs beam generated from 35 fs FWHM Ti:sa pulse

M. Schwab *et al.*,  
Appl. Phys. Lett. 103, 191118 (2013)

- > Visualize wakefield structure

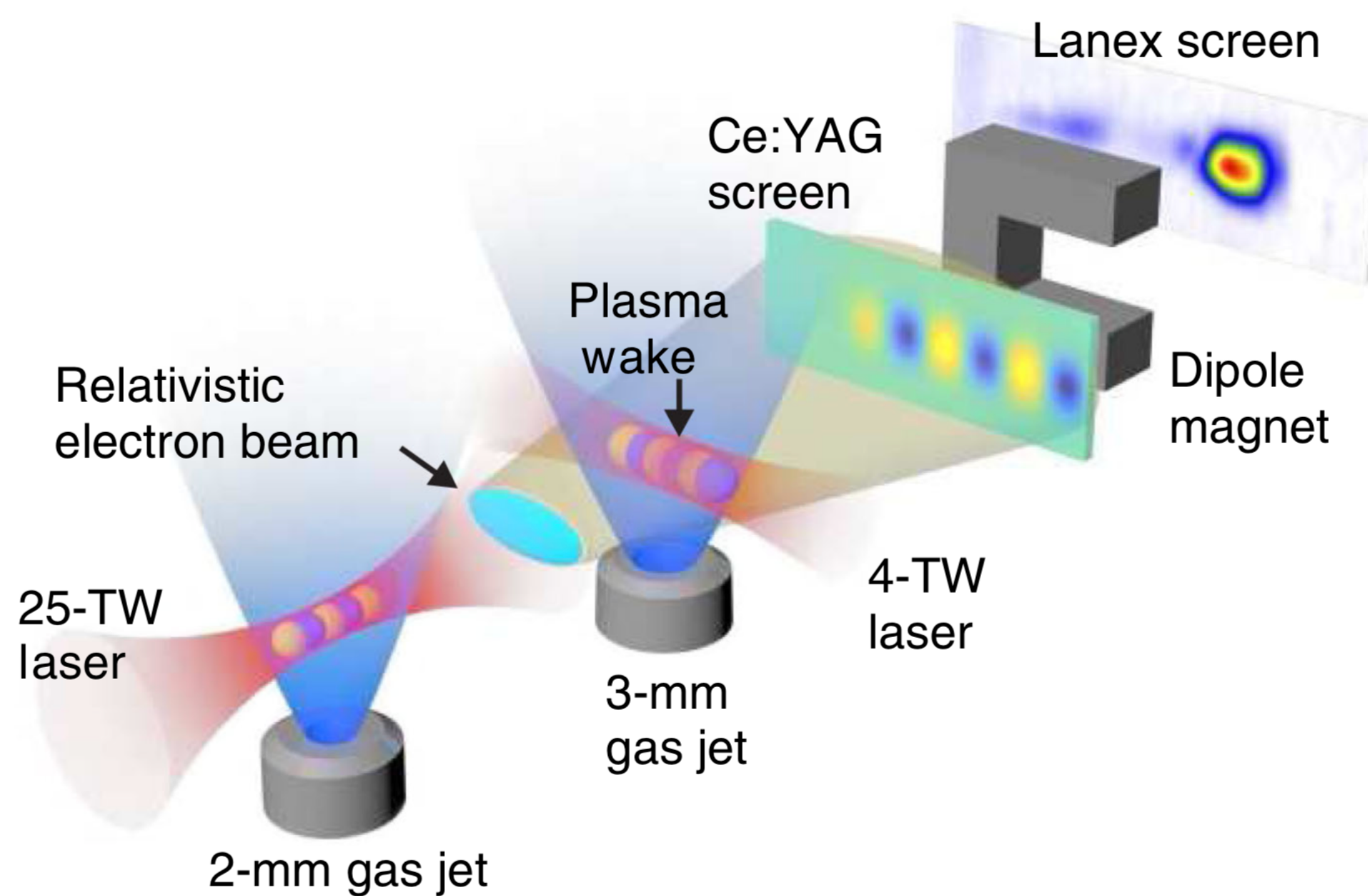


M. Schnell *et al.*, Nat. Comm. 4, 2421 (2013)

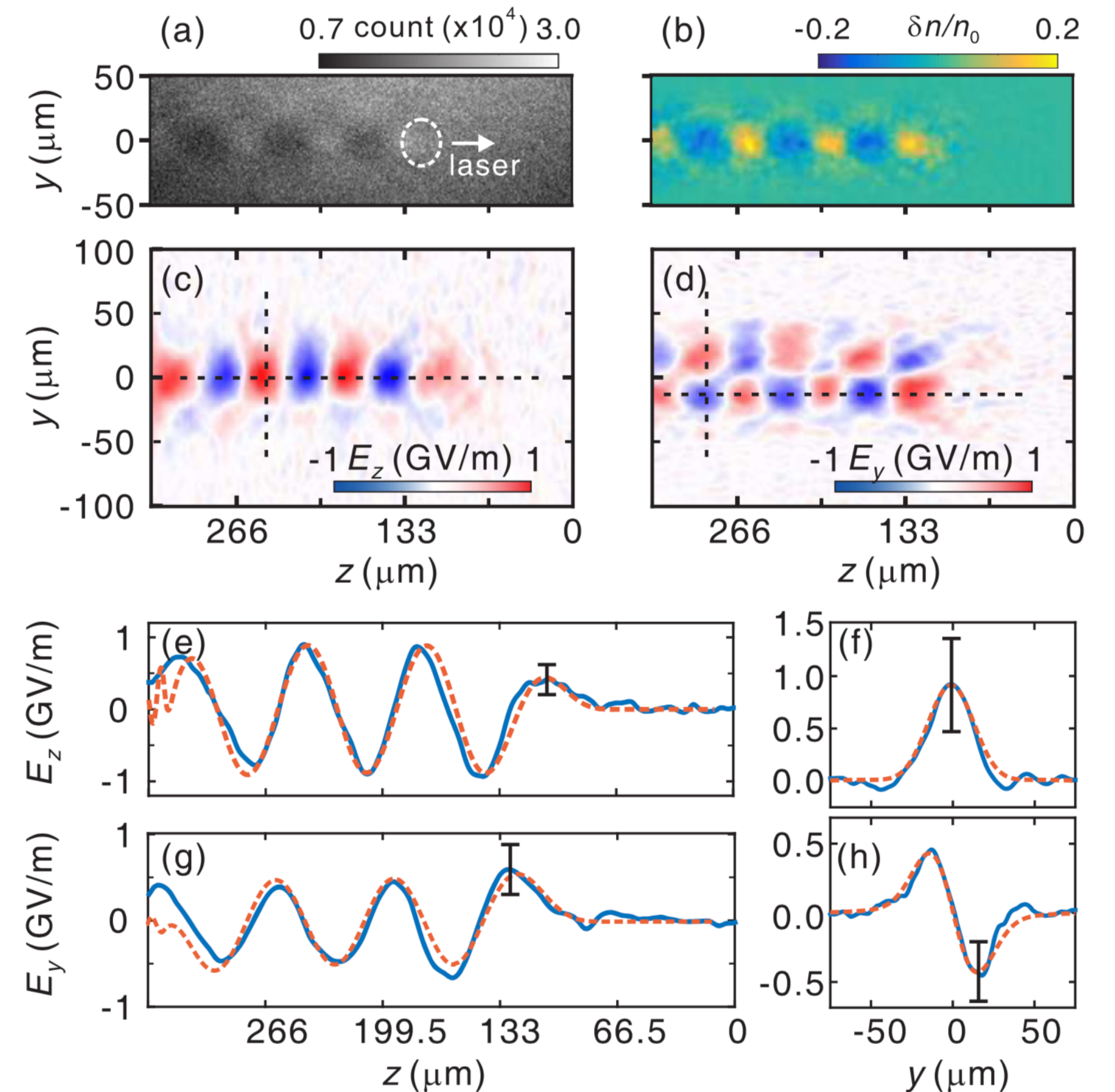


# Electron beams: electric field probes

> Relativistic electron beams can act as femtosecond transverse probes to measure electric fields

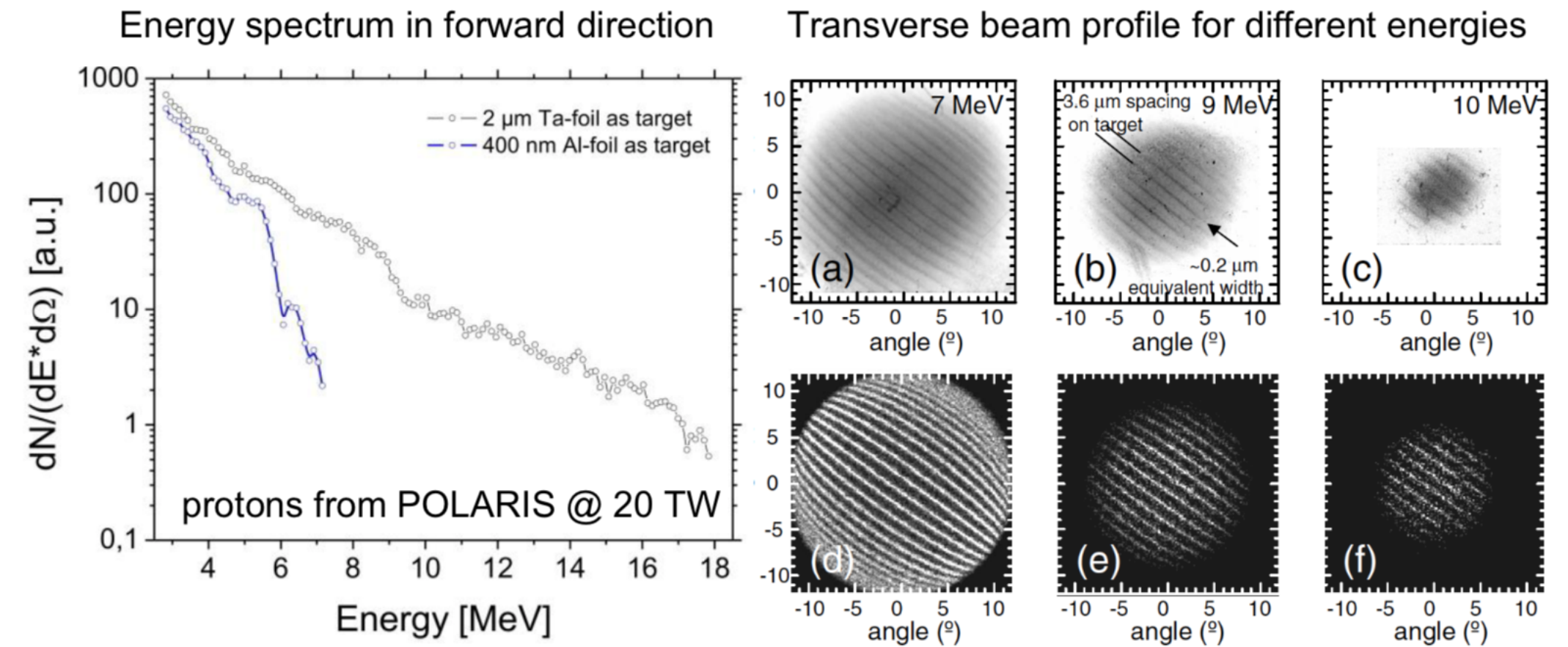


C. J. Zhang *et al.*, PRL 119, 064801 (2017)



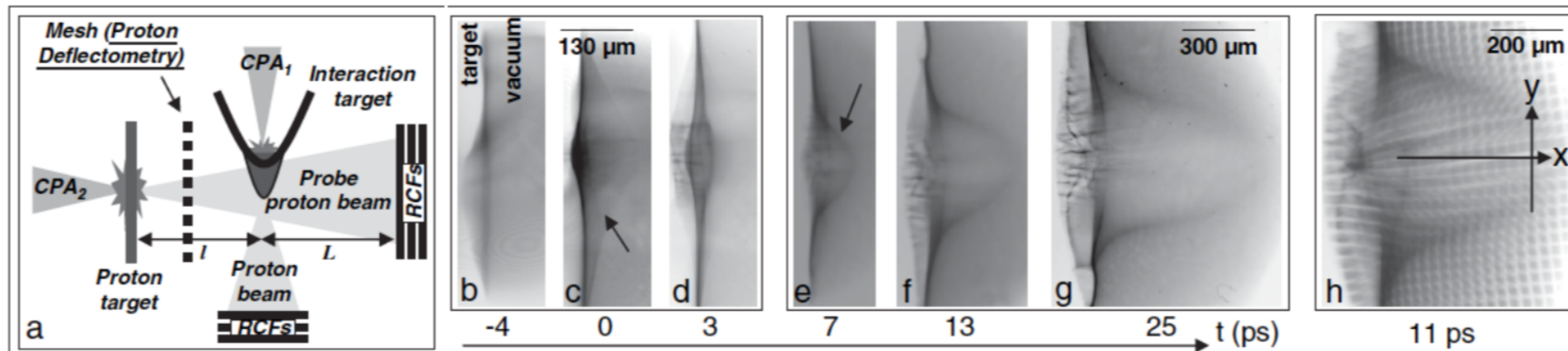
# Proton beams: electric field probes

- > Probing with laser-accelerated proton beams
  - broad energy spectrum (up to 10s of MeV)
  - laminar flow → excellent imaging properties
  - different energies arrive at target at different times → single-shot movie



T. E. Cowan, PRL (2004)

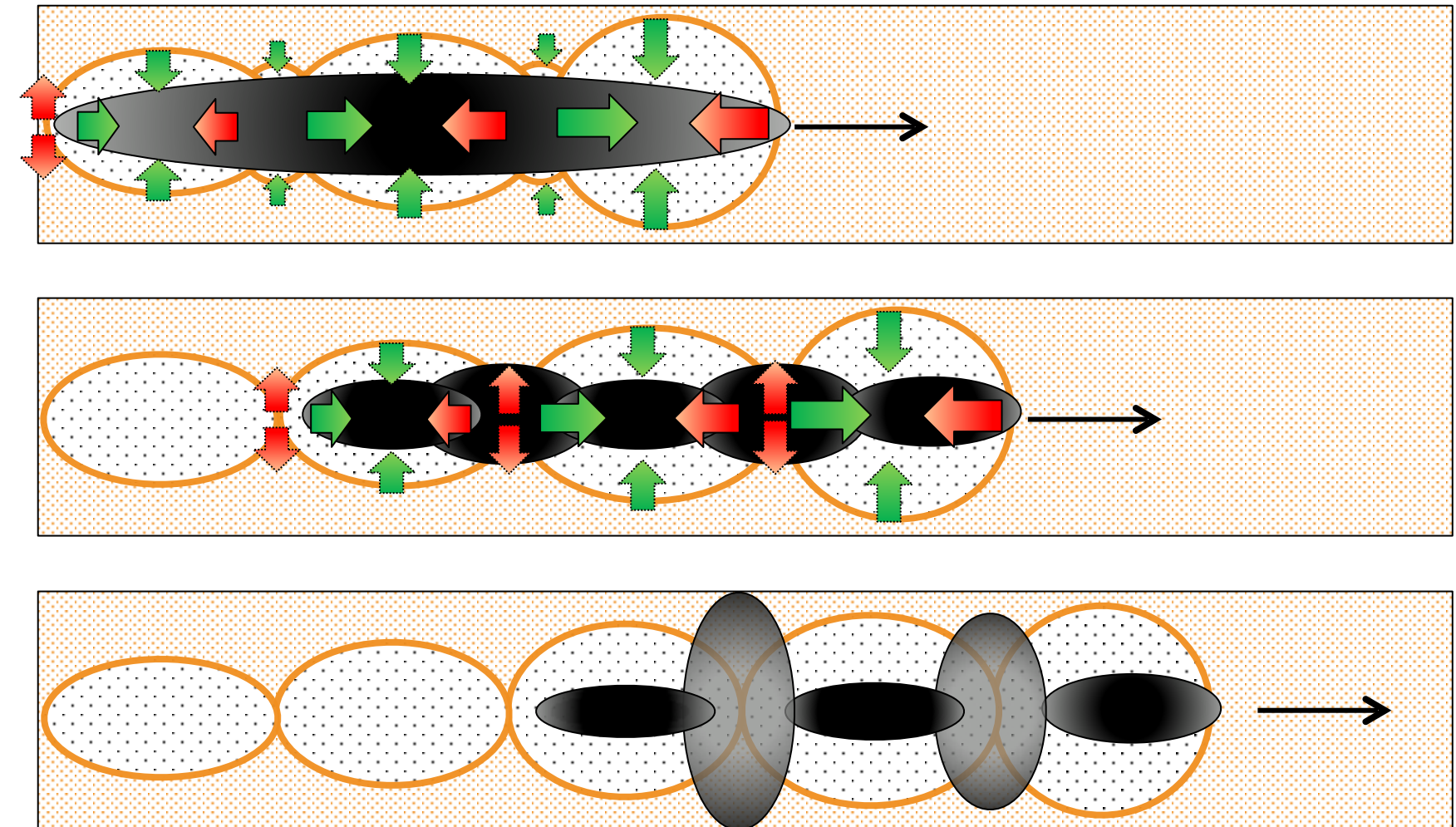
- > *Example:* record TNSA-sheath evolution in a single shot  
deduce sheath-field strength from mesh warping  $E_{\text{TNSA}} \geq 3 \times 10^{10}$  V/m



L. Romagnani, PRL (2005)

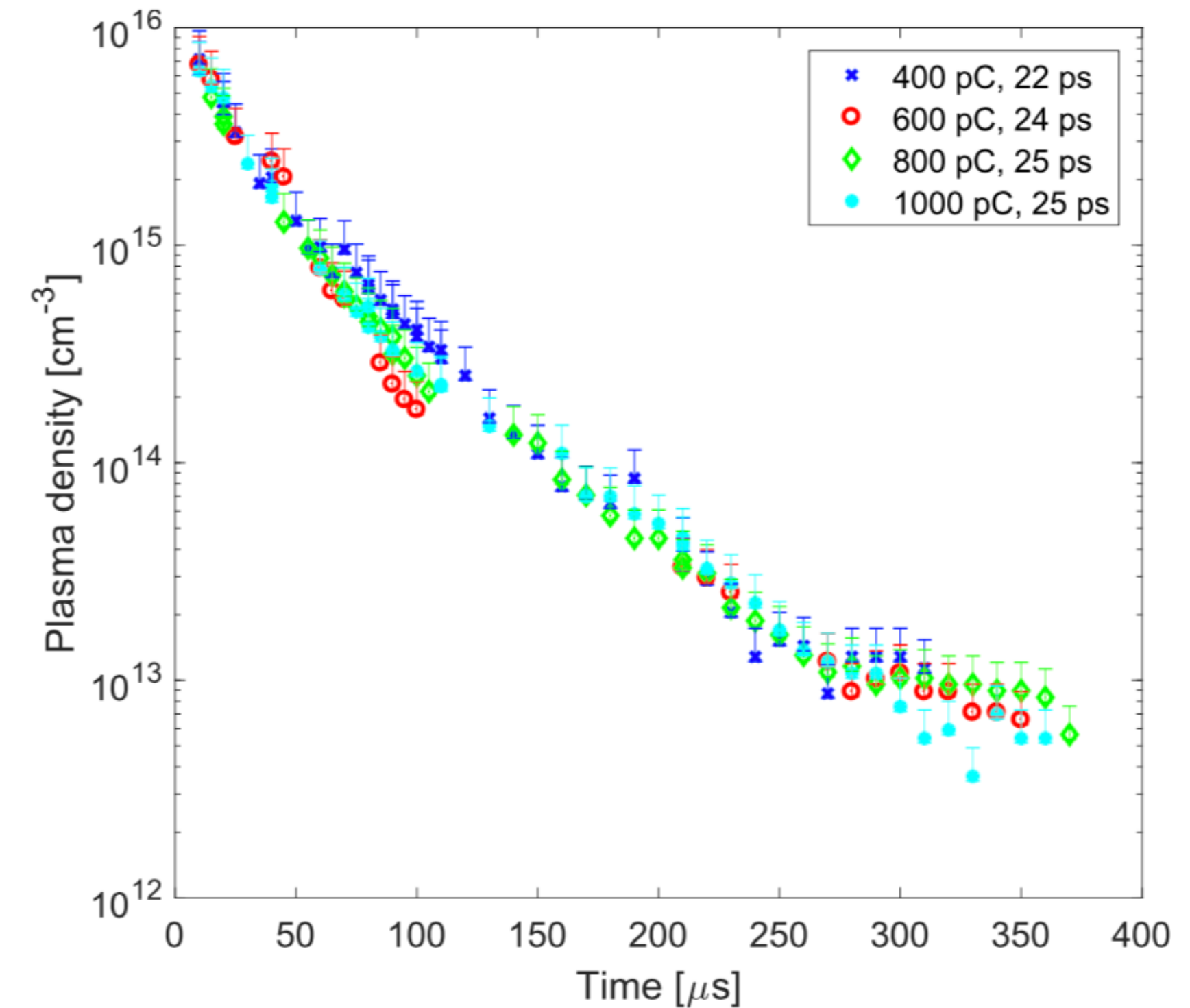
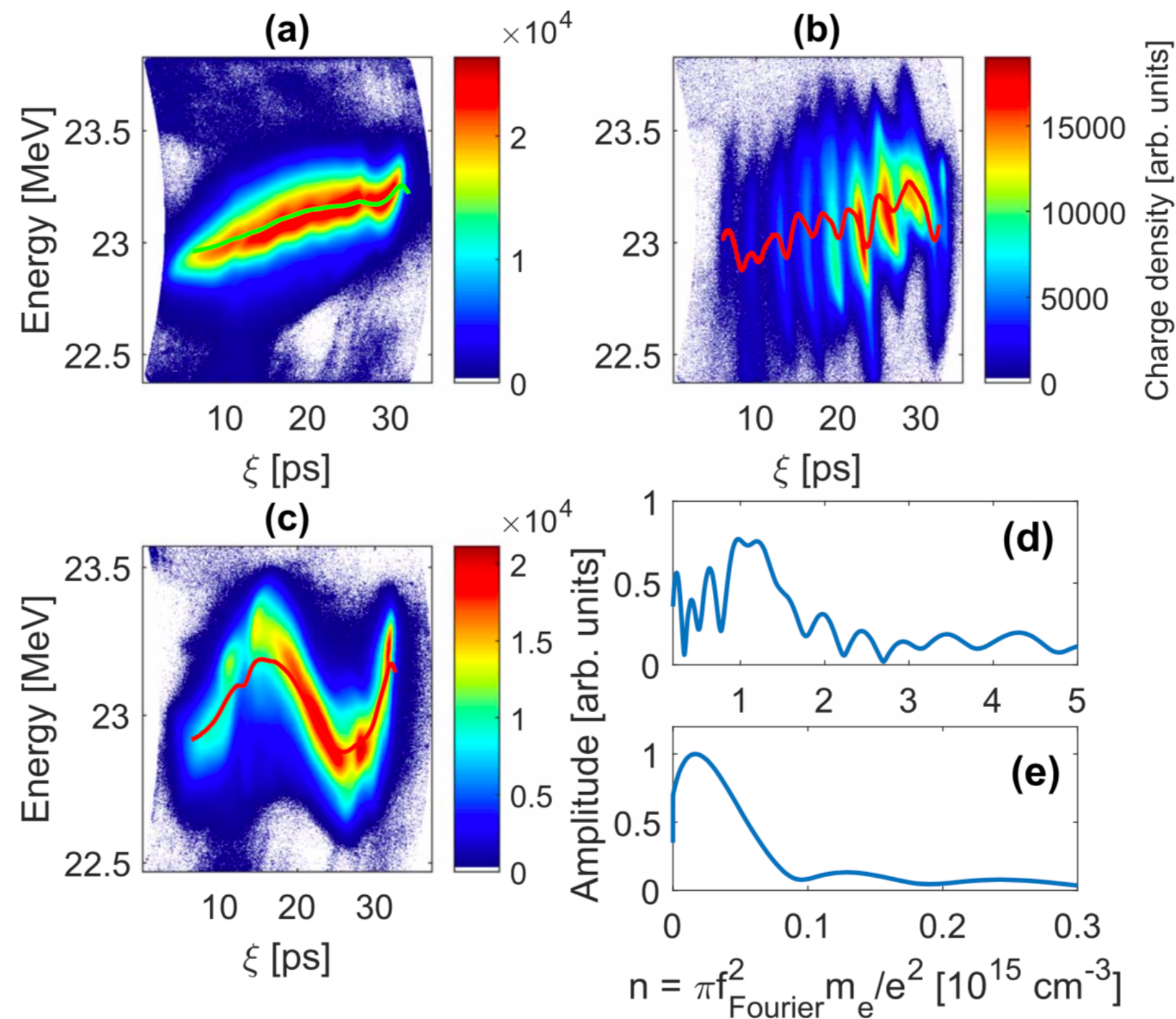
# Particle beams: self-modulation instability as a probe

- > Transverse modulation of long bunches ( $L_{\text{bunch}} > \lambda_{\text{plasma}}$ )
- > Initiated by inhomogeneities in focusing forces
- > Provides proton driver trains for AWAKE
- > Length scales are plasma density dependent  
→ diagnostic
  - Observe periodicity of longitudinal phase space
  - Dominant Fourier components reflect  $\lambda_p$
  - Longitudinally integrating technique
  - Works over large range of  $n_e$



# Particle beams: self-modulation instability as a probe

G. Loisch *et al.*, Plasma Phys. Control. Fusion **61**, 045012 (2019)

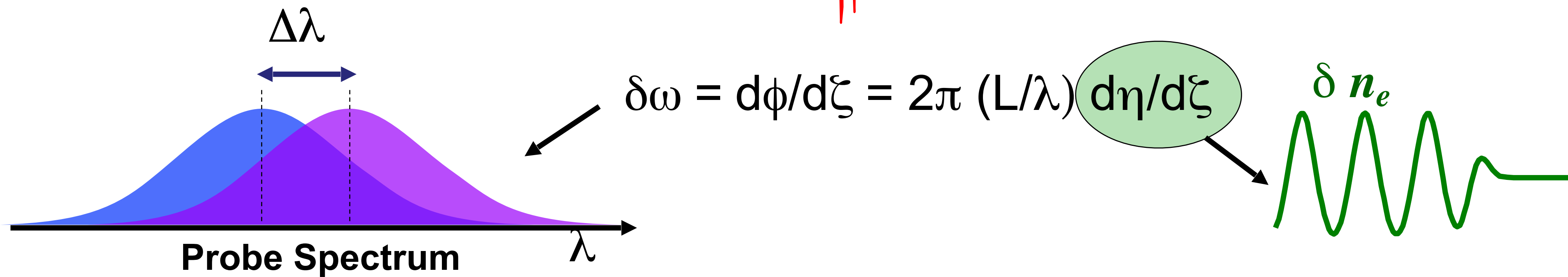
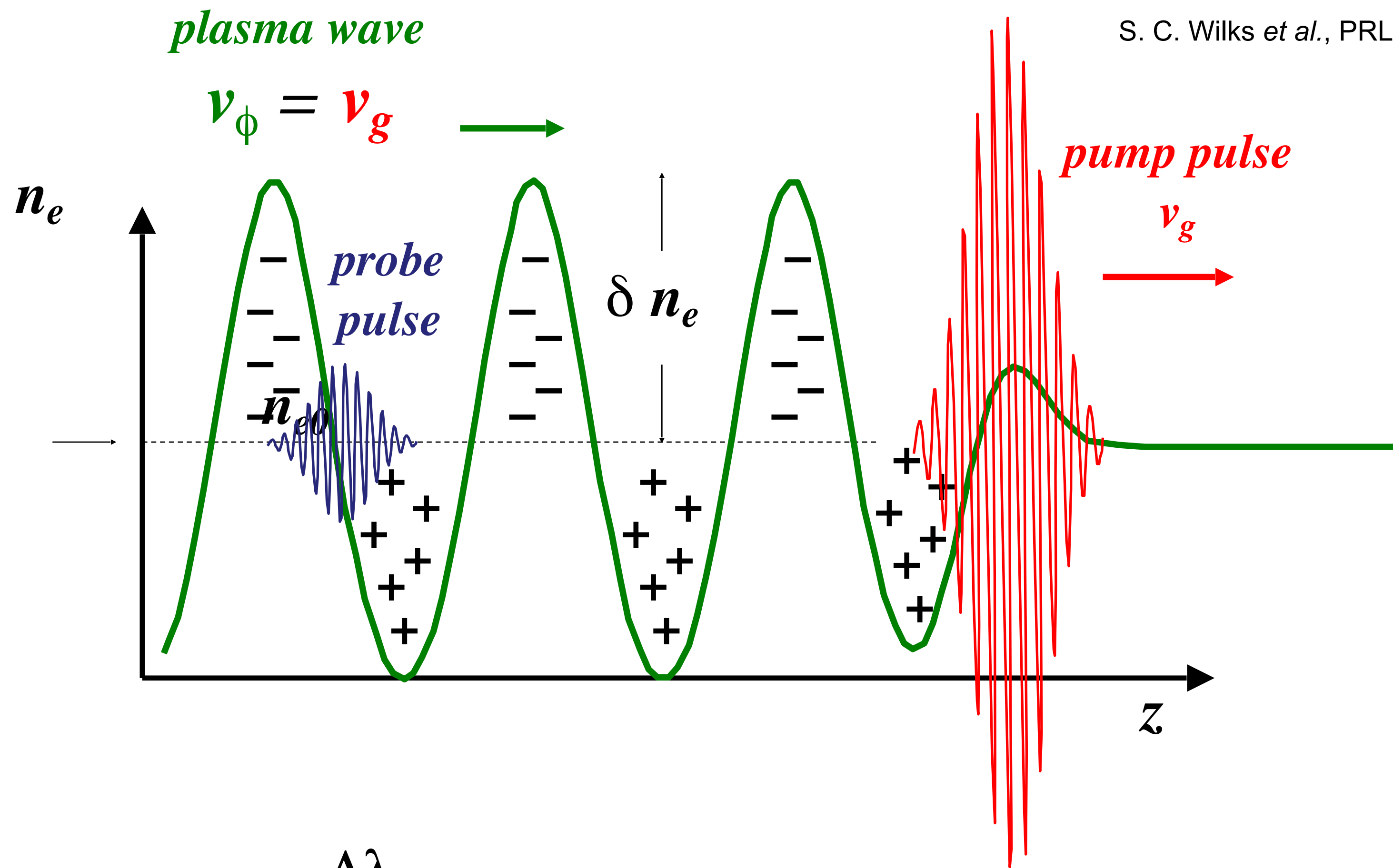


# Frequency Domain Holography

- > Thanks to Nicholas Matlis (DESY) for providing the following slides
- > For detailed info on FDH and its variants TEX and TESS, please refer to
  - FDH: N. H. Matlis *et al.*, Nature Physics 2, 749 (2006)
  - TEX: N. H. Matlis *et al.*, JOSA B 28, 23 (2011)
  - TESS: N. H. Matlis *et al.*, Optics Letters 41, 5503 (2016)

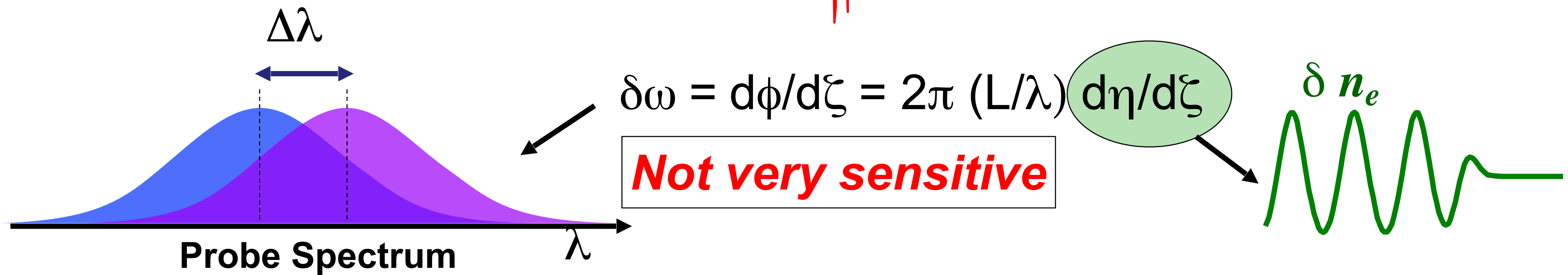
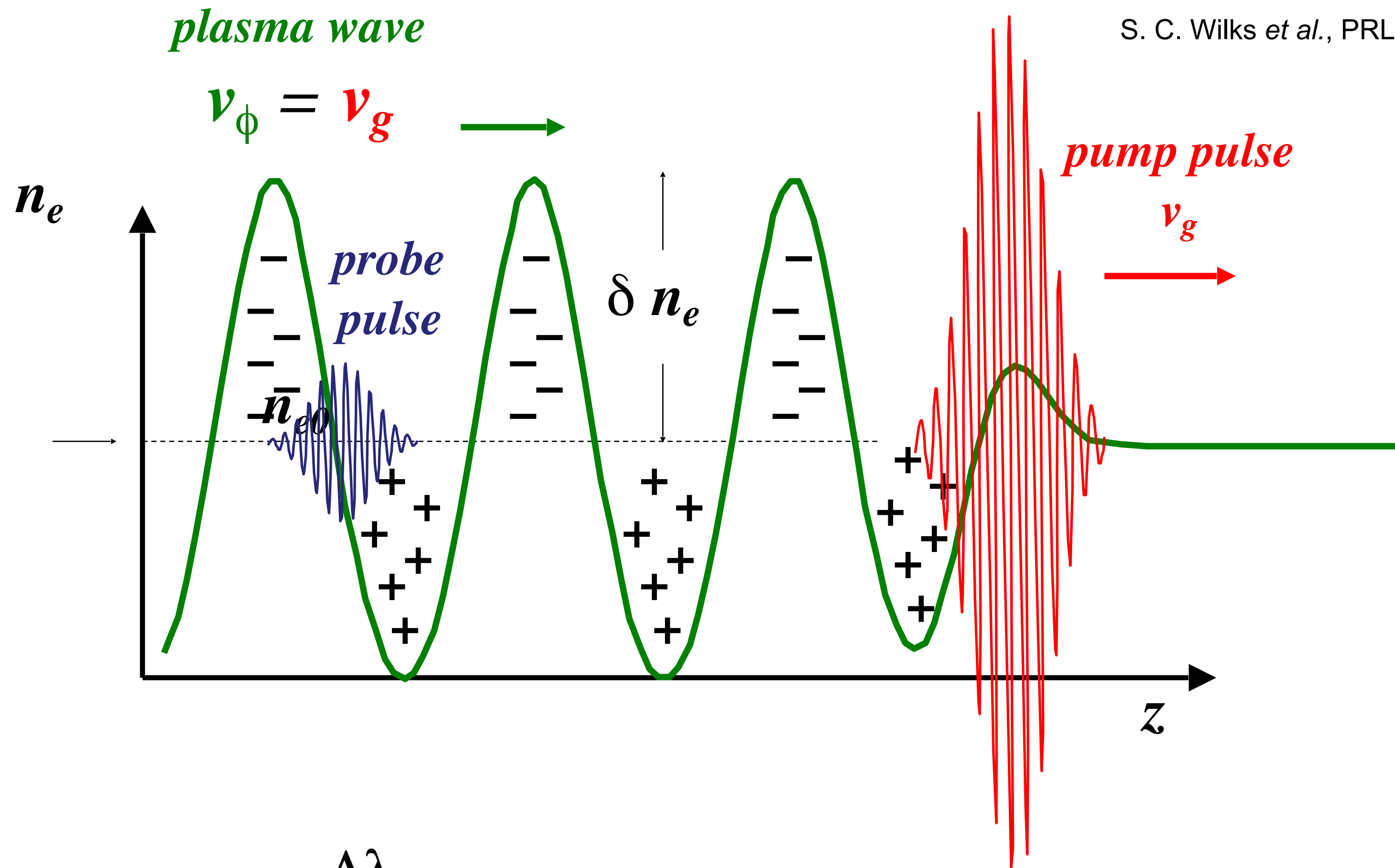
# Photon Acceleration

S. C. Wilks *et al.*, PRL (1989)



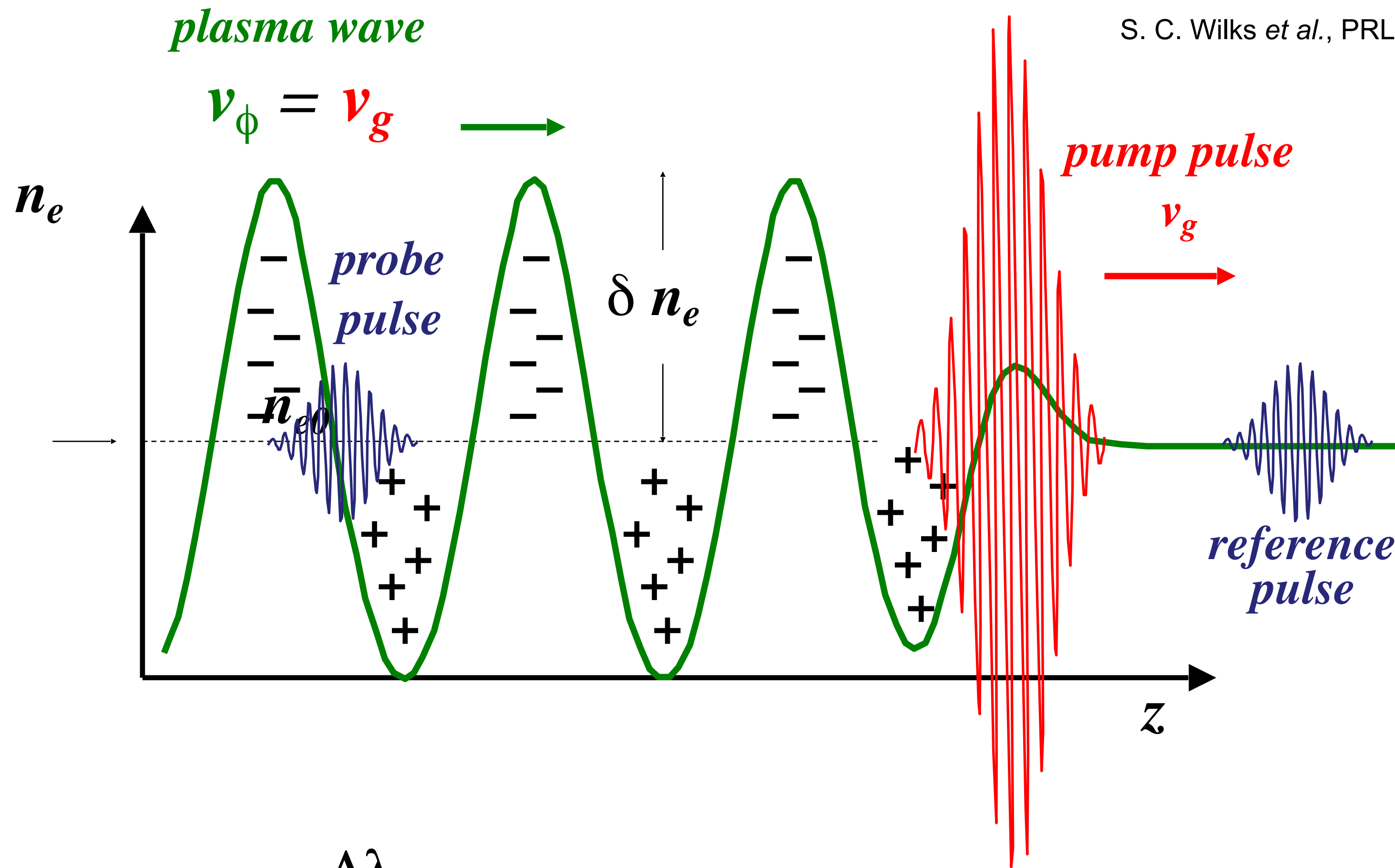
# Photon Acceleration

S. C. Wilks *et al.*, PRL (1989)

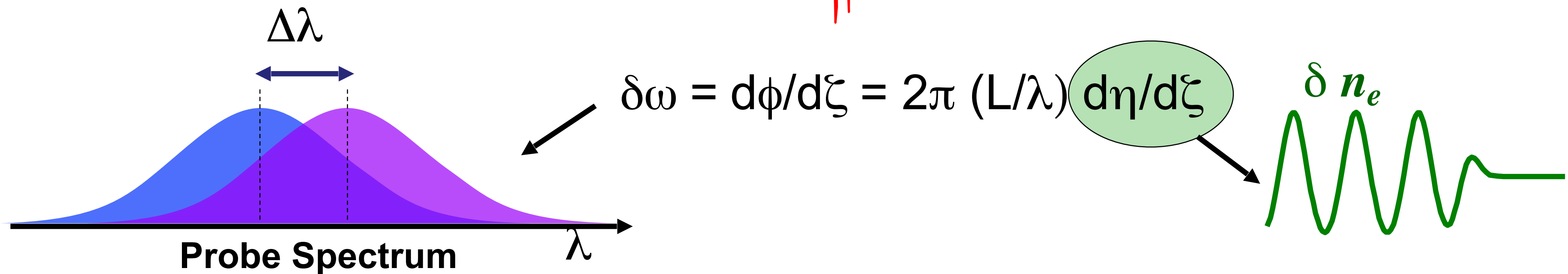


# Photon Acceleration

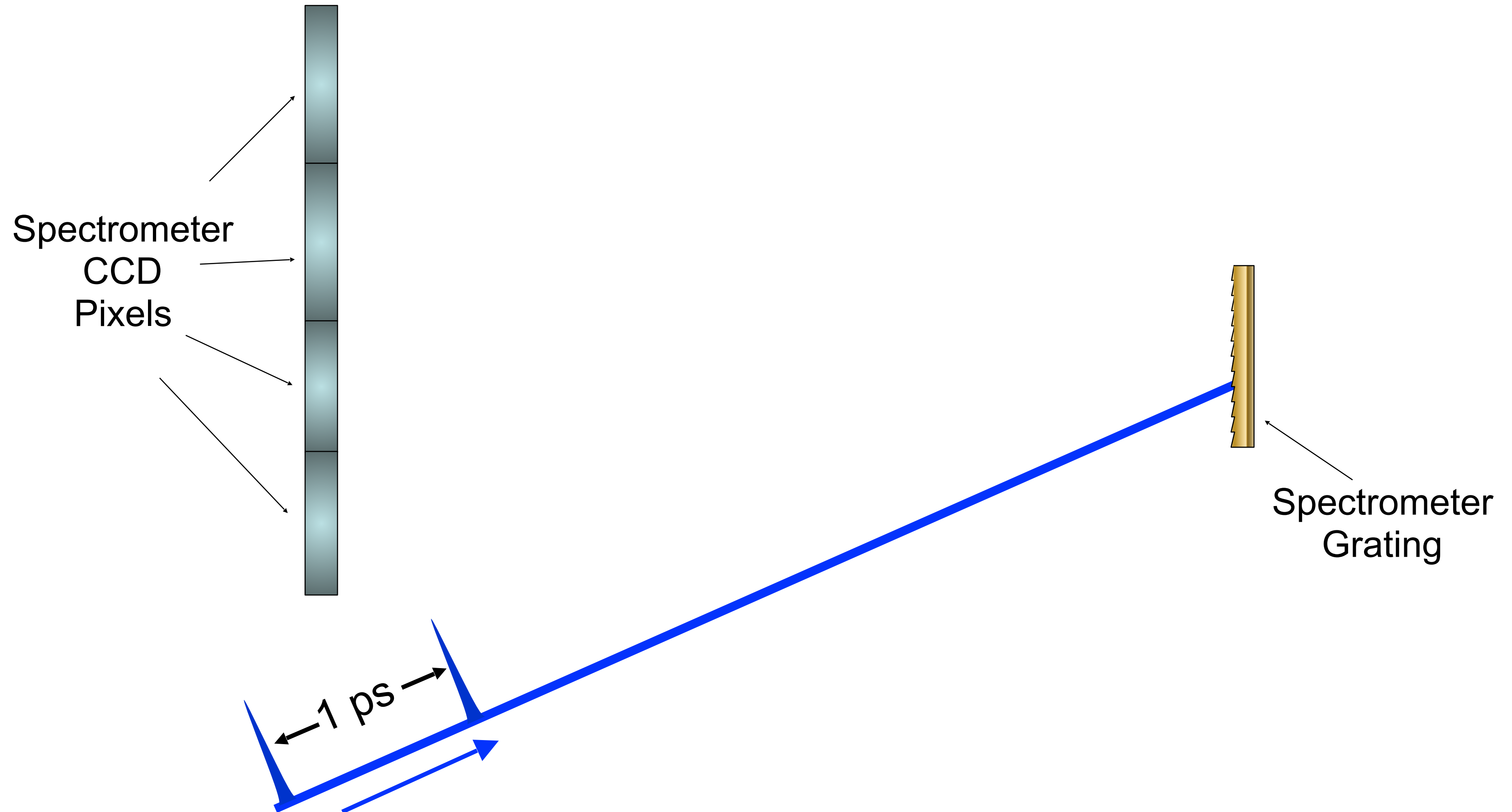
S. C. Wilks *et al.*, PRL (1989)



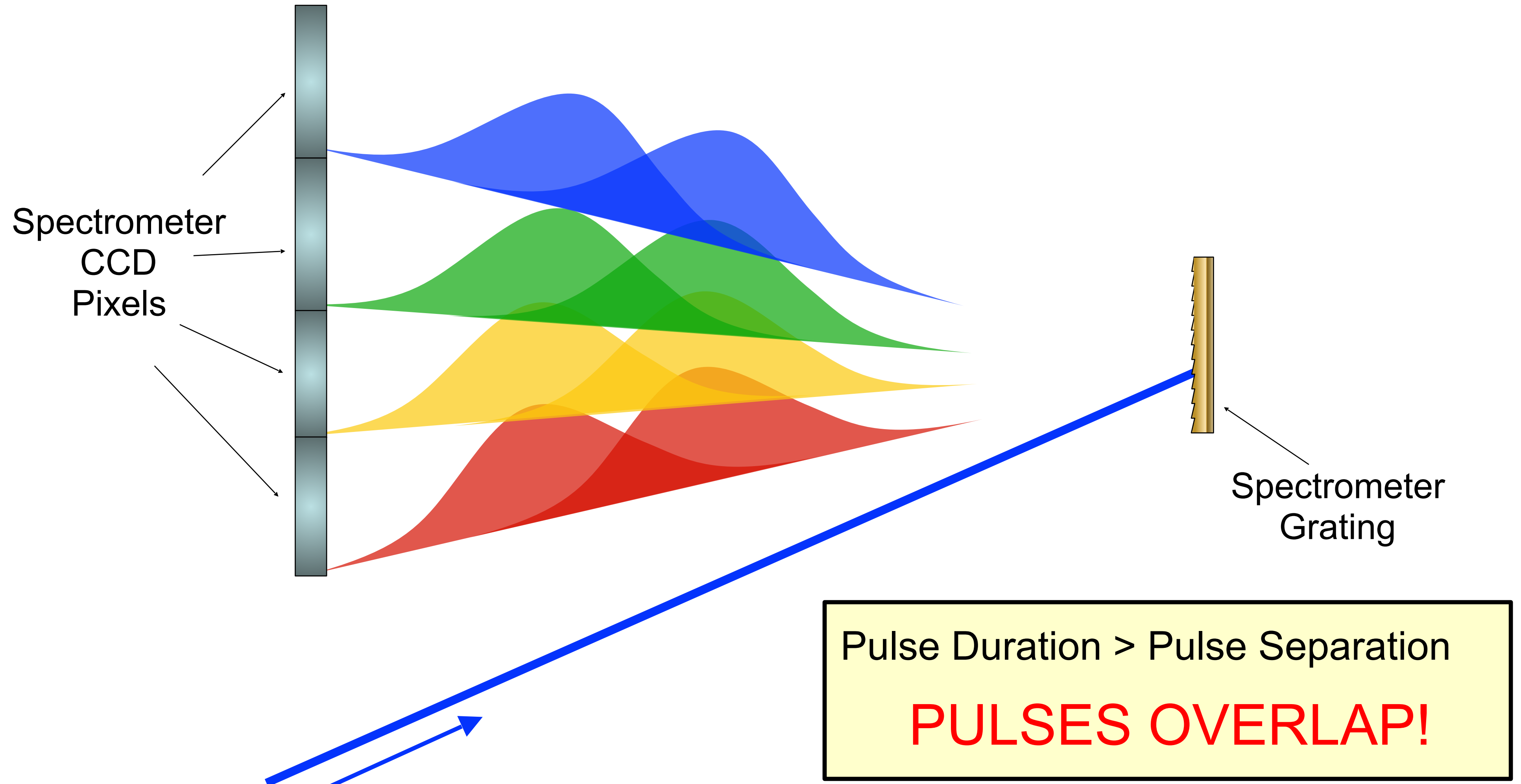
How do pulses that don't overlap interfere?



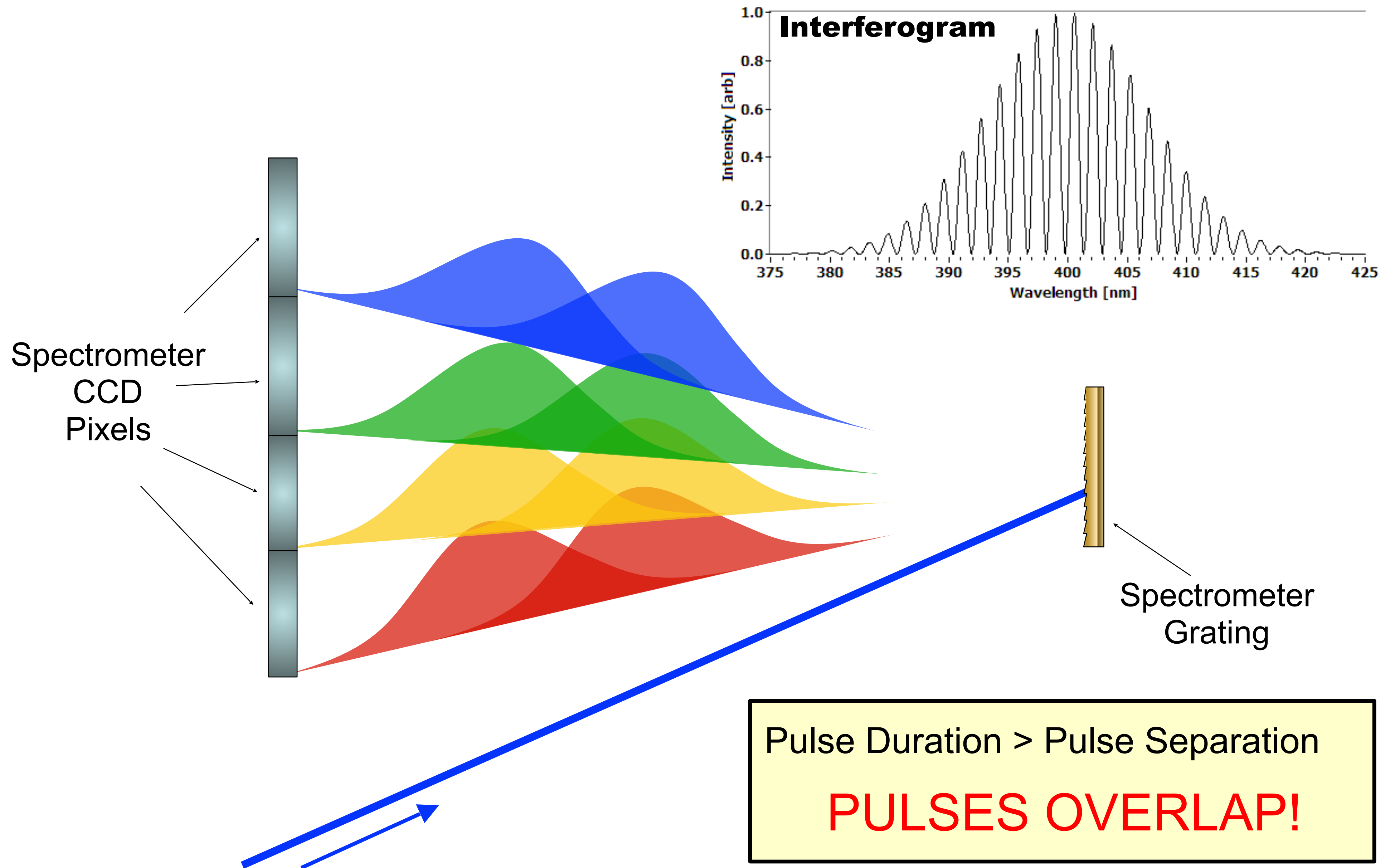
# FDI: Temporal Overlap in Spectrometer



# FDI: Temporal Overlap in Spectrometer



# FDI: Temporal Overlap in Spectrometer

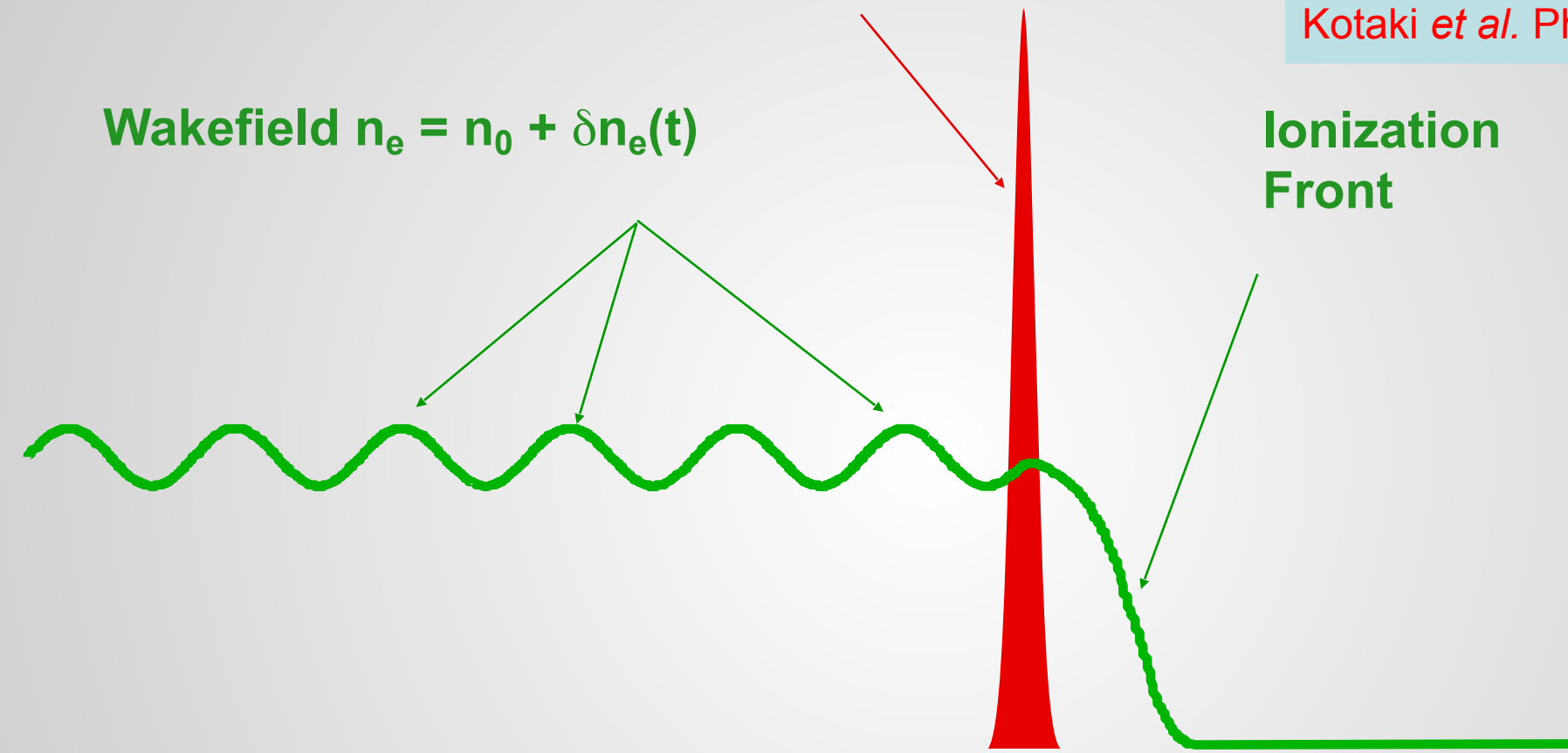


# “Frequency Domain Interferometry” probes Wakefields one point at a time

intense Pump Pulse, 25 mJ, 80 fs, 800 nm

Wakefield  $n_e = n_0 + \delta n_e(t)$

Ionization  
Front



Siders *et al.* Phys. Rev. Lett. **76**, 3570 (1996)

Marques *et al.* Phys. Plasmas **10**, 1124 (1998)

Kotaki *et al.* Phys. Plasmas **9**, 1392 (2002)

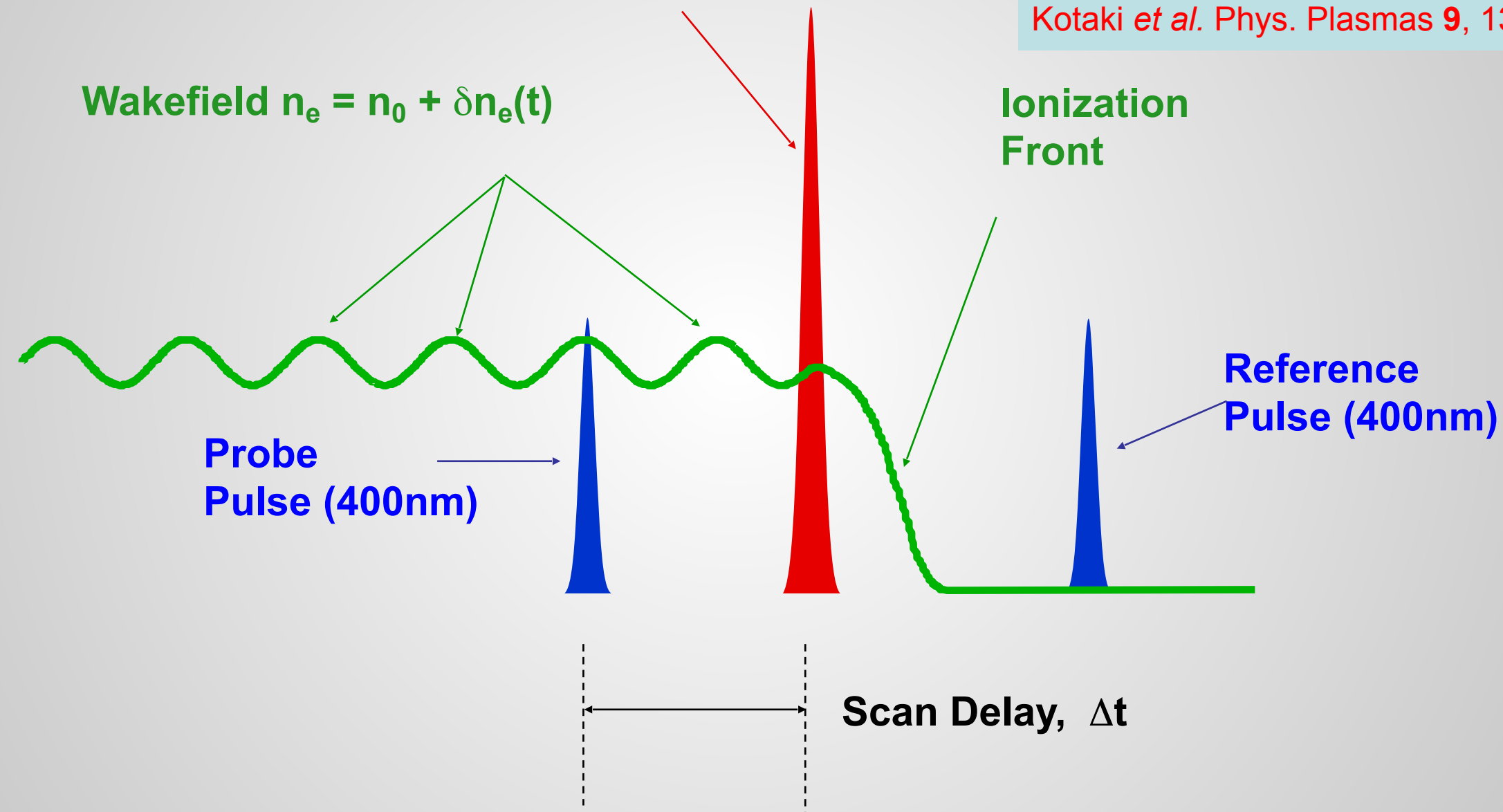
# “Frequency Domain Interferometry” probes Wakefields one point at a time

intense Pump Pulse, 25 mJ, 80 fs, 800 nm

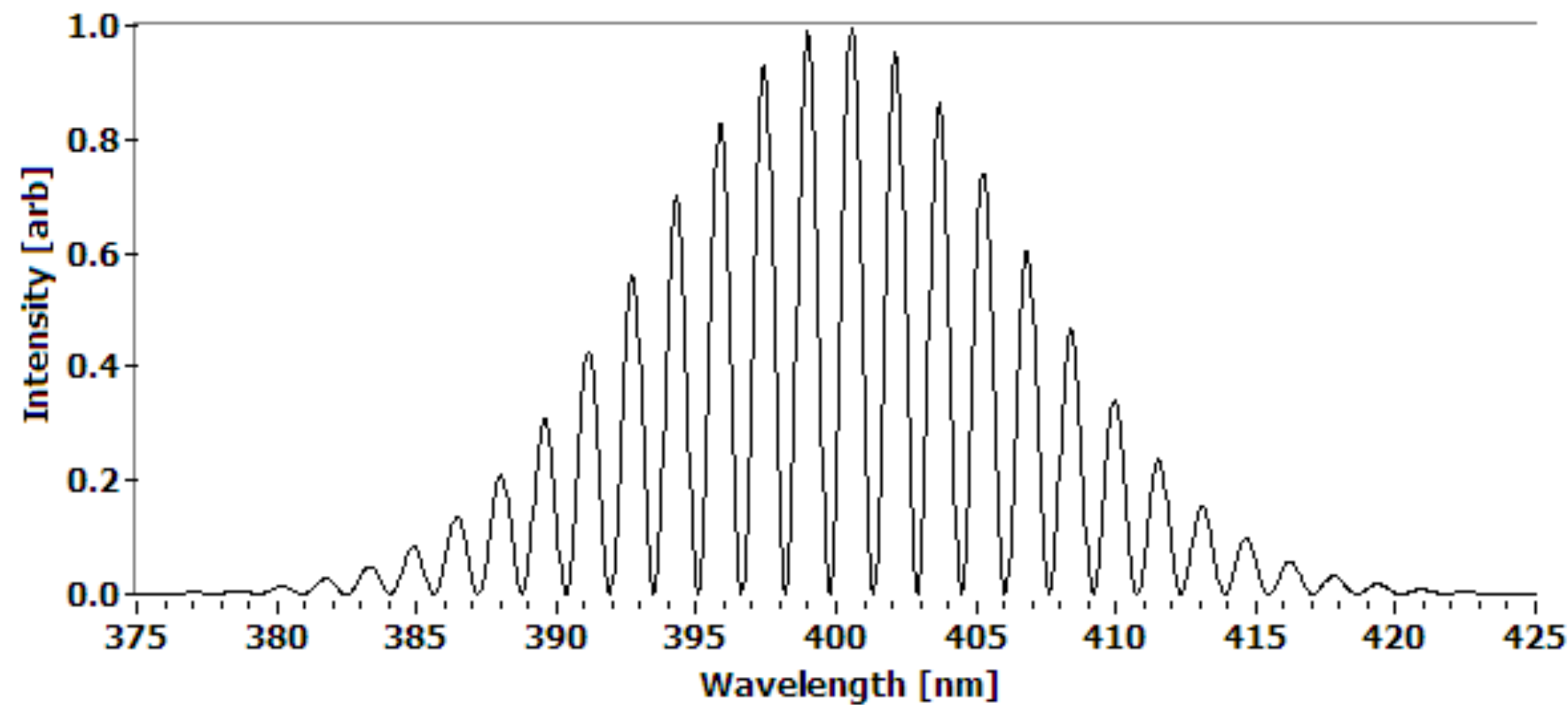
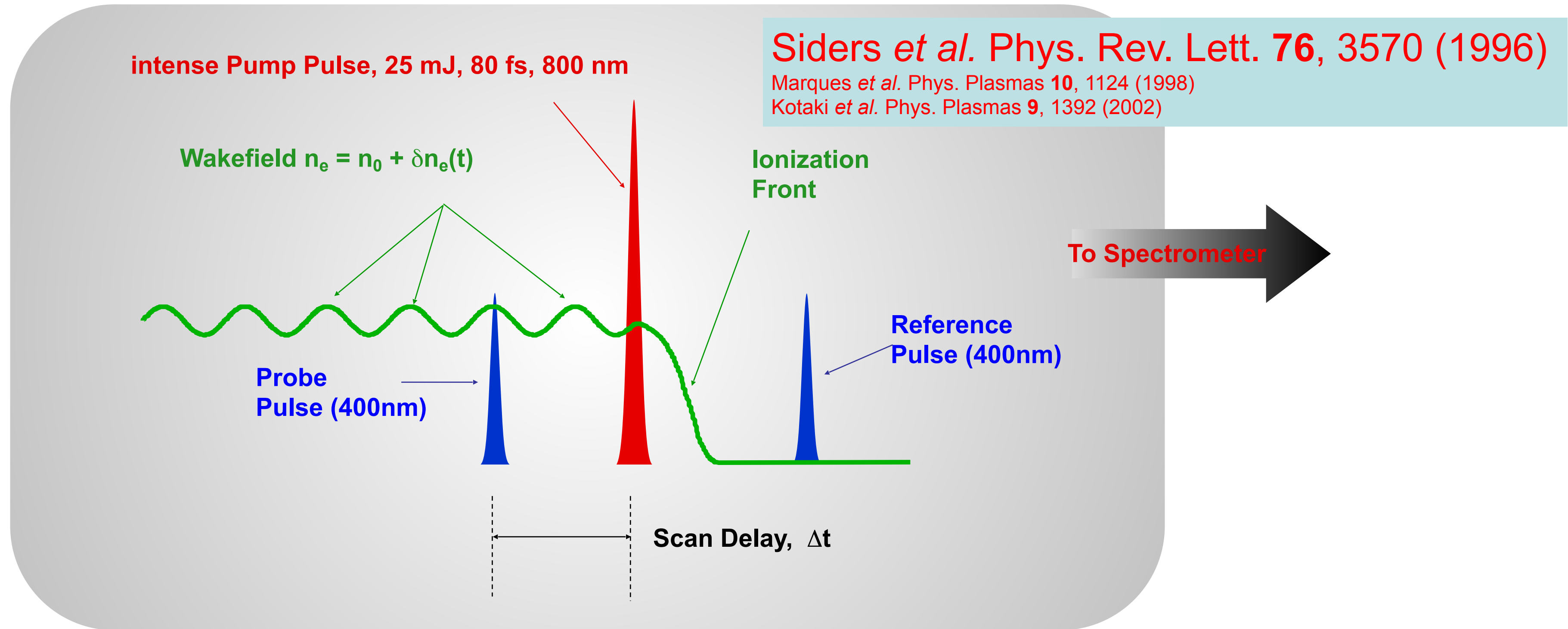
Siders *et al.* Phys. Rev. Lett. **76**, 3570 (1996)

Marques *et al.* Phys. Plasmas **10**, 1124 (1998)

Kotaki *et al.* Phys. Plasmas **9**, 1392 (2002)



# “Frequency Domain Interferometry” probes Wakefields one point at a time

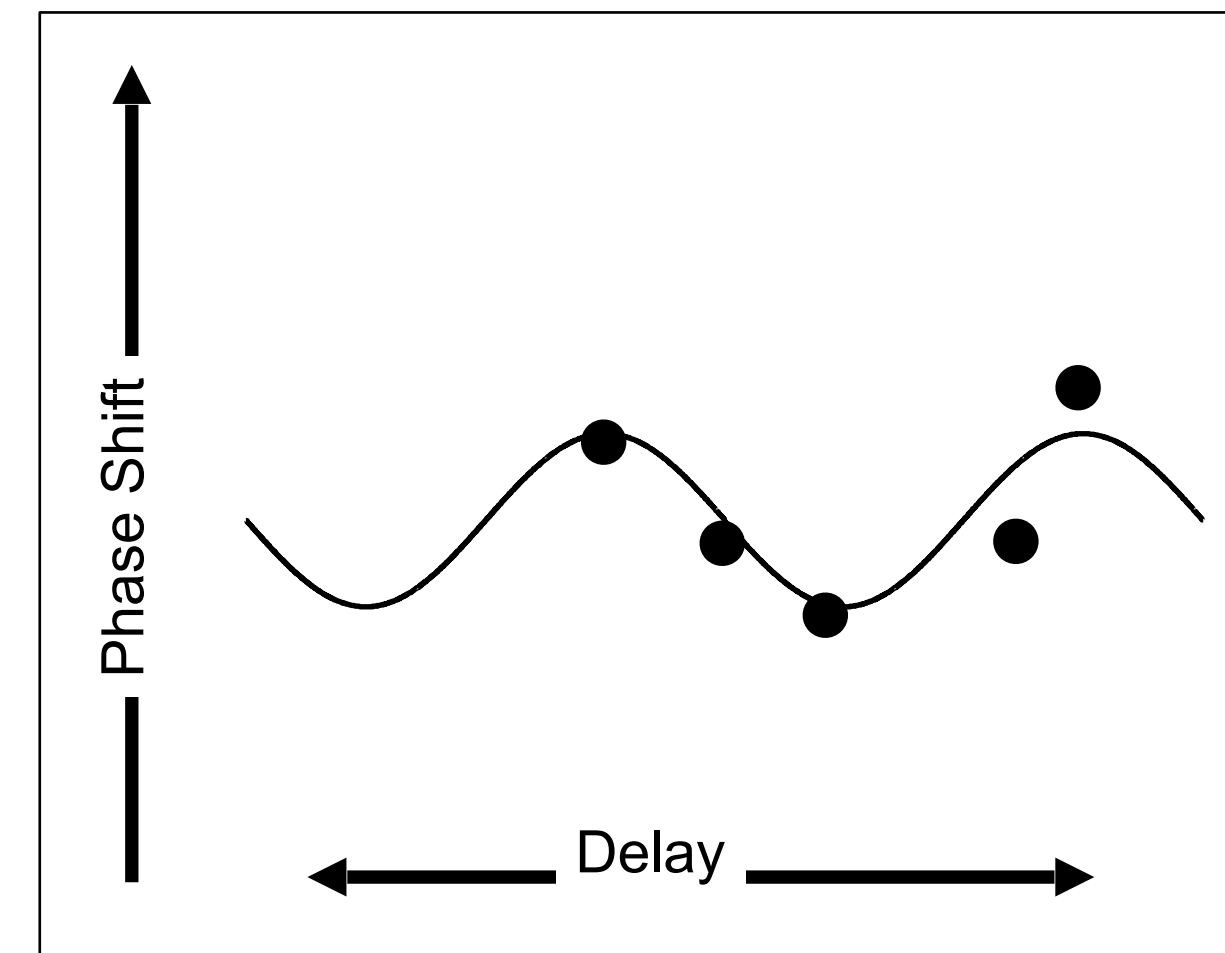
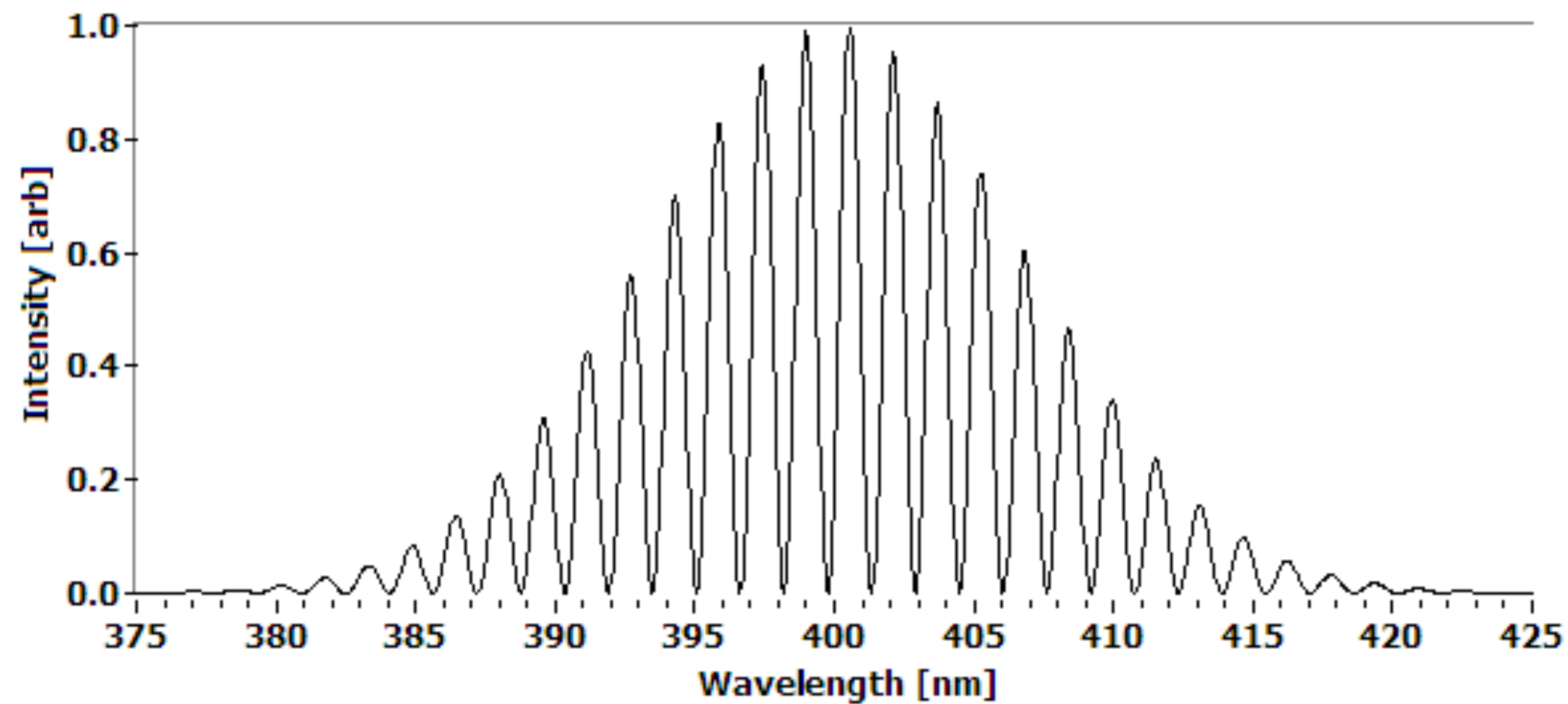
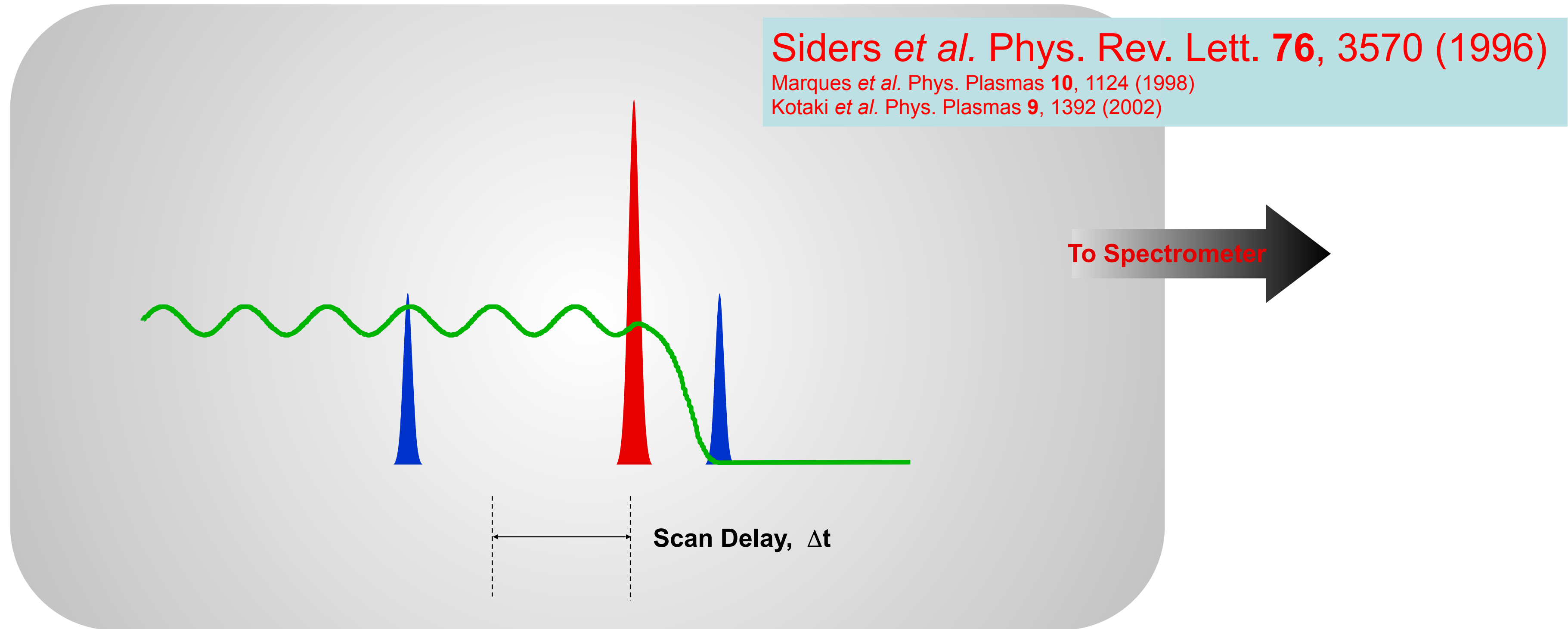


# “Frequency Domain Interferometry” probes Wakefields one point at a time

Siders *et al.* Phys. Rev. Lett. **76**, 3570 (1996)

Marques *et al.* Phys. Plasmas **10**, 1124 (1998)

Kotaki *et al.* Phys. Plasmas **9**, 1392 (2002)

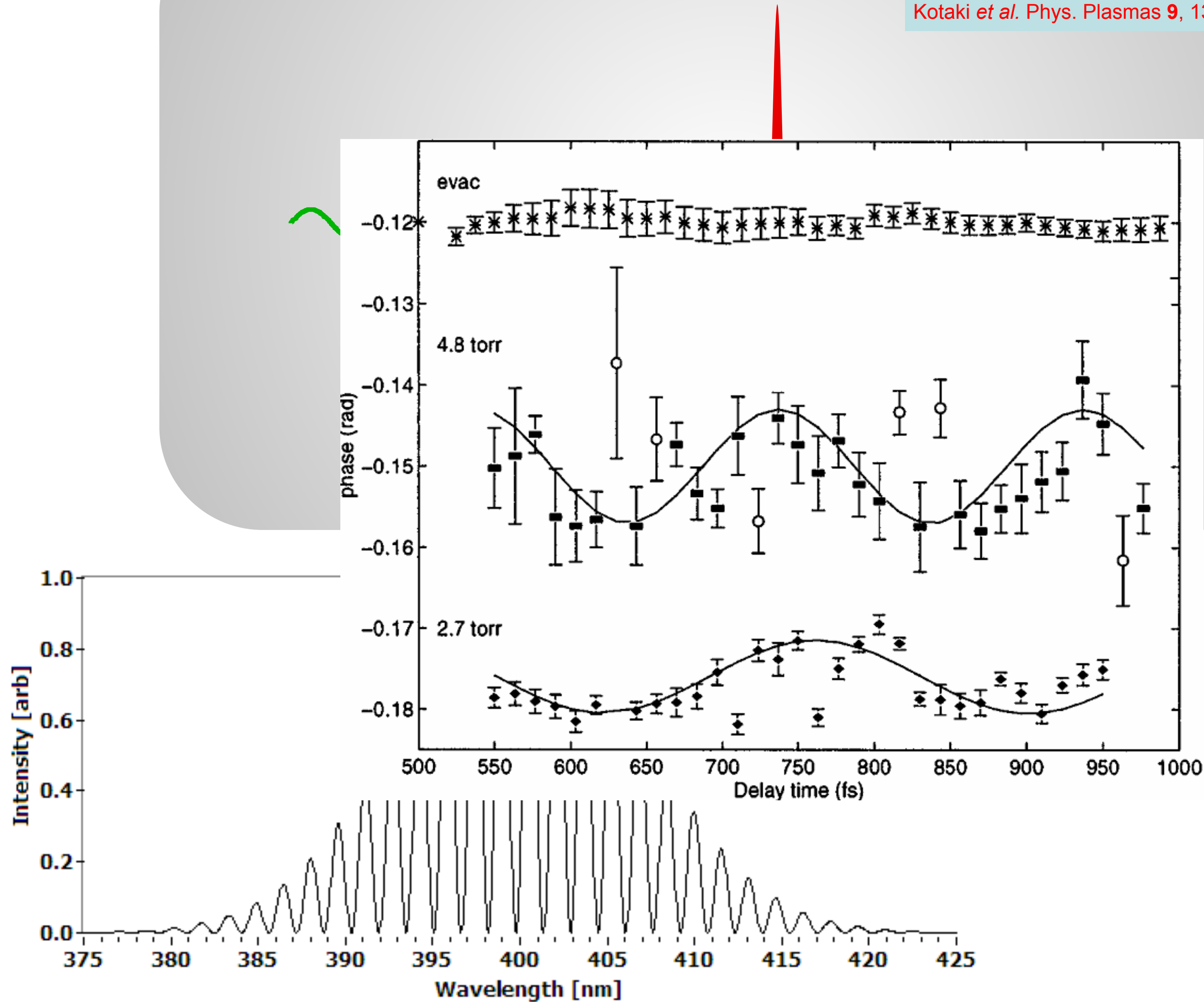


# “Frequency Domain Interferometry” probes Wakefields one point at a time

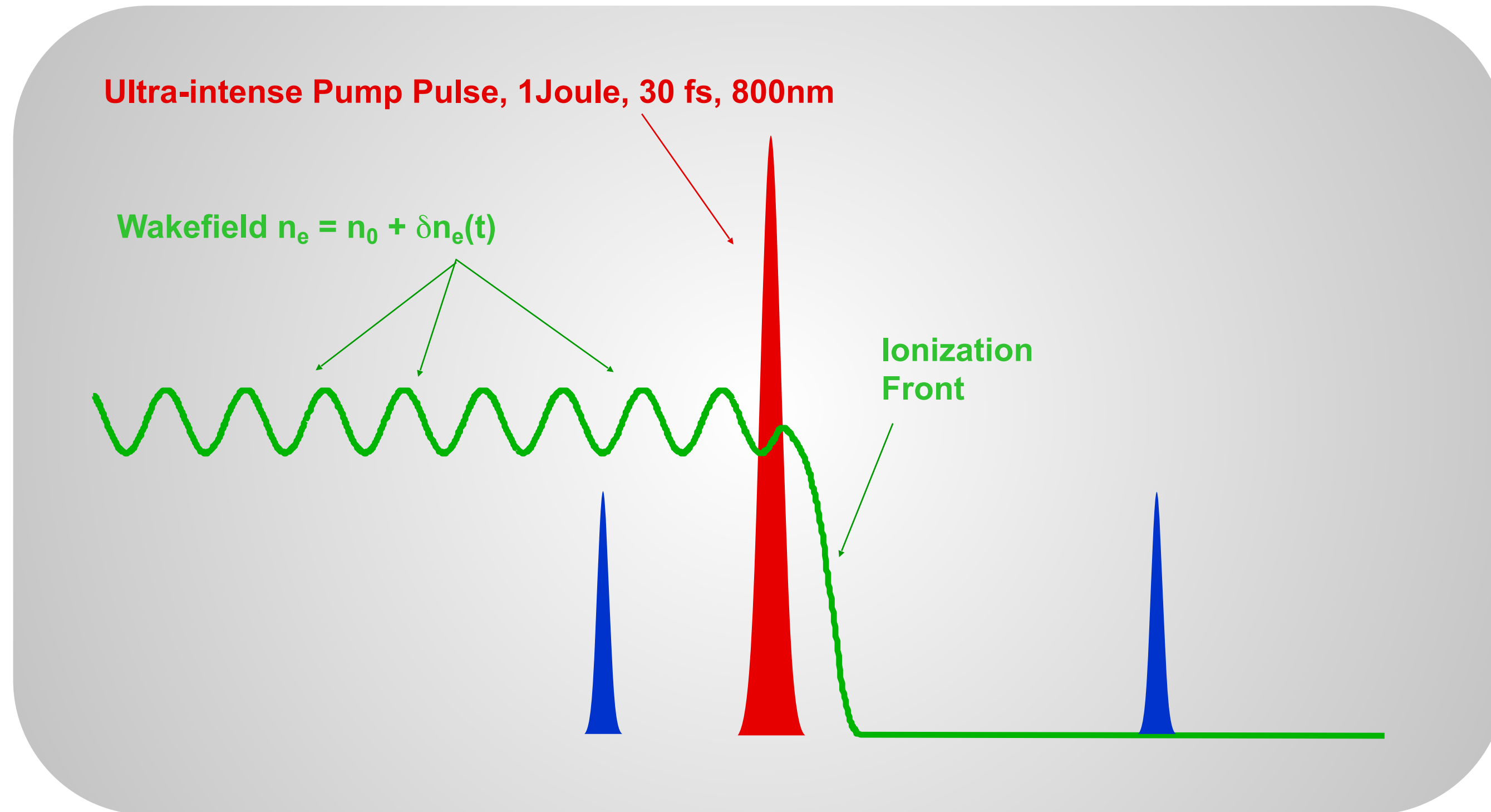
Siders *et al.* Phys. Rev. Lett. **76**, 3570 (1996)

Marques *et al.* Phys. Plasmas **10**, 1124 (1998)

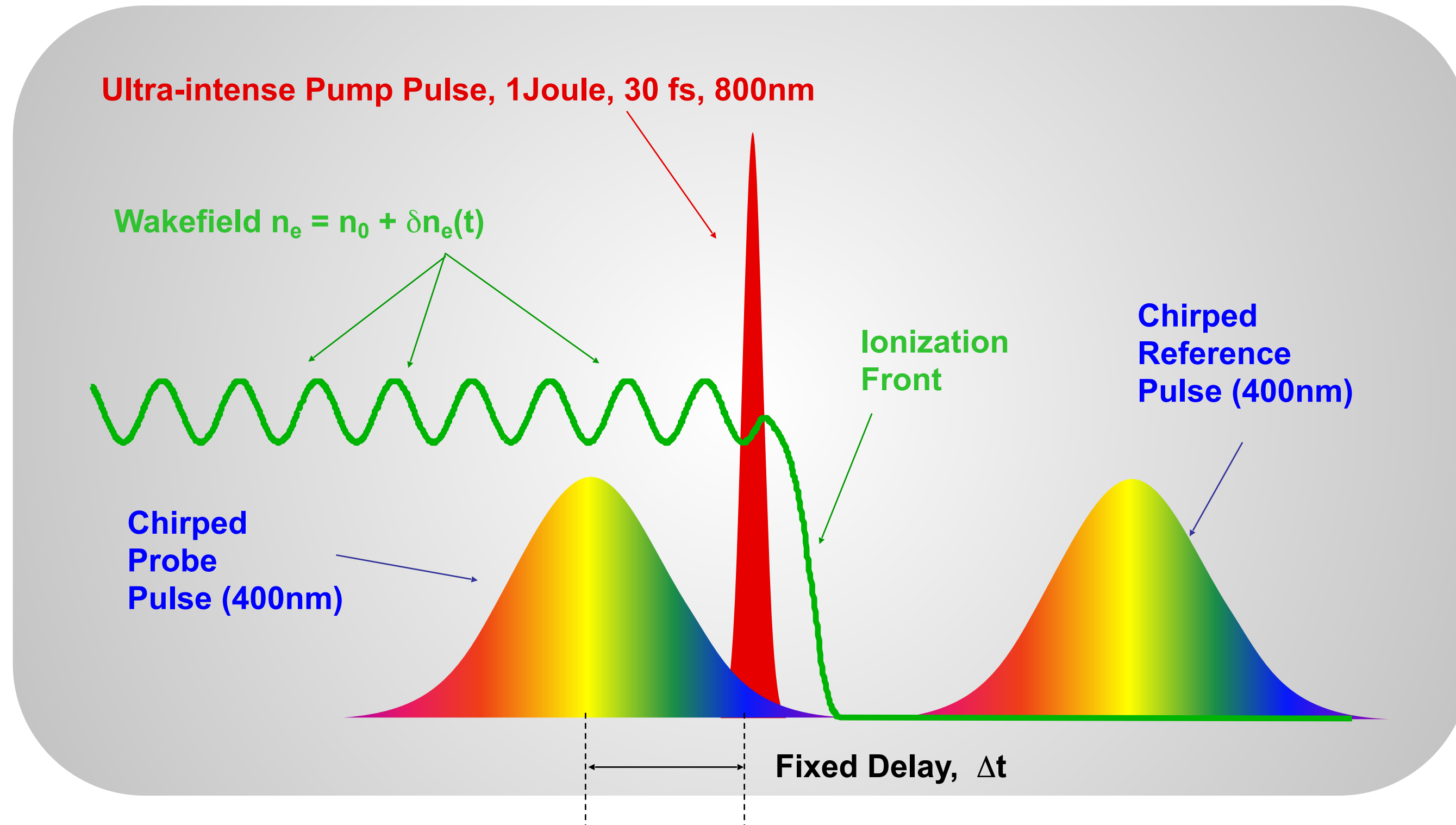
Kotaki *et al.* Phys. Plasmas **9**, 1392 (2002)



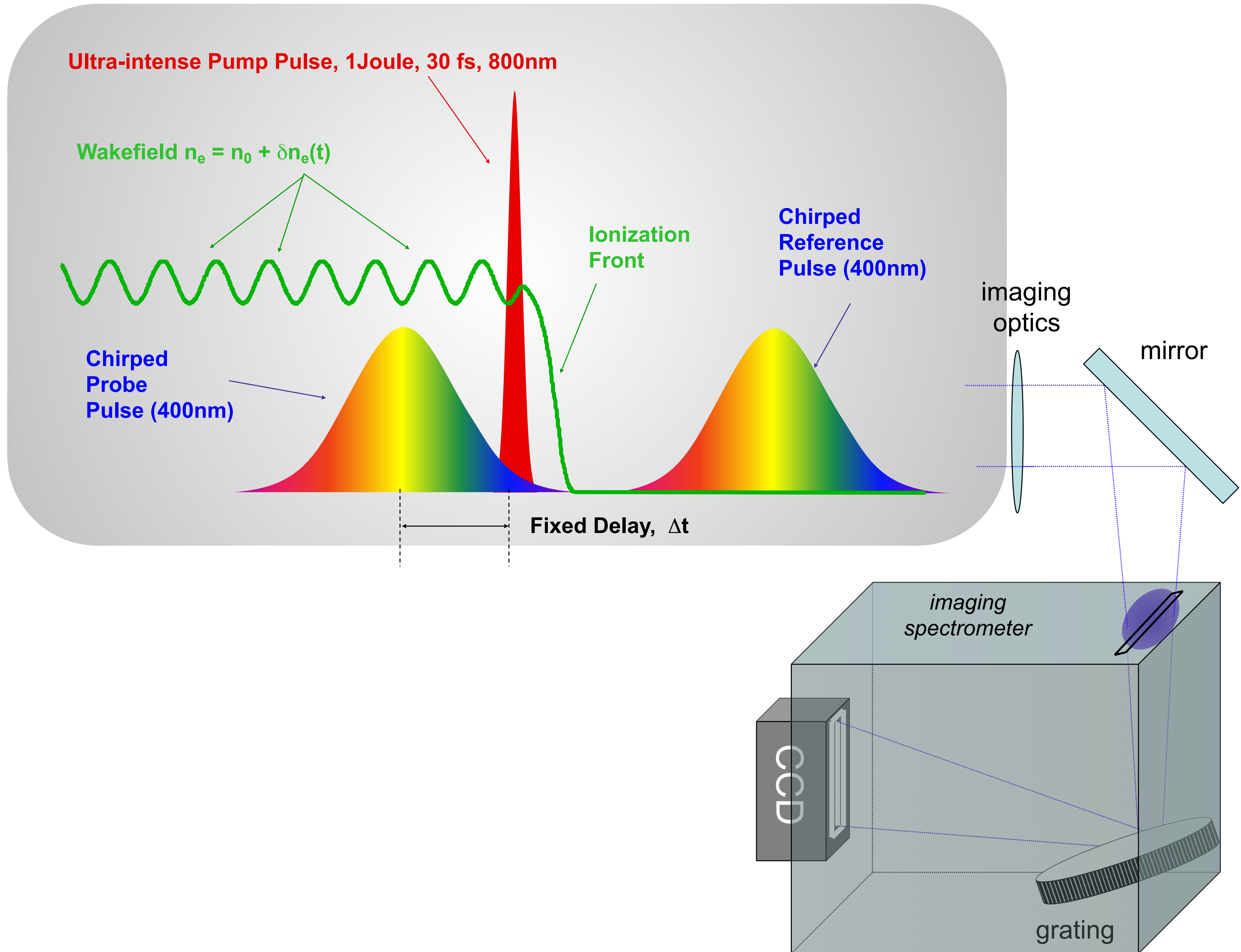
# “Frequency Domain Holography” measures Wakefields in a Single-Shot



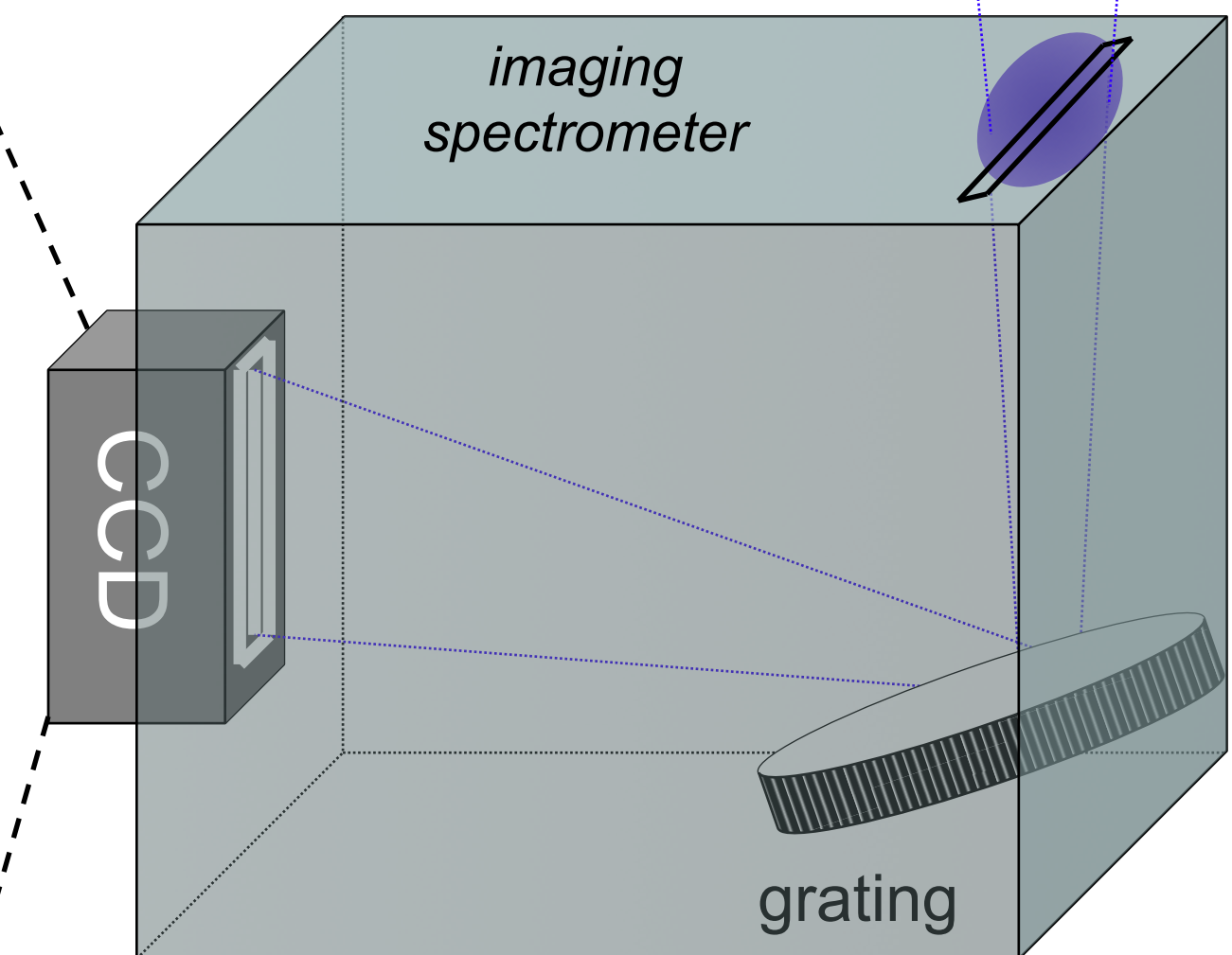
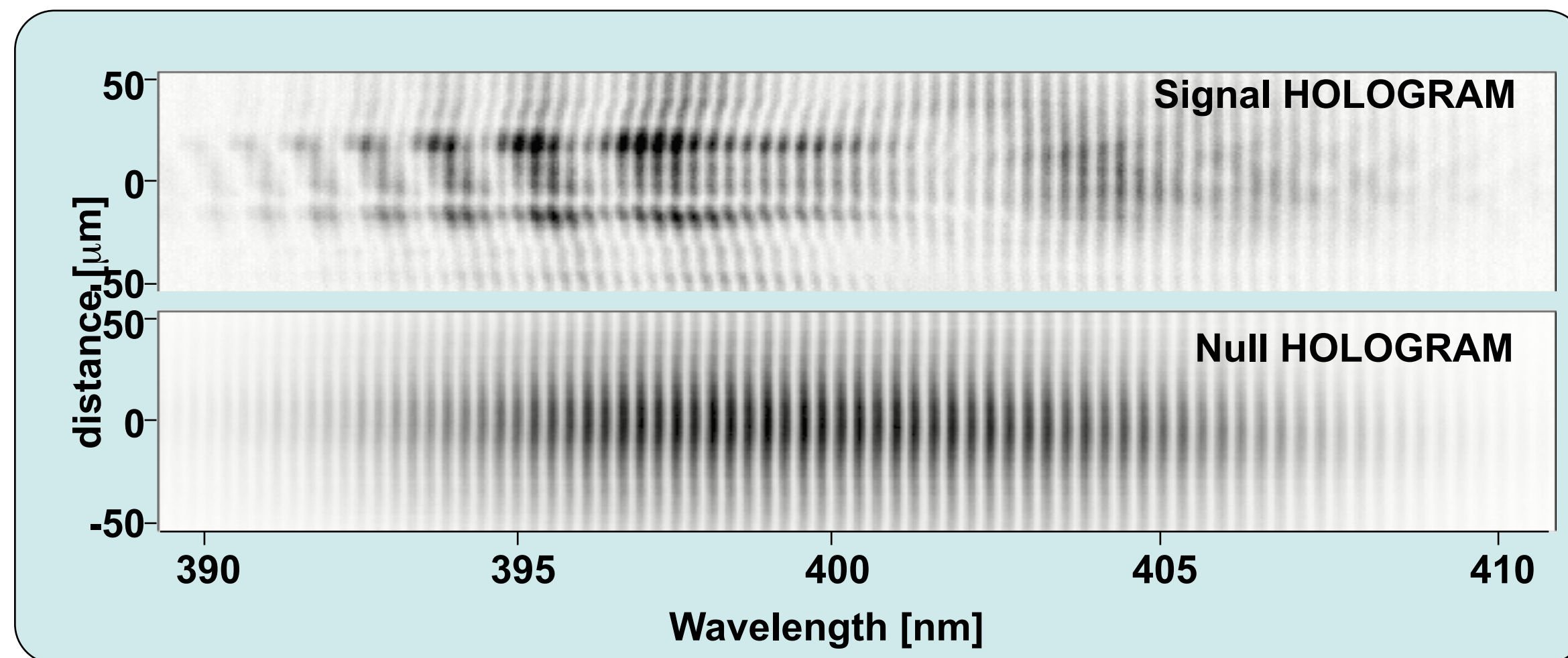
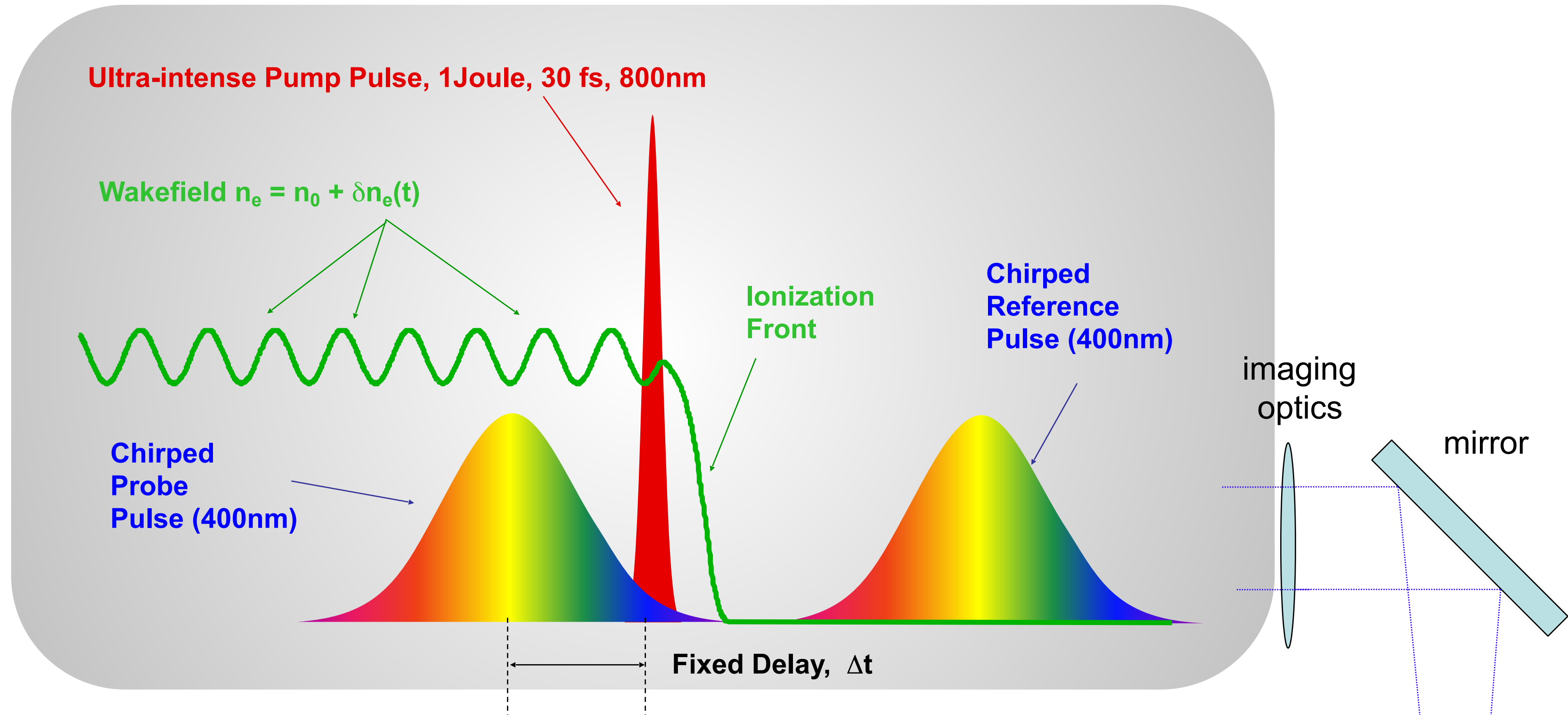
# “Frequency Domain Holography” measures Wakefields in a Single-Shot



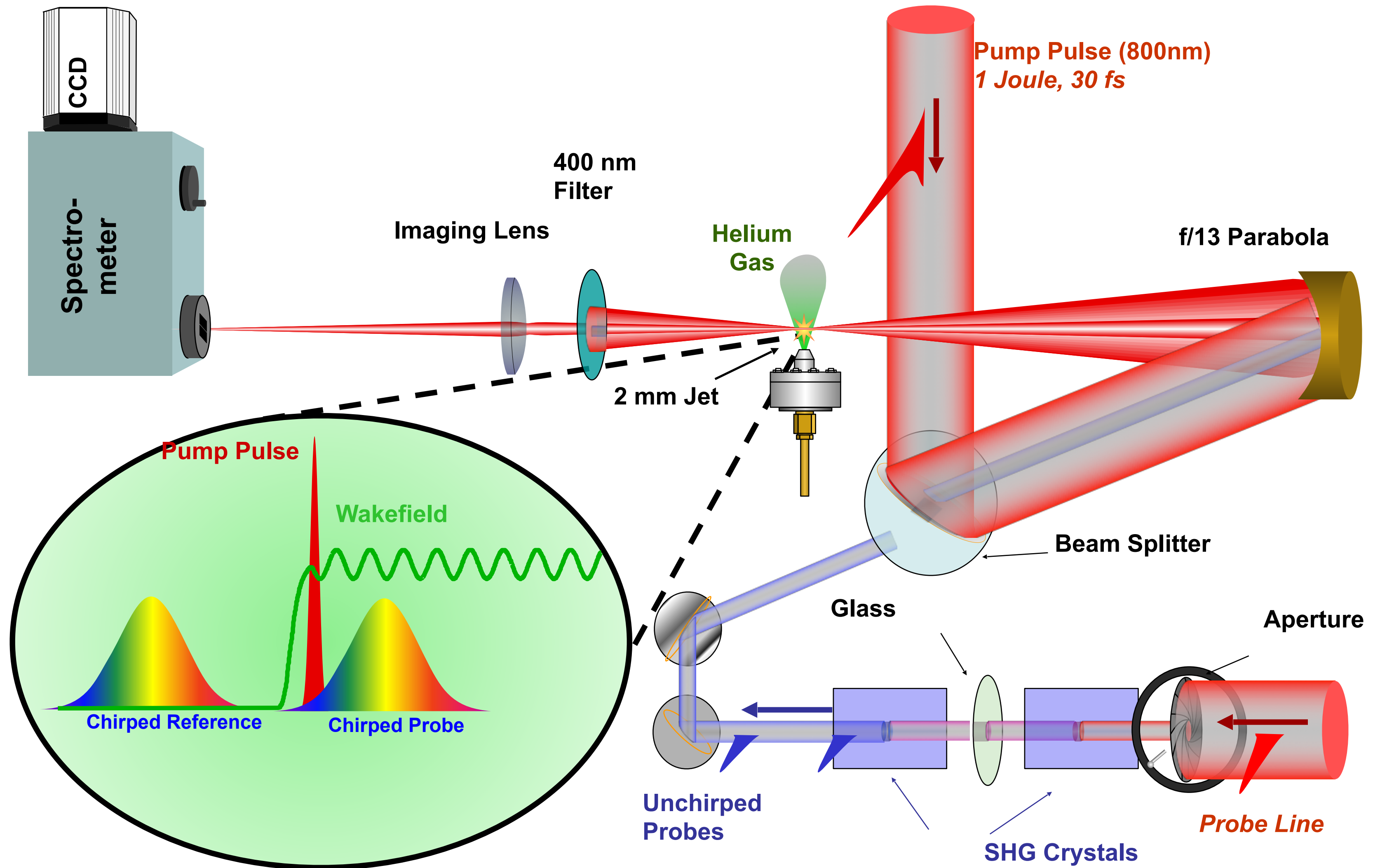
# “Frequency Domain Holography” measures Wakefields in a Single-Shot



# “Frequency Domain Holography” measures Wakefields in a Single-Shot



# Experimental Layout



# “Reading” the Hologram

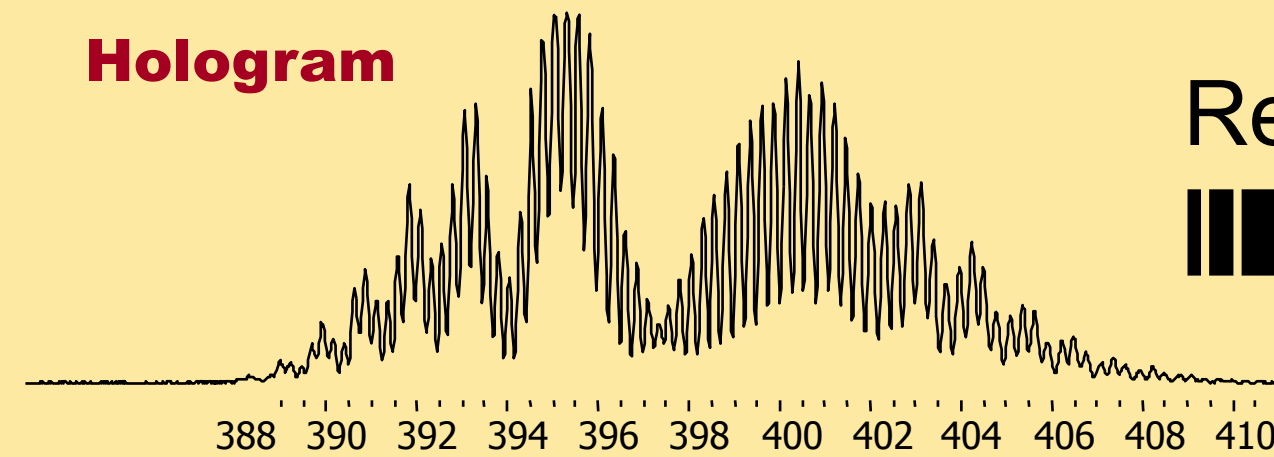
(Full Electric Field Reconstruction)

## BASIC SCHEME

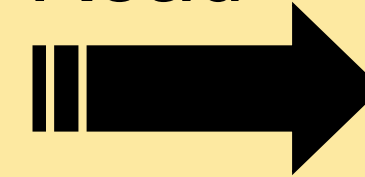
RECONSTRUCTION

TIME DOMAIN

1. Reconstruct spectral E-field of probe pulse from holographic spectrum



Read



$$E_{\text{probe}}(\omega) = |E(\omega)| e^{-i\phi(\omega)}$$

# “Reading” the Hologram

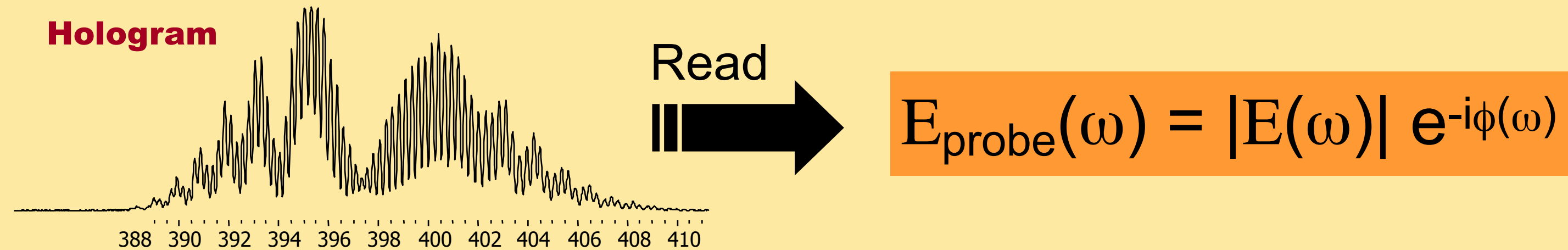
(Full Electric Field Reconstruction)

## BASIC SCHEME

RECONSTRUCTION

TIME DOMAIN

1. Reconstruct spectral E-field of probe pulse from holographic spectrum



2. Fourier Transform to the time-domain to recover temporal phase

$$E_{\text{probe}}(\omega) \xrightarrow{\text{FFT}} E_{\text{probe}}(t) = |E(t)| e^{-i\delta\phi(t)}$$

# “Reading” the Hologram

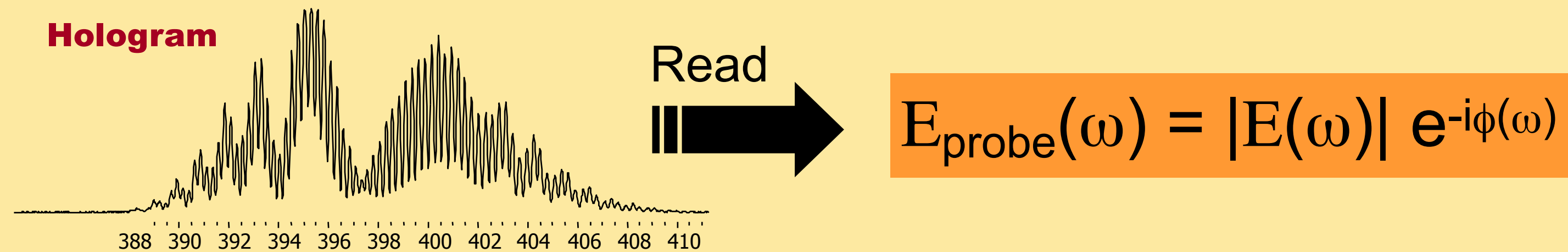
(Full Electric Field Reconstruction)

## BASIC SCHEME

RECONSTRUCTION

TIME DOMAIN

1. Reconstruct spectral E-field of probe pulse from holographic spectrum



2. Fourier Transform to the time-domain to recover temporal phase

$$E_{\text{probe}}(\omega) \xrightarrow{\text{FFT}} E_{\text{probe}}(t) = |E(t)| e^{-i\delta\phi(t)}$$

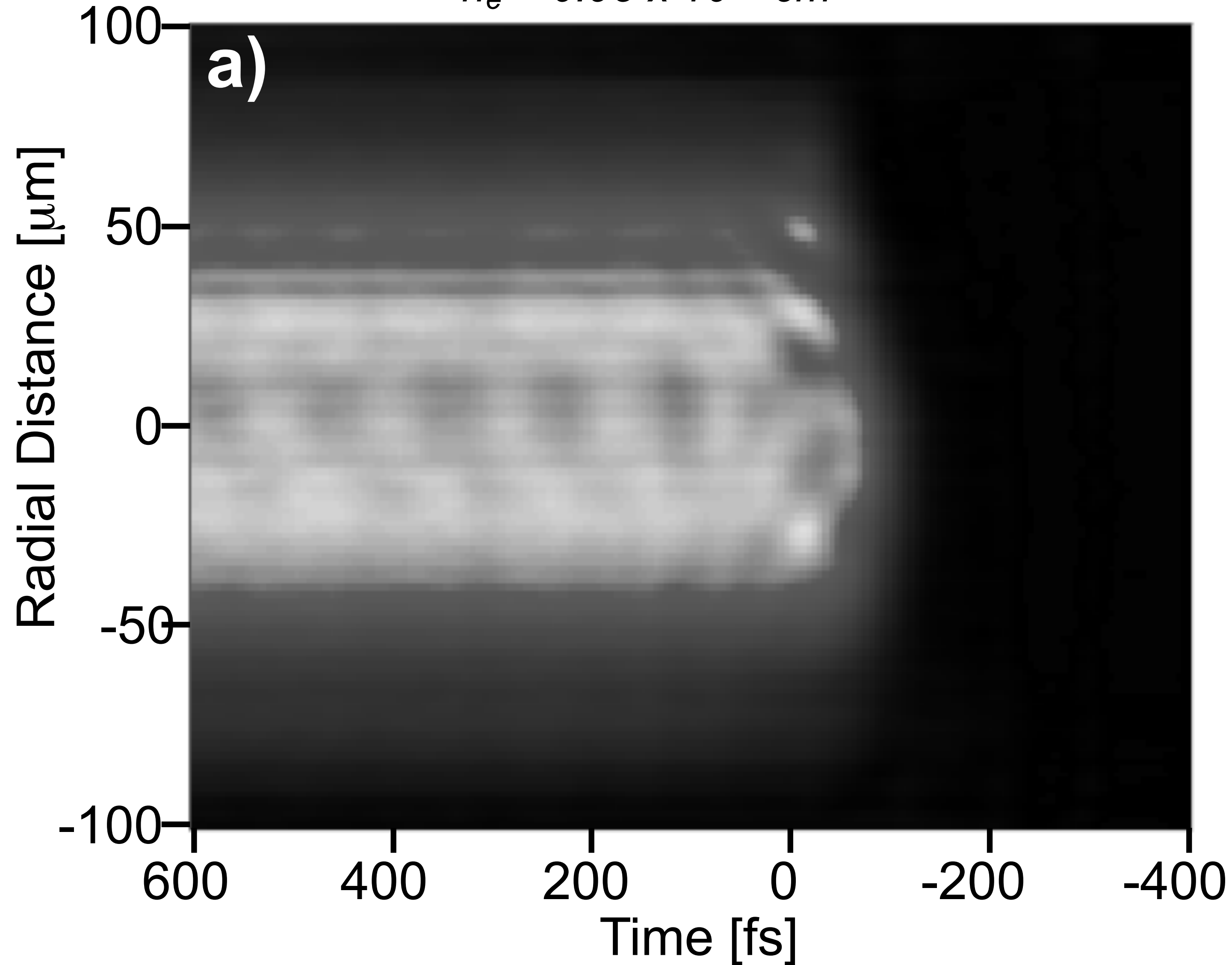
3. Calculate electron density from extracted temporal phase

$$\delta\phi(t) \xrightarrow{\text{index}} \delta n_e(t)$$


# Holographic snapshots of laser wakefields

$P \sim 10 \text{ TW}$ ,  $I \sim 10^{18} \text{ W/cm}^2$

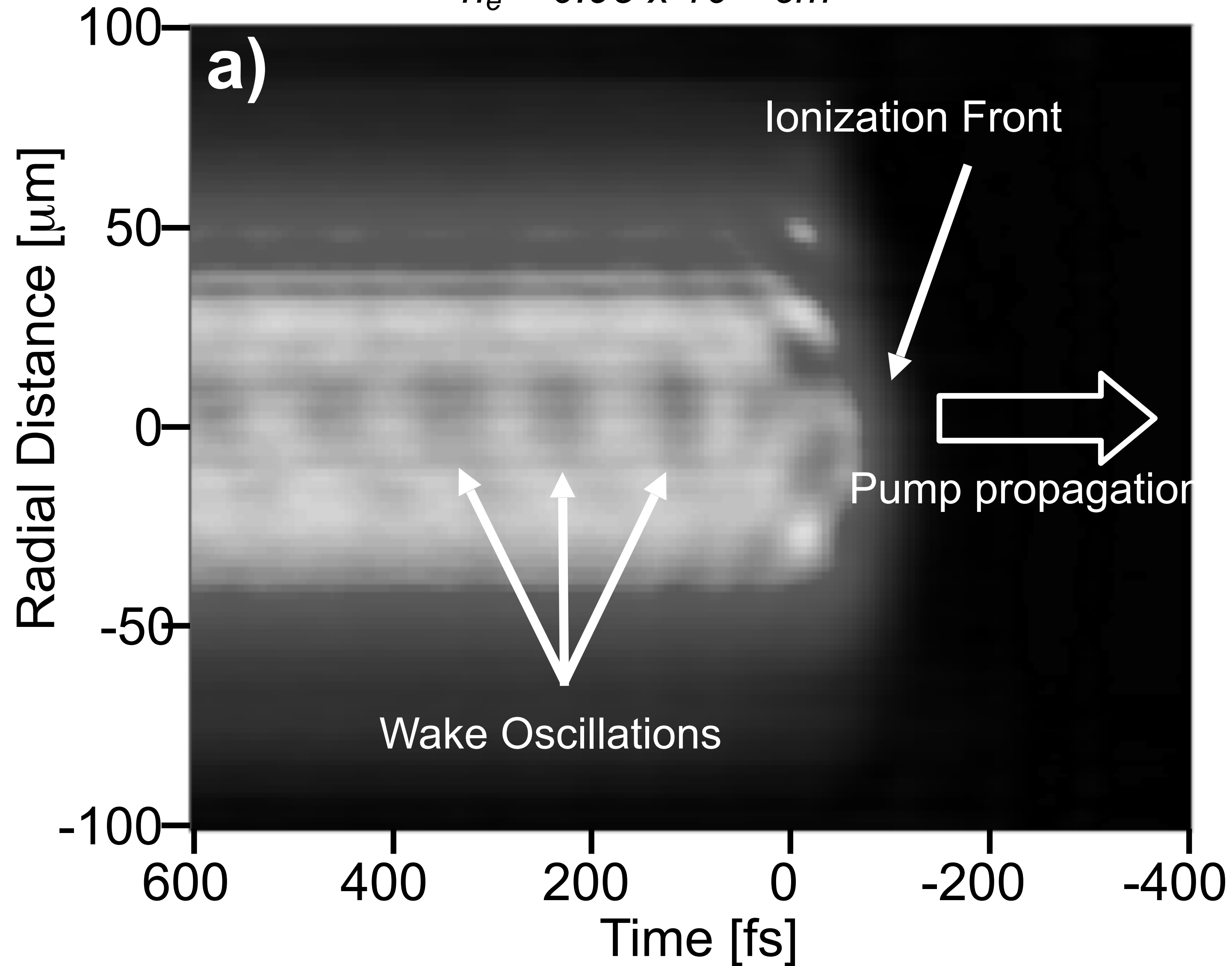
$n_e = 0.95 \times 10^{18} \text{ cm}^{-3}$



# Holographic snapshots of laser wakefields

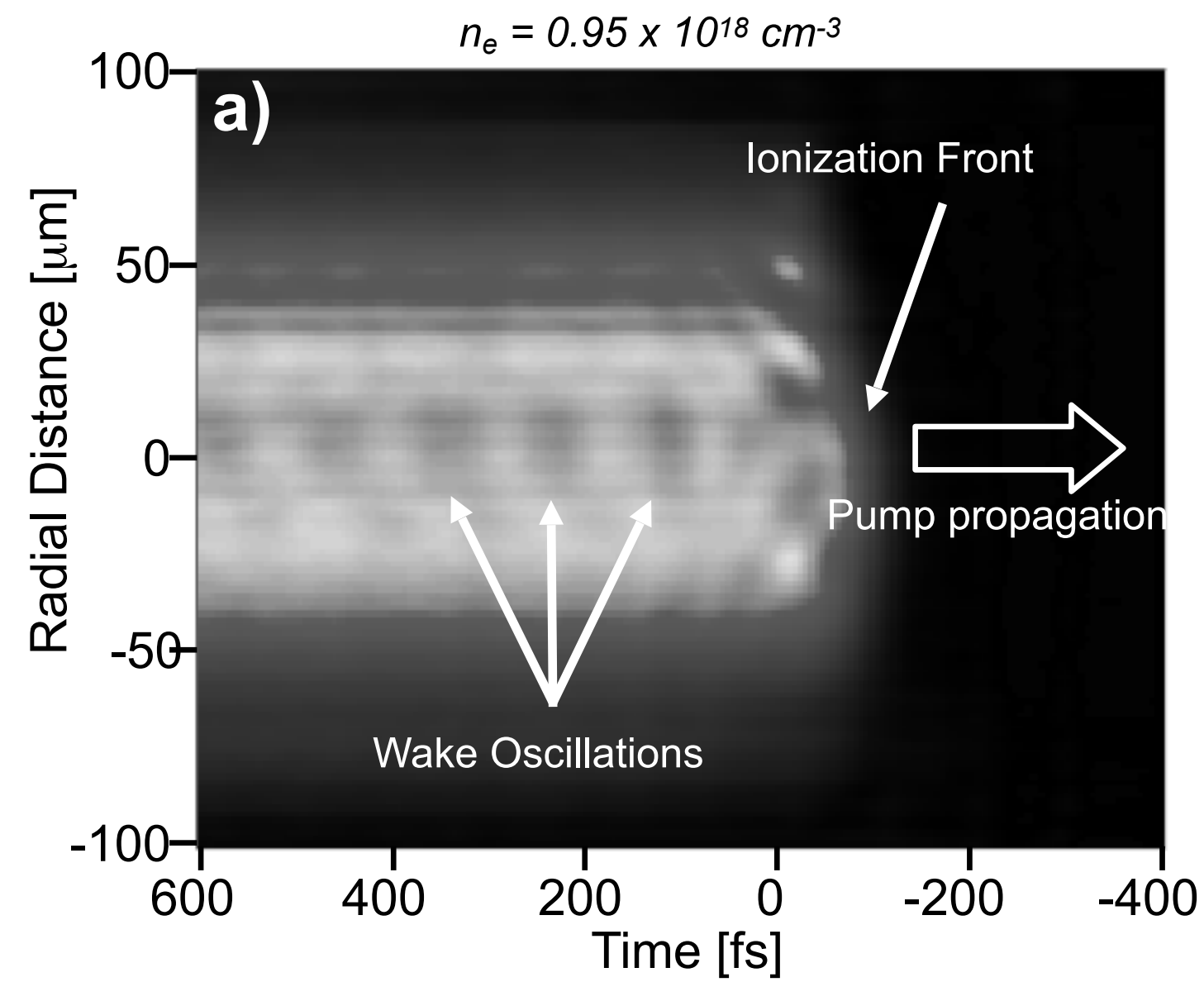
$P \sim 10 \text{ TW}$ ,  $I \sim 10^{18} \text{ W/cm}^2$

$$n_e = 0.95 \times 10^{18} \text{ cm}^{-3}$$



# Holographic snapshots of laser wakefields

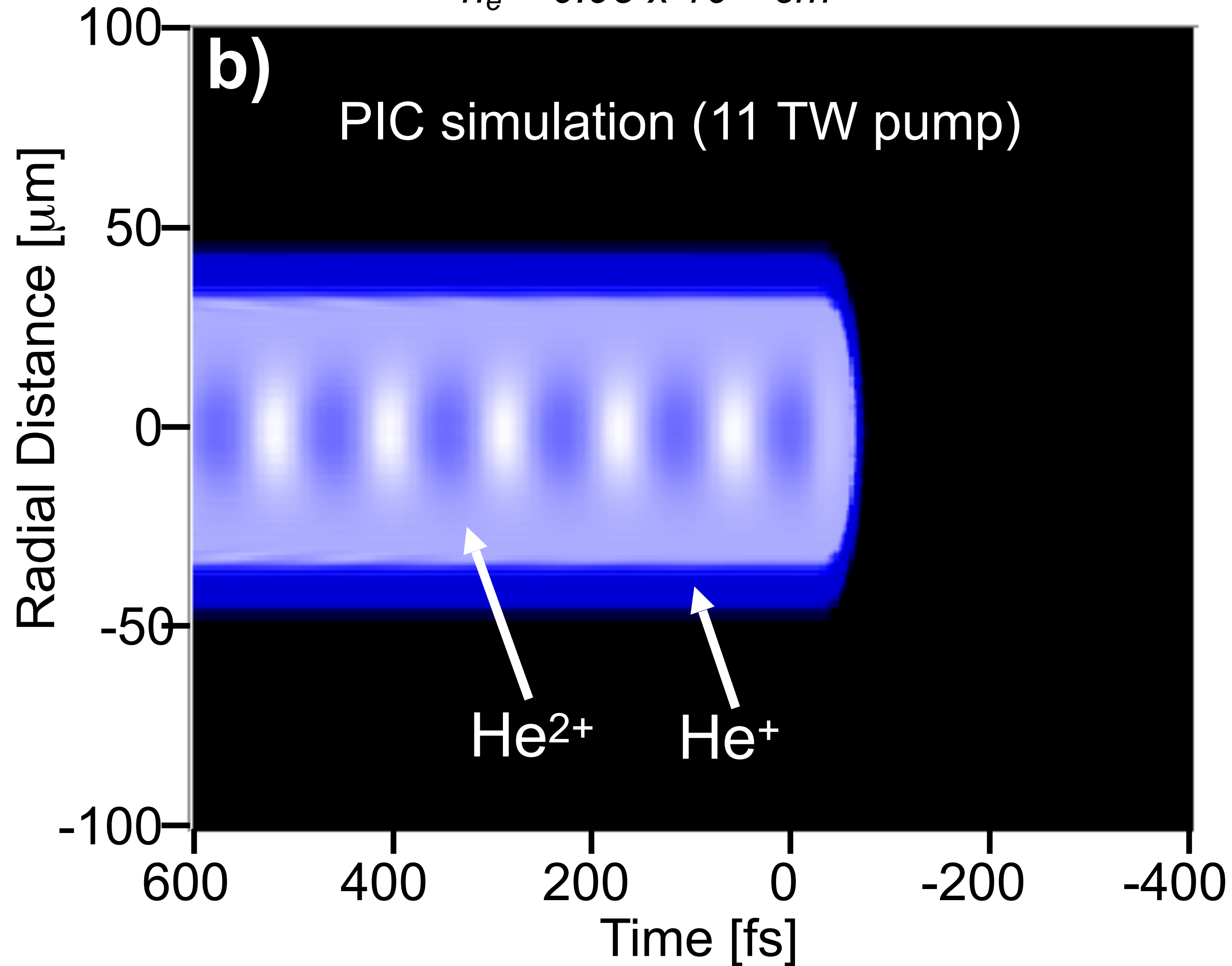
$P \sim 10 \text{ TW}$ ,  $I \sim 10^{18} \text{ W/cm}^2$



# Holographic snapshots of laser wakefields

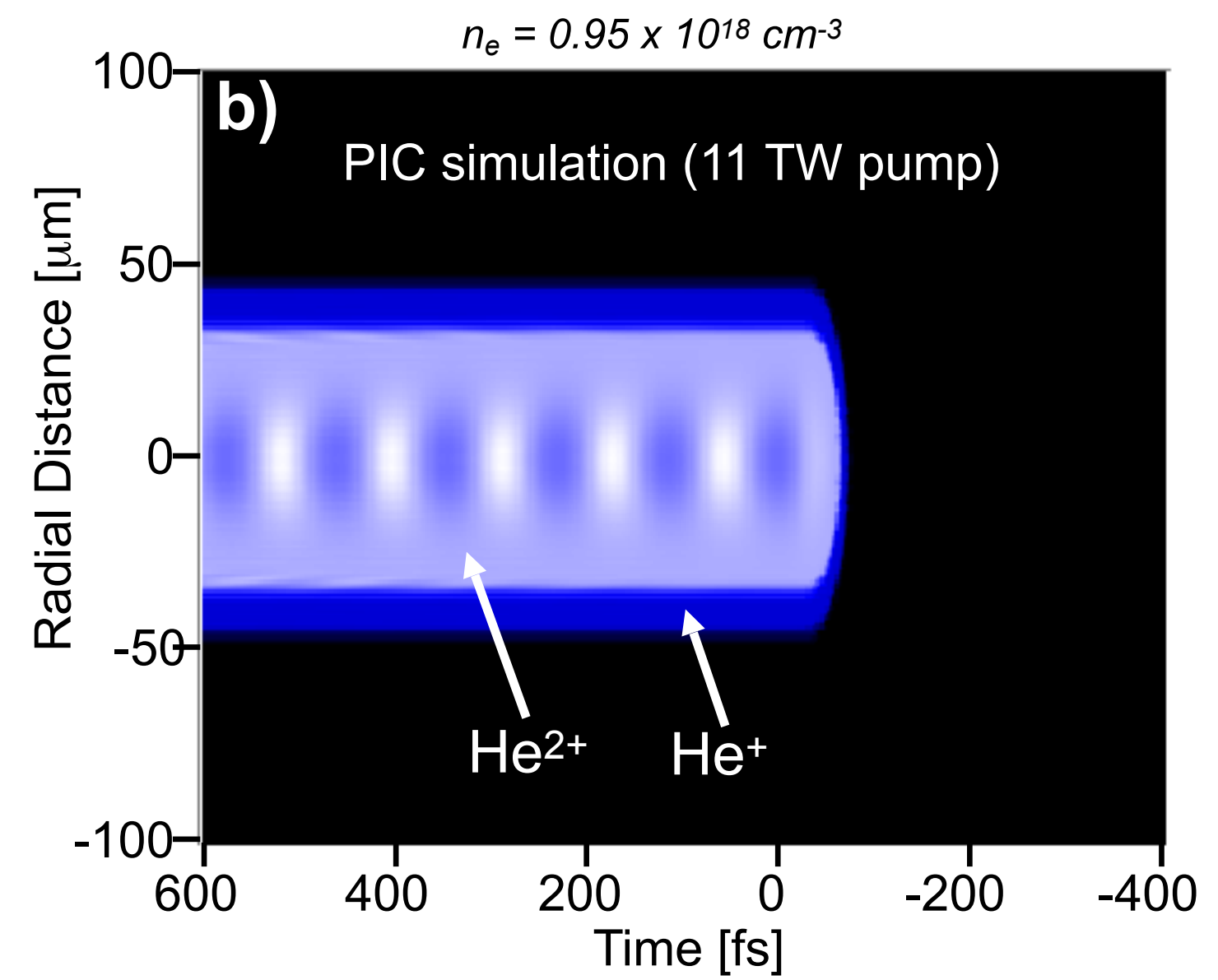
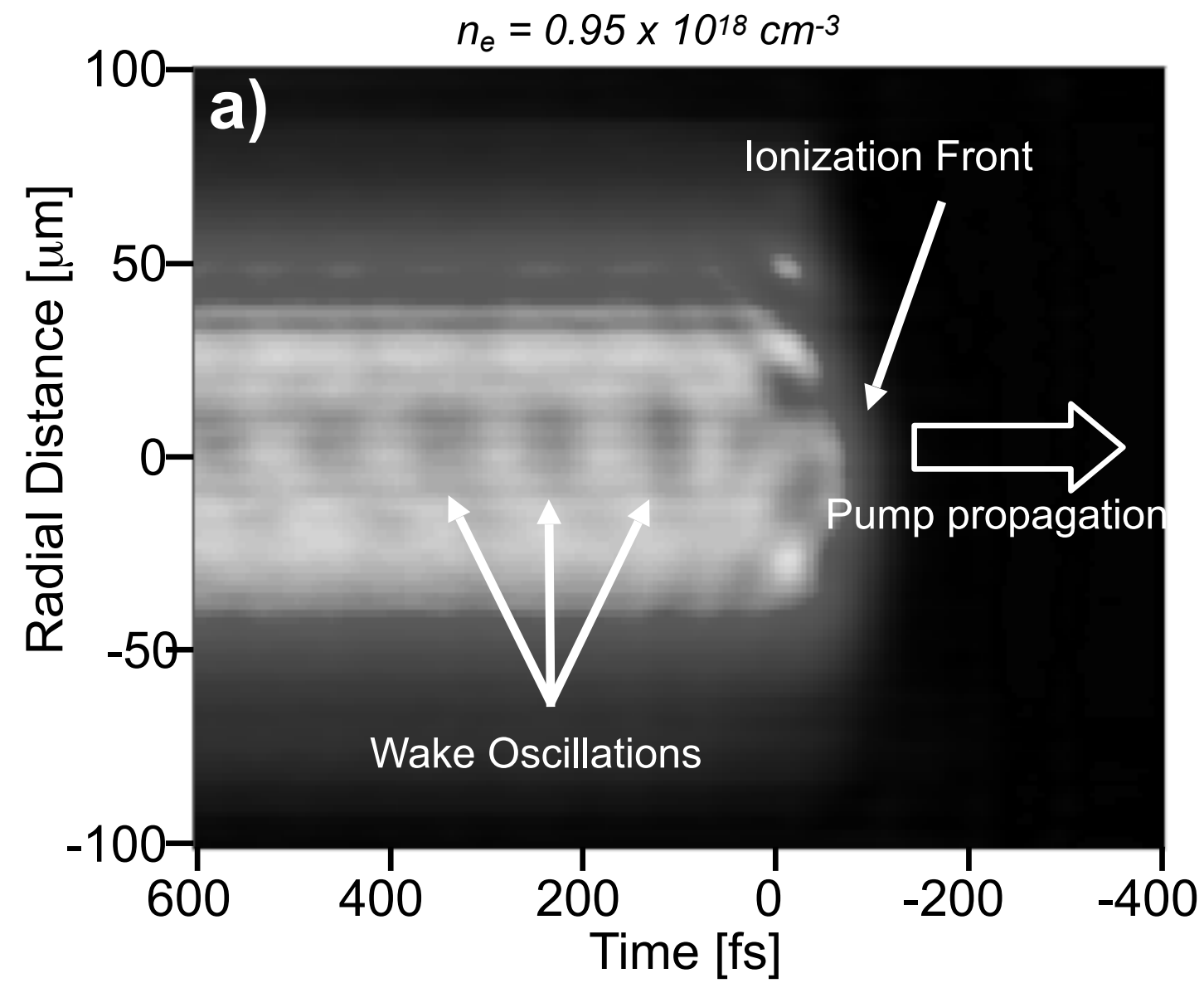
$P \sim 10 \text{ TW}$ ,  $I \sim 10^{18} \text{ W/cm}^2$

$$n_e = 0.95 \times 10^{18} \text{ cm}^{-3}$$



# Holographic snapshots of laser wakefields

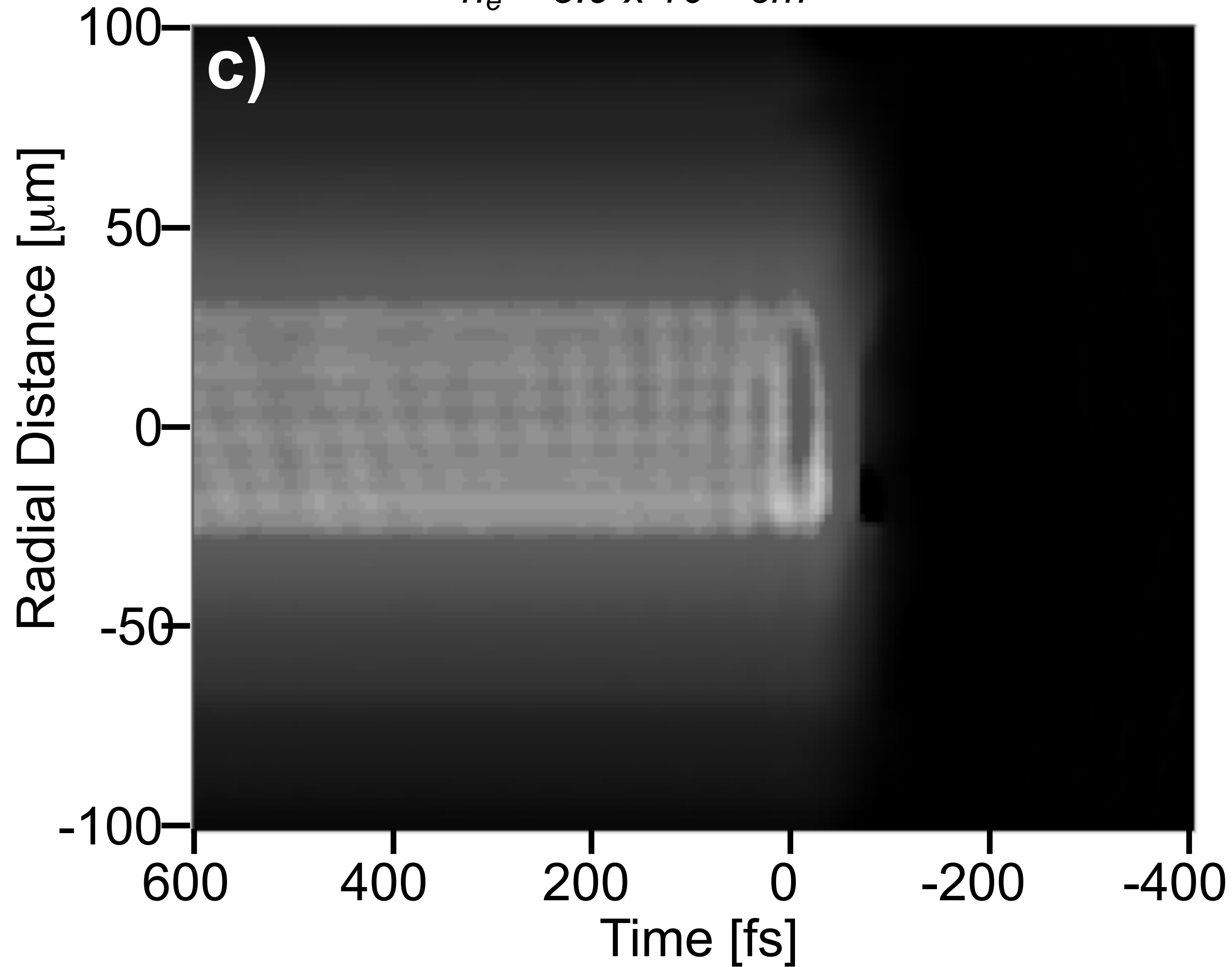
$P \sim 10 \text{ TW}$ ,  $I \sim 10^{18} \text{ W/cm}^2$



# Holographic snapshots of laser wakefields

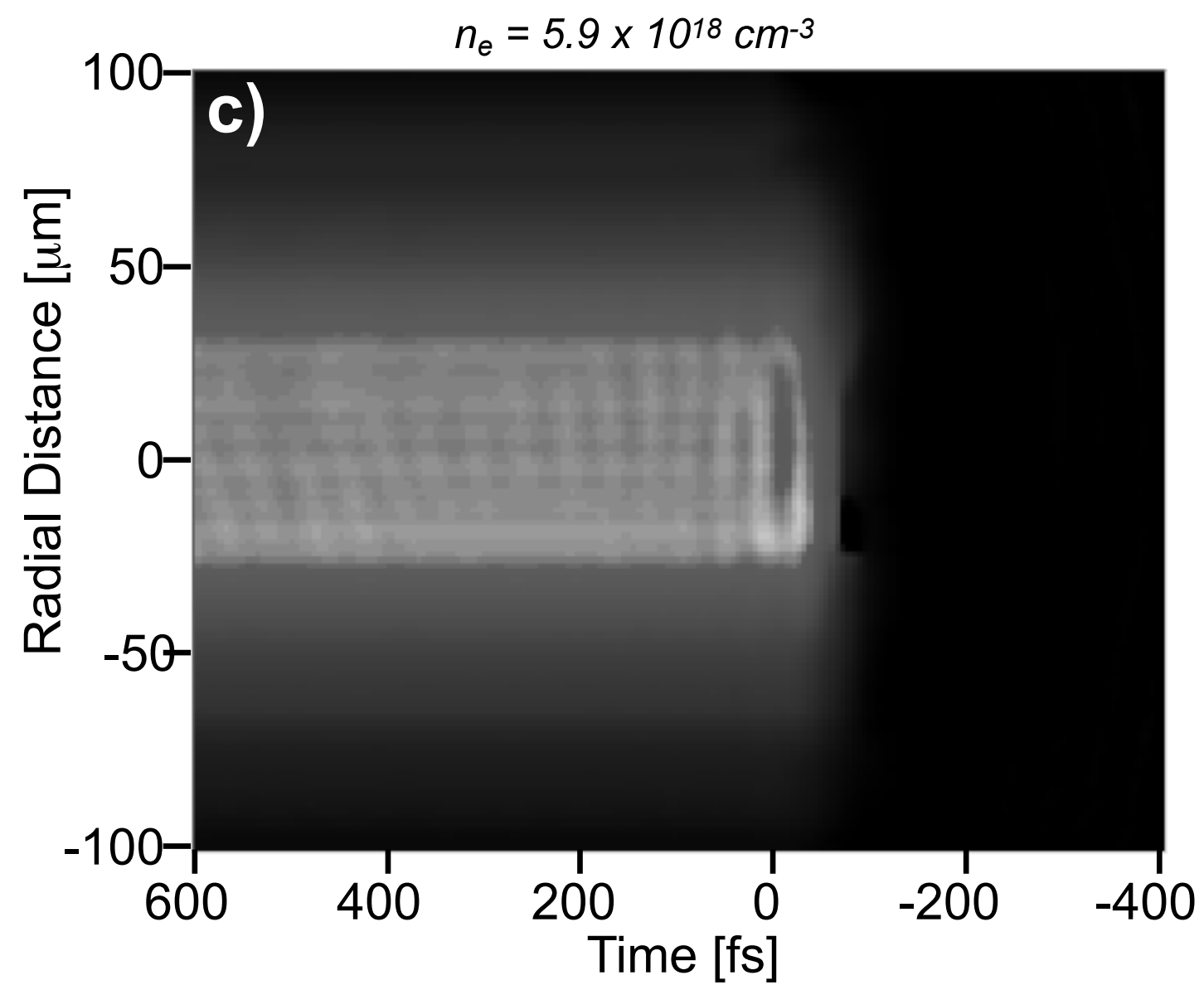
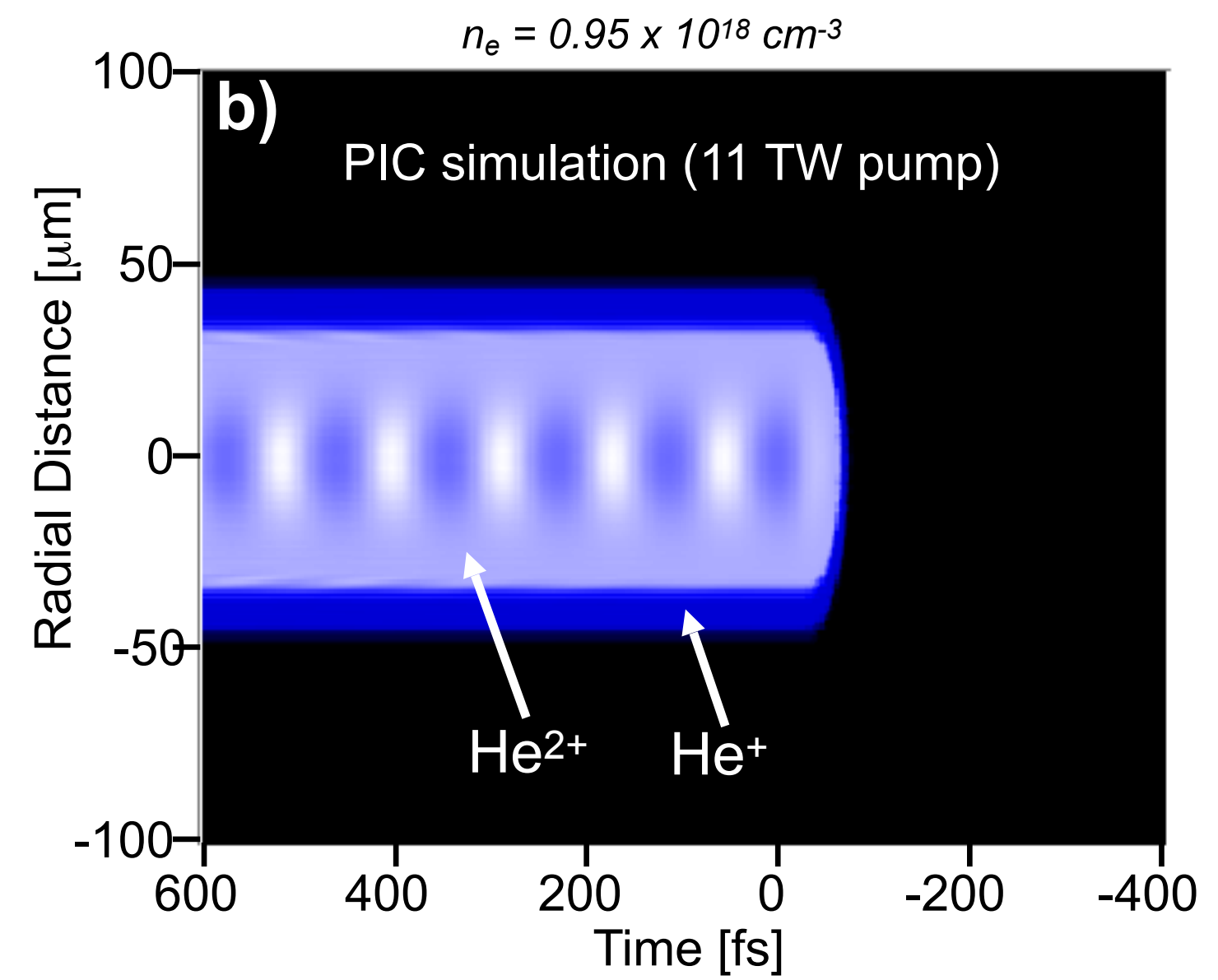
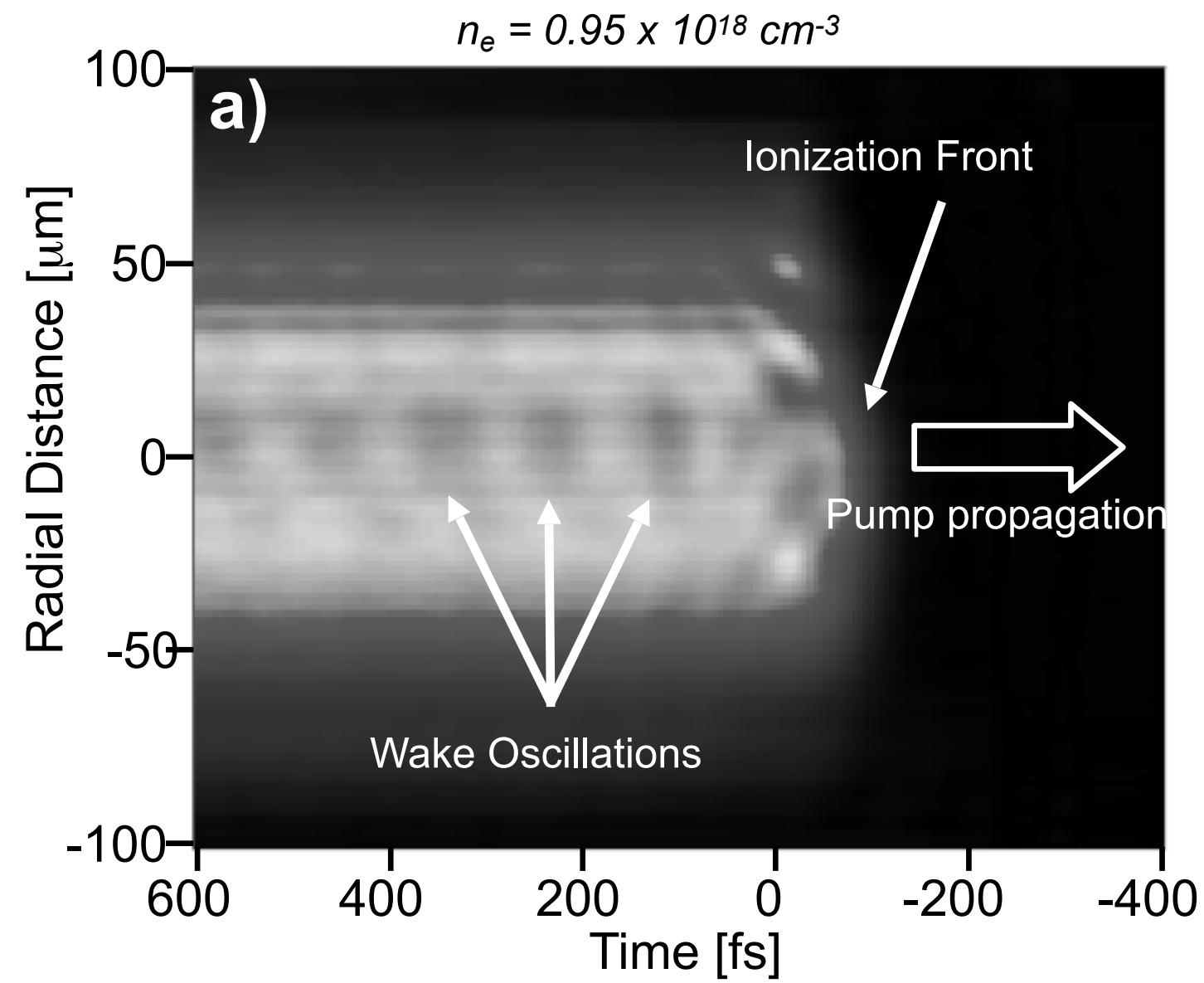
$P \sim 10 \text{ TW}$ ,  $I \sim 10^{18} \text{ W/cm}^2$

$n_e = 5.9 \times 10^{18} \text{ cm}^{-3}$



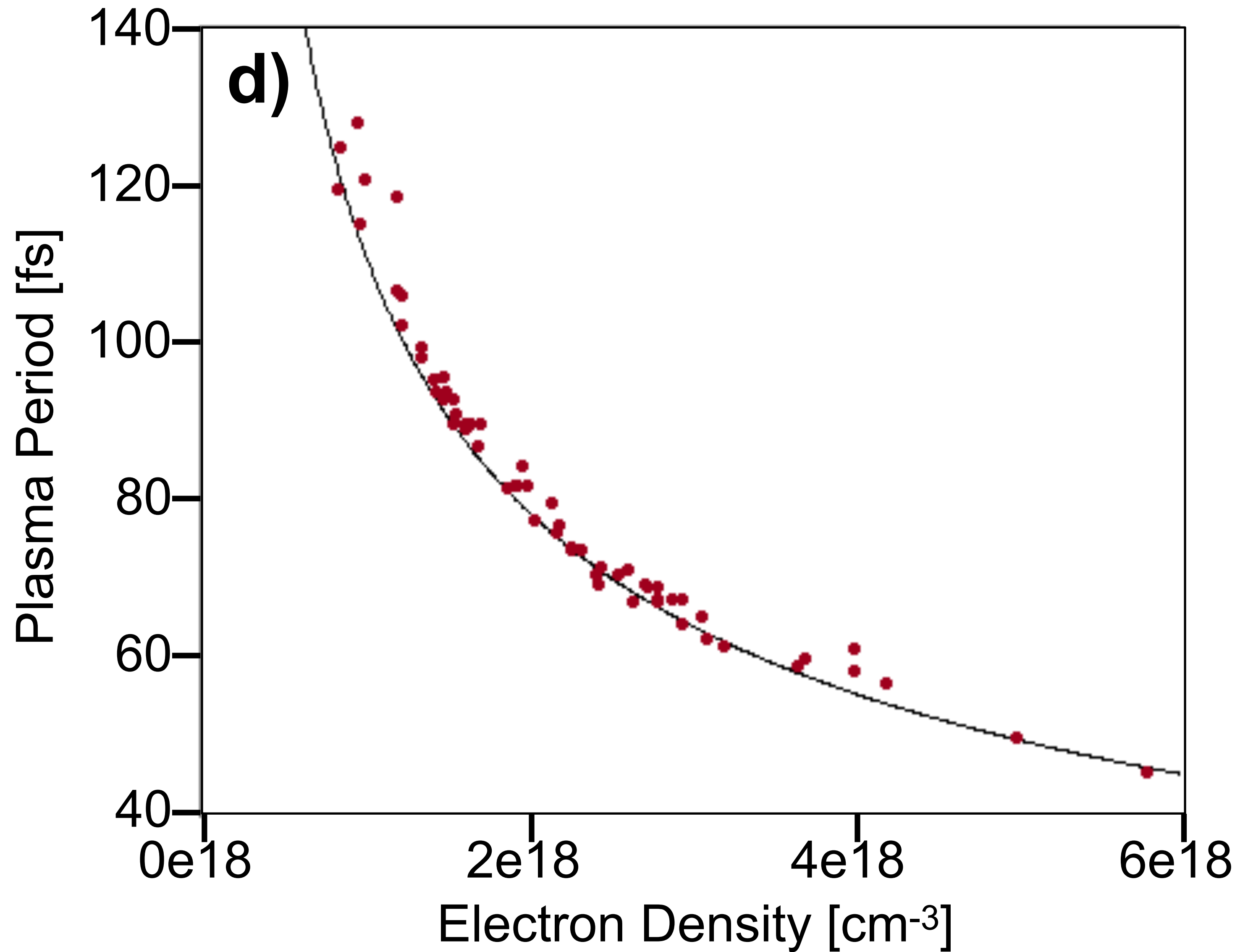
# Holographic snapshots of laser wakefields

$P \sim 10 \text{ TW}$ ,  $I \sim 10^{18} \text{ W/cm}^2$



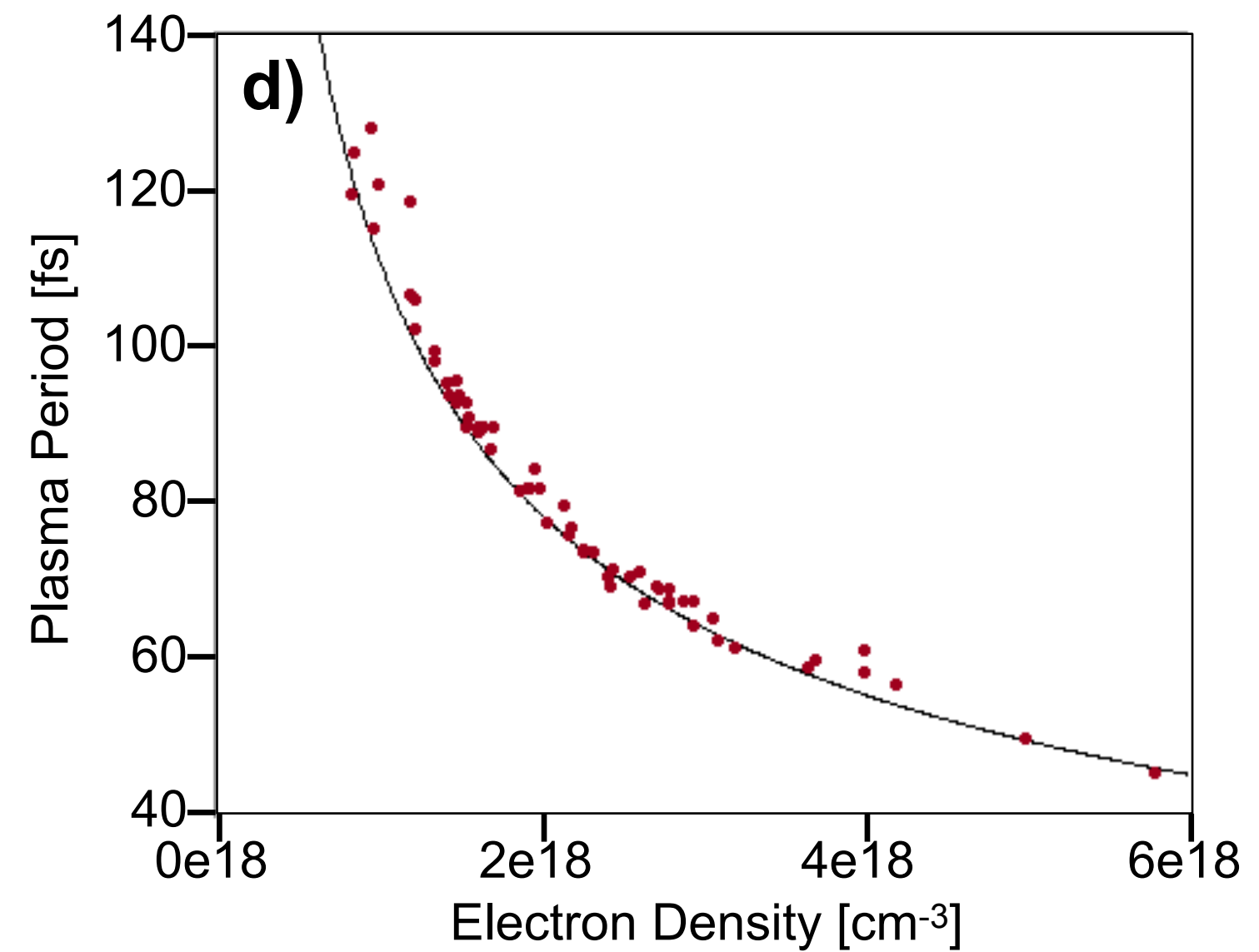
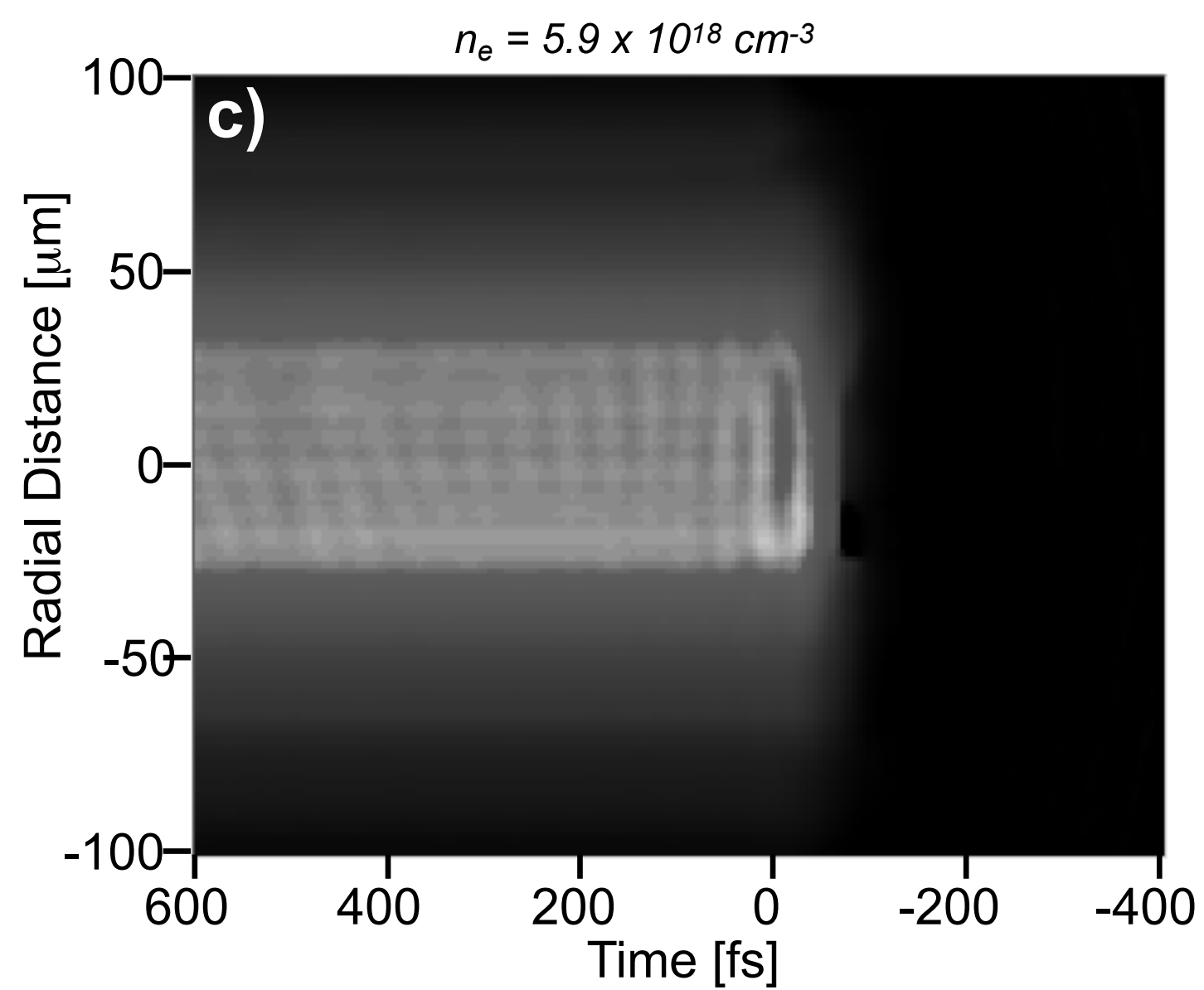
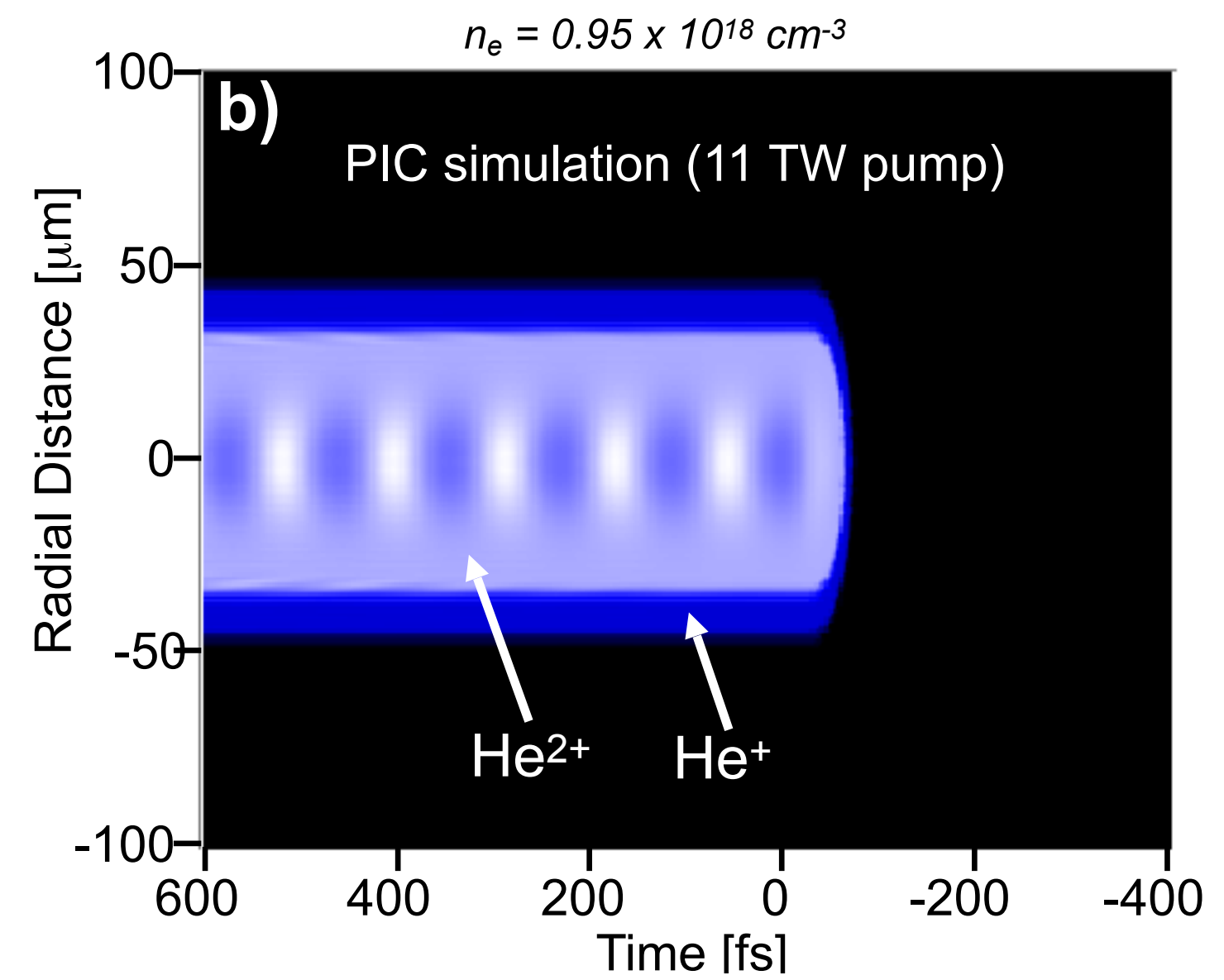
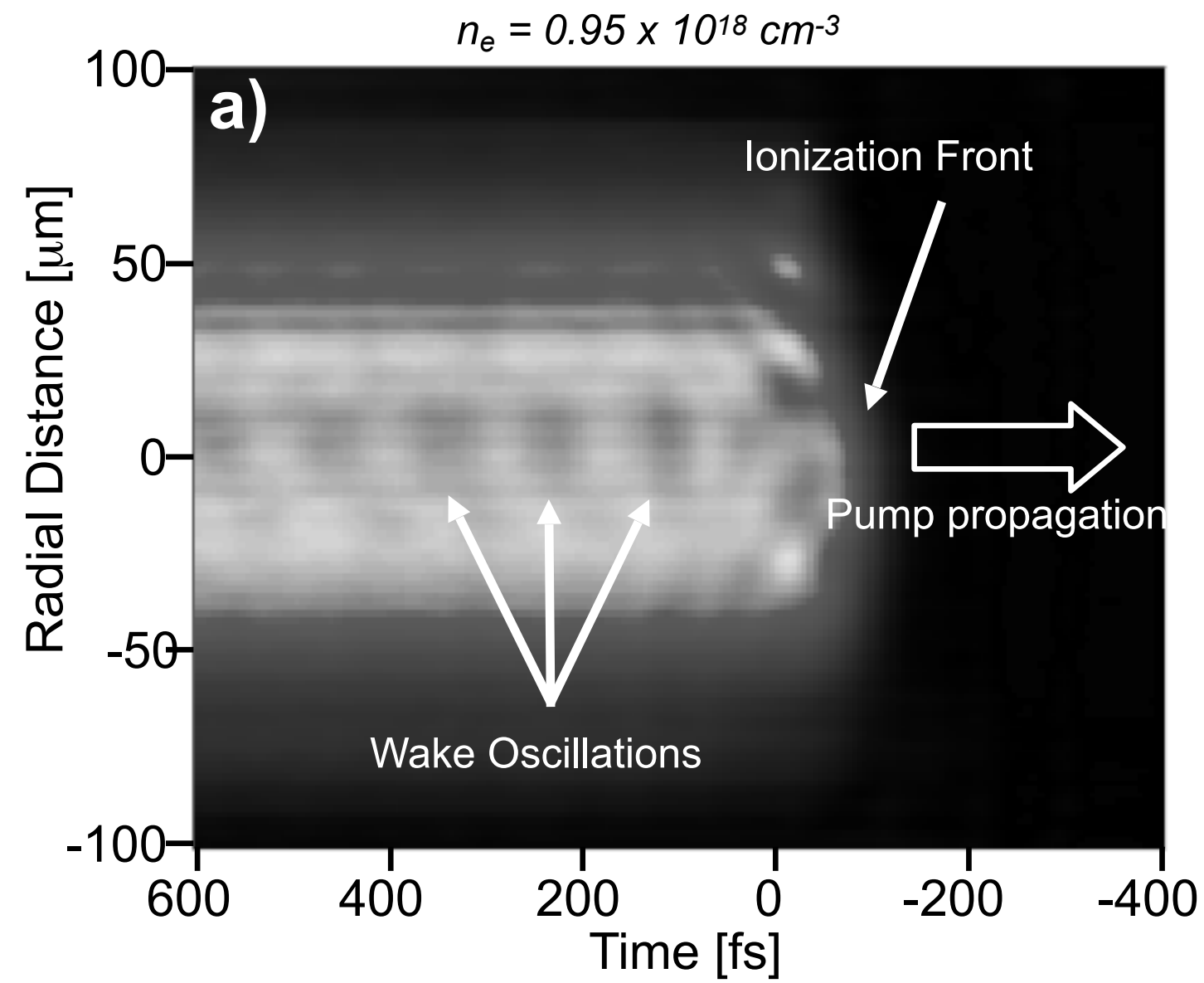
# Holographic snapshots of laser wakefields

*P ~ 10 TW, I ~ 10<sup>18</sup> W/cm<sup>2</sup>*



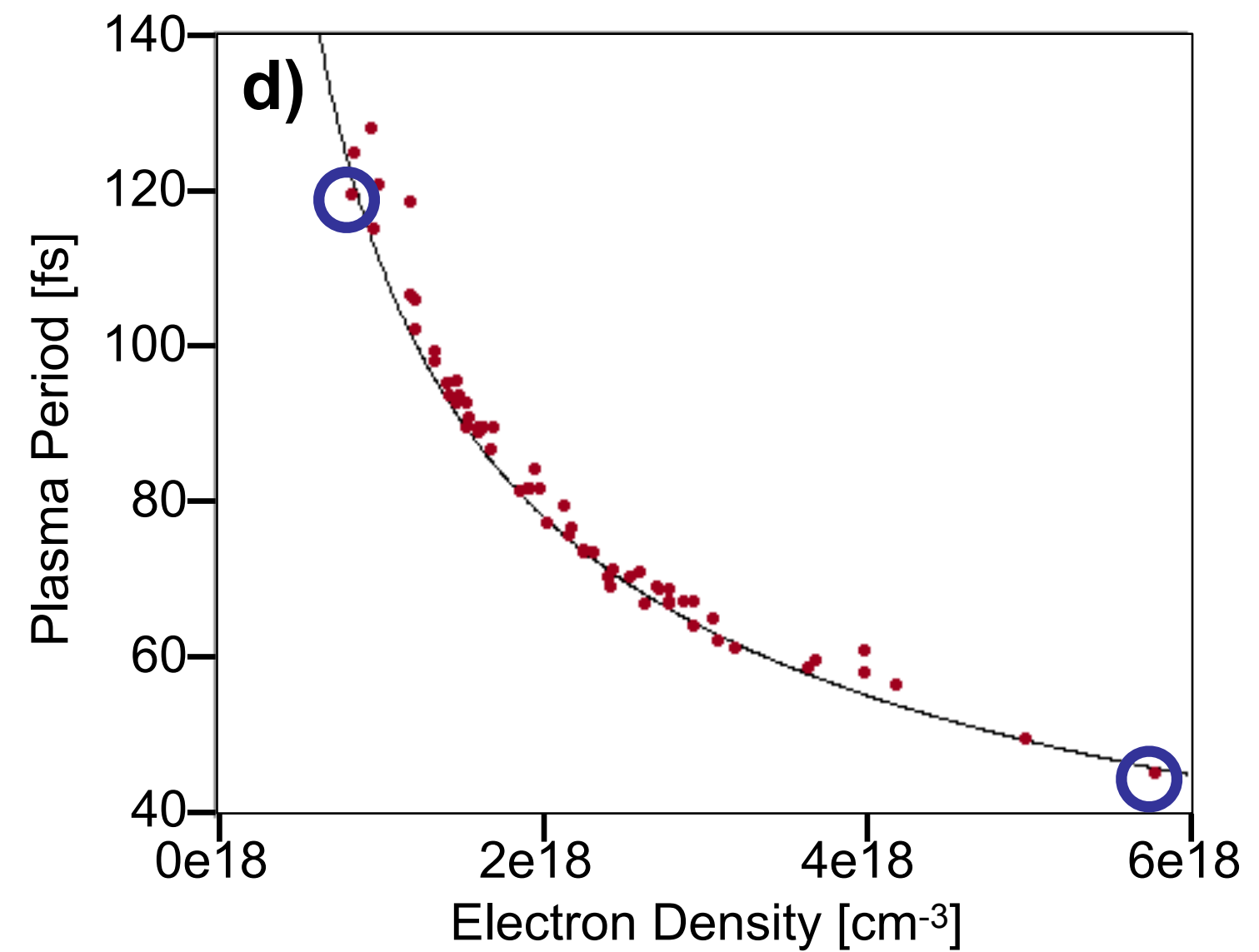
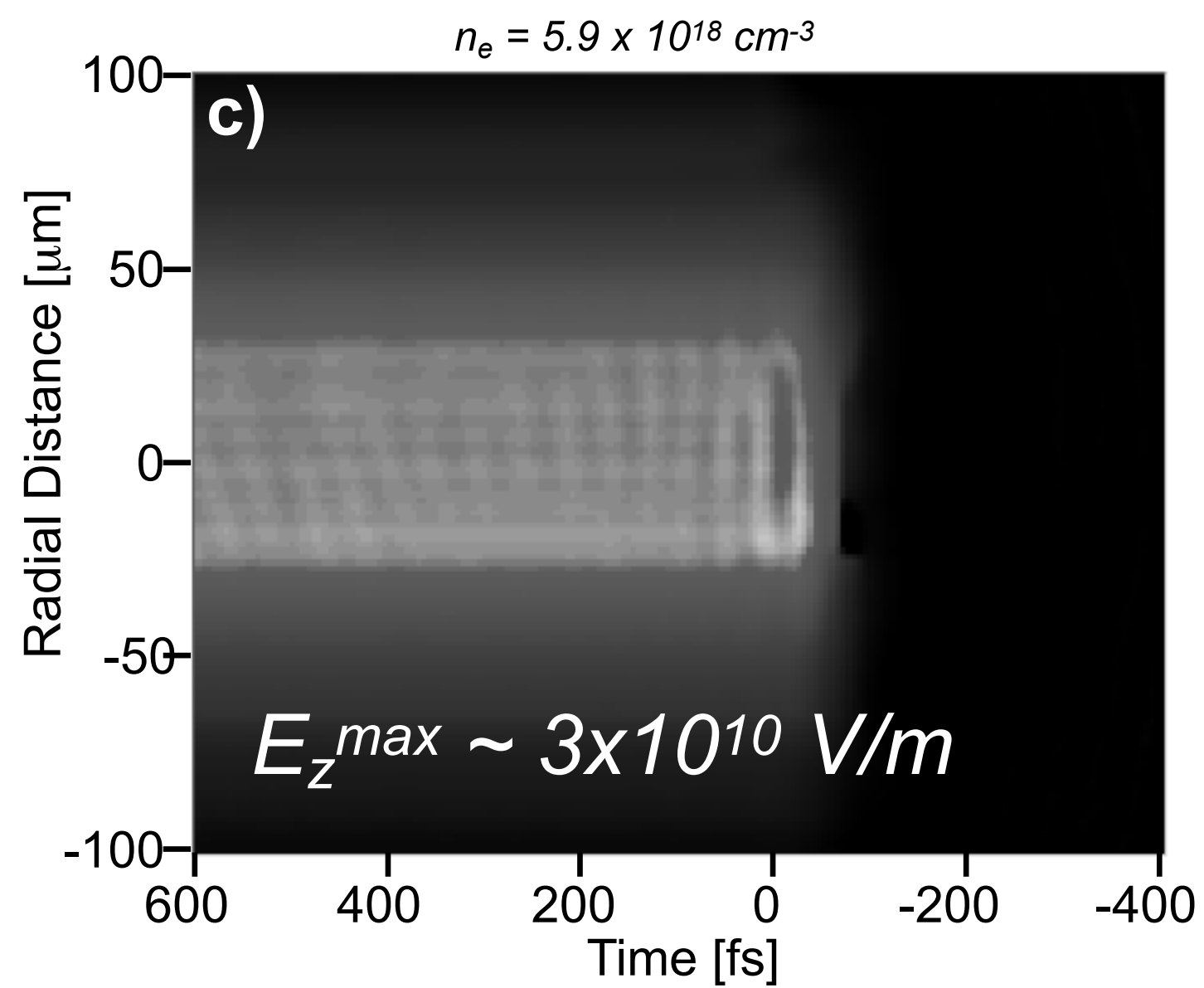
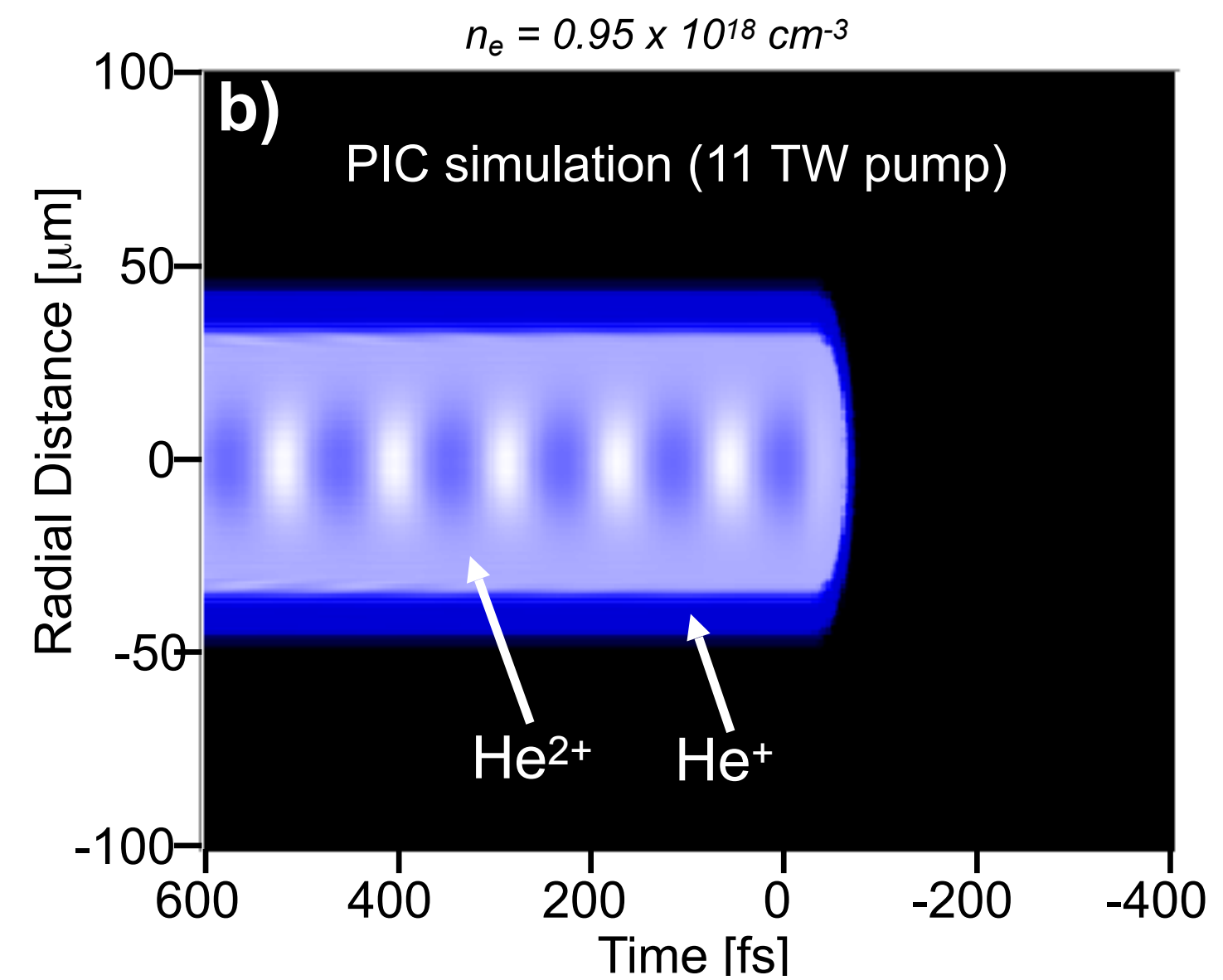
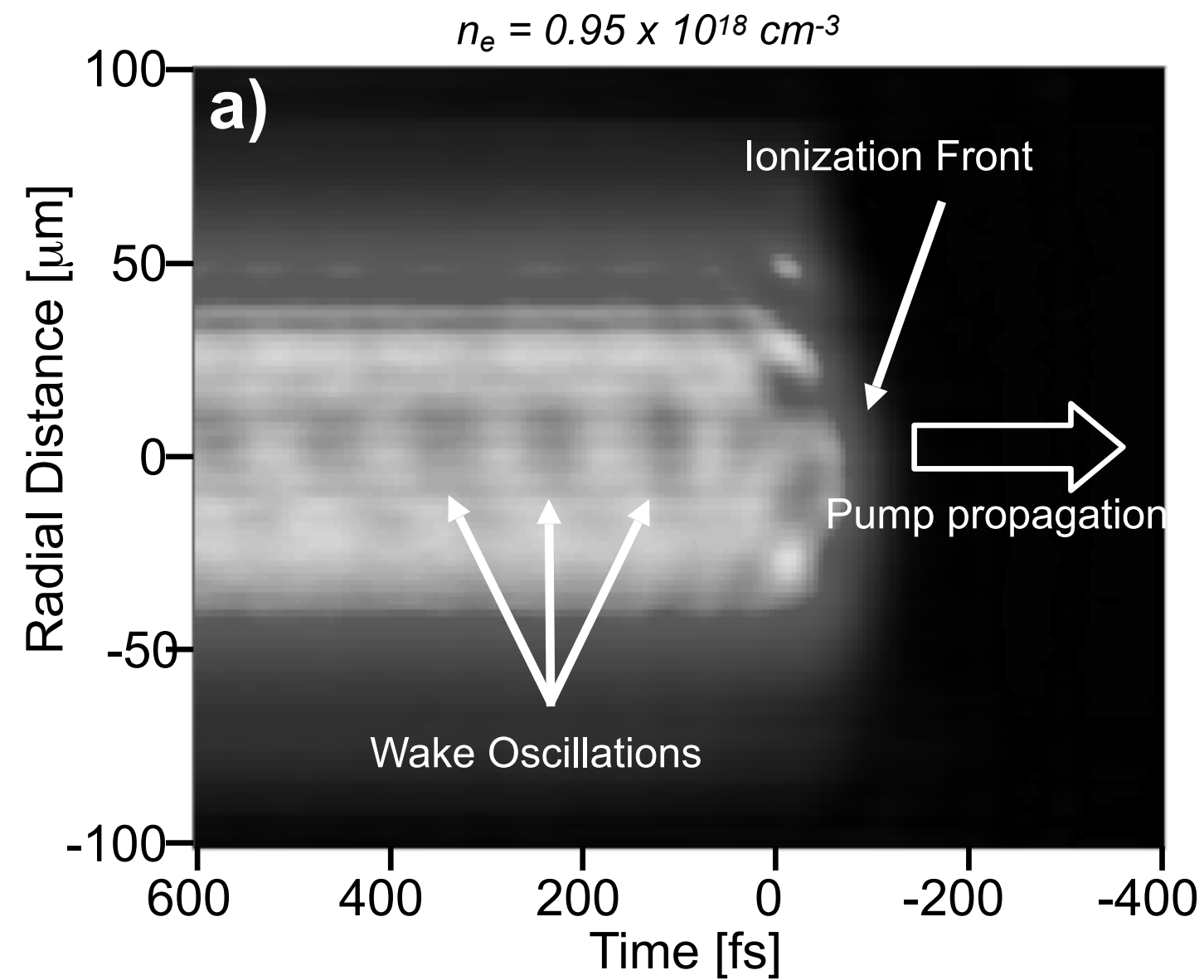
# Holographic snapshots of laser wakefields

$P \sim 10 \text{ TW}$ ,  $I \sim 10^{18} \text{ W/cm}^2$



# Holographic snapshots of laser wakefields

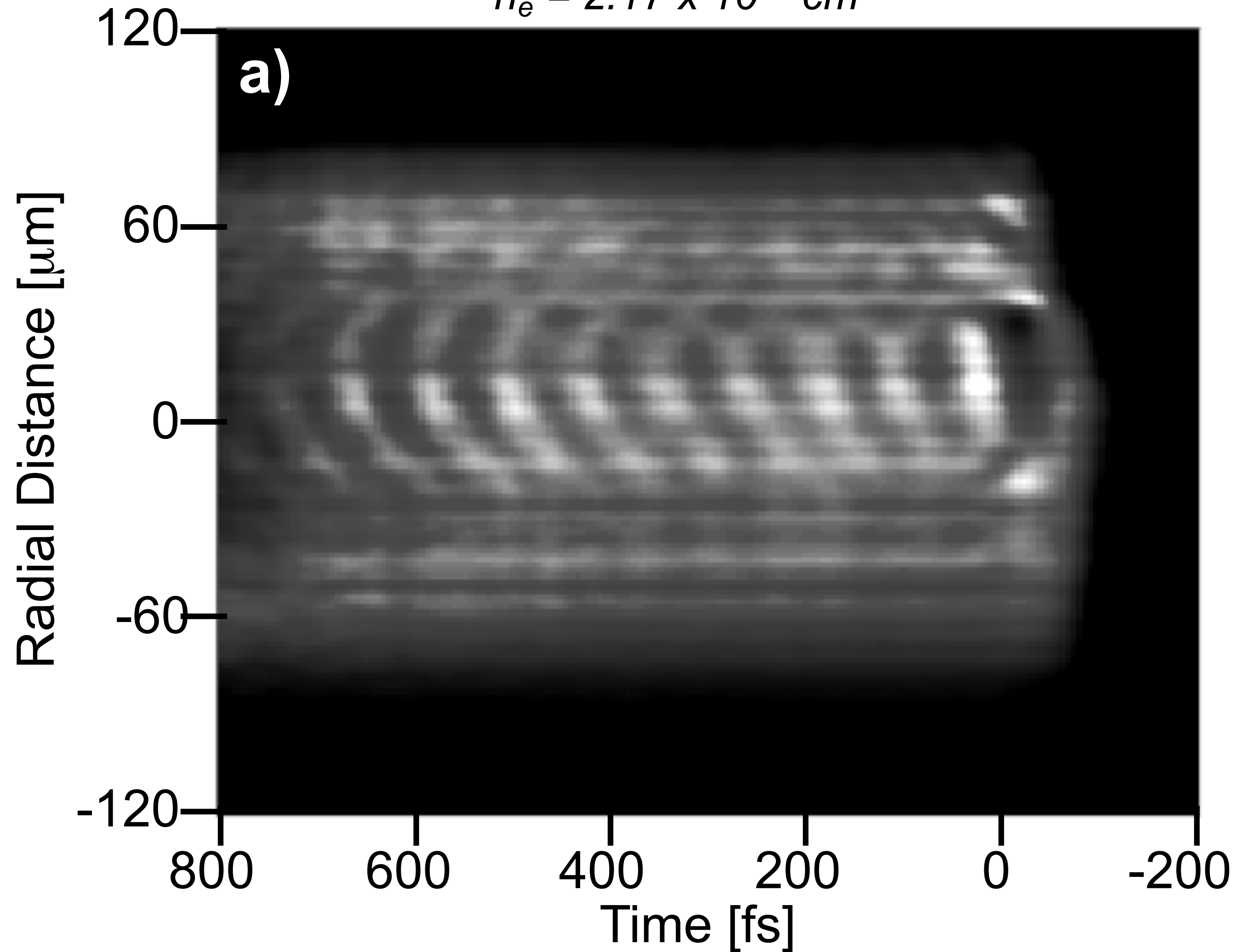
$P \sim 10 \text{ TW}$ ,  $I \sim 10^{18} \text{ W/cm}^2$



# Strong wakes have curved wavefronts

$P \sim 30 \text{ TW}$ ,  $I \sim 3 \times 10^{18} \text{ W/cm}^2$

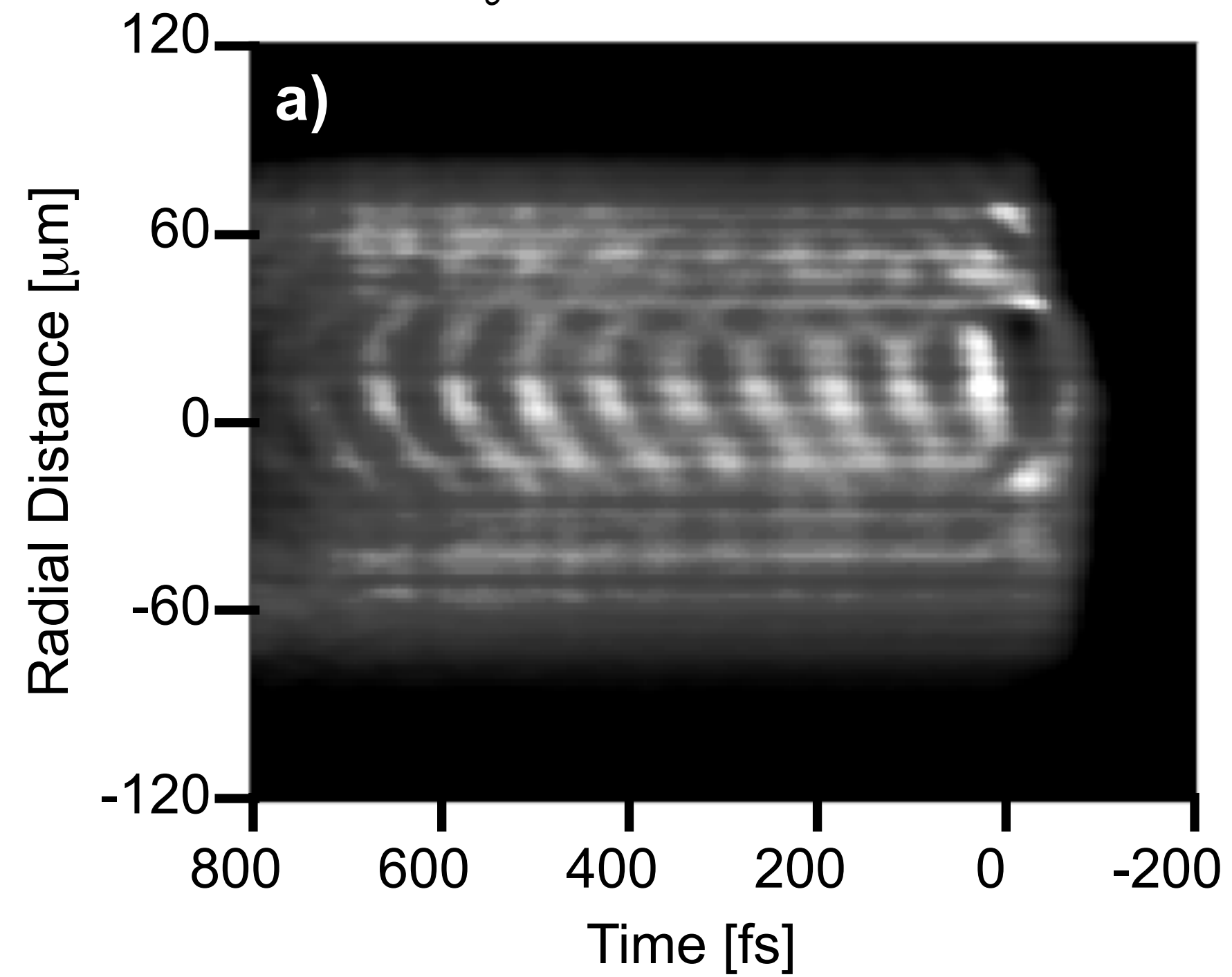
$n_e = 2.17 \times 10^{18} \text{ cm}^{-3}$



# Strong wakes have curved wavefronts

$P \sim 30 \text{ TW}$ ,  $I \sim 3 \times 10^{18} \text{ W/cm}^2$

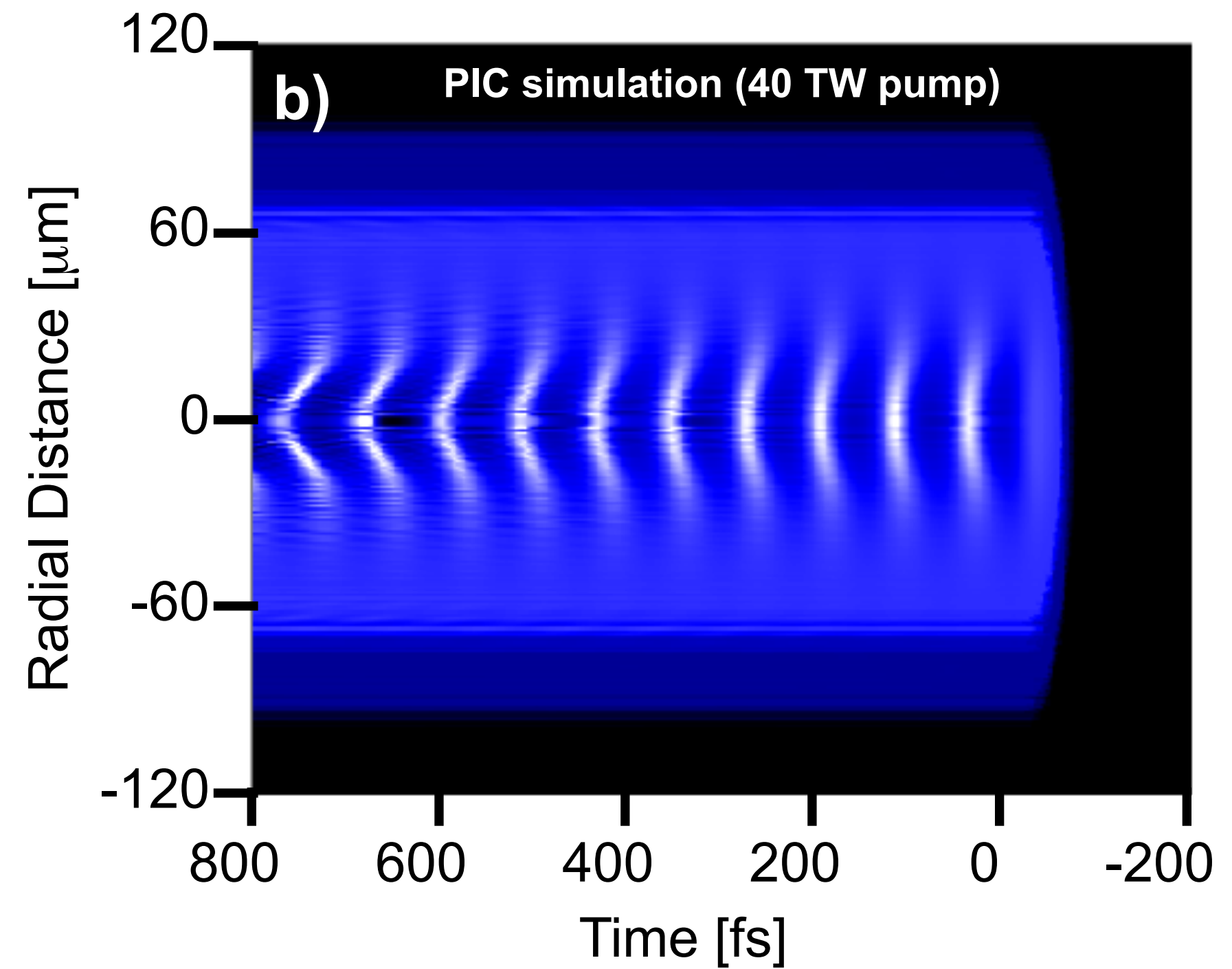
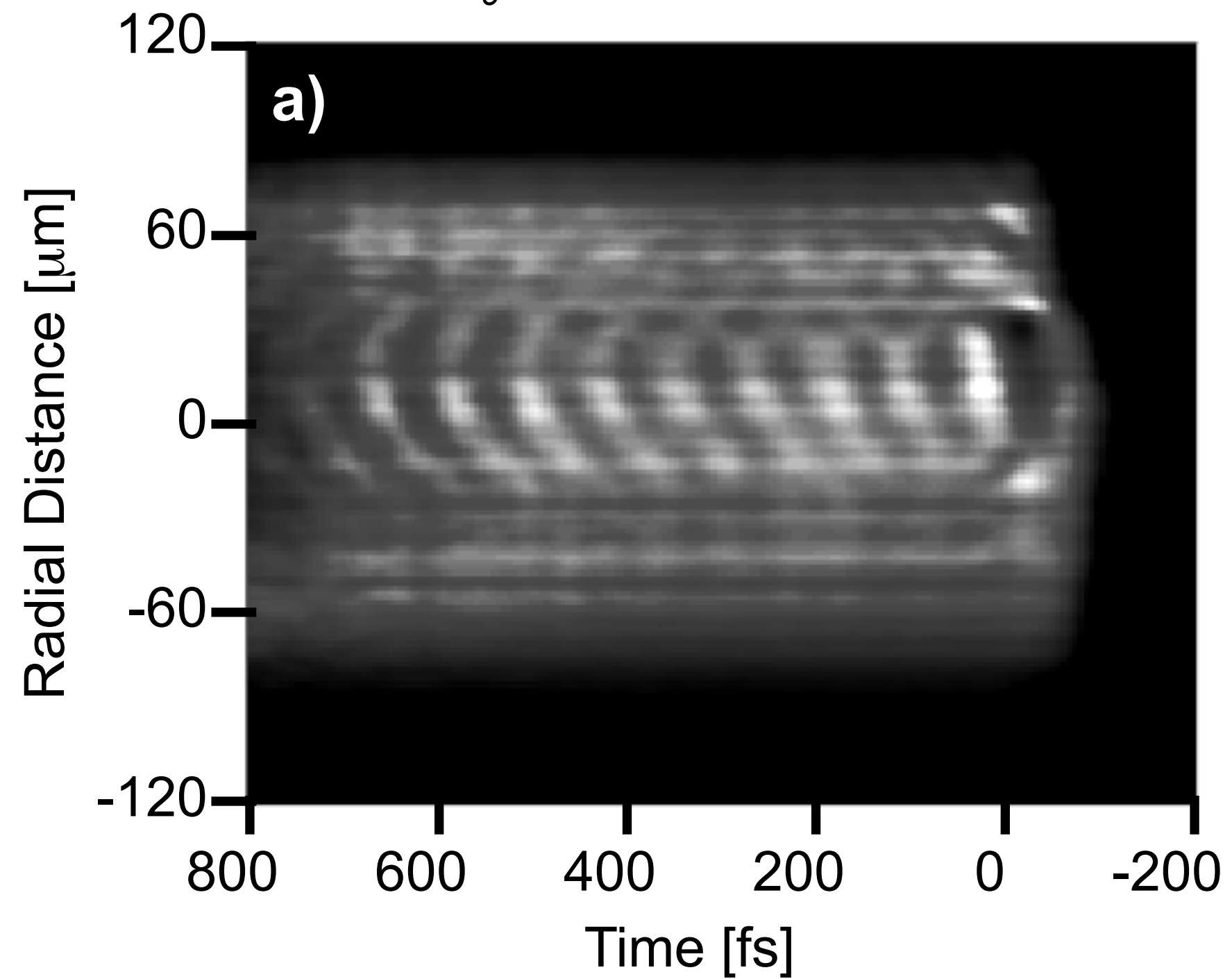
$n_e = 2.17 \times 10^{18} \text{ cm}^{-3}$



# Strong wakes have curved wavefronts

$P \sim 30 \text{ TW}$ ,  $I \sim 3 \times 10^{18} \text{ W/cm}^2$

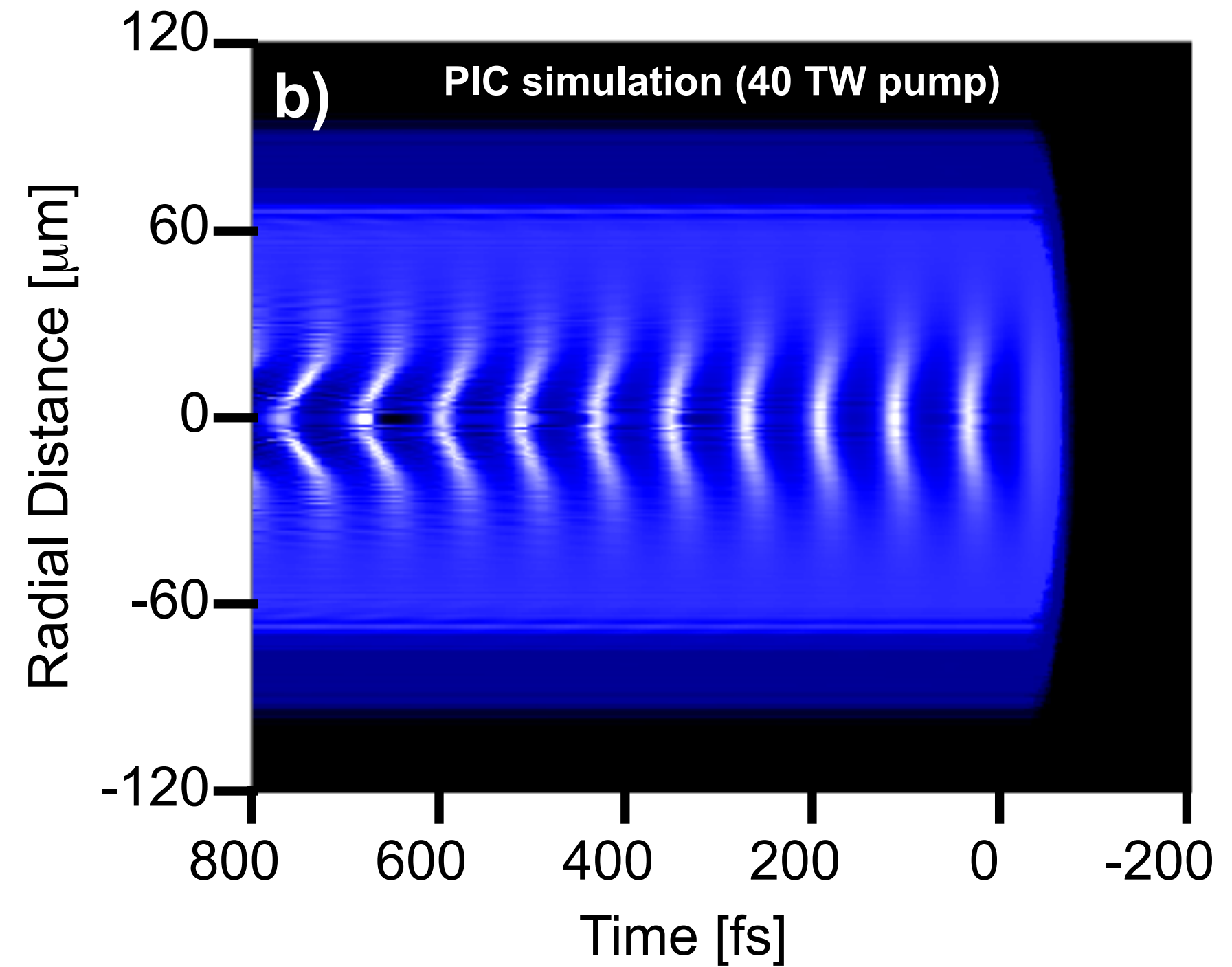
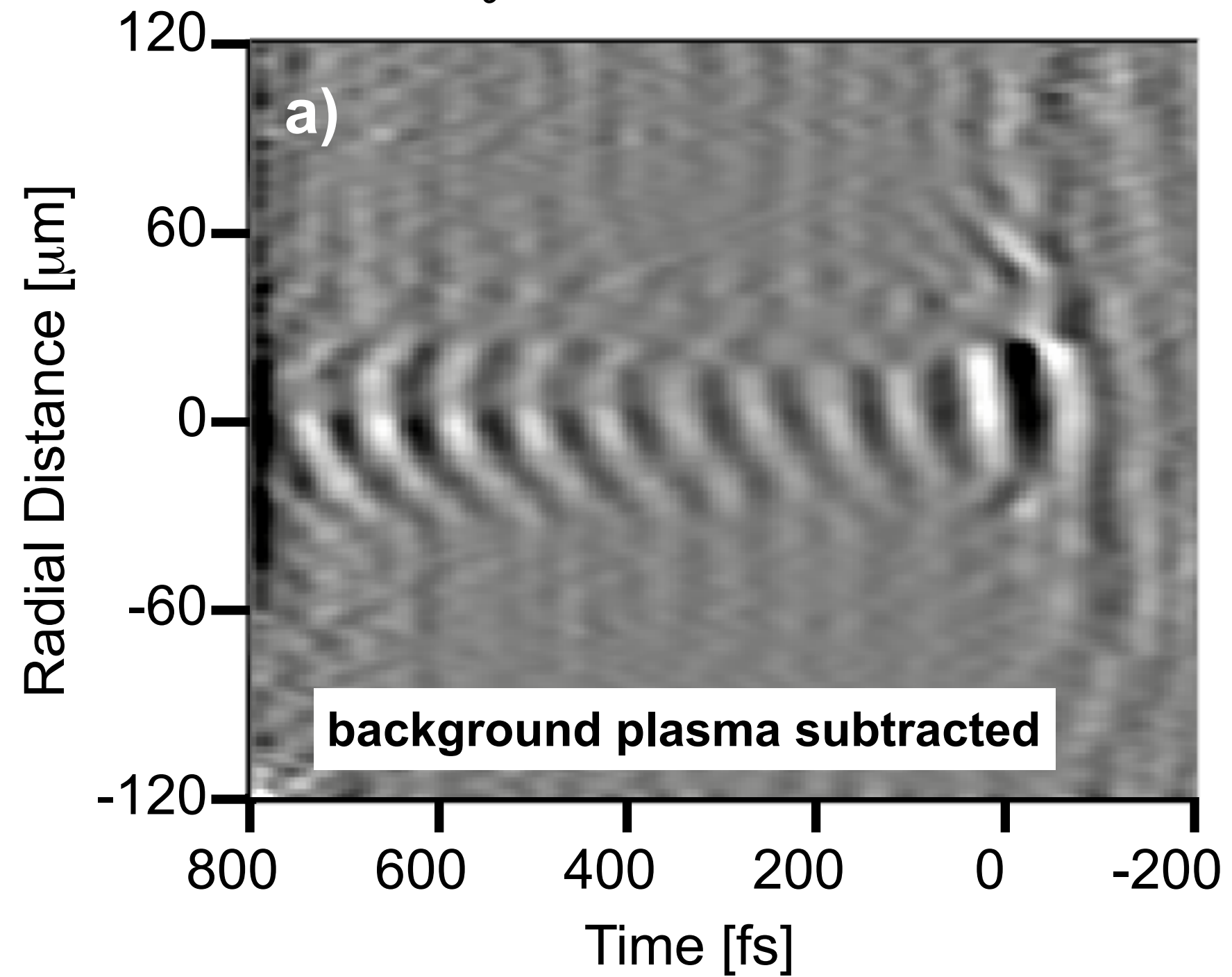
$n_e = 2.17 \times 10^{18} \text{ cm}^{-3}$



# Strong wakes have curved wavefronts

$P \sim 30 \text{ TW}$ ,  $I \sim 3 \times 10^{18} \text{ W/cm}^2$

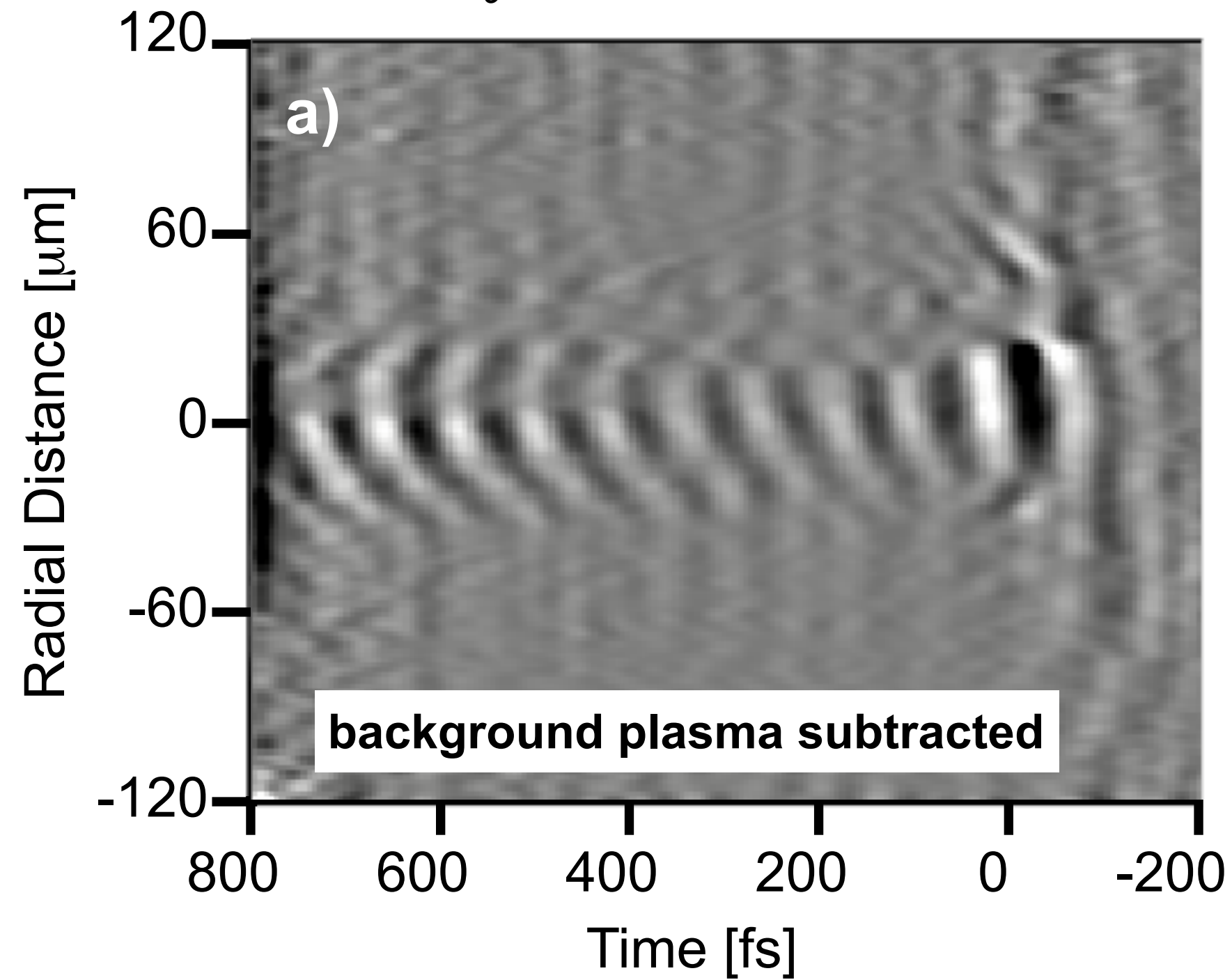
$n_e = 2.17 \times 10^{18} \text{ cm}^{-3}$



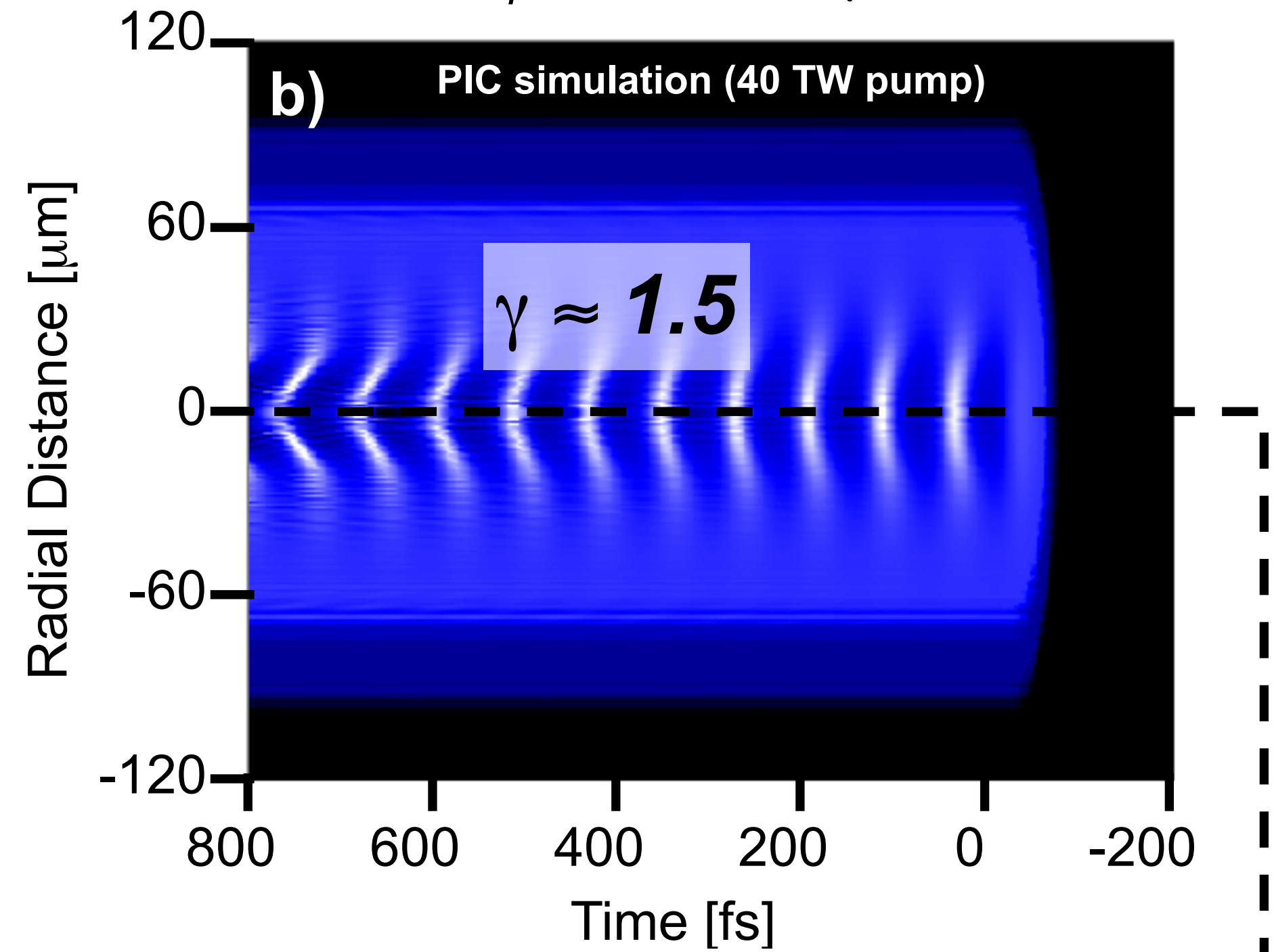
# Strong wakes have curved wavefronts

$P \sim 30 \text{ TW}$ ,  $I \sim 3 \times 10^{18} \text{ W/cm}^2$

$$n_e = 2.17 \times 10^{18} \text{ cm}^{-3}$$



$$\omega_p = [n_e e^2 / \epsilon_0 \gamma m_e]^{1/2}$$



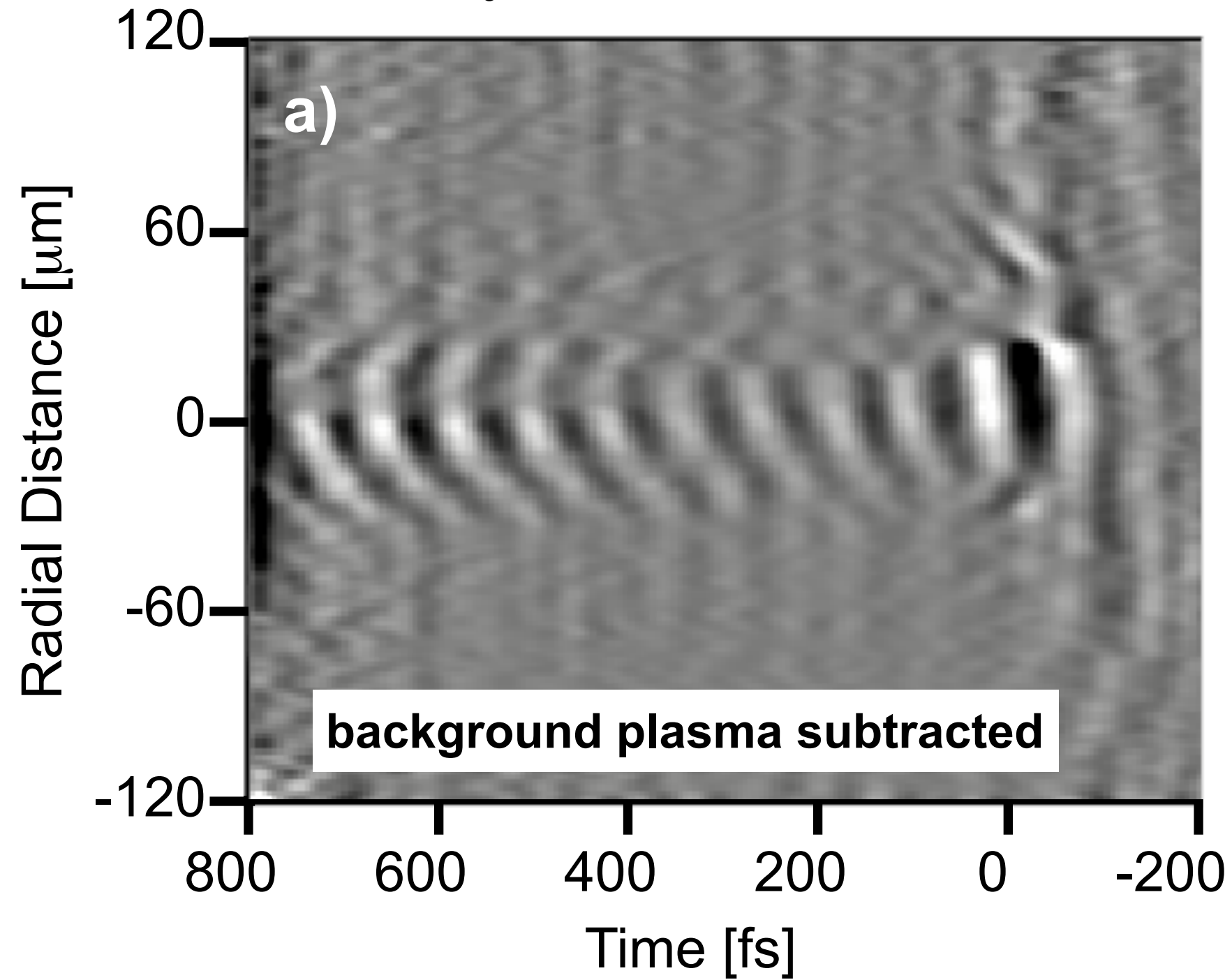
## Source of wavefront curvature:

- large wave amplitude = large  $\gamma$

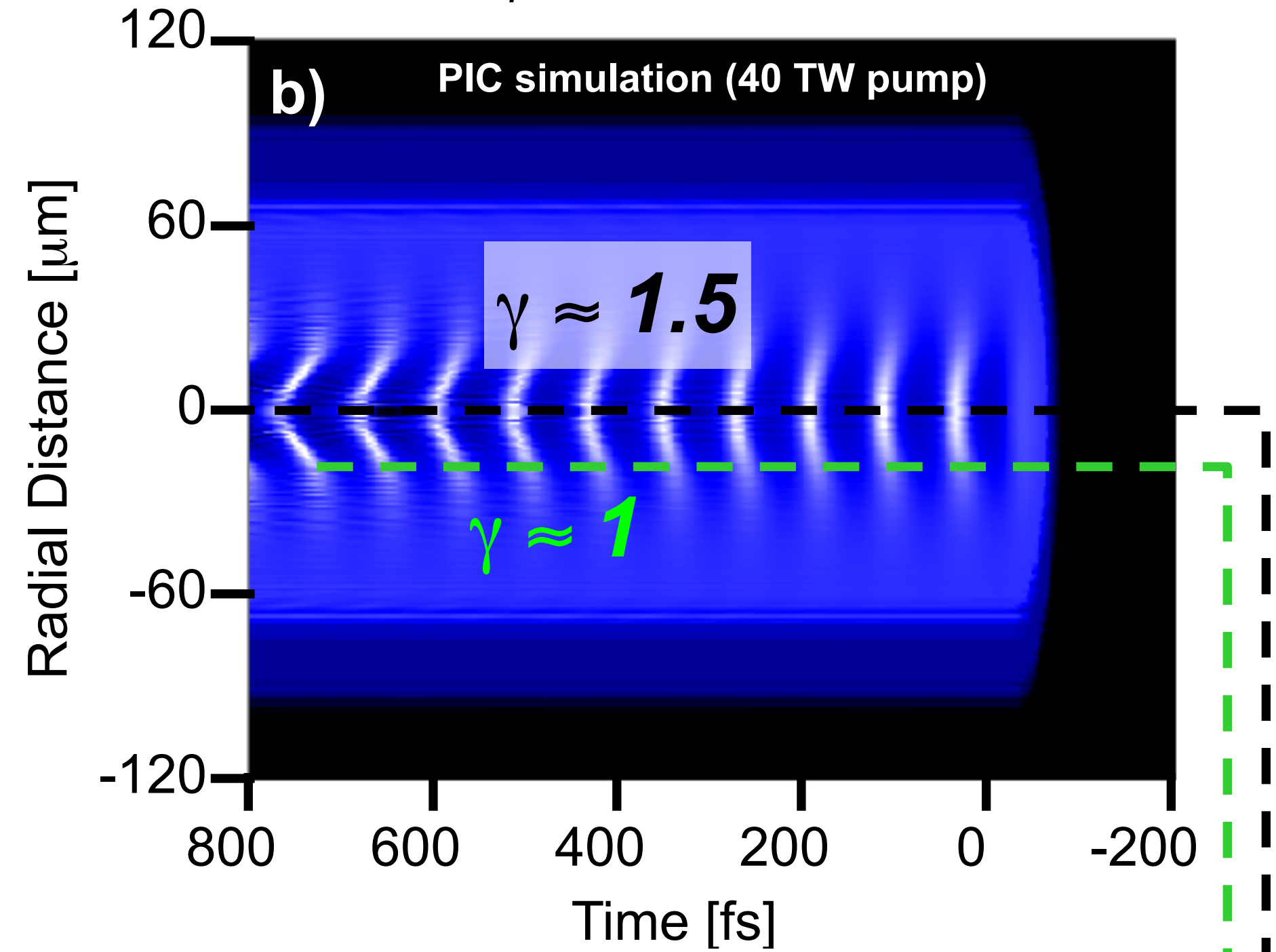
# Strong wakes have curved wavefronts

$P \sim 30 \text{ TW}$ ,  $I \sim 3 \times 10^{18} \text{ W/cm}^2$

$$n_e = 2.17 \times 10^{18} \text{ cm}^{-3}$$

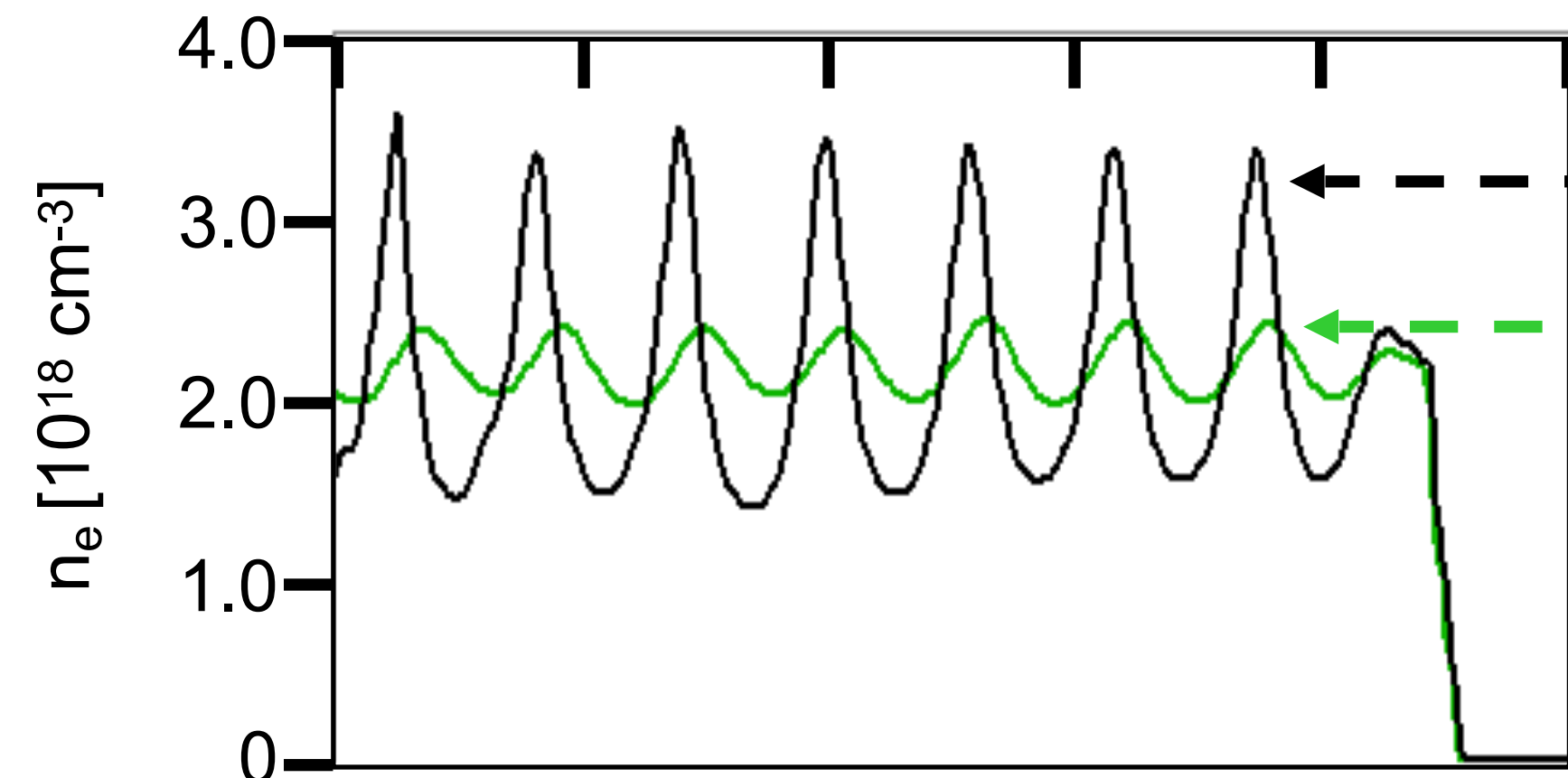


$$\omega_p = [n_e e^2 / \epsilon_0 \gamma m_e]^{1/2}$$



## Source of wavefront curvature:

- large wave amplitude = large  $\gamma$
  - small wave amplitude = small  $\gamma$
- $\lambda_p$  (relativistic)  $>$   $\lambda_p$  (non-relativistic)

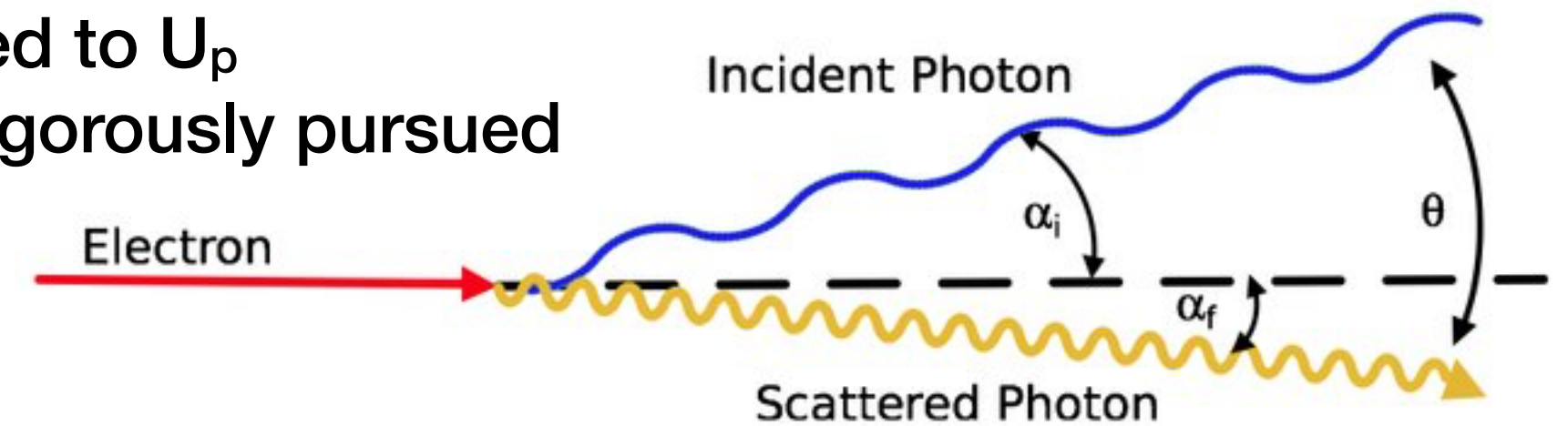


# **Plasma temperature**

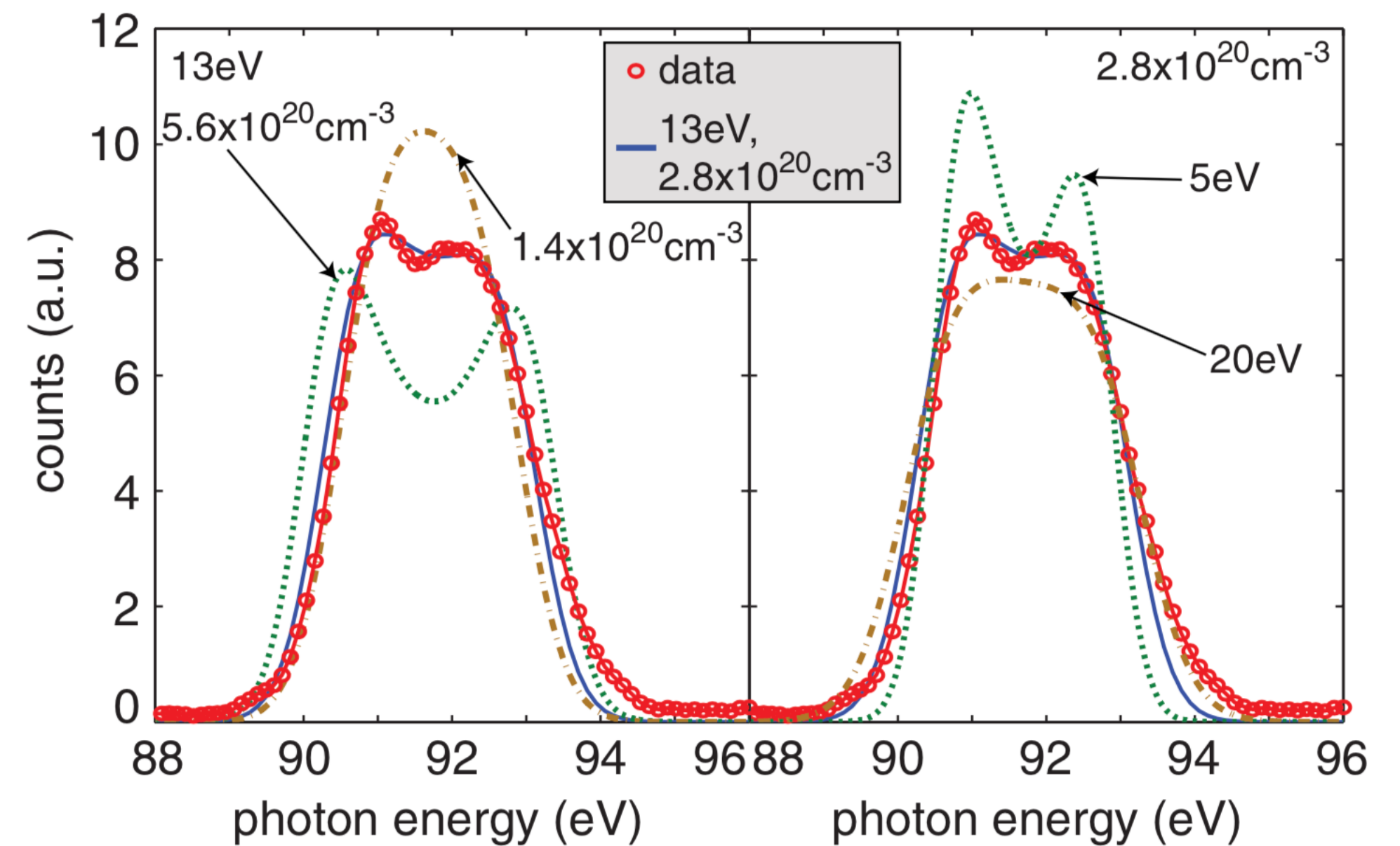
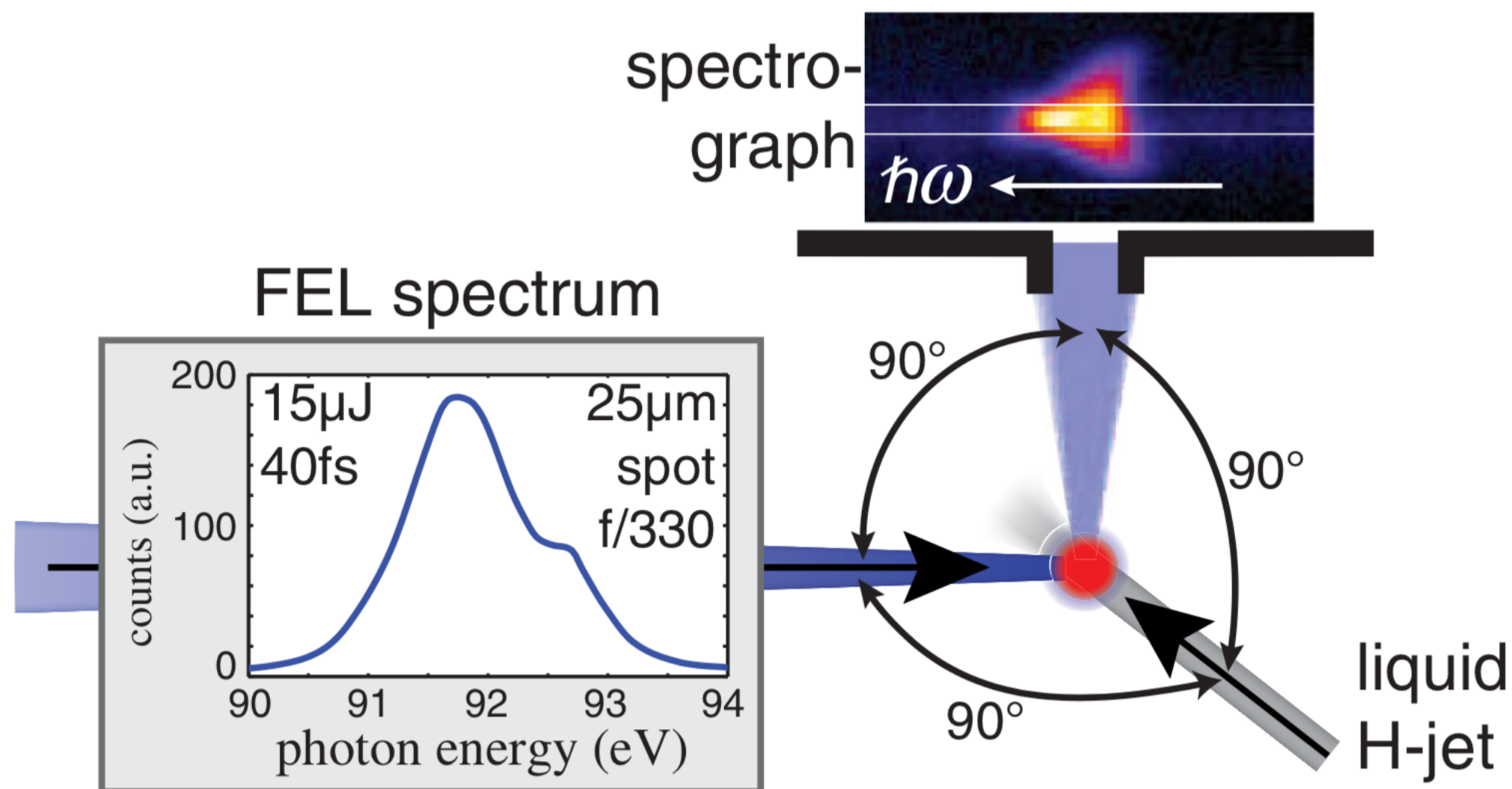
- Inverse compton scattering

# Inverse Compton scattering

- > Initial plasma temperature  $T_e(x,t)$ ,  $T_i(x,t)$  usually small compared to  $U_p$   
 → effects usually neglected, temperature measurements not vigorously pursued
- > Possible method Inverse Compton scattering



- > Example from FLASH FEL



R. R. Fäustlin *et al.*, PRL 104, 125002 (2010)

# Summary of Plasma Diagnostics

## > *Gas density*

- Raman scattering
- Interferometry

## > *Plasma density and constituents*

- Schlieren/dark-field imaging
- Laser interferometry
- Two-color phase delay spectral interferometry
- Plasma spectroscopy

## > *Internal E- & B-fields, and wake structures*

- Polarimetry
- Particle beam probes
- Frequency Domain Holography

## > *Plasma temperature*

- Inverse Compton Scattering

